AFRPL-TR-76-99

No. 9006-085-1

RELIABILITY ESTIMATING PROCEDURES FOR ELECTRIC AND
THERMOCHEMICAL PROPULSION SYSTEMS

FINAL REPORT

VOL I

BOOZ ALLEN APPLIED RESEARCH
4733 BETHESDA AVENUE
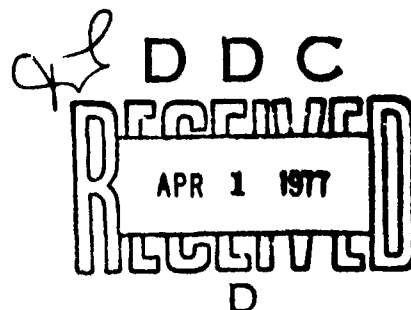BETHESDA, MARYLAND   20014

FEBRUARY 1977

APPROVED FOR PUBLIC RELEASE

DISTRIBUTION UNLIMITED

D D C

APR 1 1977

Prepared for:

AIR FORCE ROCKET PROPULSION LABORATORY
DIRECTOR OF SCIENCE AND TECHNOLOGY
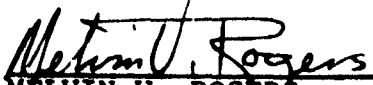AIR FORCE SYSTEMS COMMAND
EDWARDS AFB, CALIFORNIA   93523

NOTICES

This report has been reviewed by the Information Office
(OI) and is releasable to the National Technical Infor-
mation Service (NTIS). At NTIS, it will be available to
the general public, including foreign nations.

This technical report has been reviewed and is approved for
publication.

MELVIN V. ROGERS
Project Engineer

THOMAS W. WADDELL
Chief, Satellite Propulsion
Section

EDWARD E. STEIN
Deputy Chief, Liquid Rocket Division

REPORT DOCUMENTATION PAGE		READ INSTRUCTIONS BEFORE COMPLETING FORM
1. REPORT NUMBER AFRPL TR-76-99 —VOl-1	2. GOVT ACCESSION NO.	3. RECIPIENT'S CATALOG NUMBER
4. TITLE (and Subtitle) RELIABILITY ESTIMATING PROCEDURES FOR ELECTRIC AND THERMOCHEMICAL PROPULSION SYSTEMS. Vol. 1 Vol. I.		5. TYPE OF REPORT & PERIOD COVERED Final Report - March 1975 – December 1976.
		6. PERFORMING ORG. REPORT NUMBER 9006-071-8
7. AUTHOR(s)		8. CONTRACT OR GRANT NUMBER(s) F04611-75-C-0039
9. PERFORMING ORGANIZATION NAME AND ADDRESS Booz Allen Applied Research 4733 Bethesda Avenue Bethesda, Maryland 20014		10. PROGRAM ELEMENT, PROJECT, TASK AREA & WORK UNIT NUMBERS 305811TG
11. CONTROLLING OFFICE NAME AND ADDRESS Air Force Rocket Propulsion Laboratory/LKDA Edwards AFB, California 93523		12. REPORT DATE February 1977
		13. NUMBER OF PAGES 300
14. MONITORING AGENCY NAME & ADDRESS(if different from Controlling Office)		15. SECURITY CLASS. (of this report) UNCLASSIFIED
		15a. DECLASSIFICATION/DOWNGRADING SCHEDULE

16. DISTRIBUTION STATEMENT (of this Report)

APPROVED FOR PUBLIC RELEASE; DISTRIBUTION UNLIMITED

BAAR - 9006

17. DISTRIBUTION STATEMENT (of the abstract entered in Block 20, if different from Report)

18. SUPPLEMENTARY NOTES

19. KEY WORDS (Continue on reverse side if necessary and identify by block number)

Fault tree analysis
Pulse plasma systems
Ion systems
Hydrazine Monopropellant systems

Bi propellant systems
Reliability estimation

20. ABSTRACT (Continue on reverse side if necessary and identify by block number)

The primary objective of this study was to develop a sound standardized basis for reliability comparisons of thermochemical and electric propulsion concepts applicable to Air Force satellite, spacecraft, and upper-stage mission require-ments. A corollary objective was the identification of those propulsion system components which are currently the major contributors to propulsion system failures.

Nearly one hundred component level and failure mode level models were developed

over

DD FORM 1473 EDITION OF 1 NOV 65 IS OBSOLETE

in the course of the study. Constant and increasing failure rates were included to address erosion, wear, and fatigue failure, as well as random failures. Principal variables in these expressions included mission duration, operating time, and the number of operating cycles. For special cases (such as engine valves, injectors, thrust chambers) where design approaches were varied, the design life goals for the specific application were included as independent variables.

Inherent in the realiability modeling was a quantitative assessment of the uncertainty associated with each estimate. The log normal distribution was used as the uncertainty model for each component. The parameters characterizing the log normal distribution for each application were determined where possible from the scatter or statistical variance of reported failure rates for each component.

System level assessments were performed using functionally oriented fault trees. The functional approach was used to yield fault trees that are least affected by changes and revisions at the component level. System assessments were performed by aggregating the component reliability and uncertainty results through the fault tree logic using computer programs and approximation techniques which were modified or developed for this purpose.

PREFACE

This final report presents the results of a study
conducted from March 1975 through February 1977. The pri-
mary objective of the study was to develop a sound stand-
ardized basis for reliability comparisons of thermochemi-
cal and electric propulsion concepts applicable to Air
Force satellite, spacecraft, and upper-stage mission re-
quirements. A corollary objective was the identification
of those propulsion system components which currently are
the major contributors to propulsion system failures.
This study was performed for the Air Force Rocket Propul-
sion Laboratory, Edwards Air Force Base, under contract
number F04611-75-C-0039 by Booz, Allen Applied Research,
a division of Booz, Allen & Hamilton Inc.

The authors are indebted to the following organiza-
tions for their cooperation in providing data and es-
pecially for their review and critique of preliminary
results:

- Aeronutronics Division, Newport Beach, California

- AVCO Corp, Wilmington, Massachusetts.

- Bell Aerospace, Buffalo, New York

- COMSAT, Clarksburg, Maryland

- Electro Optical Systems, Pasadena, California

- Fairchild Republic, Farmingdale, New York

- Hamilton Standard, Windsor Locks, Connecticut

- Hughes Research Laboratory, Malibu, California

- Lewis Research Center, Cleveland, Ohio

- Lockheed Missiles and Space Corporation,
  Sunnyvale, California

- Phrasor Technology, Pasadena, California

D D C

APR 1 1977

iv

D
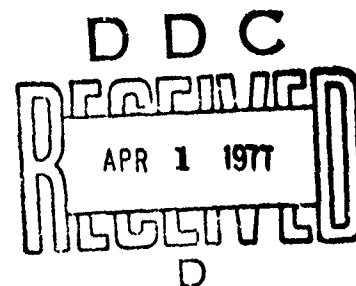
- SAMSO, Los Angeles, California

- TRW Systems, Inc., Redondo Beach, California.

v

T A B L E   O F   C O N T E N T S

Page
Number

VOLUME I

L I S T   O F   T A B L E S

L I S T   O F   F I G U R E S

TECHNICAL APPROACH

The development of reliability estimating techniques was focused on six generic propulsion systems: ion, pulsed plasma, colloid, catalytic monopropellant, electro-thermal monopropellant, and hypergolic bipropellant. Preliminary review of these systems, their expected applications, and the available reliability data has indicated that the successful approach required the following characteristics:

- The approach had to be synthesis oriented. It had to be capable of combining data and procedures that differed in origin, character, and degree of credibility.

- The approach had to take into account the uncertainties associated with the input data and estimation procedures. Furthermore, these uncertainties had to be reflected with the estimates that resulted. The approach had to avoid point estimates alone; it had to yield distributions or bounds along with central measures.

- The approach had to be directed toward defining an explicit, step-by-step methodology and was to function as a usable data base for use by designers and system analysts that are not necessarily reliability specialists.

With these considerations in mind, the study plan as shown in Figure 1 was developed and executed. This plan consisted of four general phases:

- Data Base Definition

- Electronic Component Reliability and Uncertainty Derivation

- Non Electronic Component Reliability and Uncertainty Derivation

- Propulsion System Reliability Estimation.

These phases are discussed in the following paragraphs.
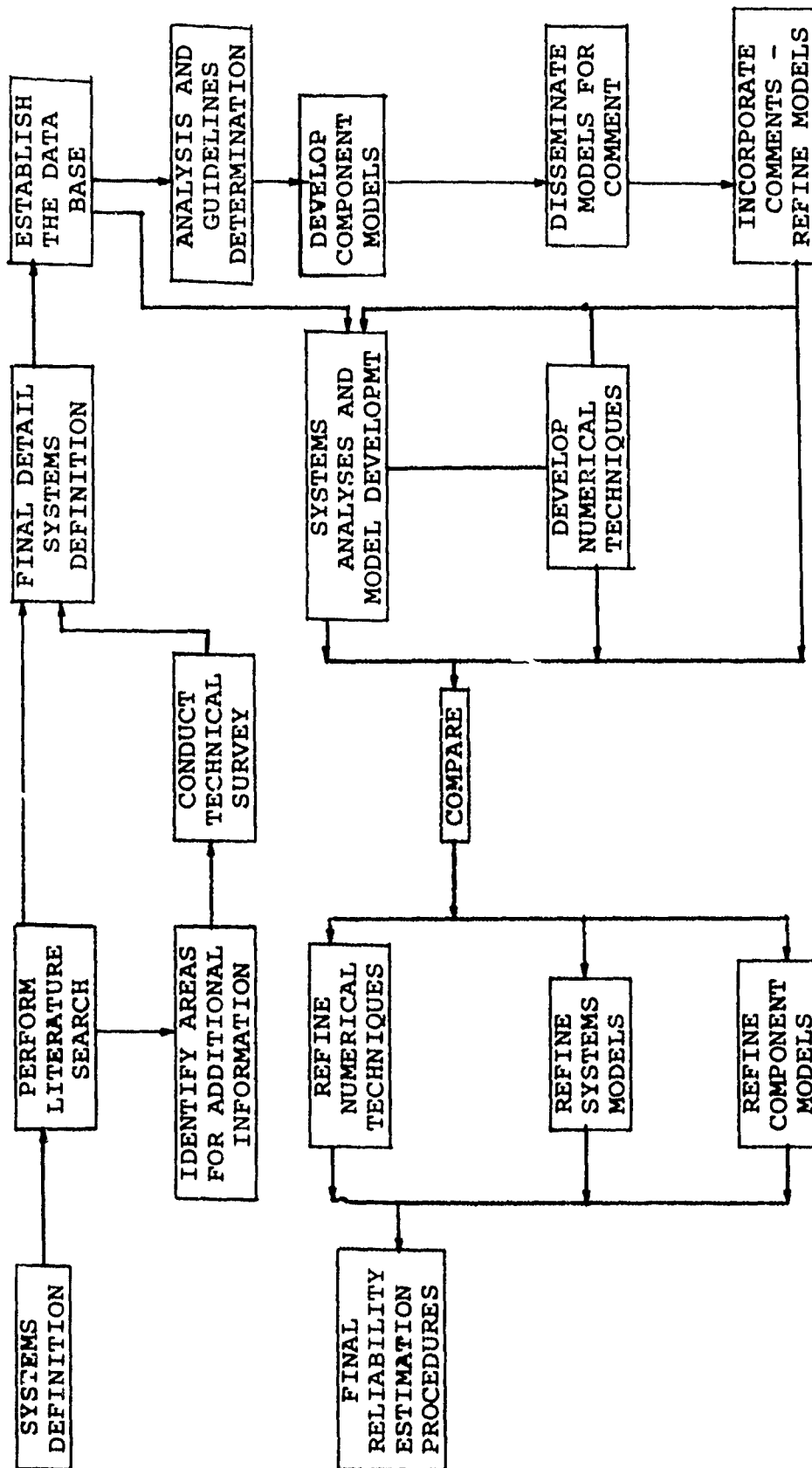
Figure 1. Reliability Estimation Procedures Study Plan

DATA BASE DEFINITION

Principally this phase consisted of the definition of the propulsion system components, data acquisition, and data representation. The six generic systems identified earlier were expanded to seven systems in order to assess two approaches to ion thrusters: the electron bombardment mercury ion thruster utilizing a Kaufman thrust chamber and the electron bombardment cesium ion thruster employing a magneto-electrostatic containment (MESC) thrust chamber. The components to be included in each of these seven systems are shown schematically with typical interfaces in Figures 2 through 8. These figures intentionally exclude multiple thruster and tankage schemes and are intended merely to identify the component types and the typical interrelationships.

Data Acquisition. Data source identification and the literature search were begun simultaneously by reviewing such data collections as AVCO, FARADA (GIDEP) and NEDCO II and by the initiation of searches at DDC and Chemical Propulsion Information Agency (CPIA). A summary representation of literature sources and the applicability of the data obtained is shown in Table 1. Review of the results of the literature search allowed the identification of those areas pertinent to reliability estimation requiring further attention. An interview guide addressing those areas was formulated for use in the technical survey which followed.

The data acquisition survey included 23 Government agencies, industrial firms and universities. Over 50 individual interviews were conducted to supplement information available from the literature search. Table 2 summarizes the organizations and applicability of data obtained from the survey.

Data Representation. The final portion of the data definition phase involved the categorization and preliminary analysis of information and data gathered from the literature search and technical survey activities. This analysis revealed the following critical characteristics of the data base that was available for the development of reliability estimation procedures:

- Actual data was limited and concentrated in two of the seven systems

- Actual data evidenced wide variability

ANODE SUPPLY   CATHODE SUPPLY   NEUTRALIZER SUPPLY

SURFACE TENSION
CESIUM TANK

FILL VALVE

START & CONTROL
VALVE

VAPORIZER

POWER
CONDITIONER

CONTROL
LOGIC

CATHODE/
HEATER

ANODIC
FEED
RING

ANODES

RING
MAGNETS

SCREEN GRID

ACCEL. GRID

CESIUM
PLASMA
ARC
NEUTRALIZER

HEATER   PLASMA ARC

MAGNETO-ELECTROSTATIC CONTAINMENT THRUSTER (MESC)

Figure 2.   Cesium Ion Electron Bombardment
Generic System Layout

I-4

FILL VALVE

PRESSURANT TANK
DIAPHRAGM

FILL VALVE

LARGE POROUS PLUG
HEATER
VAPORIZER
HIGH VOLTAGE ISOLATOR

CATHODE
HEATER

FLOW
SPLITTER

CATHODE POLE PIECE SHIELD

POWER
CONDITIONER

ELECTROMAGNET

PERMANENT MAGNET

PERMANENT MAGNET

BAFFLE

ANODE

SCREEN GRID

POLE PIECE

FROM
NEUTRALIZER
VAPORIZER

CONTROL
LOGIC

FIXED ACCELERATOR GRID · DISHED

THRUSTER

PLASMA ARC

HEATER

NEUTRALIZER

Figure 3.   Mercury Ion Electron Bombardment
Generic System Layout

I-5

Figure 4. Pulsed Plasma Generic System Layout

I-6

Figure 5. Colloid System Generic System Layout

FILL VALVE

PROPELLANT SUPPLY TANK

DIAPHRAGM

FILL VALVE

FILTER

HEATER

LATCH VALVE

CONTROL VALVE

HEATERS

INJECTOR

CHAMBER ASSEMBLY

CATALYST RETAINER

HEATERS

Figure 6. Catalytic Monopropellant
Generic System Layout

FILL VALVE

PRESSURIZED SURFACE TENSION TANK

FILL VALVE

FILTER

LATCH VALVE

HEATER

SOLENOID CONTROL VALVE

HEATERS

TO THRUSTER

THRUSTER CONFIGURATIONS

INJECTOR

HEATER

PLATINUM SCREENS

INJECTOR

PROPELLANT SWIRL

HEATERS

ROD HEATER

Figure 7.   Electrothermal Monopropellant
Generic System Layout

I-9

PRESSURANT TANK

FILL VALVE

ISOLATION VALVE

FILTER

REGULATOR

CHECK VALVE FOR
INTERCONNECT SYSTEMS

PRESSURE
RELIEF VALVE

OXIDIZER
TANK

FUEL TANK

BURST
DIAPHRAGM

BLADDER (OR SURFACE TENSION
FUEL MANAGEMENT DEVICE)

FILL VALVE

ISOLATION VALVE

FILTER

CONTROL VALVE(S)

INJECTOR

THRUST CHAMBER

Figure 8. Hypergolic Bipropellant Generic System Layout

Table 1

Literature Search Summary

#	SOURCES	Ion Thruster Cesium	Ion Thruster Mercury	Pulsed Plasma Thruster	Colloid Thruster	Catalytic Monoprop Thruster	Electrothermal Monoprop Thruster	Bi Prop Thruster	Multi System
1	JPL	X	X			X		X	X
2	Fairchild		X	X		X			
3	Lewis Research Center		X						X
4	Plasmadyne								
5	Electric Propulsion Conference 11/73	X	X	X					X
6	Space Sciences Lab			X					X
7	Electric Propulsion Conference 3/75	X	X	X					X
8	Lincoln Labs/MIT								
9	Hughes Research Lab		X	X					X
10	Princeton University	X	X			X			X
11	Martin Marietta								X
12	AFRPL								X
13	Electric Propulsion Conference 4/72					X		X	X
14	Marquardt C.					X		X	X
15	Aerospace Sciences Mtg 1/73								X
16	TRW				X		X	X	X
17	Rocket Propulsion Establishment 3/74								X
18	Rocket Research					X			
19	National Aeronautics & Space Admin.					X			X
20	Walter Kidde					X			
21	The Boeing Co					X			X
22	CPIA					X			
23	Navy Space Systems Activity								X
24	AVCO					X	X	X	X
25	Stanford Research Inst								
26	Defense Metals Info Center								
27	Reliability Analysis Center								
28	JANNAF Propulsion Conf 11/73					X			X
29	PRC System Sciences								
30	JANNAF Propulsion Conference 10/74					X			X
31	Air Force Materials Lab					X			X
32	UARL					X			X
33	McDonnel Douglas					X	X		
34	Propulsion Joint Specialist Conference 1/71								
35	AIAA	X	X	X	X	X	X	X	X
36	Monoprop Propulsion Specialist Conference 11/72					X			X
37	Hamilton Standard					X			
38	Rockwell International		X			X		X	
39	Goddard SFC	X				X			X

Table 2

Technical Survey Summary

SYSTEMS

SOURCES	Ion Thruster Cesium	Ion Thruster Mercury	Pulsed Plasma Thruster	Colloid Thruster	Catalytic Monoprop Thruster	Electrothermal Monoprop Thruster	Bi-Prop Thruster
Aerospace	X	X		X			X
Dr. Kaufman (Colorado State)	X				X		X
Martin Marietta	X				X		
Lockheed Missiles & Space Corp.	X				X	X	
Philco Aeroneutronic			X		X		
NASA-Goddard SFC							
Princeton University	X	X			X		X
COMSAT		X		X	X		
NASA-Lewis R.C.		X	X				
Hughes Research Lab		X		X		X	X
JPL			X	X	X		X
Electro-Optical Systems							
Applied Physics Lab/JHU							
Lincoln Labs							
Fairchild-Hiller							
Fairchild Republic							
TRW					X		X
SAMSO					X	X	X
Walter Kidde					X		
United Aircraft Research Lab					X		
Hamilton Standard					X		
General Electric					X		
RCA					X	X	X
Marquardt Co					X		X
Bell Aerospace							
AVCO							X
Rocketdyne							X
Aerojet General							X

- Component failure mode identification was possible for the most part, but in a qualitative sense only

- All reported data was of the constant failure rate type, and with few exceptions the failure rate was based on mission time only

- Few reliability assessments addressed the question of prediction bounds or uncertainty. Models yielding point estimates were the norm.

It was expected that the amount of data would be limited. However, its concentration in the catalytic monopropellant and bipropellant systems posed problems for the components of the five remaining systems. A significant amount of estimation of failure rates by analogy to similar component/ environment situations was thereby required. Despite the care used in selecting analogs for this purpose, this process of necessity introduced a significant amount of uncertainty. Available component failure rate data introduced its own contribution to uncertainty. Estimates of failure rates for the same component type often differed by several orders of magnitude. The importance of assessing and tracking, from the outset, the uncertainties associated with reliability estimation was underscored by the foregoing assessments of the data base.

The identification of component failure modes was made possible by the descriptive systems and component information acquired through the literature search and technical survey. With the exception of certain valves, failure rates for each of the identified component failure modes was not available from the data base. For this reason the principal reliability models were generated at the component reliability level. Partitioning to the failure mode level followed the development of system fault trees. The results of that effort served as a guide in determining which components required detailed treatment.

Most sources in the compiled data base approached reliability estimation as the determination of point estimates using constant failure rate models with mission time as the only independent variable. The complete output of any predictive process is a band of values the parameter in question is likely to assume. Point estimates such as the median and expected value are simply central measures of that predicted band. The size of that band is determined by the variance in scatter of the input data and the desired level of confidence in the expected prediction.

I-13

ELECTRONIC COMPONENT RELIABILITY AND UNCERTAINTY DERIVATION

Electronic parts or components differ from other propulsion system components in a number of important details that influence reliability prediction methodology. Electronic components generally are subject to a relatively high degree of standardization and respond to application stresses and requirements in quantitatively predictable ways. They also possess a high level of maturity and exhibit, with some important exceptions, life distributions that are well-approximated by the exponential (constant-failure-rate) distribution.

These characteristics of electronic components permit tabulations of failure rates and adjustment factors, such as those contained in MIL-HDBK-217B[1] to be used effectively. Considering the availability of reliability estimation data at the parts level for electronics and the principle that reliability estimation should be conducted, when feasible, at the level corresponding to adequate data, it is recommended that reliability prediction be performed at the parts level for electronic assemblies, such as power processors and switching units.

Failure rate variability. With rare exceptions, standard sources of failure rate data, such as MIL-HDBK-217B, provide only point estimates of failure rates; that is, a single estimate of failure rate will be obtained for each fixed combination of a specific part and a defined application. It is known, however, that actual failure rates vary significantly not only from vendor to vendor but also from production lot to production lot, under nominally identical conditions. Usually, it is impossible not only to identify the specific origin of parts that will be used in a system but also to determine the specific failure rate of parts having a particular origin. As a result, uncertainty surrounds the failure rate estimates that are used. On the basis of experience, however, it is possible to assign a specific form and estimate the parameters of a distribution characterizing that uncertainty. Because the failure rate estimates obtained from MIL-HDBK-217B reflect a mix of parts' origins, it is appropriate to treat such estimates as defining the means or expected values of the corresponding uncertainty distributions.

By examining the observed failure rates or rejection rates in screening tests, other laboratory tests, or operational experience (e.g., as reported in GIDEP/FARADA compilations), it is possible to estimate the variance associated with the uncertainty distribution for specific parts. Operational experience data need to be viewed with caution, however, because application differences are rarely identified sufficiently to permit segregation of their effects on failure rates. Similar caveats apply to screening and laboratory data unless test conditions and failure definitions are known to be consistent. For all sources except screening test data, many part types present problems in that, under realistic use conditions, failure rates are low enough so that many observations are "no failures" and at most bounding-type statements can be made. However, with some exceptions, the coefficient of variation is sufficiently consistent over a wide variety of electronic parts to justify a simpler and less time-consuming approach to uncertainty estimation.

An early examination of lot-to-lot and vendor-to-vendor variability in failure rates indicated that such variability could be represented by lognormal distributions with the square of the coefficient of variation,

$\eta^2 = 2.74$ ($\sigma_{ln} \approx 1.15$ corresponding to a 100:1 ratio

between the largest and smallest failure rates observed in a sample of 40.[2] That analysis was based largely on screening rejection rates for late-1950's transistors, diodes, resistors, and capacitors. A check on continuing validity has been conducted using data from the August 1975, revision of GIDEP, volume 1, Summaries of Failure Rate Data[3]. A scan of this document led to identification of failure rate data having the desired properties for two electronic part types: quartz crystals and circuit breakers. The desired properties, in terms of minimizing extraneous causes of variation, were reasonable sample size, multiple entries for each of several vendors, consistent environmental conditions, and single reporting source. Calculated values of σ_{ln} were 0.995 and 0.937, respectively, indicating that the earlier estimates remain valid (but may be mildly pessimistic). Accordingly, uncertainty about (constant) electronic part failure rates, with occasional exceptions, will be represented by lognormal distributions with expected values corresponding to estimates from MIL-HDBK-217B, for example, and variances based on $\sigma_{ln} \approx 1.15$. (Examples are provided in Appendix A of this section.) The following relationships may be useful in evaluating subsequent calculations:

- Parameters of the (normal) distribution of the natural logarithms of the variate:

    μ : mean=median=mode

    σ_{ln}: standard deviation

- Relationships to the (lognormal) distribution of the variate:

    Expected value $\quad E\{\lambda\} = \exp\left[\mu + \dfrac{\sigma^2}{2}\right]$

    Coefficient of variation $\quad \eta^2 = \exp(\sigma^2) - 1$

    Variance $\quad V\{\lambda\} = E^2\{\lambda\}\eta^2$

Analyses and graphic displays of the quartz crystal and circuit breaker data are presented in Tables 3 and 4 and Figures 9 and 10.

Nonconstant failure rate contributions. A substantial body of literature suggests that semiconductor failure rates tend to decrease with age, rather than remaining constant. Some recent analyses of in-orbit experience of NASA spacecraft appear to confirm this observation and extend it to some other types of electronic parts.

These observations are consistent with the first two regimes of the traditional "bathtub" curve depiction of failure rate behavior. The final regime, wear-out, will be discussed later. In the absence of convincing evidence or theoretical support for the concept of an intrinsic process that leads to monotonically decreasing failure rates, it is unwise to postulate that such decreases will prevail beyond the period of observation reflected in current data. It is suggested that the observed decreases should be disregarded for extended-mission reliability prediction purposes for the following reasons:

- The observed rate of decrease becomes too small to be of practical significance after a relatively short period

- The decrease can be viewed as reflecting the behavior of a relatively small subpopulation consisting of the "weakest" parts, and, therefore, should not be expected to continue

I-16

TABLE 3. CRYSTAL FAILURE RATES[a]
(Ground-Life Test)
(Medium Temperature Stress, Failures per 10^6 Hours)

CR-18A/U		CR-56A/U		CR-77A/U	
K[b]	3.845	K	12.409	W	49.776
H	14.298	E	1.571	M	19.015
W	22.960	Mc	4.366	M	8.643
B	15.293	E	21.999	H	3.218
H	5.957	H	11.357	H	12.872
K	5.127	K	1.551	W	54.754
B	8.496	H	7.098	H	20.455
W	18.785	Mc	1.435	W	41.513
K	6.639	M	57.513	H	17.898
K	3.319	K	7.874	M	18.224
H	13.378	K	62.992	M	15.621
H	16.054			W	59.963
B	6.086				
B	8.114				
M	5.712				
M	7.140				

	CR-18A/U	CR-56A/U	CR-77A/U
Mean Logarithm	2.1457	2.0906	3.0092
Logarithmic Standard Deviation	.5925	1.3459	.8476

TABLE 4. CIRCUIT BREAKER FAILURE RATES[c]
(Ground)
(Medium Temperature Stress)

Failures per 10^6 Hours

.311
3.62
2.62
1.89
1.05
1.34
.286
2.35
2.85

Mean Logarithm	.3011
Logarithmic Standard Deviation	.9366

[a] Source: GIDEP Vol. 1, Rev. August 1975.
[b] The letters indicate manufacturer identification.
[c] Source: GIDEP Vol. 1, Rev. August 1975 (one apparently redundant entry omitted).
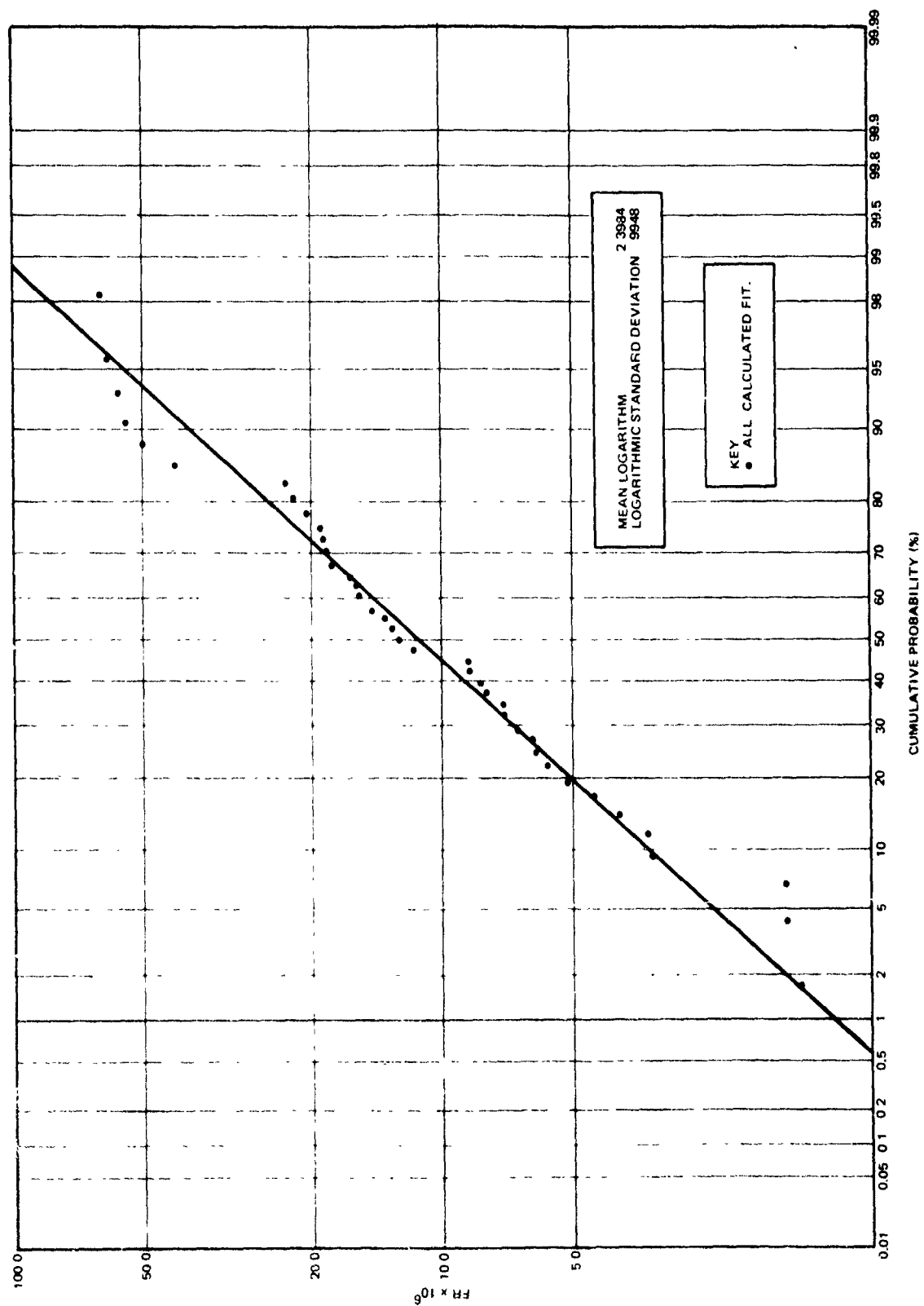
Figure 9. Crystal failure rates.
(ground-life test)
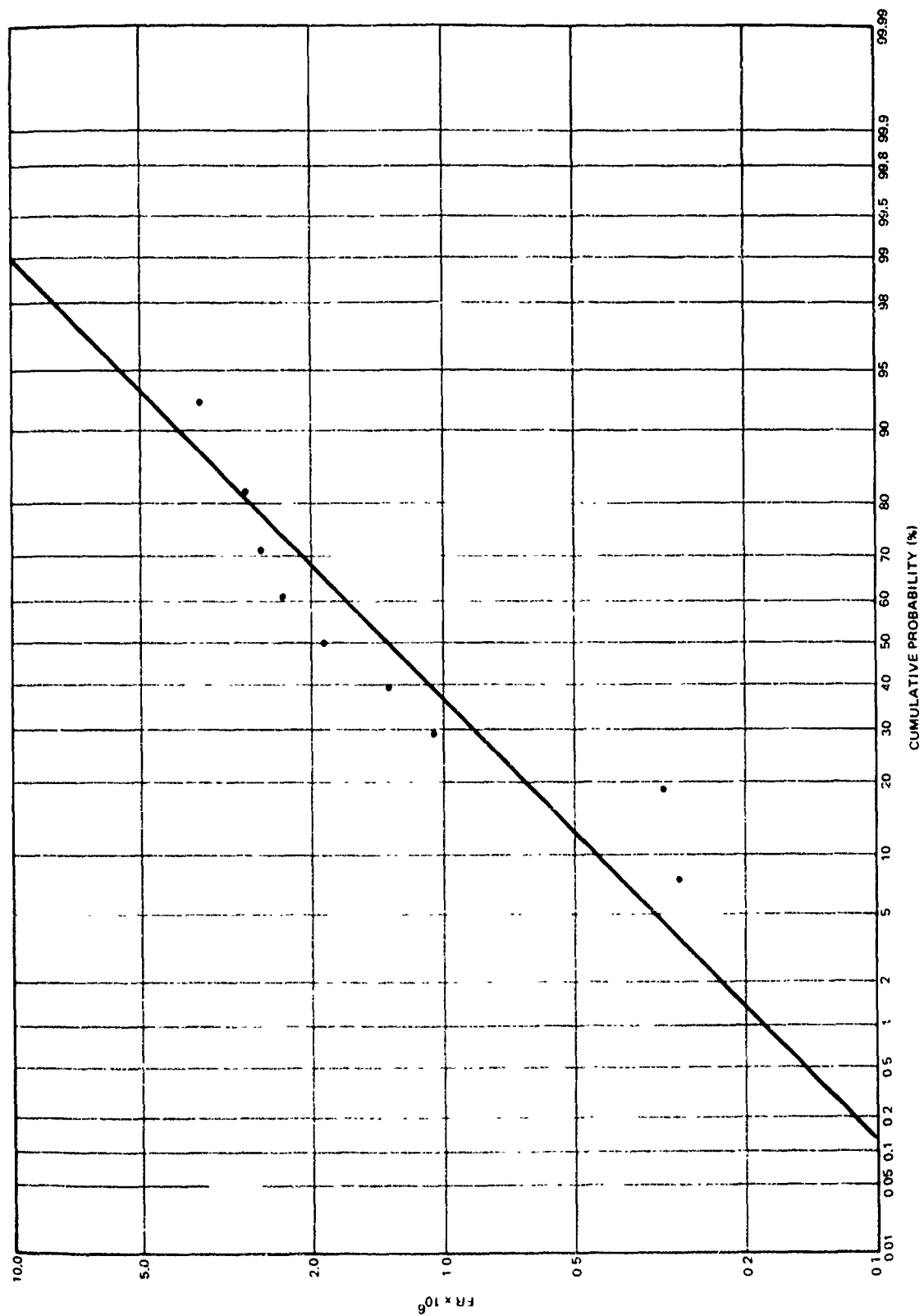
Figure 10. Circuit breaker failure rates.
(ground)

- Effective screening of electronic parts, which is mandatory for extended-duration missions, results in elimination of the individual parts whose early failure otherwise may account for the observation of decreasing failure rates

- Failure rate data in standard sources usually reflect tests or operations of sufficiently long duration to discount the decreasing failure rate effects by averaging.

Conversely, processes that may lead to increasing failure rates must be considered because they may have substantial influence late in extended missions. Furthermore, the effects of these processes are unlikely to be reflected in failure rate data. From shorter-term observations, candidate failure processes of this kind include:

- Aging of organic materials, especially insulation where dielectric properties of the material, rather than physical separation, is relied upon; for example, in coils of electromagnetic devices

- Contaminant accumulation; for example, in lubricants or on electrical contacts

- Corrosion; for example, electrolytic corrosion of electrical connections internal to resistors

- Depletion of consumable materials; for example, evaporation of lubricants, sublimation of heater elements/filaments, and erosion of electrical contacts or electrodes

- Diffusion; for example, of dopants or metallization materials in semiconductor devices, or of metals through insulators

- Radiation effects, including induced changes in bulk or surface properties of semiconductor materials and chemical changes in organic materials.

Such processes tend to lead to relatively sharply defined lifetimes for the affected parts, that is, to unimodal life distributions with small (typically, < 0.3) coefficients of variation. However, the magnitude of the modal life is likely to be very sensitive to interactions between application conditions and part design and the

low coefficient of variation is attainable only if process controls in manufacturing are stringent. Models, such as the normal distribution or the Weibull distribution with large shape parameter ($\beta > 3$, which yields results very similar to the normal distribution), are often used jointly with the exponential distribution to describe the onset of aging or wear-out effects. The problem is that extended-mission reliability estimates can be extremely sensitive to the time of onset of the effects of aging phenomena. The assumptions needed to make useful reliability estimates then become critically important; testing to assure that the onset of aging effects occurs sufficiently late will usually be necessary. Fortunately, such tests, which can usually be accelerated, can be conducted with much smaller sample sizes than those necessary to determine constant failure rates.

(From the standpoint of minimizing testing burdens, it also is worth noting that wear-out life characterization for components of complex, nonrepairable systems need not be exhaustive. Usually, the system will have failed by the time the median life for any component has been reached, thus reducing the interest in statistical details of component life distribution for longer periods. However, it may be important to know whether the wear-out failure process competes as a cause for failure for all members of a component population or applies only to a subpopulation having special characteristics, such as the presence of a contaminant or the absence of an inhibitor. Truncation of testing can lead to serious estimation errors in the latter case.)

Of the candidate failure processes identified previously, some may be ruled out by proper precautions in system design. Solid-state diffusion and insulation aging are sharply temperature-dependent and, for 10-year or shorter mission durations, can be virtually eliminated as significant failure processes if component temperatures can be held to moderate levels. Radiation effects also can be minimized if the radiation environment is moderate and/or shielding is possible. For some components, however, wear-out processes constitute potentially significant problems. A more specific discussion of these components appears to be in order.

Components subject to wear-out processes. There are at least two electronic components of candidate propulsion systems for which avoidance of significant wear-out effects may be impracticable. It happens that both components

are peculiar to high-voltage applications and are found in solid propellant pulsed plasma systems: energy storage capacitors and arc-initiation ("ignition") electrodes. Such electrodes also may be found in other plasma systems and may be subject to similar phenomena but are regarded as special cases to be discussed in the context of the systems with which they are associated.

Energy storage capacitors. Energy storage capacitors for pulsed plasma applications are required to provide un-usually high energy/weight ratios (energy densities). The capacitors described in AFRPL-TR-74-50[5] appear to be reasonably typical at 40 J/lb (2,500 volts, 50 microfarads). Energy densities as high as 125J/lb (5,000 volts, 35 micro-farads) have been offered commercially[6] but with life expectancies on the order of 3,000 discharges at full rated voltage. It is widely accepted that life expectancy for capacitors varies inversely with the fifth power of applied voltage.

High-energy densities are obtainable only with di-electrics that are thin or have high dielectric constants; current technology requires both. This limits the choice of materials and generally prevents choosing conservative derating policies (low ratios of applied voltage to rated voltage). Some high dielectric-constant materials also have relatively low maximum-temperature limits with sharply decreasing life expectancy above 50°C, making conservatism impracticable with respect to operating temperatures. In addition, some otherwise desirable dielectrics and impreg-nants are quite vulnerable to radiation. Since shielding of these capacitors is rather difficult because of their relatively large size and location near the thrusters, missions involving substantial radiation doses or rates place further restrictions on choices of materials. AFRPL-TR-74-50[6] describes a construction using a sandwich di-electric (one layer of paper between two layers of poly-vinylidene flouride, a high dielectric-constant material) and castor oil impregnant. The capacitors made by Maxwell Laboratories for Fairchild Republic Company use mylar di-electric and monoisopropylbiphenol (MIPB) as the impreg-nant, the latter substituted for silicone oil for reasons of radiation resistance[7].

There is an indication that Maxwell Laboratories lack failure rate and life data for capacitors using MIPB. One of the authors of the present report was directly involved in a major life test experiment on paper/mylar capacitors

(MIL-C-14157) using related impregnants[8]. The report
on that life test is generally unavailable but a subsequent
paper provides some of the major results and conclusions
In the absence of more recent, definitive data, a
qualitative discussion will be based on the earlier
results. The salient results of the test were:

- The capacitor life test observations could be
  described reasonably well by Weibull distri-
  butions, but with both shape and scale para-
  meters differing among manufacturers and for
  differing voltage stresses.

- In most cases, equally good or better fits to
  the data could be obtained by using mixed expo-
  nential distributions. Suspected heterogeneity
  within capacitor populations makes mixed models
  more appealing.

- Results for capacitors from one manufacturer
  are important because certain failures clearly
  involved impregnant problems and constituted a
  distinct subpopulation physically and statis-
  tically. The most satisfactory model consisted
  of an exponential distribution and a normal dis-
  tribution.

As noted previously, exponential/normal mixed models
are attractive and widely used for electronic devices
subject to wear-out phenomena. In the case of the par-
ticular capacitor life test cited, 9 percent of the capa-
citors of one manufacturer failed by case rupture when
tested at 100 percent of rated voltage and 125°C (the tem-
perature limit for mylar if phase change is to be avoided).
The remainder, and virtually all capacitors from other
manufacturers, failed electrically.

Considered separately, case-rupture failures could be
described by a normal distribution with a mean of 9,400
hours and a standard deviation of 1,400 hours.* Later
diagnosis of the case ruptures indicated gas evolution
from the impregnant as the cause. A concurrent "blind"
analysis of impregnant from new and life-tested capacitors
by infrared spectroscopy indicated bond breakage and in-
dependently predicted gas evolution. The capacitor manu-
facturer stated that an inhibitor which is customarily

See Example 3 and Figure 6 of preceding reference.

used had deliberately been reduced or omitted in manufacture of the capacitors supplied for the test.

It is not clear whether a distinct subpopulation would have existed in the absence of the specific actions reported by the manufacturer. It is also impossible to be sure that similar phenomena would not have been encountered in other capacitors at a later time (the life test was terminated at 16,000 hours). However, the results indicate that wear-out phenomena approximating normal distributions can exist, that population heterogeneity is a definite possibility, and that life limitations due to impregnant characteristics can be important within the mission durations contemplated. It remains to be considered which stresses are likely to be important, whether they can be reduced sufficiently to delay failure beyond mission requirements, and whether it is possible to devise tests that can provide the necessary data without prohibitive costs or durations.

The problem is complicated by further observations from the life test. Infant mortality is in evidence for some manufacturers at the higher voltage stresses; nonrupture wear-out modes also appear. Failure-rate discontinuities indicate that distinct failure mechanisms are operative, although no physically obvious differences were observed. Perhaps the most compelling argument favoring distinct failure mechanism lies in the differences in the effects of applied voltage:

- As already noted, the failure rate during the period of essentially "random" failures varied approximately as the fifth power of voltage

- Infant mortality failure rates typically varied approximately as the seventh to ninth power of applied voltage

- Nonrupture wear-out failure rates varied almost directly with applied voltage

- Applied voltage had little or no effect on failure rates for rupture

- For all types of wear-out failure, the time of onset of wear-out was virtually independent of applied voltage.

I-24

Clearly, increased voltage would not be useful as a way of reducing test time for evaluation of wear-out phenomena. (Applied voltage in life tests ranged from about 50 to 200 percent of rated voltage).

It remains likely that temperature constitutes a useful accelerating stress; unfortunately, the life test cited was restricted to 125°C, a temperature considerably in excess of most use conditions. The impregnant bond-breakage phenomenon held responsible for ruptures is of the kind that would be expected to follow the Eyring (or Arrhenius) equations, with the rate doubling for every 7° to 10°C increase in temperature. For the rupture phenomenon, one might anticipate an increase in mean life from 9,000 hours at 125°C to the vicinity of 3,000,000 to 40,000,000 hours at 40°C. It would, of course, be unwise to rely on such an extrapolation without exploratory testing at intermediate temperatures, although the model is supported by a large body of data involving insulation aging in electromagnetic devices.

The potential importance of radiation effects suggests their exploration through life tests also. Among a variety of possible effects, two are likely to be synergistic with heat while a third may be mitigated by elevated temperature:

- Bond breakage and bond formation (i.e., changes in polymer structure) are likely to be induced by radiation with rates that may be enhanced by available thermal energy

- Radiation may induce ionization; temperature will determine ion mobility; and electrical fields may determine the resulting damage, including the possibility of runaway electrical breakdown

- Decreases in electrical conductivity of capacitor foils and leads may be reversible by annealing at elevated temperatures.

Potential interactions such as these make it necessary to conduct tests with stress combinations. Such interactions also may interfere with attempts to use accelerated testing. Even if radiation testing can be performed in isolation, there may be difficulties due to confounding of rate and dose effects under accelerated conditions.

Arc-initiation electrodes. Arc-initiation electrodes in pulsed plasma systems are provided in the form of solid-state plugs that somewhat resemble automotive spark plugs. In an internal combustion engine, spark plugs are intended to furnish the energy needed to initiate combustion and are exposed to fuel-air mixtures and exhaust gases above atmospheric pressure. In a pulsed plasma system, igniter plugs generate ionized debris, which initiates electrical breakdown across the fuel face. The igniter plugs are exposed alternately to hard vacuum and the debris, and to remnants of a plasma derived from tetrafluoroethylene. The two devices share one failure mechanism, electrode erosion, but otherwise differ sufficiently to make relia-bility extrapolation hazardous.

It appears likely that the reliability of arc-initia-tion electrodes is largely determined by two factors:

- A low and possibly constant failure rate contri-bution due to manufacturing flaws, such as cracks in insulator bodies

- A relatively narrow wear-out type distribution reflecting electrode and surface erosion.

This conjecture concerning arc-initiation electrodes is supported by laboratory and flight experience described by the Fairchild Republic Company and the Applied Physics Laboratory of the Johns Hopkins University.

Typical applications of pulsed plasma systems involve intermittent use. This suggests the possibility of ac-celerated testing by increasing duty cycles but not to the point where effects due to temperature excursions inherent in normal use are averted. In some applications [10], dual igniter plugs have been used in an alternating mode. Where it is feasible to use such a configuration to obtain igniter plug redundancy, the time intervals for demonstrating wear-out free performance can be shortened substantially.

Summary. Analyses of applications of electronic components to advanced propulsion systems lead to the following key observations:

- It is almost always possible to generate some meaningful reliability predictions for electronic components and assemblies from available data

- Inherent variability, not just application uncertainties, makes it necessary to provide quantitative estimates of prediction uncertainties.

- The validity of such predictions is contingent upon adequate assurance that wear-out phenomena will not become dominant within anticipated mission durations. Such assurance sometimes will require application-oriented life testing. Accelerated testing techniques often may be applied with care for this purpose.

In general, electronic component failure rate uncertainties can be represented adequately by lognormal distributions whose expected value is determined from MIL-HDBK-217B, and whose coefficient of variation is a constant. Exceptions arise when the degree of standardization is low and when age-dependence of reliability is non-negligible. Examples 1, 2, and 3 contained in Appendix A illustrate the procedures to be used.

NON ELECTRONIC COMPONENT RELIABILITY AND UNCERTAINTY DERIVATION

As in the case of electronic devices, observed failure rates for nonelectronic components can be expected to deviate substantially from average values due to vendor-to-vendor and lot-to-lot variations. Additional uncertainties surround nonelectronic components for several reasons:

- Their sensitivity to application-specific efforts

- Probable existence of poorly characterized aging effects

- A generally lower degree of component standardization.

In the presence of aging or life-limiting effects of significant magnitude, it is impossible to characterize component failure rates, reliability estimates, or life expectancies by single-parameter distribution. At a minimum, two-parameter distributions, such as the normal, gamma, or Weibull (without delay), must be employed; often, a mixture of distributions representing different failure processes is appropriate. These conditions increase both model complexity and the difficulties of parameter estimation.

I-27

Earlier studies. To put these modeling and estimation problems into perspective, Table 5 displays some results derived from earlier studies of aircraft flight control components[11, 12]. These results apply to single-parameter (exponential) reliability models and do not directly address time-dependent effects; nevertheless, they provide some indication of the magnitude of uncertainties.

For each device listed in Table 5, a lognormal distribution was fitted to failure rate data (principally from FARADA). The coefficient of variation and the lower (5 percent) and upper (95 Percent) Bayesian confidence bounds were obtained from the fitted distribution. The adequacy of fit of the lognormal model was checked for device types providing sufficient data; device types providing fewer than five data points have been omitted from the table.

For the devices marked by [c], sufficient data points had been available to permit some investigation of significant time-related failure rate trends out to at least 2,500 operating hours. No trends significant from both statistical and engineering viewpoints were found. (Unfortunately, the absence of such trends in 2,500 operating hours of operation in aircraft environments will not usually justify dismissing the possibility of important time-related effects in long-duration space missions.)

It is interesting to note that the coefficient of variation tends to be lowest for components that are highly standardized, produced by a small number of manufacturers, or comparatively insensitive to application peculiarities. (The coefficient of variation used in this report for electronic components is 1.66.) However, values at the low end of the range may be illusory in view of a possible unrecognized duplication of specific device designs or applications in a relatively small data base. This does not preclude use of the data as a guide to relative variability as a function of device type.

Some additional considerations. The usual objective of component-level reliability prediction is to allow the estimation of system reliability for various mission durations or specific time intervals within a mission. Aside from modeling of relationships within the system, this requires component-level estimates for corresponding time intervals.

I-28

TABLE 5. FAILURE RATE UNCERTAINTIES[a]

Device type[b]	Coefficient of variation	Failure rate (per million hours)		
		Lower bound	Mean	Upper bound
Bolt	0.5	3.7	9.1	17.7
Regulator, tension	0.6	14.4	41.8	89
Indicator, airspeed[c]				
bomber and transport	0.74	84.3	310	739
fighter	1.37	225	2081	6660
Servomechanism, hydraulic	0.78	25.9	102	251
Bearing, ball, low speed	1.0	2.8	15.5	43.1
Accumulator, hydraulic[c]	1.25	28.34	224	689
Gyro, rate	1.3	43.6	367	1150
Actuator, electric	1.49	49.1	520	1715
Bearing, journal	1.6	1.74	21.0	71
Cable, mechanical	1.7	1.51	20.3	70
Motor, torque	1.8	2.85	42.4	149
Spring	2.1	2.43	47.9	175
Cylinder, hydraulic[c]	2.14	10.2	208	761
Bellcrank	2.4	2.64	66.6	249
Accelerometer	2.7	15.9	500	1890
Solenoid	2.8	4.03	136	519
Sheave	2.8	0.23	7.6	29.0
Filter, oil	3.0	4.28	164.2	630
Lamp	3.2	2.0	86.5	333
Tube, torque	3.2	0.53	22.8	88
Actuator, hydraulic[c]	3.52	10.82	559	2160
Switch, pushbutton	5.3	1.6	173	657

[a] For selected components, aircraft environment; fitted lognormal distributions; data from AFFDL-TR-67-20 (Table 5 and Appendix B) and AFFDL-TR-67-183 (Appendix II).

[b] Listed in ascending order of coefficient of variation.

[c] Sufficient data to indicate absence of aging effects on failure rate to 2,500 hours.

The most limited useful component-level estimate for characterizing uncertainty consists of a statement of two values for a single specific interval; for example, the expected value and a lower confidence bound on the reliability of a component for an interval beginning at 0 and ending at some time, T_O. In the absence of any additional information, the only further statements that can be made from such estimates are that the corresponding reliability estimates must be at least as high for any elapsed time ending sooner, and no higher for any elapsed time ending later. More formally, denoting the expected value of reliability for an interval beginning at 0 and ending at t is denoted by $R(t)$ and the corresponding lower bound by $R_{.05}(t)$.

$$\left.\begin{array}{l} R(t) \geq R(T_o) \\[2mm] R_{.05}(t) \geq R_{.05}(T_o) \end{array}\right\} \quad 0 < t < T_o$$

$$\left.\begin{array}{l} R(t) \leq R(T_o) \\[2mm] R_{.05}(t) \leq R_{.05}(T_o) \end{array}\right\} \quad T_o < t < \infty$$

Of course, the usual definition of reliability requires that both $R(t)$ and $R_{.05}(t)$ converge to 1 as t shrinks to 0, and to 0 as t increases without limit. However, the rate of convergence is not specified, and the limiting values are not useful in themselves.

At the other extreme, if one accepts as "known" that the applicable reliability model is the exponential distribution, $R(T_O)$ and $R_{.05}(T_O)$ are sufficient to determine the estimates of $R(t)$ and $R_{.05}(t)$ for all values of t. This occurs because the expected value and upper confidence bound on the failure rate have one-to-one relationships with the T_O reliability estimates. This condition does not hold for distributions specified by two or more parameters. For example, there is an unlimited number of μ, σ pairs yielding any specified value of $R(T_O)$ for the normal distribution but with differing values of $R(t)$ for $t \neq T_O$.

A variety of intermediate situations can be postulated, each implying certain kinds and amounts of information or a willingness to place restrictions on the form of the

reliability model. For example, one may be willing to stipulate that a Weibull distribution with known and fixed shape parameter applies because this model and parameter value are "known" to apply to the class of components under consideration. Another fairly common type of intermediate situation is one in which a great deal is considered "known" to apply to the class of components under consideration. Another fairly common type of intermediate situation is one in which a great deal is considered "known" for $t \leq T_O$ and very little is "known" for $t \geq T_O$. This would be the case when the failure process(es) to T_O can be determined from observation; however, a subsequent wear-out phenomenon due to other processes is anticipated.

Procedures. Since the ultimate use of component-level reliability prediction will be in the derivation of system reliability estimates, it is desirable to anticipate the requirements of the latter. The system reliability models that will be used are based on combinatorial calculations, propagation of variance, and beta distribution models for reliability uncertainties at component and higher assembly levels. This implies a requirement for estimation of component reliability expectations and uncertainties for any selected time within the intended mission duration.

For system reliability estimation purposes, the beta distribution model for each component at each selected time must be defined. It is possible to fit a beta distribution to any two fractiles, central measures, or moments (e.g., mean and variance) of a reliability uncertainty distribution derived from other sources. In general, it is not possible to obtain a beta distribution that exactly matches another distribution, such as one derived from a lognormal uncertainty distribution of failure rates over the range of possible values. However, a very good match over the range of maximum interest -- from the fifth percentile to the expected value -- can be obtained by making the distributions congruent at the fifth percentile and at the median. Further discussion of the beta distribution is provided in Appendix B.

If the form of the component life distribution is "known" and has a single uncertain parameter (e.g., the constant failure rate in the exponential distribution or the scale parameter of the Weibull distribution), that life distribution can be evaluated at any selected time, t, and for any desired points in the uncertainty distribution. For example, assume that the exponential distribution

I-31

describes component life and that the failure rate (per
million hours) is described by a lognormal uncertainty
distribution with mean natural logarithm 2.28 and logarith-
mic standard deviation 1.2. Then the median and 95th per-
centile failure rates (rounded to one decimal place) are:

$$\lambda_{.5} = e^{2.28} = 9.8 \text{ per } 10^6 \text{ hours}$$

$$\lambda_{.95} = e^{2.28+1.97} = 70.4 \text{ per } 10^6 \text{ hours.}$$

Since fractiles hold in transformation, we may evaluate
the median and 5th percentile of the reliability uncer-
tainty distribution directly for any value of t. For
t = 2,000 hours, the results are:

$$R_{.5} = e^{-2,000 \times 9.8 \times 10^{-6}} = 0.981$$

$$R_{.05} = e^{-2,000 \times 70.4 \times 10^{-6}} = 0.869.$$

Consider the alternative that the observations on which
reliability estimates are to be based involved a 5,000-
hour exposure of the components and led to the conclusion
that:

$$R_{.5}(5,000) = 0.5$$

$$R_{.05}(5,000) = 0.25.$$

How can these conclusions be translated to uncertainty
distributions for time intervals other than 5,000 hours?
In general, estimation procedures will need to be dif-
ferent for intervals ending earlier than the 5,000-hour
observation time and for those ending later.

     One possibility involves a willingness to attribute
a particular life-distribution form with fixed parameters
to the median ($R_{.05}$) only. Estimation of the median of
the uncertainty distribution then involves merely the sub-
stitution of the desired values of t. The alternative is
to draw a smooth curve connecting the starting point (0,1)
with the observed point (5,000, 0.5), choosing a curve

shape that is consistent with the evaluation of failure processes involved (e.g., with an increasing failure rate). In either case, it is extremely important to bear in mind that:

- The component under consideration usually will be only one of many components in a system

- Time intervals for which the system reliability is low are not of interest if the system is nonrepairable

- Reliability of the component will need to be quite high if the system reliability is not so low as to be uninteresting, unless the component is used in a highly redundant configuration

- The important component reliability estimation region (the important part of the life distribution), therefore, usually will be one in which the predicted reliability is well in excess of 0.9.

These observations have two major implications. One is that $R_{.5} = 0.5$ is a poor choice for a starting point; a value on the order of $R_{.5} = 0.9$ would be much more suitable. (In practice, it also is much more likely to be available for the long-lived components of interest.) The other implication is that essentially we are dealing with tail behavior of life distributions, which reduces both the dependability of, and the sensitivity to, distributional forms and parameters. Dependability is reduced because extreme tail behavior usually is determined by outliers rather than by the main population; if not, tail behavior is often very sensitive to distribution parameters. Sensitivity is reduced by convergence. This point may be illustrated by examining a fairly wide variety of distributions in an example shown in Table 6, all having the value $R(40,000) = 0.9$ in common:

TABLE 6 . EXAMPLE: DISTRIBUTION WITH COMMON R(40,000)

Form	Condition for $R(40,000) = 0.9$	Parameters
Exponential	$.105361/\lambda = 40,000$	$\lambda = 2.634 \times 10^{-6}$
Weilbull	$(.105361\alpha)^{1/\beta} = 40,000$	$\beta = 0.5, \ \alpha = 1,898$

Table 6 (continued)

Weilbull $\quad (.105361\alpha)^{1/\beta} = 40,000 \quad \beta = 2 \quad , \alpha = 1.5186 \times 10^{10}$

Weilbull $\quad (.105361\alpha)^{1/\beta} = 40,000 \quad \beta = 4 \quad , \alpha = 2.4297 \times 10^{19}$

Normal $\quad \mu - 1.28\sigma = 40,000 \quad \mu = 60,000, \sigma = 15,625$

Normal $\quad \mu - 1.28\sigma = 40,000 \quad u = 80,000, \sigma = 31,250$

Normal $\quad \mu - 1.28\sigma = 40,000 \quad \mu = 100,000, \sigma = 46,875$

For this example shown in Table 6, the reliability values at four lower ages and one greater age are tabulated:

TABLE 6 . EXAMPLE: DISTRIBUTION WITH COMMON R(40,000)
(Continued)

Distribution	R(5000)	R(10,000)	R(20,000)	(R30,000)	R(80,000)
Exponential					
2.634×10^{-6}	0.9869	0.9740	0.9487	0.9240	0.8100
Weibull					
0.5, 1898	0.9634	0.9477	0.9282	0.9128	0.8616
2, 1.5186×10^{10}	0.9984	0.9934	0.9740	0.9425	0.6561
4, 2.4297×10^{19}	0.99997	0.9996	0.9934	0.9672	0.1853
Normal					
60,000, 15,625	0.9998	0.9993	0.9948	0.9726	0.1000
80,000, 31,250	0.9918	0.9875	0.9726	0.9452	0.5000
100,000, 46,875	0.9786	0.9726	0.9561	0.9323	0.6652

The differences displayed in Table 6 are far from trivial. Selecting the most appropriate distributional models therefore is important. For ages less than the common point, however, relatively little added observational information is needed for adequate parameter estimation if the appropriate distributional form has been selected.

If the additional information is substantial, even the choice of distributional form may not be too critical. If, for example, we know that R(10,000) = 0.99 as well as R(40,000) = 0.9, the parameters of a Weibull distribution model are fixed at $\beta = 1.695$, $\alpha = 5.996 \times 10^8$, and for a

normal distrubution model $\mu = 76,570$, $\sigma = 28,570$. The single-parameter exponential distribution cannot be fitted to the two known points. If we are willing to consider the two-parameter version (exponential distribution with delay or guarantee time), we find $\lambda = 3.177 \times 10^{-6}$, $\alpha = 6,840$. These models yield the values presented in Table 7.

TABLE 7. TWO-POINT FITTED DISTRIBUTIONS

Distribution	R(5000)	R(10,000)	R(20,000)	R(30,000)	R(80,000)
Exponential w/delay 3.177×10^{-6}, 6,840	1.0000	0.9900	0.9591	0.9291	0.7926
Weilbull 1.695, 5.996×10^{8}	0.9969	0.9900	0.9680	0.9374	0.7110
Normal 76,570, 28,570	0.9939	0.9900	0.9762	0.9485	0.4522

The results displayed in Table 7 serve to illustrate an important and obvious, but often neglected, point: Any reasonable distributional model fitted to observed data can provide a good description within the range of observations (in the example, for ages up to 40,000 hours), but extrapolation beyond the range of observation is strongly dependent on the model chosen. Furthermore, the existence of a good observational fit does not guarantee model validity. Thus, it is concluded that extrapolation is risky even when no new failure processes need to be anticipated at greater component ages, and that the choice of the life distribution model usually needs to be supported by information beyond that available from fitting of curves to observational data. In general, that information comes from insight into manufacturing process variations and failure processes or from knowledge about the long-term behavior of related devices.

Selection of a suitable life distribution model for R.5(t) must be accompanied by the choice of a corresponding model for R.05(t) or for some other measure of reliability estimation uncertainty, unless, as discussed previously, there is sufficient faith in distributional form and parameters (e.g., exponential with λ .95) to permit direct evaluation. One difficulty that should be noted immediately arises from the fact that life distributions from the same family generally cross unless some restrictive conditions

are met. Two Weibull distributions with parameters α_1, β_1; α_2, β_2,   will cross at

$$t = \left(\frac{\alpha_1}{\alpha_2}\right)^{\frac{1}{(\beta_1 - \beta_2)}}$$

unless $\beta_1 = \beta_2$, while two normal distributions will cross at two values of t unless $\mu_1 = \mu_2$, when $R(\mu_1) = R(\mu_2) =$ 0.5. Unless the crossings occur outside the time period of interest, $R_{0.5}(t) > R_{.5}(t)$ for some range of t. In addition to this illogical inversion, there will be understatement of uncertainty as the crossing point is approached. Modifications of models may be necessary if $R_{.05}(t)$ is to be handled in life-distribution form.

Alternatively, one may address the uncertainty distribution or the relationship between R.05(t) and R.5(t) directly. This approach also presents some problems. As an example, consider the observation R.5(5000) = 0.9032, $R_{.05}(5000) = 0.7499$. Attributing the exponential distribution to $R_{.5}(t)$ yields $R_{.5}(2005) = 0.96$. Suppose we choose to model the uncertainty about R(t) by a beta distribution.* The beta distribution having $R_{.5} = 0.9032$ and $R_{.05} = 0.7499$ has the parameters $\alpha = 15$, $\beta = 1$.+ From a Bayesian viewpoint, the sum $\alpha + \beta$ can be interpreted as an "equivalent" sample size; that is, it would characterize all possible posterior distributions derivable from go-no go testing of a sample of size $\alpha + \beta$ and the uniform beta prior distribution with $\alpha_0 + \beta_0 = 0$. On the grounds that any "test" yielding 15 successes and 1 failure as of 5,000 hours would have been observable in principle at any earlier time with sample size 16, one may argue in the absence of any other information that $\alpha + \beta = 16$ should apply to the uncertainty distribution used to describe information at any lesser age. It happens that $R_{.5} = 0.96$ is the median of the beta distribution with $\alpha = 16$, $\beta = 0$, and for that distribution, $R_{.05} = 0.8384$.

---

*A detailed discussion of this convenient model is presented in Appendix B.

+There are two common notations for the beta distribution; the notation used here corresponds to $f(R) = \dfrac{\Gamma(\alpha+\beta+2)}{\Gamma(\alpha+1)\Gamma(\beta+1)} R^{\alpha}(1-R)^{\beta}$.

In order to determine if the value of $R_{.05}(2005)$ is consistent with the available information and/or intuition, one possibility is to seek to define a reasonable life distribution that yields $R_{.05}(2005) = 0.8384$, $R_{.05}(5000) = 0.7499$. These values are satisfied by a Weibull distribution with $\beta = 0.5766$, $\alpha = 335.81$ (not to be confused with the similarly labeled parameters of the beta distribution). This is an increasing failure-rate distribution, implying that the uncertainty attached to the 2,005-hour reliability estimates is larger than would be the case if we were willing to attribute the exponential distribution to $R_{.05}$ as well as to $R_{.5}$. That approach would yield $R_{.05}(2005)= 0.981$. In many cases, the implied increase in uncertainty for interpolation would be acceptable as being in accord with intuition and available information, but the judgment should be made on a case-by-case basis after examining the implications. For example, the model would be inappropriate if additional, contradictory evidence were available from a separate 2,500-hour test.

(It should be evident that the process of reliability and uncertainty estimation involves ad hoc procedures and subjective judgment. This approach is not at all inconsistent with the Bayesian approach but probably is unacceptable to the statistician with a "classical" inclination. Unfortunately, he is powerless to deal with the problem in any practical way.)

There remains the problem of extrapolation to component ages beyond the observed data coverage. Statistical theory provides no information other than the absolute requirements that any reliability function be monotonically nonincreasing and tend to 0 as age approaches infinity. General experience adds to this that reliability functions are smooth (i.e., continuous). It is necessary to look elsewhere for useful reliability estimates.

The act of choosing life distribution models within the span of observable data and information implies some belief that the models relate to the physical processes that lead to device failure. The degree of belief will vary and will be reflected in the uncertainty models chosen. It follows that the first step in extrapolation involves two questions:

- Is it reasonable to expect the same physical processes to continue?

● How rapidly does uncertainty about the validity
of the life distribution model or its parameters
increase?

The first question is related primarily to the life
distribution model; the second, to the uncertainty dis-
tribution model. (Continuity and monotonicity are not re-
quirements for the latter; it is quite reasonable to
specify increasing uncertainty as one moves away from a
"known" point in either direction.)

The answer to the first question almost always will
be affirmative. However, a further question must be asked:
Are there additional failure processes (or changes in im-
pact of the same failure processes) that may become signi-
ficant during the time interval to be considered in the
extrapolation? For example, frictional wear may be the
predominant failure process reflected in the life distri-
bution model. At greater component ages, wear may con-
tinue, but fatigue may become the primary failure process.

Thus, extrapolation must rely entirely on knowledge,
analysis, and judgment, in the domain of engineering and
the physical sciences; statistical methods serve only to
describe the results with one exception. The purpose of
reliability prediction and estimation of uncertainties is
to aid in decisionmaking, and Bayesian statistical methods
are closely related to decision theory, especially to the
notion of loss functions. The choice of models may be in-
fluenced by the consequences to be expected from decisions
that formally rely on the models. Most importantly, the
models should be used to decide how to allocate limited
test resources among tests of the components of a proposed
system to maximize information gain (uncertainty reduction),
a topic addressed in the description of computer program
BETAL1 in the Computer Program Section of this report.

Component Reliability Derivation. Analysis of the data
base revealed an exclusive use of single parameter con-
stant failure rate component reliability expressions.
Furthermore, the single parameter was almost always mis-
sion time. While this uniformity of approach was very
attractive, especially when aggregation to the systems
level was intended, it was not the most descriptive of
the components, their duty cycles, or their operating en-
vironments.

The approach employed in developing this methodology was the individual assessment of each component and letting that assessment determine the type of failure rate to be employed and the parameter or parameters to be used in the model. As can be expected, with the broad range of components, the result of this approach was a diverse collection of models. However, it decided to proceed along these lines, developing the more complex aggregating techniques requiring rather than artificially constraining the component level models in the interest of methodology simplicity.

The derivation process can be characterized by the following steps:

- Component assessment in the context of its system application

- Structuring the component reliability model

- Model quantification

- Model verification

- Failure mode modeling.

Component Assessment. Rather than impose generalization across systems, each component was assessed within the context of its system application. While this required multiple assessments of similar components, it yielded generalized component models based on demonstrated similarities rather than a priori assumptions. These assessments identified the principal failure modes, mechanisms, and the parameters to which component reliability seemed sensitive.

Structuring the Component Reliability Model. The results of the foregoing assessment were converted next into discrete expressions. Some failure mechanisms (such as manufacturing flaws) implied random failure situations which were best modeled by constant failure rate models. Others (such as erosion, wear, or compaction) implied increasing failure rate situations. The Weibull model was used to model these situations. Several components exhibited mechanisms of both types. These were modeled using a composite expression containing constant failure rate and increasing failure rate contributions.

While failure rates and types are of obvious impor-
tance, a second equally important consideration is the
variable upon which they are dependent. These, too, were
identified in the assessment process and were included in
the modeling process. Typically, these parameters were
number of cycles, operating time, and mission time. Exam-
ples of the resulting models are shown below.

Constant Failure Rate, Simple   (Fill Valve)

$R = \exp(-\lambda t)$ Where t=elapsed mission
                                                 time

Constant Failure Rate, Compound   (Relief Valve)

$R = \exp[-\lambda_m t - \lambda_c N]$ where t=elapsed mission
                                                 time
                                                 N=Number of cycles

Increasing Failure Rate, Simple   Electric Isolator)

$R = \exp\left[-\dfrac{t^\beta}{\alpha}\right]$ where t=elapsed mission
                                                 time
                                                 α=Weibull scale
                                                 parameter
                                                 β=Weibull shape
                                                 parameter

Increasing Failure Rate, Compound   (Catalyst Bed - Steady State)

$R = \exp\left[-\dfrac{N^2}{\alpha_{ns}} - \dfrac{n^3}{\alpha_s} - \dfrac{t^2_{ss}}{\alpha_s}\right]$ where N=number of steady
                                                 state firings
                                                 n=number of cold starts
                                                 t_{ss}=steady state oper-
                                                 ating time

Composite Model   (Filter)

$R = \exp\left[-\lambda t_m - \dfrac{t_{op}^{1.5}}{\alpha}\right]$ where t_m=elapsed mission
                                                 hours
                                                 t_{op}=operating hours

Uncertainty distribution modeling presented a situation requiring a different approach. Component failure rate data was too sparse to directly identify the type of distribution that would best characterize failure rate's variability. Rather than rely simply on judgment, previous experience suggested a simplifying alternative. It has been found, almost universally that the uncertainty distribution of a generic failure rate is skewed to the right. Values much larger than the expected value are more likely to occur than values correspondingly smaller. This is also in accord with intuition; a failure rate much worse than the generic mean seem. more likely to be observed than one that is much better. Good fits to the log normal distribution, which corr· ponds to this behavior, have been found to be common. This distribution was assessed against all available failure rate data on a component by component basis. It was found that this distribution could be used in the uncertainty distribution to characterize the reported variability in all but a few component failure rates. The exceptions were best modeled using a normal distribution.

Model Quantification. Assigning values to the model parameters was the next step in the development process. Available data provided overall component failure rates. With the exception of valves there was virtually no partitioning of failure rates to failure modes. A second problem was the exclusive use of constant failure rate models for all components in previous reliability assessment efforts. Moreover, virtually all used mission time-related failure rates; only a few developed cycle-or pulse-dependent failure rates. Finally, for some of the more novel propulsive systems, virtually no failure rate data was available on a large number of components. For these items, the failure rates employed were derived from analogous component/environment situations for which data was available. In addition, significant extrapolation was required to bridge the gap between the documented endurance tests and the long mission durations (> 5 yrs) of interest. In short, the process of model quantification was far from a rigorous statistical exercise. Extensive use of engineering judgments was required to yield usable component reliability models. As can be expected, the uncertainty involved in these judgments is relatively high. This situation further underscored the need for tracking the uncertainties associated with the reliability estimating procedures. As the experience base grows with additional test and in service use and more explicit failure rates are identified, this uncertainty can be expected to decrease.

Two procedures used in the model quantification process are worth highlirhting. The first involved the adaptation of reported constant failure rate data for use in models involving Weibull expressions. Two judgments were required by the process: first, an estimate of the point when the failure rate would begin to increase, and second, an assessment of the Weibull shape factor. The shape factor strongly influences the severity of the slope of the increasing failure rate. With these two estimates, the constant failure rate model and the increasing failure rate (Weibull) model could be equated and the Weibull scale factor could be determined. That is, the reliability model using constant failure rate is expressed as:

$$R = \exp_1\left[-\lambda x\right]$$ where λ = constant failure rate

    x = parameter upon which
        reliability is dependent

    (such as operating time,
    flight time cycles, etc.)

and the increasing failure rate (Weibull) model is given as:

$$R = \exp\left[-\frac{x^{\beta}}{a}\right]$$ where x = parameter upon which
        reliability is dependent

    β = Weibull shape factor

    a = Weibull scale factor

At that value of x where the failure rate λ begins to change, both models will yield the same estimate of reliability. If this value and the value of β (characteristically between 1 and 3) are estimated, the Weibull scale parameter can be found directly:

This approach was used in conjunction with the procedure used to transition from constant to increasing failure rate models. For components evidencing a strong design sensitivity to expected mission life, the transition point to increasing failure rate was defined as a percent of the design life rather than a fixed number of hours or cycles.

I-42

$$R = \exp\left[-\lambda x^\circ\right] = \exp\left[-\frac{x^{\circ\,\beta^\circ}}{a}\right]$$

where x° = the value of x where
is expected to change

β° = the estimated value of
the shape factor

taking the logarithms,

$$\lambda x = \frac{x^{\circ\,\beta^\circ}}{}$$

$$= \frac{x^{\circ\,\beta^\circ}}{\lambda x^\circ}$$

$$= \frac{x^{\circ\,\beta^\circ} - 1}{\lambda}$$

The second procedure involved the introduction of component design life into the reliability model. The design of some components is relatively insensitive to operating life. Whether the planned use calls for one thousand or one million operating hours or cycles, the component design is virtually the same. Other components, typically those prone to corrosion, erosion, wear, fatigue, etc., have their design strongly tailored to the expected mission life. For these components it would not be appropriate to extrapolate conditions in evidence at the end of one year's use. This would be simply unrealistic. If a 5-year mission were anticipated, then a component designed for this expected life would have been used. Where comparison of two components (such as the 1- and 5-year designs) was desired, comparisons were based upon service life as a percent of design life, for example, suppose an estimate of conditions is desired after 4 years on a component designed for 5-year life. The data base available for assessment is drawn from a similar component designed for 1-year life. Rather than simply extrapolating from the available data, examination of conditions at the four-fifths or 80 percent design life of the 1-year component should be made. The results of this assessment form a more realistic estimate of what might be expected after 4 years of the operation of a component designed for 5 years life. This approach was used in conjunction with the procedure used to transition f.om constant to increasing failure rate models. For components evidencing a strong design sensitivity to expected mission life, the transition point to increasing failure rate was defined as a percent of the design life rather than a fixed number of hours or cycles.

Two types of partitioning readily identified them-
selves in this modeling process. The first was one where
the failure modes and portions of the component model
aligned themselves on a one-to-one basis. The second re-
quired subdivision of component model elements in order
to generate the failure mode model. These situations are
best described by the following examples.

Example 1. One-to-One Correspondence

Component: Filter

Model: $R = \exp\left[-\lambda t \dfrac{-t_{op}{}^{\beta}}{\alpha}\right]$

Fail Modes: Leaking, Clogging

Partitioning:

Leaking Mode $\qquad R = \exp(-\lambda t)$

Clogging Mode $\qquad R = \exp\left[\dfrac{-t_{op}{}^{\beta}}{\alpha}\right]$

Example 2. Component Model Subdivision

Component: Isolation Valve (Normally Closed)

Model: $R = \exp\left[-\lambda_c N - \lambda_m t\right]$

Failure Modes: Fail Open, Fail Closed, Fail Partial, Leak
to space

Failure Mode Frequency: Based on data base and judgment

Mode	Frequency	Factor by Failure Rate	
		λ_I	λ
Open	10%	$K_o = .1$	$K_o{}^c = .1$
Closed	30%	$K_c = .3$	$K_c = .3$
Partial	55%	$K_p = .55$	$K_p = .6$
Leak to Space	5%	$K_l = .05$	$K_l = 0$

The final step in the component reliability modeling process was the quantification of the uncertainty distribution. As mentioned earlier the log normal distribution would be used throughout. The variability in reported failure rates evidenced by each component was used to tailor the log normal distribution to reflect the uncertainty associated with that particular component's reliability expression. The log normal distributions were characterized by specifying the coefficient of variation and the mean. Wherever possible these parameters were determined directly from the reported failure rates for the component. Where no failure rates or a few divergent estimates were available, judgment once again had to be relied upon to yield credible and realistic results.

Model Verification. Upon completion of the component reliability model development, a request for comments was initiated. The models, supporting rationale, and other descriptive material were submitted to 26 selected Government and industry organizations representing a cross section of auxiliary propulsion system designers, developers, manufacturers, prime contractors and user agencies.

The responses, received from more than half of the addressees, were very useful in refining the methodology. There was general agreement with the approaches taken and the results achieved. Where differences existed alternatives were always suggested. Almost all suggestions were incorporated in the refinement process. Since analogous component/environment combinations were often used in developing component models, it was found that alternative analogs were especially useful. A second major outcome of this process was the completion of the model generalization process. Component models were initially generated by assessing each component within the context of its system application. While generalizations were suspected, it was considered preferable to have these generalizations result from demonstrated similarities in the models and from concurrence in the review process. As a result of this review it was possible to replace the seven systems categories of components with two: electric propulsion systems components and thermochemical propulsion systems components.

Component Model Partitioning. The component level analysis yielded nearly sixty reliability models. Because of the limitations of the available data, subdivision of these

models to the failure mode level was conducted on a selective basis. Indiscriminate (and, for lack of definitive data, often arbitrary) partitioning to the failure mode level would have introduced undesirable increases in system level uncertainty without increasing understanding of component or system reliability behavior.

Approach to Component Model Partitioning. Fault tree requirements were used as the partitioning criteria. Components often appeared in several places in a system fault tree each time reflecting a different failure mode. For example, under a fault tree portion entitled "Propellant Flow Too Low" a number of valves appeared as failing closed or partially open. In another portion of the same tree "Propellant Flow Too High", the same valves appeared as failing open or leaking to space. Neither situation required the entire failure model but rather some subdivision. In these cases partitioning to component failure modes was conducted.

Partitioning Techniques. Review of the available component models produced two readily identifiable partitioning techniques, direct and K-factor.

The direct method was used in those cases where a one to one relationship existed between a failure mode and a portion of the component model. For example, the developed filter model was:

$$R = \exp\left[-\lambda t - \frac{t_{op}^{\beta}}{\alpha}\right]$$

where λ = constant failure rate dependent on mission time

β, α = increasing (Weibull) failure rate parameters dependent on operating time, t_{op}

The identified failure modes were clogging and excessive flow (due to leakage or fracture). The clogging mode failure rate was assessed as increasing with increasing filtration (that is with increasing operating time) and the leakage mode failure rate as being constant throughout the mission. This resulted in a direct partitioning of the model. The model for the clogging mode became:

$$R = \exp\left[\frac{-t_{op}}{\alpha}\right]$$

and the model for leaking became

$$R = \exp(-\lambda t)$$

I-46

Other component types (principally valves) had failure modes that reflected part of each of the model constituents. Partitioning factors (k factors) had to be developed in these cases to subdivide the model. For example the latch valve model was formulated as

$$R = \exp\left[-\lambda_c N - \lambda_f t\right]$$

where λ_c = failure mode per cycle
N = number of cycles
λ_f = failure mode per mission hour
t = mission hours elapsed

The identified failure modes for this valve were fail open, fail closed, fail partial, and leak to space. A simple breakdown was not possible in this case. Both number of cycles and elapsed mission time influenced the failure modes and had to be so reflected. The result was the following matrix

Mode	K-factor	λ_c	λ_f
Fail Open	K_D	.1	.1
Fail Closed	K_C	.3	.3
Fail Partial	K_P	.55	.6
Leak to Space	K_L	.05	.0

The values of the K factors were developed from what ever partitioning information was available (principally from the GIDEP source) and judgment in application to the component/environment situation. They were then applied to the expected value of the failure rate, $E\{\lambda\}$. [The expected value $E\{\lambda\}$ was the parameter obtained from analysis of the data base.] The procedure was as follows. For the Fail Open mode:

$$E\{\lambda_{CO}\} = K_O E\{\lambda_c\}$$

where $E\{\lambda_{CO}\}$ = expected value of the cyclic failure rate in in the fail open mode.
K_O = K factor determined for the fail open mode.
$E\{\lambda_c\}$ = expected value of the component model cyclic failure rate.

I-47

The variance of the failure rate (a basis for uncertainty about the component results) must also be carried to the failure mode level:

$$V \{\lambda_{CO}\} = K_O V \{\lambda_C\}$$

where $V \{\lambda_{CO}\}$ = is the variance of the expected value of the cyclic failure rate in the open mode
= the open mode
$V \{\lambda_C\}$ = is the variance of the component model cyclic failure rate.

The following development of uncertainty parameters will deal with the cyclic failure rate in the open mode, only so the subscript "CO" will be dropped for clarity.

The coefficient of variation, η, for the log normal distribution characterizing the failure mode is given by

$$\eta = \frac{\sqrt{V \{\lambda\}}}{E \{\lambda\}}$$

where $V \{\lambda_{CO}\}$ and $E \{\lambda_{CO}\}$ were defined above.

The standard deviation, σ for the required lognormal distribution can be obtained from

$$\eta^2 = \exp[\sigma^2] - 1$$
$$\sigma = \sqrt{\ln(\eta^2 + 1)}$$

The mean of the distribution, μ, is given by

$$E \{\lambda\} = \exp\left(\mu + \frac{\sigma^2}{2}\right)$$

or

$$\mu = \ln[E \{\lambda\}] - \frac{\sigma^2}{2}$$

The median and the bounds on the cyclic failure rate in the open mode follow:

. Median

$$\lambda_{.5} = \exp(\mu)$$

I-48

- 5% Lower Bound (L.B.)

$$\lambda_{.05} = \exp[\mu - 1.64485\sigma]$$

- 95% Upper Bound (U.B.)

$$\lambda_{.95} = \exp[\mu + 1.64485\sigma]$$

This process was then repeated for the cyclic failure rate in the closed mode, partial mode and leak mode and for the flight time failure rate in applicable modes to complete the characterization at the failure mode level.

SYSTEMS RELIABILITY ESTIMATION

At this point in the development of the methodology, reliability (and uncertainty) models for all the required components had been formulated and quantified. What was required at the system level was a framework to:

- Describe the systems and identify the appropriate component models required by each.

- Provide the system specific logic network to allow for proper model aggregation.

Alternative Approaches. The most common approaches to the analysis and description of component/system relationships are failure modes, effects and criticality analysis (FMECA) and fault tree analysis (FTA). FMECA displays are in tabular form, and are usually accompanied by reliability block diagrams to aid understanding and to facilitate construction of mathematical reliability models. FTA analyses and displays are in logic-diagram form, so that the equivalent of a reliability block diagram is inherent.

FTA can be characterized as a "top-down" approach; the principal thrust is successive definition of all conceivable failure events at the system level, the subsystem level, and on down to the component failure mode level. FMECA is "bottom-up" and is conducted principally in the inverse order by identifying component failure modes and tracing their consequences up through the system.

In principle, the results of FTA and FMECA should be equivalent; experienced analysts frequently alternate between top-down and bottom-up modes in the process of analyzing a system.

Selection Rationale. The FTA approach was selected as the framework for the systems level assessment. Its principal advantages included:

- Display of functional relationships among system elements in a graphic form readily understood by engineers and analysts.

- Ready assimilation and application by systems analysts

- Ready isolation of similarities and differences among competing system configurations

- Easily converted into algebraic models

- Development of a fault tree need be carried down only to the level at which failure rate information is available.

With respect to the last item, the fault trees presented in the results section of this report were developed beyond the available failure rate information. The analysis was continued in this manner to reflect qualitative failure mode information and to accommodate failure rate data (or assessments) that may result from on-going testing and developmental efforts.

A further advantage was realized by emphasizing functional (system-oriented rather than hardware oriented) failure-event definitions in the upper levels of the fault trees. This yielded upper portions of the trees that could be common to a number of alternative system configurations. (Lower portions of fault trees are inherently applicable to specific components types regardless of usage). Fault tree modification to represent an alternative system configuration would then entail major changes only in the intermediate levels of the tree. This implied reduced effort for multiple analyses, and thus, greater flexibility.

The results of this reliability modeling study are
three fold: the component and failure mode reliability
models, the systems analyses using the fault tree framework
and the mathematical tools developed to support the assess-
ment process. Examples of methodology application are pro-
vided in Appendix A.

COMPONENT RELIABILITY MODELS

The total number of models developed including failure
mode partitioning was nearly one hundred. This was an un-
wieldy number for presentation in tabular form. Therefore,
the following uniform format was used for each component.

Component Title and Description. The component was identi-
fied and a brief description of the approach used and the
applicable failure modes was provided.

Component Reliability Model. The component level reliability
model was presented and all the parameters defined.

Failure Rate Uncertainty Distribution Model. The distribu-
tion was identified and its principal parameters (coefficient
of variation, mean and standard deviation) were quantified.
For cases where multiple failure rates were present in the
model, uncertainty model parameters were developed and pre-
sented for each rate.

It must be noted that the failure rate uncertainty
distribution model can be applied directly to constant
failure rates, λ , only. For those models using increasing
failure rates, the uncertainty distribution is implicitly
presented through the upper and lower bound values of α and
its equivalent mean and median.

Failure Rate Mean and Bounds. The 5% Lower Bound, Median,
Mean and 95% Upper Bound are presented for each of the
failure rates, λ , (or scale factors, α , in the component
model.

Partition by Failure Modes. For each of the identified modes,
the model, the failure rates (or scale factors) and the Mean
and Bounds are given in the format used at the component
level.

I-51

ELECTRIC PROPULSION COMPONENTS
RELIABILITY MODELS

INDEX TO ELECTRIC PROPULSION
RELIABILITY MODELS

As stated in preceding sections of this report the piece part approach MIL-HDBK 217B was used in assessing the reliability of electronic assemblies. This approach used without modification yields simply point estimates of failure rates. Since it is known that actual failure rates vary significantly the resulting uncertainty surrounding the point estimate had to be addressed. From the arguments presented in the Electronic Components and Assemblies Section, the log normal distribution with coefficient of variation $\eta = 1.655$ was chosen to model the uncertainty at the component level.

Aggregation of this uncertainty to the PCC level followed the following process:

1. Determination of component variance - From the MIL-HDBK 217B assessment the expected value of the component rate $E\{\lambda\}$ was obtained. The variance was calculated using the relationships

$$V = \eta^2 E^2 \{\lambda\} \qquad \text{and as discussed above}$$

$$\eta = 1.655,$$

$$V = 2.74 \, E^2 \{\lambda\}$$

2. Variance Aggregation. This process followed two paths. For identical components

$$\text{Total } V = (V_i)^n$$

For dissimilar components

$$\text{Total } V = \sum_{c=1}^{n} V_i$$

Representation of the PCC level failure rate and variance in the form chosen for other components used the same relations set forth at the start of this section. Uncertainty distribution parameters were given by

$$\eta_{PCC} = \frac{\sqrt{V_{PCC}}}{E\{\lambda_{PCC}\}}$$

$$\sigma_{PCC} = \sqrt{\ln(\eta_{PCC} + 1)}$$

$$\mu_{PCC} = \ln\left[E\left\{\lambda_{PCC}\right\}\right] - 1/2 \ \sigma^2_{PCC}$$

Failure rate bounds and central measures were obtained from

$$\text{Median} = \quad \lambda_{.5} = \exp(\mu_{PCC})$$

$$5\% \text{ Lower Bound} = \quad \lambda_{.05} = \exp\left[\mu - 1.645\,\sigma\right]$$

$$95\% \text{ Upper Bound} = \quad \lambda_{.95} = \exp\left[\mu + 1.645\,\sigma\right]$$

The results presented for the Cesium Ion, Colloid and Pulsed Plasma PCC were obtained by analysis of available parts lists of the system (13, 14, 15); grouping of parts by subassemblies was available only for the Pulsed Plasma System (Ref 7). Therefore, only this system shows entries in the fault tree below the PCC level.

The results shown for the Mercury Ion PCC are taken from a recently completed study performed by Hughes Research Lab for Lewis Research Center (Ref 16). While parts lists were not available for this study, the results presented in Ref 16 were obtained using the MIL-HDBK 217B approach. This satisfied our requirement for $E\{\lambda_{PCC}\}$ but left no direct method for assessing the variance associated with $E\{\lambda_{PCC}\}$. Since the Cesium Ion System is also an Electron Bombardment Ion System, with similar thrust levels and mission profiles, the variance calculated for that PCC was arbitrarily assigned to the Mercury Ion PCC.

(PCC (Mercury Ion System)

Component Reliability Model

$$R = \exp(-\lambda t) \qquad \text{where } t = \text{mission time}$$
$$\text{(elapsed mission hours)}$$

Failure Rate Uncertainty Distribution Model

    Log Normal

    Coefficient of Variation $\eta = 2.341$

    Mean $\mu = -15.61$

    Standard Deviation $\sigma = 1.367$

Failure Rate Mean and Bounds

5% Lower Bound	Median	Mean	95% Upper Bound
$\lambda_{.05}$	$\lambda_{.5}$	$E\{\lambda\}$	$\lambda_{.95}$
0.0175	0.166	0.422	1.57

$$x\ 10^{-6} \text{ per hour}$$

PCC (Cesium Ion System)

Component Reliability Model

    $R = \exp(-\lambda t)$ where t = mission time

Failure Rate Uncertainty Distribution Model

    Log Normal

    Coefficient of Variation $\eta = 0.915$

    Mean $\mu = -13.18$

    Standard Deviation $\sigma = 0.78$

Failure Rate Mean and Bounds

5% Lower Bound	Median	Mean	95% Upper Bound
$\lambda_{.05}$	$\lambda_{.5}$	$E\{\lambda\}$	$\lambda_{.95}$
0.52	1.88	2.55	6.79

$$x\ 10^{-6} \text{ per hour}$$

PCC (Colloid System)

Component Reliability Model

$R = \exp(-\lambda t)$ where t = mission time

Failure Rate Uncertainty Distribution Model

Log Normal

Coefficient of Variation $\eta = 1.655$

Mean $\mu = -13.91$

Standard Deviation $\sigma = 1.148$

Failure Rate Mean and Bounds

5% Lower Bound	Median	Mean	95% Upper Bound
$\lambda_{.05}$	$\lambda_{.5}$	$E\{\lambda\}$	$\lambda_{.95}$
0.138	0.91	1.758	6.01

$$x\ 10^{-6} \text{ per hour}$$

Control Logic (Pulsed Plasma)

Component Reliability Model

$R = \exp(-\lambda t)$ where t = operating time

Failure Rate Uncertainty Distribution Model

Log Normal

Coefficient of Variation $\eta = 0.2095$

Mean $\mu = -13.47$

Standard Deviation $\sigma = 0.2073$

Failure Rate Mean and Bounds

5% Lower Bound	Median	Mean	95% Upper Bound
$\lambda_{.05}$	$\lambda_{.5}$	$E\{\lambda\}$	$\lambda_{.95}$
1.01	1.42	1.45	2.0

$$x\ 10^{-6}\ \text{per hour}$$

Low Voltage Converter (Pulsed Plasma)

Component Reliability Model

$R = \exp(-\lambda t)$ where t = operating time

Failure Rate Uncertainty Distribution Model

Log Normal

Coefficient of Variation $\eta = 0.5772$

Mean $\mu = -13.6$

Standard Deviation $\sigma = .536$

Failure Rate Mean and Bounds

5% Lower Bound	Median	Mean	95% Upper Bound
$\lambda_{.05}$	$\lambda_{.5}$	$E\{\lambda\}$	$\lambda_{.95}$
0.516	1.247	1.44	3.01

$$x\ 10^{-6}\ \text{per hour}$$

High Voltage Converter (Pulsed Plasma)

Component Reliability Model

$R = \exp(-\lambda t)$ where t = operating time

Failure Rate Uncertainty Distribution Model

Log Normal

Coefficient of Variation $\eta = 0.322$

Mean $\mu = -13.37$

Standard Deviation $\sigma = 0.314$

Failure Rate Mean and Bounds

5% Lower Bound	Median	Mean	95% Upper Bound
$\lambda_{.05}$	$\lambda_{.5}$	$E\{\lambda\}$	$\lambda_{.95}$
0.93	1.56	1.64	2.62

$$x\ 10^{-6}\ \text{per hour}$$

System Power Converter (Pulsed Plasma)

Component Reliability Model

$R = \exp(-\lambda t)$ where t = operating time

Failure Rate Uncertainty Distribution Model

Log Normal

Coefficient of Variation $\eta = 0.594$

Mean $\mu = -13.67$

Standard Deviation $\sigma = 0.55$

Failure Rate Mean and Bounds

5% Lower Bound	Median	Mean	95% Upper Bound
$\lambda_{.05}$	$\lambda_{.5}$	$E\{\lambda\}$	$\lambda_{.95}$
0.466	1.15	1.34	2.85

$$x\ 10^{-6}\ \text{per hour}$$

Sense Circuit (Pulsed Plasma)

Component Reliability Model

$R = \exp(-\lambda t)$ where t = operating time

Failure Rate Undertainty Distribution Model

Log Normal

Coefficient of Variation	$\eta = 3.14$
Mean	$\mu = -15.43$
Standard Deviation	$\sigma = 1.54$

Failure Rate Mean and Bounds

5% Lower Bound	Median	Mean	95% Upper Bound
$\lambda_{.05}$	$\lambda_{.15}$	$E\}\lambda\{$	$\lambda_{.95}$
0.0157	0.199	.649	2.5

$$x\ 10^{-6} \text{ per hour}$$

Pulse Buffer (Pulsed Plasma)

Component Reliability Model

$R = \exp(-\lambda t)$ where t = operating time

Failure Rate Uncertainty Distribution Model

Log Normal

Coefficient of Variation	$\eta = 0.3675$
Mean	$\mu = -14.007$
Standard Deviation	$\sigma = 0.3559$

Failure Rate Mean and Bounds

5% Lower Bound	Median	Mean	95% Upper Bound
$\lambda_{.05}$	$\lambda_{.5}$	$E\{\lambda\}$	$\lambda_{.95}$
0.46	0.826	.828	1.48

$$x\ 10^{-6}\ \text{per hour}$$

PCC SWITCH

While this component had not been defined as part of
the system to be assessed, the use of redundant PCC's imply
its use. Since all the electric propulsion systems assessed
included redundant PCC's, the PCC switch was included. Its
function is analyzed in the fault trees for each system.
The identified failure modes for the switch are failing
active and passive. The former implies a failure during
the switching process leaving neither PCC connected to the
propulsion system. The fail passive mode implies failure
to switch, leaving the PCC/thruster configuration existing
upon initiation of the switch command unchanged.

Component Reliability Model

$$R = \exp(-\lambda N) \qquad \text{where N = operating cycles}$$

Failure Rate Uncertainty Distribution Model

Log Normal

Coefficient of Variation	$\eta = 1.66$
Mean	$\mu = -16.6$
Standard Deviation	$\sigma = 1.15$

Failure Rate Mean and Bounds

5% Lower Bound	Median	Mean	95% Upper Bound
$\lambda_{.05}$	$\lambda_{.5}$	$E\{\lambda\}$	$\lambda_{.95}$
0.0094	0.062	0.12	0.41

$$x\ 10^{-6} \text{ per cycle}$$

Partition to Failure Modes

1. <u>Fail Active</u>

   1.1 <u>Model</u>

   $$R = \exp(-\lambda t)$$

   1.2 <u>Failure Rate</u>

   $$E\left\{\lambda_A\right\} = 50\% \; E\{\lambda\}$$

   1.3 <u>Failure Rate Means and Bounds</u>

5% Lower Bound	Median	Mean	95% Upper Bound
$\lambda_{.05}$	$\lambda_{.05}$	$E\{\lambda\}$	$\lambda_{.95}$
0.00025	0.0024	0.06	0.022

2. <u>Fail Passive</u> – $\times 10^{-6}$ per cycle

   2.1 <u>Model</u>

   $$R = \exp(-\lambda t)$$

   2.2 <u>Failure Rate</u>

   $$E\left\{\lambda_A\right\} = 50\% \; E\{\lambda\}$$

   2.3 <u>Failure Rate Means and Bounds</u>

5% Lower Bound	Median	Mean	95% Upper Bound
$\lambda_{.05}$	$\lambda_{.05}$	$E\{\lambda\}$	$\lambda_{.95}$
0.00025	0.0024	0.06	0.022

   $\times 10^{-6}$ per cycle,

UNPRESSURED SURFACE TENSION TANK (CESIUM)

The contribution due to corrosion is an age-dependent phenomenon that occurs only in a reservoir subpopulation in which efforts to prevent carbon precipitation have been unsuccessful; the mean life for this subpopulation appears to be on the order of 10,000 hours.* A normal distribution is an appropriate model for the subpopulation.

Even if the two life-distribution models are considered "known", there are four uncertain parameters:

- The constant failure rate, λ

- The mean of the normal distribution (we shall use μ' to distinguish this from the lognormal uncertainty distribution parameter, μ)

- The standard deviation of the normal distribution, σ'

- The relative size of the subpopulation, K.

It would be meaningless to consider uncertainty in each of these parameters with available data and insight. Instead, fixed estimates will be used for two: $\mu' = 10,000$ hours, $\sigma' = 1,500$ hours. Noting that the noncorrosion failure rate has the expected value $E\}\lambda\{ = 1.5 \times 10^{-6}$ and applying the 3.6×10^{-6} estimate as an equivalent expected failure rate at 10,000 hours, we obtain

$$e^{-10,000 \times 1.5 \times 10^{-6}} \cdot [1 + .5E\}K\{] = e^{-10,000 \times 3.6 \times 10^{-6}}$$

$$E\}K\{ \approx .04$$

---

*See ref 17, 18, 19, 20, 21, 22

Component Reliability Model

$$R_i(t) = e^{-\lambda_{(1-i)}t} \cdot (1-K_{(1-i)})N(t)$$

is the overall model, which yields the following for
selected values of t:

t	$R_{0.05}(t)$	$R_E(t)$	$R_{0.5}(t)$	$R_{0.95}(t)$
5,000	0.999	0.995	0.993	0.977
10,000	0.996	0.972	0.965	0.912
15,000	0.993	0.949	0.939	0.849
20,000	0.992	0.944	0.932	0.830
50,000	0.987	0.918	0.891	0.722
87,000	0.980	0.886	0.842	0.607

Failure Rate Uncertainty Distribution

Parameters

Coefficient of Variation	$\eta = 1.25$
Mean	$\mu = -0.065$
Standard Deviation	$\sigma = 0.97$
Bounds and Central Measures	$(x10^{-6}$ per hr.$)$

5% Lower Bound	Median	Mean	95% Upper Bound
$\lambda_{.05}$	$\lambda_{.05}$	$E\{\lambda\}$	$\lambda_{.95}$
0.19	0.94	1.5	4.63

The uncertainty about K will be described by a beta
distribution:

$$P(x \leq C) \approx \frac{\Gamma(50)}{\Gamma(2)\,\Gamma(48)} \int_0^C x(1-x)^{47}\,dx$$

I-66

<u>Subpopulation relative size pounds and central</u>
<u>measures ($\times 10^{-6}$ per hour)</u>

5% Lower Bound   Median   Mean   95% Upper Bound

$K_{0.05} = 0.004$ $K_{0.5} = 0.038$ $E\{K\} = 0.04$ $K_{0.95} = 0.09$

Since it is likely that λ and K are strongly correlated
(because both are determined by design and process controls),
we may treat K_i as being associated with λ_i. For notational
convenience, let $N(\cdot)$ denote the complement of the normal
cumulative probability.

<u>Partition to Failure Modes</u>

1.1 Tank Leakage
     Assessed at 40% of all tank failures. In terms of
     reliability

$$R_{Leak} = \left(R_{Tank\ Total} \right)^{.4}$$

1.2 Tank Fins Unwetting
     Assessed at 40% of all tank failures. In terms of
     reliability

$$R_{(Fins)} = \left(R_{Tank\ Total} \right)^{.4}$$

1.3 Trapped Gas
     Assessed at 20% of all tank failures. In terms of
     reliability

$$R_{Gas} = \left(R_{Tank\ Total} \right)^{.2}$$

I-67

TRAPPED GAS IN RESERVOIR (Cesium Ion Only)

This condition is not clearly assessable to one component bur rather to two. During the interval between tank charging and orbit insertion gas trapping is possible. It may result from a tank leak or a fill valve leak. The details of each of these component failure modes are assessed under the appropriate component. The resulting composite model is presented below:

Component Reliability Model

$R = R$ (fill valve gas leakage) x R (tank gas leakage)

$$R_{\text{tank gas leak}} = \left[R_{\text{tank total}}\right]^{.2}$$ (see cesium reservoir

$$R_{\text{(fill valve}} = \exp)\ (-\lambda_L t)$$

> where t = mission hours
> L = leakage failure rate
> (see fill valve for values)

then

$$R = \left[R_{\text{tank total}}\right]^{.2} \times \exp(-\lambda_L t)$$

PRESSURIZED TANK

The failure modes for this component are rupture and leakage. Most imperfections will be minute, leading to leak failure rather than rupture (a distribution of 80% leak failure and 20% rupture failure is indicated). Typical failure locations include diaphragm (or bladder) and tank interface, valve and tank interface, and welded joints. The principal failure mechanisms include handling and workmanship and corrosion. Metal fatigue has also been suggested as a possible mechanism of lower importance.

Component Reliablity Model

$$R = \exp(-\lambda t) \qquad \text{where } t = \text{pressurized time}$$
$$\lambda = \text{failure rate}$$

Failure Rate Uncertainty Distribution

Log Normal

Coefficient of Variation	$\eta = 2.5$
Mean	$\mu = -16.27$
Standard Deviation	$\sigma = 1.4075$

Failure Rate Mean and Bounds

5% Lower Bound	Median	Mean	95% Upper Bound
$\lambda_{.05}$	$\lambda_{.5}$	$E\{\lambda\}$	$\lambda_{.95}$
.0085	0.086	.231	.87

$$X10^{-6} \text{ per hour}$$

Partition by Tank Halves (to accommodate tank/bladder systems)

1. Propellant Half Failure

    1.1 Model $R = \exp(-\lambda t)$

    1.2 Failure Rate

        $E\left\{\lambda_{prop}\right\} = 50\% \ E\{\lambda\}$

    1.3 Failure Rate Mean and Bounds

5% Lower Bound	Median	Mean	95% Upper Bound
$\lambda_{.05}$	$\lambda_{.5}$	$E\{\lambda\}$	$\lambda_{.45}$
0.0022	0.032	0.116	0.452

    $$X10^{-6} \text{ per hour}$$

2. Pressurant Half Failure

    2.1 See 1.1

    2.2 See 1.2

    2.3 See 1.3

ELASTOMERIC BLADDER/DIAPHRAGM

While the pressure in the propellant reservoir of the mercury ion system is similar to that in the thermochemical systems, the materials compatibility was assessed as being the principal device in determining the reliability model for the bladder. While virtually no failure rate data exists for bladders of similar service, reliability assessmen s of this situation have been performed (Ref 23). The point estimate failure rate cited in Ref 23 shall be used as the starting point for this model. Since Ref 23 does not assess uncertainty, the uncertainty model for the thermochemical bladder will be used.

Failure modes for these expulsion devices are leakage and rupture, which are caused by (1) imperfections in materials and fabrication, and (2) folding tears.

Component Reliability Model

$R = \exp(-\lambda t)$ where t = pressurized time

Failure Rate Uncertainty Distribution

Log Normal

Coefficient of Variation	$\eta = 0.75$
Mean	$\mu = -16.08$
Standard Deviation	$\sigma = 0.668$

Failure Rate Mean and Bounds

5% Lower Bound	Median	Mean	95% Upper Bound
$\lambda_{.05}$	$\lambda_{.5}$	$E\{\lambda\}$	$\lambda_{.95}$
0.035	0.104	0.17	0.312

$$x\ 10^{-6}\ \text{per hour}$$

FILL VALVE (Cesium Ion System)

The similar pressures and mission times allow the use of the thermochemical fill valve model in the mercury ion system. The cesium fill valve presents a different situation. During the period between tank charging and orbit insertion this valve experiences a pressure differential opposite to that of the fill valve in the above mentioned system. After orbit insertion the pressure differential is negligible and ceases to be of concern as a failure mechanism. This dual mode of operation is reflected in the selected reliability model. Because of the long duration at very low pressures the starting point for this model was the colloid fill valve.

Component Reliability Model

$$R = \exp\left[-\lambda_G t_o - \lambda_L t_m\right]$$

where λ_G = gas leak fail rate

t_o = elapsed time between pressurization and orbit insertion

λ_l = propellant leak fail rate

t_m = mission duration

Failure Rate Uncertainty Distribution Model

Log Normal	λ_G	λ_L
Coefficient of Variation	1.91	1.91
Mean	-12.81	-15.69
Standard Deviation	1.24	1.24

Failure Rate Mean and Bounds

5% Lower Bound	Median	Mean	95% Upper Bound
$\lambda_{.05}$	$\lambda_{.5}$	$E\{\lambda\}$	$\lambda_{.95}$

	5% Lower Bound	Median	Mean	95% Upper Bound
λ_G	0.356	2.7	5.9	21.0
λ	0.02	0.153	0.33	1.18

$$x\ 10^{-6}\ \text{per hour}$$

Partition to Failure Modes

1. **Propellant Leakage**

    1.1 **Model**

    $R = \exp(-\lambda_L t)$ $\qquad$ t = mission hours

    1.2 **Failure Rate**

    $E\{\lambda_L\} = 0.33 \times .5^{-6}$ per hour

    1.3 **Failure Rate Mean and Bounds**

5% Lower Bound	Median	Mean	95% Upper Bound
$\lambda_{.05}$	$\lambda_{.5}$	$E\{\lambda\}$	$\lambda_{.95}$
0.02	0.153	0.33	1.18

$$x10^{-6}\ \text{per hour}$$

2. **Gas Leakage to Tank**

    2.1 **Model**

    $R = \exp(-\lambda_G t)$ $\qquad$ t = time elapsed between tank charging and orbit insertion

    2.2 **Failure Rate**

    $E\ \lambda_G = 5.9 \times 10^{-6}$ per hour

    2.3 **Failure Rate Mean and Bounds**

5% Lower Bound	Median	Mean	95% Upper Bound
0.356	2.7	5.9	21.0

$$x10^{-6}\ \text{per hour}$$

FILL VALVE

This component is used to introduce the pressurant or propellant into its storage tank. Upon completion of fluid loading the valve is closed and if launch occurs on schedule it remains in this position throughout the remainder of the mission. Failure modes of this component are rupture and internal leakage of the valve seat. Rupture can be caused by flaws appearing randomly in the material and by stresses during launch. Redundancy for this component is achieved by capping with valve closure caps:

Component Reliability Model

$$R = \exp(-\lambda t)$$

where t = pressurized time
λ = failure rate

Failure Rate Uncertainty Distribution

Lognormal

Coefficient of Variation $\eta = 10.5$

Mean $\mu = -16.21$

Standard Deviation $\sigma = 2.1703$

Valves in general are exposed to repeated cyclic operation and their reliability models reflect the situation with cyclic dependent functions that can often drive the overall expression. Fill valves however, can be expected to be cycled only a few times in system pressure tests and finally once more upon charging the propellant storage tank prior to launch. It will then become a passive component of the system; expected to last the mission in the finally closed condition. Therefore its reliability model includes a time dependent function only. The deleterious effects of test cycling prior to final charging are included in the

developed failure rate to be applied throughout the mission.

Failure Rate Mean and Bounds

5% Lower Bound	Median	Mean	95% Upper Bound
$\lambda_{.05}$	$\lambda_{.5}$	$E\{\lambda\}$	$\lambda_{.95}$
.003	0.091	.09	.323

$$\times 10^{-6} \text{ per hour}$$

HEATERS (LINE, TANK AND VALVE)

Heaters of this type employed in electric systems are used in duty cycles and environments very similar to those employed in thermochemical propulsion systems. This led to the use of the same reliability model and parameter and values as used in the thermochemical propulsion system; see that section for further discussion of this heater type (page I-153).

Component Reliability Model (unchanged)

$$R = \exp(-\lambda t)$$

where λ = failure rate
t = Mission time

Failure Rate Uncertainty Distribution

Lognormal

Coefficient of Variation η = 2.016

Mean μ = -17.68

Standard Deviation σ = 1.274

Failure Rate Rounds and Central Measures

5% Lower Bound	Median	Mean	95% Upper Bound
$\lambda_{.05}$	$\lambda_{.5}$	$E\{\lambda\}$	$\lambda_{.95}$
.0026	0.0209	.047	.169

$$\times 10^{-6} \text{ per hour}$$

VAPOR VALVE (CESIUM)

The principal working elements of the vapor valve are bimetallic washers designed to produce a valve opening at temperatures above 100°C. These washers can function as designed only if the bond of the dissimilar materials is preserved over an extended period under the corrosive action of cesium propellant. Obstacles to thorough reseating appear improbable.

Component Reliability Model

$R = \exp(-\lambda t)$ where t = operating time

Failure Rate Uncertainty Distribution Model

Log Normal

Coefficient of Variation	$\eta = 1.7$
Mean	$\mu = -12.59$
Standard Deviation	$\sigma = 1.165$

Failure Rate Mean and Bounds

5% Lower Bound	Median	Mean	95% Upper Bound
$\lambda_{.05}$	$\lambda_{.5}$	$E\{\lambda\}$	$\lambda_{.95}$
0.5	3.4	6.7	23.1

$\times\ 10^{-6}$ per hour

Partition to Failure Modes

1. Fail Open

   1.1 Model

      $R = \exp(-\lambda t)$ where t = operating time

   1.2 Failure Rate

      $E\{\lambda_o\} = 1/3 \; E\{\lambda\}$

   1.3 Failure Rate Mean and Bounds

5% Lower Bound	Median	Mean	95% Upper Bound
$\lambda_{.05}$	$\lambda_{.5}$	$E\{\lambda\}$	$\lambda_{.95}$
0.06	0.72	2.23	8.6

$$x \; 10^{-6} \text{ per hour}$$

2. Fail Closed

   2.1 Model   (see 1.1)

   2.2 Failure Rate   (see 1.2)

   2.3 Failure Rate Mean and Bounds   (see 1.3)

3. Fail Partial

   3.1 Model (see 1.1)

   3.2 Failure Rate (see 1.2)

   3.3 Failure Rate Mean and Bounds (see 1.3)

ISOLATOR

The CIV*assembly incorporates the main isolator to decouple the thruster high voltage from the propellant feed system. The propellant feed lines are potential conductors that could parallel a short across all units on a common feed system. In one current design, isolation enables the single reservoir tc supply the main and neutralizer cathodes. Endurance tests totaling over 17,000 hours indicate that failure modes mav include insulation breakdown due to both metal deposits and ceramic failure (24, 25, 26). The mechanism of differential thermal expansion described for the vaporizer disk may be applicable to the ceramic spacers.

Guidance on estimating an isolator failure rate is gained by noting that some capacitors utilize similar materials for an analogous function, at least to the extent of insulating against leakage current,

The available data suggest an equivalent failure rate, $E\{\lambda\} = 4.6 \times 10^{-6}$, which is a somewhat conservative estimate. Leakage current data suggest an autocatalytic type of process, consistent with knowledge about basic phenomena: the negative temperature coefficient of resistance in ceramics leads to channeling of leakage current and potentially to thermal runaway. A Weibull model with shape parameter $\beta = 2$ appears appropriate.

Component Reliability Model

$$R = \exp\left[\frac{-t^{\beta}}{\alpha}\right]$$

where t = operating time

β = shape factor, set equal to 2, based on similarity of isolator to ceramic capacitor

α = scale factor

The failure rate ($\lambda = 4.6 \times 10^{-6}$, per hour) is intended for use in an exponential model. Transition to a Weibull model was obtained by setting both models equal at a selected value of operating time, t. Using 8 cm test history as a guide a value of t = 6,000 was used.

─────────────────────

*Cathode-Isolator-Vaporizer

Then;

$$e^{-\lambda t} = \exp\left[-\frac{t^2}{\alpha}\right]$$

taking the logrithms, $\quad \lambda t = \dfrac{t^2}{\alpha}$

and at $t = 6,000$ hours,

$$\alpha = \frac{6,000}{\lambda}$$

Failure Rate Uncertainty Distribution Model

Log normal

Coefficient of variation $\eta = 13.08$

Mean $\qquad\qquad \mu = 0.2036$

Standard deviation $\qquad \sigma = 1.626$

Weibull Parameter Values and Bounds

Shape Parameter, $\beta = 2$

Scale Parameter, α, Equivalent Mean and Bounds

5% Lower Bound	Equivalent Mean	Median	95% Upper Bound
$\alpha_{.05}$	α_E	$\alpha_{.5}$	$\alpha_{.95}$
3.374×10^8	1.305×10^9	4.89×10^9	7.198×10^{10}

VAPORIZER

Several modes of failure for the vaporizer plug can be visualized (25, 26, 29). During application of heat at the periphery of the porous plug, there will be a transient period when the outer regions are warmer than the core with nonuniform expansion inducing stresses. The same will happen during cooling. While 20,000 cycles of stress is not a large number and reduces the fracture point of a material only slightly below its zero-cycle level, the nonuniform wall structure between cells could be vulnerable. Then, if one or a few cell walls were fractured, the nearby walls would take higher loads and a crack could propagate. Vapor flow through the cells will accelerate the process due to the extremely thin walls subjected to wear. Should malperformance of the vaporizer heater occur and produce an uneven temperature distribution in the porous plug housing, there will be an acceleration of the tendency of the plug to develop a crack. The consequences of this type of failure vary between small degradation in performance, such as a higher flow of vapor than predicted, and or catastrophic due to complete loss of propellant. The distribution of failures under this mechanism will increase with the number of operating cycles.

The porous plug can also develop failures analogous to failures of liquid and gaseous material filters. The failure mechanism is a clogging of the filter passages as foreign matter is removed from the material being filtered. Every effort is expended in filtration of propellant to remove impurities prior to reservoir filling, but 100-percent removal may not be achievable. Impurities could migrate to the porous plug and clog passages, thus reducing propellant flow for a given setting of the vaporizer. Another possible effect observed during testing was that impurities countering the nonwetting property of liquid metal against tungsten allowed loss of propellant.

Component Reliability Model

$$R = \exp\left[- \lambda_{op} t_{op} - \lambda_c N\right]$$

where λ_{op} = operating time failure rate

λ_c = cyclic failure rate

t_{op} = operating time

N = number of cycles

Failure Rate Uncertainty Distribution Model (Applicable to both failure rates)

Log normal

Coefficient of Variation $\eta = 1.71$

Mean $\mu = -13.19$

Standard Deviation $\sigma = 1.168$

Failure Rate Mean and Bounds (Cyclic and Time Components)

	5% Lower Bound	Median	Mean	95% Upper Bound
	$\lambda_{.05}$	$\lambda_{.5}$	$E\{\lambda\}$	$\lambda_{.9}$
λ_c	0.273	1.87	3.69	12.74
λ_{op}	0.273	1.87	3.69	12.74

$$X10^{-6} \text{ per hour (cycle)}$$

Partition to Failure Modes

1. Clogging

    1.1 Model $R = \exp(-\lambda_{cl}\, t)$ where t = operating hours
    λ_{cl} = clogging failure rate

    1.2 Failure Rate

    $$E\{\lambda_{cl}\} = 25\% \; E\{\lambda\}$$

    1.3 Failure Rate Mean and Bounds

5% Lower Bound	Median	Mean	95% Upper Bound
$\lambda_{.05}$	$\lambda_{.5}$	$E\{\lambda\}$	$\lambda_{.95}$
0.019	0.259	0.923	3.185

$$\times 10^{-6} \text{ per hour}$$

2. Excessive Flow, e.g. Leaking, Fracture

    2.1 Model $R = \exp[-\lambda'_{op} t_{op} - \lambda'_{c}\, N]$

    2.2 Failure Rate

    $$E\{\lambda'_{c}\} = 100\% \; E\{\lambda_{c}\}$$
    $$E\{\lambda'_{op}\} = 75\% \; E\{\lambda_{op}\}$$

    2.3 Failure Rate Mean and Bounds

	5% Lower Bound	Median	Mean	95% Upper Bound
	$\lambda_{.05}$	$\lambda_{.5}$	$E\{\lambda\}$	$\lambda_{.95}$
λ'_{c}	0.273	1.87	3.69	12.74
λ'_{op}	0.16	1.25	2.77	9.96

$$\times 10^{-6} \text{ per hour (cycle)}$$

VAPORIZER HEATER

The heating coil is subject to failure even after the design is qualified for the application. The corrosion problem of electrical heaters operating in oxidizing atmospheres is not present in a spacecraft ion engine. Nevertheless, absolute purity of the heater conducting element is impossible; the inclusions can be a source of outgassing. The cumulative timewise effect is that enough material can be lost to lead to a fracture. Thermal cycling contributes to this mode of failure. As material is lost, the resistance of the heater coil will be increased, and propellant flow control will be more difficult. In the event of coil fracture no propellant can be passed. Failures of this part will increase with time of operation, roughly analogous to a fatigue phenomenon.

For the vaporizer heating coil the NRN* contains the following failure rate:

Heaters, electrical-satellite: $0.450 + 375\%$, -95% per 10^6 part-hours.

The variance about the mean value is greater than encountered for most data. However, there is no reason to assume that any of the heaters in the failure rate data base have been rated more or less conservatively than the data for the vaporizer heater. The present application does contain a thermal cycling operation that could accelerate the deleterious effects of undetected flaws in material or fabrication (25, 26, 29). In fact, an open circuit failure occurred during cycle and life testing of the mercury ion thruster after 594 cycles, which resulted in a redesign to alleviate high thermal stresses. Therefore, an estimate is made that the mean failure rate for the heating coil in the vaporizer application will be 75 percent above the NRN value:

$$\lambda = 0.79 \text{ per } 10^6 \text{ part-hours.}$$

A straight time dependence (constant failure rate) is suggested for the heater. There will be an expansion in the length of the heater coil and a possible stress condition because of a constrained installation. However, this line of reasoning is more speculative than the case for undetected imperfections.

---

* NEDCO Reliability Notebook

Component Reliability Model

$$R = \exp(-\lambda t) \qquad \text{where } t = \text{operating time}$$

Failure Rate Uncertainty Distribution Model

Log Normal

Coefficient of Variation $\qquad \eta = 1.71$

Mean $\qquad\qquad\qquad\qquad \mu = -14.73$

Standard Deviation $\qquad\quad \sigma = 1.168$

Failure Rate Mean and Bounds

5% Lower Bound	Median	Mean	95% Upper Bound
$\lambda_{.05}$	$\lambda_{.5}$	$E\{\lambda\}$	$\lambda_{.95}$
0.06	0.40	0.79	2.73

$$x\ 10^{-6} \text{ per hour}$$

HOLLOW CATHODE

Some of the so-called random failures that might occur prior to predicted end of life could originate in materials and fabrication. The electron beam welding process used for joining the cathode tip to the body has been known to leave particles, which later become free of the parent metal. In swaging the keeper cap over the heater shield, minute cracks may be introduced which become evident at a later point in the operating life. The application of insulator material to the heater coil and carbonate coating to the insert may produce non-uniformities which become crack originations under thermal cycling. Additionally, spot welds join the wire connecting the foil insert to the cathode body (25, 26, 27, 28).

It must be assumed that before development is complete, requirements for the cathode service life will have been demonstrated. Because failures are unpredictable, they may appear at the end of the useful life or develop prematurely. Similarly, failures may be due to imperfections in fabrication or materials as discussed previously.

Electron tubes show these same failure characteristics. Examples in data compilation include such failure items as excessive heat, caused by arcing, leading to melting of insulator material at base; shorting due to erosion of particles; hot spots in filamentary material and opens; and low electron rates due to cathode material deterioration. The similarity of these kinds of failures to potential thruster cathode failures suggests that tube failure rates may be applicable. In particular, the operation of the ion engine has been likened to a magnetron operated at current cutoff. Several sources provide failure rates for this type of tube.

Component Reliability Model

$$R = \exp(-\lambda t)$$

where t = operating time
λ = failure rate per hour

Failure Rate Uncertainty Distribution Model

Log normal

Coefficient of variation	$\eta = 13.08$
Mean	$\mu = -12.28$
Standard Deviation	$\sigma = 1.626$

Failure Rate Mean and Bounds

5% Lower Bound	Median	Mean	95% Upper Bound
$\lambda_{.05}$	$\lambda_{.5}$	$E\{\lambda\}$	$\lambda_{.95}$
0.32	4.67	17.5	67.7
		$\times 10^{-6}$ per hour	

DISCHARGE CHAMBER (Kaufman type)

The production of ions to be accelerated and focused into an ion current takes place in the discharge chamber, sometimes referred to as an ion chamber. Arbitrarily, this assembly will be defined as including the so-called optics and excluding the cathode discussed previously. The components comprising the discharge chamber assembly are outer shell, thruster endplate (forward end), anode, and accelerator and screen grids.

Endurance testing of the SIT-8 unit accumulated 7,400 hours with 229 startups. A significant interruption occurred at about the 1000-hour point when the composite graphite tantalum baffle delaminated and fractured (26). This item was replaced by a redesigned part of isotropic graphite. Otherwise, there were some operational anomalies; for example, the accelerator drain current became roughly half its initial value before steadying while there was an increase in propellant flow. Measurements on weight loss (or gain) were made during halts in testing. The tentative conclusion at Lewis Research Center appeared optimistic that the target on useful life can be reached.

While it does not constitute a catastrophic failure in itself, the erosion problem may produce various consequences. If the rate of erosion can be controlled and the parts experiencing loss of material are proportioned accordingly, there will be only a tolerable loss of thruster performance out to the predicted end of service life. However, some researchers have reported a rapid increase in erosion rates when the loss reaches approximately 75 percent of the available material (30, 31, 32).

There is a small probability that a total loss of thrust could result from sputtering erosion, such as the case of a particle shorting the grids. When the particle is metal, a discharging capacitor has been used to cause the particle to melt and remove the short. Specific design measures have been taken to correct known or suspected points of vulnerability to the effects of sputtered particles. The neutralizer is now positioned to avoid a recurrence of the accelerator grid erosion experienced during flight of the 15-centimeter unit. Sputter shields are included at the terminals installed on the endplate. Insulating materials, such as those at the anode shell mount and the accelerator grid mount, are selected as appropriate for the application.

The conclusion to be drawn from the previous discussion is that a structural wear-out mode of failure will be the most probable. However, other failures may include premature and unpredicted failures of a wear-out type together with apparently random occurrences of failure due to fabrication or material imperfections. The observations during test periods are consistent with these statements. Additionally, by examining the origins of the failure mechanism, a similar conclusion can be reached. The parts are large enough to enable fabrication and inspection to be free from the need for absolute perfection. There are no concentrated heat sources to induce the thermal gradients and cycling that could accelerate the anomalous behavior of minute imperfections. The problem of thermal distortion of the accelerator and screen grids because of temperatures higher in their central regions than their edges has been solved by the dished design, at least for the period before deep erosion.

On the other hand, erosion damage is inevitable. The high velocity impact of charged particles on the walls erodes the metal surfaces. Sputter yield, that is, the number of atoms eroded per incident ion, has been studied and its rates are known. However, the resulting weight loss can be uneven and lead to catastrophic consequences. In other cases, it may develop that lost weight and thermal gradients during on-off cycling may interact to steepen the gradients and accelerate the fatigue-like action of cycling. Furthermore, the material loss rate is widely believed to accelerate as it progresses.

The flaking problem may be delayed rather than completely cured by the design improvements. Erosion rates may be slowed by the use of resistant materials and, at some locations, by further protective coatings. Nevertheless, the buildup on the anode and its screen insert can be expected to persist. Ultimately, the buildup may span the meshes of the screen and result in particles produced by flaking, which may be as large as those produced before design improvements. Another beneficial procedure consists of shot-blasting the anode surface to effect better adherence of sputtered material.

Component Reliability Model

$$R = \exp\left[-\lambda t - \frac{(t-5000)^\beta}{\alpha}\right]$$

where λ = failure rate (per operating hour)

t = operating time

$\beta = 3.0$

α = Scale Factor

Failure Rate Uncertainty Distribution

Log Normal

Coefficient of Variation $\eta = 3.86$

Mean $\mu = -14.79$

Standard Deviation $\sigma = 1.663$

Exponential Component Failure Rate Mean and Bounds

5% Lower Bound	Median	Mean	95% Upper Bound
$\lambda_{.05}$	$\lambda_{.5}$	$E\{\lambda\}$	$\lambda_{.95}$
.024	0.38	1.5	5.8

$$\times \, 10^{-6} \text{ per hour}$$

Weibull Component Parameter Values and Bounds*

Shape Factor, $\beta = 3.0$

Scale Factor α,   Equivalent Mean and Bounds

5% Lower Bound	Mean	Median	95% Upper Bound
$\alpha_{.05}$	α_E	$\alpha_{.5}$	$\alpha_{.95}$
1.146×10^{11}	4.435×10^{11}	1.767×10^{12}	2.722×10^{13}

* The same relative scale was applied to the uncertainty distribution for α, bearing in mind that α is analogous to $1/\lambda$

I-90

DISCHARGE CHAMBER, MESC

The magnetoelectrostatic plasma containment concept influences the form of the discharge chamber. Bounding surfaces of the discharge chamber act as a magnetic wall to reflect most of the ions and electrons approaching them. This greatly reduces ion losses to the walls, increases mass utilization efficiency, and provides a uniform plasma for efficient ion extraction.

Some erosion data are available from an abbreviated life test. The objective of the test was 18,000 hours, but a termination occurred at 4348 hours because of a failure of the neutralizer cathode heater. The accelator electrode evidenced erosion on the downstream face by charge exchange ions consisting of pits about 0.1 inch deep and a ring groove about the radius of the ground potential housing. Electrode alignment was rated excellent because the pits were symmetric with respect to the apertures. The loss due to pits and the ring was found to be 0.15 gram; a further loss of 0.24 gram was uniform over the downstream face, for a total of 0.39 gram out of an original part of mass of 30 grams. An extrapolation by the developers based on steady erosion indicated that penetration would occur at 39,500 hours. It is also possible, however, that as material loss accumulated beyond an operating period that has been reached in test the discharge chamber operation becomes vulnerable to the kind of misalignments reported. In fact, the loss of material can cause higher local temperatures, which can accelerate the loss of material in a regenerative process. (33, 34, 35, 36, 37)

The kinds of failures that can occur within the cesium ion thruster discharge chamber assembly have already been noted for the discharge chamber of the the mercury unit and to some extent for other components of this unit. Early development tests uncovered a few deficiencies for which fixes were found and reported. An inability to deflect thrust through the required excursion angle was traced to an initial misalignment in the accelerator electrode. Later, additional anomalies were found but were not fully rectified until the improved accelerator suspension was adopted.

A number of structural members and joints can be the source of failures under the interaction of undetected flaws in material and fabrication processes, thermal cycling, and erosive effect of partical bombardment. The discharge chamber design includes a multiplicity of anode members that must be

mounted and maintained at a set value of electric potential. The magnets must be maintained in position. The beam extraction grids must be mounted in precise alignment and the alignment retained under the thermal cycling of start up and shutdown. The alignment must further be controlled as a means of thrust vector control, which involves eight electric heater elements with compound functions of structural support and position control. The anode feed ring must be supported in position to feed cesium vapor, a function that includes the operation of an electric heater and connectors for electric potential setting. The shell of the discharge chamber also provides a mounting for the main cathode.

Component Reliability Model

$$R = \exp\left[-\lambda t - \left(\frac{t-6000}{\alpha}\right)^{\beta}\right]$$

where t = operating time
λ = constant failure rate
α = Weibull scale factor
β = Weibull shape factor

Failure Rate Uncertainty Distribution Model

Log Normal

Coefficient of Variation	$\eta = 5.44$
Mean	$\mu = -12.82$
Standard Deviation	$\sigma = 1.85$

Failure Rate Mean and Bounds

5% Lower Bound	Median	Mean	95% Upper Bound
$\lambda_{.05}$	$\lambda_{.5}$	$E\{\lambda\}$	$\lambda_{.95}$
0.129	2.71	15	56.8

$$\times\ 10^{-6}\ \text{per hour}$$

Weibull Parameter Values and Bounds

Shape Parameter $\quad \beta = 2.0$

Scale Parameter $\quad \alpha$, Equivalent Mean and Bounds

5% Lower Bound	Equivalent Mean	Median	95% Upper Bound
$\alpha_{.05}$	α_E	$\alpha_{.5}$	$\alpha_{.95}$
7.31×10^7	2.8×10^8	1.3×10^9	2.313×10^{10}

NEUTRALIZER ASSEMBLY

The neutralization function is required to maintain the overall charge neutrality (current neutralization) of the space vehicle, so that the ion beam does not cause any image charge on the vehicle thereby retarding the ions and reducing engine thrust (charge neutralization). The neutralizer cathode is similar in function to the main cathode and was, in fact, first developed to provide a long-life neutralizer. Except for the reduced mercury flow, the form of the neutralizer assembly, including isolator and vaporizer, is close to the main CIV assembly. Since there is no evident relationship of flow rate to the probability of failure, the previously developed failure data are considered to be directly applicable. Also, the incorporation of the plasma bridge emitter into the hollow cathode has enabled placement of the neutralizer device some distance from the ion beam, thus inhibiting tip erosion.

Neutralizer Isolator Reliability Model

$$R = \exp\left[-\frac{t^{\beta}}{\alpha}\right]$$

where t = operating time
β = shape factor = 2
α = scale factor = 1.305×10^9

See Isolator Model, page I-79 for details

Neutralizer Vaporizer Reliability Model

$$R = \exp(-\lambda t)$$

where t = operating time
λ = failure rate per hour

See Vaporizer Model, page I-81 for details

Neutralizer Cathode Reliability Model

$$R = \exp(-\lambda t)$$

where t = operating time
λ = failure rate per hour

See Hollow Cathode Model, page I-78 for details

The failure rate and scale factor values at the 5%, Median, Mean and 95% bounds for these values are the same as their CIV counterparts.

Neutralizer Probe Reliability Model (Cesium Ion Only)

Use Cathode Model, page I-78.

THRUST VECTORING ASSEMBLY (TVA)

The current prominent approach to thrust vector control is mechanical gimbaling. With the incorporation of dished grids at the accelerator/screen grid assembly, translation becomes more difficult to execute. Additionally, the gimbal mechanism is favored over an all-electrostatic device on the basis of longer probable useful life. A summary parts list includes the following:

- Lower support joint - two axes of rotation with three relative motion bearings, including spacecraft mount

- Upper support joint - one rotary bearing combined with slotted longitudinal strut

- Linear actuator (two required) - jack screw type with geared stepping motor drive, engage mount ring from spacecraft support

- Mount ring - provides bearing mounts and engages endplate of discharge chamber.

The parts of this assembly have fairly well-established failure histories since functionally similar mechanisms have been operated on many aeronautical applications and onboard spacecraft, star tracker drives, for example. Bearings at the gimbal axes may weld after sustained space exposure. If misalignments occur as a consequence of launch forces or spacecraft thermal deformation, driving torques may exceed capacities of actuators, gearing, or stepping motors. The jackscrews are inherently high-friction devices which can jam or score the screw thread. If overloaded, the stepper motors may develop hot spots, loss of insulation, and open circuits.

TVA   Lower Support

Component Reliability Model

$$R = \exp(-\lambda t)$$ where t = operating time

Failure Rate Uncertainty Distribution Model

    Log Normal

    Coefficient of Variation $\eta = 3.785$

    Mean $\mu = -14.45$

    Standard Deviation $\sigma = 1.652$

Failure Rate Mean and Bounds

5% Lower Bound	Median	Mean	95% Upper Bound
$\lambda_{.05}$	$\lambda_{.5}$	$E\{\lambda\}$	$\lambda_{.95}$
0.035	0.53	2.07	8.03

$$X\ 10^{-6}\ \text{per hour}$$

TVA - Motor and Bearing

Component Reliability Model

$R = \exp(-\lambda t)$ where t = operating time

Failure Rate Uncertainty Distribution Model

Log Normal

Coefficient of Variation $\eta = 2.45$

Mean $\mu = -13.19$

Standard Deviation $\sigma = 1.395$

Failure Rate Mean and Bounds

5% Lower Bound	Median	Mean	95% Upper Bound
$\lambda_{.05}$	$\lambda_{.5}$	$E\{\lambda\}$	$\lambda_{.95}$
0.188	1.87	4.93	18.5

$$X\ 10^{-6} \text{ per hour}$$

TVA - Linear Actuation

Component Reliability Model

$R = \exp(-\lambda t)$ where t = operating time

Failure Rate Uncertainty Distribution Model

Log Normal

Coefficient of Variation $\eta = 2.49$

Mean $\mu = -13.24$

Standard Deviation $\sigma = 1.405$

Failure Rate Mean and Bounds

5% Lower Bound	Median	Mean	95% Upper Bound
$\lambda_{.05}$	$\lambda_{.5}$	$E\{\lambda\}$	$\lambda_{.95}$
0.176	1.78	4.76	17.9

$$X\ 10^{-6}\ \text{per hour}$$

TVA - Upper Support

Component Reliability Model

$R = \exp(-\lambda t)$ where t = operating time

Failure Rate Uncertainty Distribution Model

Log Normal

Coefficient of Variation	$\eta = 4.629$
Mean	$\mu = -15.05$
Standard Deviation	$\sigma = 1.764$

Failure Rate Mean and Bounds

5% Lower Bound	Median	Mean	95% Upper Bound
$\lambda_{.05}$	$\lambda_{.5}$	$E\{\lambda\}$	$\lambda_{.95}$
0.016	0.291	1.38	5.3

$$X\ 10^{-6}\ \text{per hour}$$

SPARK INITIATOR

As indicated in the Electronic Components and Assemblies section, igniters (arc-initiation electrodes) also can be described by the combination of a (low) constant failure rate contribution and a relatively narrow wear-out-type distribution. For the latter, we shall use a normal distribution with $\frac{\sigma_N}{\mu_N} = 0.2$. Both contributions are regarded as dependent on the number of firing pulses.

Flight and laboratory test data indicate $\mu_N > 36 \times 10^6$ pulses and $\lambda < 2$ per billion pulses. These will be used as the $\mu_{N_{.05}}$ and $\lambda_{.95}$ estimates.* The coefficient of variation for λ must be larger than the standard electronic component value; we shall use $\eta = 2.5$.

The normal contribution uncertainty is comparable to those for the colloid thruster system neutralizer, with $\eta = .304$.

In this case, the failure processes associated with the two contributions appear to be distinct and uncorrelated. It will be found convenient to deal with the two contributions at the system level, as if there were two components in series, one providing the normal contribution and the other providing the exponential contribution.

Component Reliability Model

$$R = [\exp(-\lambda t)] \int_t^{\infty} \frac{1}{s\sqrt{2\pi}} \exp\left[-\frac{(t-m)^2}{2s^2}\right] dt$$

where t = mission time

---

* To avoid confusion with the uncertainty parameters σ and μ, σ_N and μ_N shall hereafter be replaced by s and m, respectively.

Note: Second component of model is a normal distribution. It is commonly tabulated with table look-up using

$$K = \frac{t-m}{s}$$

Failure Rate Uncertainty Distribution Model

Coefficient of Variation $\eta = 2.5$

Mean $\mu = -22.33$

Standard Deviation $\sigma = 1.407$

The normal contribution uncertainty is comparable to that of the colloid thruster system neutralizer, with $\eta = 0.304$.

Failure Rate λ Mean and Bounds

5% Lower Bound	Median	Mean	95% Upper Bound
0.00002	0.0002	0.00053	0.002

$$X10^{-6} \text{ per pulse}$$

Normal Contribution Parameter Values and Bounds

5% Lower Bound	Median = Mean	95% Upper Bound
$m_{.05}$	$m_{.5}$	$m_{.95}$
36	24	12

$$X10^{-6} \text{ per pulse}$$

ENERGY STORAGE CAPACITOR

This component has been discussed in some detail in the Electronic Components and Assemblies section with the conclusion that useful reliability estimates will require testing. The discussion also indicated that a combination exponential-normal model is attractive:

$$R(t) = \exp(-\lambda t) \int_t^{\infty} \frac{1}{\sigma\sqrt{2\pi}} \exp\left[-\frac{(t-\mu)^2}{2\sigma^2}\right] dt$$

It was noted that heterogeneity has been observed in some capacitor populations; the model omits subpopulation effects, although these should be considered when sufficient information becomes available.

Because these capacitors are highly specialized, use of MIL-HDBK-217B data for estimation involves unusually large uncertainties that should be reflected in larger-than-usual coefficients of variation. This means that test results will outweigh prior information as to the exponential contribution early in any test program.

As indicated in the Electronic Components and Assemblies section, temperature and voltage strongly influence reliability. Radiation effects also may be important. In addition, voltage effects differ with capacitor age, and radiation effects may interact with both voltage and temperature effects. Temperature is expected to affect both the exponential and the normal contributions. Rate-dependent radiation effects should be expected to affect the exponential contribution, and dose-related effects should be expected to affect primarily the normal contribution.

Component Reliability Model

$$R = \left[\exp\ (-\lambda_c N)\right] \left\{ \int_t^\infty \frac{1}{s\sqrt{2\pi}}\ \exp\ \left[-\frac{(t-m)^2}{2s^2}\right]\ dt\right\}$$

Note: Second component of model is a normal distribution. It is commonly tabulated with table look-up using $K = \frac{t - m}{s}$; t = mission time

For this capacitor the models for m, s and λ are:

$$m = \left(\frac{V_R}{V_A}\right)^{7.5}\ x\ 10^4\ cycles \qquad \text{where } V_R = \text{rated voltage}$$
$$V_A = \text{applied voltage}$$

Convert m to time using $\left(\dfrac{\text{mission life}}{\text{total number of cycles}}\right)$

$$s = 0.165\,m$$

$$\lambda = 5\ \left(\frac{V_A}{V_R}\right)\ x10^{-12}\ \text{per cycle}$$

Uncertainty Distribution Model

	λ_c	λ_m
Coefficient of Variation $\eta =$	4.35	1.3
Mean $\mu =$	$\left[\ln\left(\frac{V_A}{V_R}\right) - 27.518\right]$	$\left[7.5\ln\left(\frac{V_R}{V_A}\right) + 8.71\right]$
Standard Deviation $\sigma =$	1.73	1.0

Parameter Values and Bounds

	5% Lower Bound	Median	Mean	95% Upper Bound
λ_c:	$\exp\left[\mu - 1.645\sigma\right]$	$\exp(\mu)$	$\exp\left[\mu + \frac{\sigma^2}{2}\right]$	$\exp\left[\mu + 1.645\sigma\right]$
μ:	$\exp\left[\mu - 1.645\sigma\right]$	$\exp(\mu)$	$\exp\left[\mu + \frac{\sigma^2}{2}\right]$	$\exp\left[\mu + 1.645\sigma\right]$

MAIN ELECTRODES[*]

   While a build up of charred propellant has been
observed in tests (10), no performance degradation has been
noted. The performance of the main electrodes are much
less sensitive to wear than the initiators. Therefore, the
random failure constant failure rate portion of the initiator
model will be used for the main electrodes.

Component Reliability Model

   $R = \exp(-\lambda N)$ where N = number of pulses
                            λ = failure rate per pulse

Failure Rate Uncertainty Distribution Model

   Lognormal

   Coefficient of Variation $\eta = 0.29$

   Mean $\mu = -22.33$

   Standard Deviation $\sigma = 0.505$

Failure Rate Mean and Bounds

5% Lower Bound	Median	Mean	95% Upper Bound
$\lambda_{.05}$	$\lambda_{.5}$	$E(\lambda)$	$\lambda_{.95}$
0.00002	0.0002	0.0005	0.002

$$X10^{-6} \text{ per pulse}$$

---

[*]Pulsed Plasma

NEGATOR SPRING

This component was assessed as having a nearly negligible failure rate. The failures are considered to be random; the failure rate is constant throughout the mission. Manufacturing flaws and material flaws are the identified failure mechanisms.

Component Reliability Model

$R = \exp(-\lambda t)$ where t = mission time
λ = failure rate per hour

Failure Rate Uncertainty Distribution Model

Lognormal

Coefficient of Variation $\eta = 3.77$

Mean $\mu = -22.3$

Standard Deviation $\sigma = 1.2$

Failure Rate Mean and Bounds

5% Lower Bound	Median	Mean	95% Upper Bound
$\lambda_{.05}$	$\lambda_{.5}$	$E(\lambda)$	$\lambda_{.95}$
0.00005	0.0004	0.0008	0.003

$$X10^{-6} \text{ per hour}$$

PROPELLANT BELLOWS RESERVOIR (Colloid)

In addition to containing the propellant until demanded by the thruster the bellows has a spring force that pressurizes the propellant so that it can flow against the various impedances of the system (14).

Development problems have occurred that are normal for a new system; there was a structural problem that involved the upper flange, upper dome, and convolution weld joints. The flange was placed in torsion when the bellows was in an extended position. Design changes have been recommended that would eliminate the moments that caused the torsion.

Distortion of the base flange of the bellows during assembly caused its coplanarity to go out of . ecification. This distortion is a result of the welding of the inner bellows and bellow convolution to the base flange (14).

Aging and stress relief may be failure mechanisms that could prevent propellant bellows storage system from supplying proper pressure required to operate the system. A uniform tensile force is required to compress the fluids and to supply working pressure.

A leak in the fill-valve, bellows, weld joints, or plumbing that leads to the control valve would be catastrophic, as the bellows is constantly supplying pressure to the fluid.

Component Reliability Model

$R = \exp(-\lambda t)$ where t = pressurized time
                                 λ = failure rate per hour

Failure Rate Uncertainty Distribution Model

Log Normal

Coefficient of Variation	$\eta = 0.984$
Mean	$\mu = -16.84$
Standard Deviation	$\sigma = 0.823$

Failure Rate Mean and Bounds

5% Lower Bound	Median	Mean	95% Upper Bound
$\lambda_{.95}$	$\lambda_{.5}$	$E\{\lambda\}$	$\lambda_{.95}$
0.0009	0.049	0.068	0.188

$$X\ 10^{-6}\ \text{per hour}$$

FILL VALVE (Colloid System)

The pressure differential across the colloid system
feed valve is very low when compared to the differentials
of the thermochemical system. The TRW Colloid Interim Final
Report #1 (Ref 14) uses a fill valve failure rate value of
0.073×10^{-6} per hour in the reliability assessment. This
is approximately an order of magnitude lower than the
expected value for the thermochemical fill valve failure
rate, and seems reasonable in light of the very low pressure
differentials in the colloid system. The value from Ref 14
will be used as the expected value of this assessment.
Since that report did not address failure rate uncertainties,
the thermochemical system fill valve uncertainty model will
be applied herein.

Component Reliability Model

$R = \exp(-\lambda t)$ where t = mission time
λ = failure rate per hour

Failure Rate Uncertainty Distribution Model

Log Normal

Coefficient of Variation	$\eta = 10.5$
Mean	$\mu = -18.79$
Standard Deviation	$\sigma = 2.17$

Failure Rate Mean and Bounds

5% Lower Bound	Median	Mean	95% Upper Bound
$\lambda_{.05}$	$\lambda_{.5}$	$E\{\lambda\}$	$\lambda_{.95}$
0.0002	0.0069	0.073	0.246

$$x\ 10^{-6} \text{ per hour}$$

PROPELLANT FILTER[*]

The similar function resulted in the use of the thermo-chemical filter model. The principal difference in application is the absence of a significant pressure differential across the colloid filter. While use of the thermochemical filter model should therefore yield conservative results in the colloid system, its use is recommended until endurance testing or flight experience indicates the appropriate modification.

Component Reliability Model

$$R = \exp\left[-\lambda t - \frac{t_{op}^{\beta}}{\alpha}\right]$$

λ_L = leaking failure rate

t = mission time

t_{op} = operating time

α = Weibull scale factor

β = Weibull shape factor

Failure Rate Uncertainty Distribution Model

Log Normal

Coefficient of Variation $\eta = 1.33$

Mean $\mu = -18.35$

Standard Deviation $\sigma = 1.667$

Failure Rate Mean and Bounds

5% Lower Bound	Median	Mean	95% Upper Bound
$\lambda_{.05}$	$\lambda_{.5}$	$E\{\lambda\}$	$\lambda_{.95}$
0.00067	0.0107	0.043	0.166

$$x\ 10^{-6}\ \text{per hour}$$

[*]Colloid System

Weibull Parameter Values and Bounds

Shape Parameter $\qquad \beta = 1.5$

Scale Parameter $\qquad \alpha \qquad$ Equivalent Mean and Bounds

5% Lower Bound	Mean	Median	95% Upper Bound
$\alpha_{.05}$	α_E	$\alpha_{.5}$	$\alpha_{.95}$
1.9×10^7	7.35×10^7	2.95×10^8	4.5×10^9

Partition by Failure Modes

1. Leakage

 1.1 Model

$$R = \exp\left(-\lambda_L t\right)$$

 1.2 Failure Rate Mean and Bounds

5% Lower Bound	Median	Mean	95% Upper Bound
$\lambda_{.05}$	$\lambda_{.5}$	$E\{\lambda\}$	$\lambda_{.95}$
0.00067	0.0107	0.043	0.166

$$X\ 10^{-6}\ \text{per hour}$$

2. Clogging

 2.1 Model

$$R = \exp\left[-\frac{t_{op}}{\alpha}\right]$$

 2.2 Weibull Parameter Values and Bounds

 Weibull Shape Parameter $\beta = 1.5$

 Weibull Scale Parameter α

5% Lower Bound	Mean	Median	95% Upper Bound
$\alpha_{.05}$	α_E	$\alpha_{.5}$	$\alpha_{.95}$
1.9×10^7	7.35×10^7	2.95×10^8	4.5×10^9

CONTROL BELLOWS (COLLOID)

The control bellows serves two purposes: initially, it assists in opening and closing the ball valve; in addition, it creates extra contraction that pulls back the propellant from needle tips and also allows for a small amount of leakage past the ball valve. Pullback is classified as a major goal of program; there are further hardware modifications that will result in increased reliability and that will also improve the startup procedure. The same reliability and uncertainty models and values are proposed as were used for the propellant storage bellows.

Component Reliability Model

$$R = \exp(-\lambda t)$$

where t = operating time
λ = failure rate per hour

Failure Rate Uncertainty Distribution Model

Lognormal

Coefficient of Variation $\eta = 0.985$

Mean $\mu = -16.84$

Standard Deviation $\sigma = 0.8236$

Failure Rate Mean and Bounds

5% Lower Bound	Median	Mean	95% Upper Bound
$\lambda_{.05}$	$\lambda_{.5}$	$E\{\lambda\}$	$\lambda_{.95}$
0.0125	0.0485	0.068	0.188

$$X10^{-6} \text{ per hour}$$

BALL VALVE (COLLOID SYSTEM)

The tungsten ball valve operates on a pressure differential basis similar to a one-way check valve. The valve is susceptible to leakage as a result of objects being trapped in the valve seat. The supply pressure, a result of the tension established by the bellows acting to close the valve, is about 3.5 in. of mercury(14). Failure mechanisms would be corrosion or contamination in the propellant storage system rather than any stuctural failure.

Component Reliability Model

$R = \exp(-\lambda t)$ where t = mission time
λ = failure rate per hour

Failure Rate Uncertainty Distribution Model

Lognormal

Coefficient of Variation η = 13.08

Mean μ = -17.31

Standard Deviation σ = 2.27

Failure Rate Mean and Bounds

5% Lower Bound	Median	Mean	95% Upper Bound
$\lambda_{.05}$	$\lambda_{.5}$	$E\{\lambda\}$	$\lambda_{.95}$
0.0007	0.03	0.4	1.27

$$X10^{-6} \text{ per hour}$$

Partition by Failure Modes

1. Fail Open

1.1 Model

$$R = \exp\{-\lambda_o t\}$$

t = mission time
λ_o = fail open rate

1.2 Failure Rate

$$E\{\lambda_o\} = 50\% \; E\{\lambda\}$$

1.3 Failure Rate Mean and Bounds

5% Lower Bound	Median	Mean	95% Upper Bound
$\lambda_{.05}$	$\lambda_{.5}$	$E\{\lambda\}$	$\lambda_{.95}$
0.0002	0.0108	.2	0.575

$$X10^{-6} \text{ per hour}$$

2. Fail Closed

2.1 Model

$$R = \exp\{-\lambda_c t\}$$

where t = mission time
λ_c = fail closed rate

2.2 Failure Rate

$$E\{\lambda_c\} = 50\% \; E\{\lambda\}$$

2.3 Failure Rate Mean and Bounds

5% Lower Bound	Median	Mean	95% Upper Bound
$\lambda_{.05}$	$\lambda_{.5}$	$E\{\lambda\}$	$\lambda_{.95}$
0.002	0.0108	0.20	0.575

$$X10^{-6} \text{ per hour}$$

ZEOLITE CANNISTER

When heated, zeolite releases CO_2, which increases the pressure, expands the control bellows, and actuates the tungsten ball valve. Allowing the zeolite to cool absorbs much of the CO_2 and reduces the internal pressure within the bellows. The power to the heater located in the zeolite cannister is regulated by comparing the exhaust beam current to a reference current(14). Reliability of system propellant delivery is based upon operation of the regulator mechanism and the heater. Failure of either mechanism would result in failure of the propulsion system in either the on or off position. Since the heater is assessed separately, the principal failure mode for the cannister is leaking.

Component Reliability Model

$$R = exp\ (-\lambda t)$$

where t = operating hours
λ = failure rate per hour

Failure Rate Uncertainty Distribution Model

Log Normal

Coefficient of Variation $\eta = 2.016$

Mean $\mu = -17.68$

Standard Deviation $\sigma = 1.27$

Failure Rate Mean and Bounds

5% Lower Bound	Median	Mean	95% Upper Bound
$\lambda_{.05}$	$\lambda_{.5}$	$E\{\lambda\}$	$\lambda_{.95}$
0.0026	0.0209	0.047	0.169

$$X\ 10^{-6}\ per\ hour$$

SYSTEM PROPELLANT MANIFOLD[*]

The propellant feed line model, failure rate and uncertainty distribution were used to model the colloid propellant manifold.

Component Reliability Model

$$R = \exp(-\lambda t)$$

where t = operating time
λ = failure rate per hour

Failure Rate Uncertainty Distribution Model

Lognormal

Coefficient of Variation	$\eta = 0.643$
Mean	$\mu = -16.39$
Standard Deviation	$\sigma = 0.588$

Failure Rate Mean and Bounds

5% Lower Bound	Median	Mean	95% Upper Bound
$\lambda_{.05}$	$\lambda_{.5}$	$E\{\lambda\}$	$\lambda_{.95}$
0.029	0.076	0.09	0.02

$X10^{-6}$ per hour

[*] Colloid System

ELECTROFLUIDIC ISOLATION VALVE

This component is yet to be developed. Its need, however, to minimize system damage upon thruster module failure, is evident. It would be premature at this time to assess in detail failure modes and rates. In order to allow system modeling, a model for this component was synthesized by joining the electric isolator model and the propellant isolation valve model from the thermochemical section.

Component Reliability Model

$$R = \exp \left[- \lambda_c N - \lambda_m t - \frac{t_{op}}{\alpha}^{\beta} \right]$$

where
λ_c = cycle fail rate
N = number of cycles
λ_m = mission time fail rate
t = mission time
t_{op} = operating time
α = Weibull scale factor
β = Weibull shape factor

Failure Rate Uncertainty Distribution Model

Log normal

	λ_c	λ_f
Coefficient of Variation	$\eta = 0.5155$	0.5165
Mean	$\mu = -17.17$	-17.26
Standard Deviation	$\sigma = 0.4855$	0.4863

Failure Rate Mean and Bounds

	5% Lower Bound	Median	Mean	95% Upper Bound	
	$\lambda_{.05}$	$\lambda_{.5}$	$E\{\lambda\}$	$\lambda_{.95}$	
λ_c	0.016	0.035	0.32	1.11	per cycle
λ_m	0.014	0.032	0.29	1.01	per hour

$$X\ 10^{-6}$$

Weibull Model Parameter Values and Bounds

Shape Factor $\beta = 2$

Scale Factor α

5% Lower Bound	Equivalent Mean	Median	95% Upper Bound
$\alpha_{.05}$	α_E	$\alpha_{.5}$	$\alpha_{.95}$
3.374×10^8	1.305×10^9	4.89×10^9	7.198×10^{10}

Partition by Failure Modes

1. Electric Isolation Failure

    1.1 Model
    $$R = \exp\left[-\frac{t_{op}}{\alpha}^{\beta}\right]$$

    1.2 Model Parameter Values and Bounds

    Weibull Shape Factor $\beta = 2$

    Weibull Scale Factor α

5% Lower Bound	Equivalent Mean	Median	95% Upper Bound
$\alpha_{.05}$	α_E	$\alpha_{.5}$	$\alpha_{.95}$
3.374×10^8	1.305×10^9	4.89×10^9	7.198×10^{10}

2. Fluidic Isolation Failure

    2.1 Model
    $$R = \exp\left[-\lambda_m t - \lambda_c N\right]$$

    2.2 Failure Rate Mean and Bounds

	5% Lower Bound	Median	Mean	95% Upper Bound
	$\lambda_{.05}$	$\lambda_{.5}$	$E\{\lambda\}$	$\lambda_{.95}$
λ_m	0.014	0.032	0.29	1.01 per hour
λ_c	0.016	0.035	0.32	1.11 per cycle

THRUSTER FRAME [*]

The thruster frame assembly includes the module frames, two temperature transducers and a heater. The reliability assessment of Ref. 14 assigns a value of 0.0447 per million operating hours. Previous assessment of a line, tank or valve heater indicate that this is a reasonable failure rate for the heater alone. The inclusion of the other components and the location of the frame relative to the extractor insulators, indicate that the failure rate assigned by Ref. 14 can best be used as a guide to the 5% Line Bound on the failure rate.

Component Reliability Model

$R = \exp(-\lambda t)$ where t = mission time
λ = failure rate per hour

Failure Rate Uncertainty Distribution Model

Lognormal

Coefficient of Variation $\eta =$ 3.64

Mean $\mu =$ -14.25

Standard Deviation $\sigma =$ 1.63

Failure Rate Mean and Bounds

5% Lower Bound	Median	Mean	95% Upper Bound
$\lambda_{.05}$	$\lambda_{.5}$	$E\{\lambda\}$	$\lambda_{.95}$
0.0445	0.65	5	9.47

$$X. \quad \text{per hour}$$

[*] Colloid Thruster System

I-118

THRUSTER MODULE [*]

Data collection for the colloid system reveals that the largest uncertainty of the system concerns the failure rates that have been assumed for the needle assemblies. The failure rates available for the needle/extractor assembly are arbitrary because of lack of historical data(14). Degrading effects revealed during a 4350-hour test program in which there was no evidence of approaching failure are discussed below.

Needle uniformity of construction is necessary to maintain high beam efficiencies. Early tests indicated that lack of quality control in fabrication was responsible for geometry variations and low efficiencies. Variations in rim geometry and needle depth contributed to wide variations in charge and velocity of the ejected droplets.

Contamination is possible if there is a lack of care in preparing the feed system and in establishing proper loading techniques. Oil-like contamination film on the needles prevents a complete wetting of the emitter source and a variation in the electrostatic field (non-uniform thrusting).

Three performance-degrading phenomena were noted (during the ground life test) that supposedly will be reduced in effect during operation in space and when suggested design changes are incorporated: (1) needle tar buildup, (2) material buildup on the shield, and (3) needle erosion.

The following assessment is based on a specific design and reflects failure rate estimates (Ref. 14) that seem nearer to a lower bound than to $E\{\lambda\}$. To facilitate analysis of other configurations, the estimates are for a submodule that consists of 36 needles, shield electrodes, and needle seals; three extractor insulators; and one plenum, with $\lambda_{0.05} = 0.031 \times 10^{-6}$.

---

[*] Colloid Thruster

Failure rate uncertainty distribution. The uncertainty is comparable to that associated with the mercury ion engine main isolator:

$$\eta^2 = 13.08$$
$$\sigma^2 = 2.645$$
$$\sigma = 1.626.$$

Constant failure rates are used despite possible redundancies that apply if degraded performance is allowable; redundancy can be imputed to submodule combinations when component/system relationships are examined.

Component Reliability Model

$R = \exp(-\lambda t)$ where t = mission time
λ = failure rate per hour

Failure Rate Uncertainty Distribution Model

Lognormal

Coefficient of Variation $\eta = 3.616$

Mean $\mu = -15.29$

Standard Deviation $\sigma = 1.62$

Failure Rate Mean and Bounds

5% Lower Bound	Median	Mean	95% Upper Bound
$\lambda_{.05}$	$\lambda_{.5}$	$E\{\lambda\}$	$\lambda_{.95}$
0.031	0.45	1.69	6.53

$$X10^{-6} \text{ per hour}$$

FILAMENT NEUTRALIZER

The purpose of the neutralizer is to provide a
sufficient quantity of electrons (by means of a heated
tungsten wire) to equal the positive current from the
thruster (14). Included with the filament is a positive po-
tential monitor, which is used to collect excess electrons from
the neutralized exhaust plasma. Two are used per system (one
redundant). Failure of the neutralizer would prevent
formation of a neutral plasma (at 50v) that extends through-
out the beam and merges with space potential.

Three possible failure modes are identified that can
influence the reliability of the colloid neutralizer:
(1) burnout of the filament (filament evaporation),
(2) filament wire cyclic fatigue, and (3) mounting spring
preload or variation of the spring constant (14). Filament
burnout is based upon a normal wear-out distribution,
whereas the other failure modes are time and cyclic
sensitive.

The primary failure mode of the neutralizer is
filament evaporation. An accelerated life test was conducted
by operating the filament at higher temperatures than
normal ones seen during operation. Initial analyses had
correlated failure with 6 percent change in filament
diameter. However, the accelerated life tests indicated
that complete burnout occurred after a 12 percent reduction
in filament diameter. The life expectancy is based at
24,000 hr. when 8.5 percent reduction in diameter has
occurred. Operation beyond 8.5 percent reduction will
result in nonuniform electron emission, which would require
a higher injection potential and would promote further
burnout.

Component Reliability Model

$$R = [\exp(-\lambda t)] \left\{ \int_t^\infty \frac{1}{\sqrt{2\pi}\, s_b} \exp\left[-\frac{(t-m_b)^2}{2s_b^2} \right] dt \right\}$$

$$\left\{ \int_t^\infty \frac{1}{\sqrt{2\pi}\, s_c} \exp\left[-\frac{(t-m_c)^2}{2s_c^2} \right] dt \right\}$$

where t = mission time

Note: The second and third components of the model are normal distributions for filament burnout and on-off cycling respectively. The normal distribution is commonly tabulated with table look up using $K_b = \dfrac{t - m_b}{s_b}$ and $K_c = \dfrac{t - m_c}{s_c}$ definitions of t, m, s.

Failure Rate, λ, Uncertainty Distribution Model

Coefficient of Variation	$\eta =$	3.804
Mean	$\mu =$	-14.78
Standard Deviation	$\sigma =$	1.655

Failure Rate Mean and Bounds

5% Lower Bound	Median	Mean	95% Upper Bound
$\lambda_{.05}$	$\lambda_{.5}$	$E\{\lambda\}$	$\lambda_{.95}$
0.024	0.38	1.5	5.8

$$X10^{-6} \text{ per hour}$$

Burnout Normal Contribution Parameter, m_b, Values and Bounds

5% Lower Bound	Mean = Median	95% Upper Bound
$m_{b.05}$	$m_{b.05}$	$m_{b.95}$
10,000	20,000	30,000

$$s_b = 3\, M_b$$

Cyclic Normal Contribution Parameter, m_c, Values and Bounds

5% Lower Bound	Mean = Median	95% Upper Bound
$m_{c.05}$	$m_{c.5}$	$m_{c.95}$
9,250	18,500	27,750

I-122

Conversions

1. m_b already in terms of time conversion not required.
2. Convert m_c to time base using $\left(\dfrac{\text{total mission hours}}{\text{total number of cycles}}\right)$

as the conversion factor.

THERMOCHEMICAL PROPULSION COMPONENTS
RELIABILITY MODELS

INDEX TO THERMOCHEMICAL PROPULSION
COMPONENTS RELIABILITY MODELS

PRESSURIZED TANK

The failure modes for this component are rupture and leakage. Most imperfections will be minute, leading to leak failure rather than rupture (a distribution of 80% leak failure and 20% rupture failure is indicated). Typical failure locations include diaphragm (or bladder) and tank interface, valve and tank interface, and welded joints. The principal failure mechanisms include handling and workmanship and corrosion. Metal fatigue has also been suggested as a possible mechanism of lower importance.

Component Reliablity Model

$R = \exp(-\lambda t)$ where t = pressurized time
λ = failure rate

Failure Rate Uncertainty Distribution

Log Normal

Coefficient of Variation $\eta = 2.5$

Mean $\mu = -16.27$

Standard Deviation $\sigma = 1.4075$

Failure Rate Mean and Bounds

5% Lower Bound	Median	Mean	95% Upper Bound
$\lambda_{.05}$	$\lambda_{.5}$	$E\{\lambda\}$	$\lambda_{.95}$
.0085	0.086	.231	.87

$$X10^{-6} \text{ per hour}$$

Partition by Tank Halves (to accommodate tank/bladder systems)

1.   Propellant Half Failure

   1.1 Model $R = \exp(-\lambda t)$

   1.2 Failure Rate

      $E\{\lambda_{prop}\} = 50\% \ E\{\lambda\}$.

   1.3 Failure Rate Mean and Bounds

5% Lower Bound	Median	Mean	95% Upper Bound
$\lambda_{.05}$	$\lambda_{.5}$	$E\{\lambda\}$	$\lambda_{.45}$
0.0022	0.032	0.116	0.452

$$\times 10^{-6} \text{ per hour}$$

2.   Pressurant Half Failure

   2.1 See 1.1

   2.2 See 1.2

   2.3 See 1.3

BLADDER/DIAPHRAGM

The function of these devices is to provide for expulsion of the propellants while simultaneously preventing the pressurant gases from flowing further downstream in the system. A well defined choice of materials for these components must be made on the basis of the design operating life of the system. Elastomerics (such as EPT and the AFE series) can be considered for life times of about 7 years with hydrazine fuels and about 3 years with oxidizers. For longer periods of time metallic devices must be considered, primarily because of swelling and permeation of elastomerics when in contact with propellants such as nitrogen tetroxide.

Failure modes for these expulsion devices are primarily leakage and rupture, which are caused by (1) imperfections in the materials and fabrication processes and (2) folding tears (elastomeric) and fracture (metallic) and (3) pinholing. Corrosion of the metallic moving parts and metal to metal seals during long missions is another failure mechanism.

Component Reliability Model, Elastomerics

Elastomerics bladders and diaphragms were assessed as having a 5-7 year life time with hydrazine fuels and a 3 year life time with oxidizers. The life limiting mechanisms are swelling and permeation after prolonged contact with the propellants. In order to model this behavior the following composite model was selected:

	Fuel	Oxidizer
$R = \exp(-\lambda t)$	for $0 \leq t \leq 2.5$ yrs	$0 \leq t \leq 1.5$ yrs
$R = \exp\left[-\lambda t - \dfrac{(t - \delta)^{\beta}}{\alpha}\right]$	for 2.5 yrs $\leq t$	1.5 yrs $\leq t$
	δ: 2.2×10^{4} hrs	1.3×10^{4} hrs

where λ = random time dependent failure
rate

t = mission time

α = Weibull model scale factor

β = Weibull model shape factor

δ = delay factor.

1.   Fuel (Hydrazine) application: Data was available
to determine a failure rate (λ) and uncertainty distri-
bution for the random failure component. The Weibull
component parameters (α, β) were calculated to reflect
the reported upper limits (5 to 7 years) for elastomeric
hydrazine compatibility.

2.   Oxidize application: The same random failure rate
and uncertainty distribution was used as identified for
fuels application. The Weibull model component param-
eters were calculated to reflect the reported life limit
(3 years) for use of elastomerics with oxidizer (N_2O_4).

Failure Rate Uncertainty Distribution Elastomerics

Log Normal

Coefficient of Variation	$\eta = .75$
Mean	$\mu = -14.56$
Standard Deviation	$\sigma = .688$

Failure Rate Mean and Bounds, Elastomerics

5% Lower Bound	Median	Mean	95% Upper Bound
$\lambda_{.05}$	$\lambda_{.5}$	$E\{\lambda\}$	$\lambda_{.95}$
.15	.48	.6	1.48

$$X\ 10.^{-6}\ \text{per hour}$$

Weibull Scale Factor Mean and Bounds, Elastomerics

	5% Lower Bound $\alpha_{.05}$	Mean α_E	Median $\alpha_{.5}$	95% Upper Bound $\alpha_{.95}$
Hydrazine Application	5×10^5	1.233×10^6	1.54×10^6	4.93×10^6
Oxidizer (N_2O_4) Application	3.7×10^8	9.085×10^8	1.135×0^9	3.63×10^9

Weibull Shape Factor, β and Delay Factor δ, Elastomerics

	β	δ
Hydrazine Application	1.2	2.2×10^4 hrs
Oxidizer (N_2O_4) Application	2	1.3×10^4 hrs

Component Reliability Model, Metallics

$$R = \exp(-\lambda t) \quad , \text{ for } 0 \le t \le 5 \text{ year}$$

$$R = \exp\left[-\lambda t - \frac{(t - \delta)^\beta}{\alpha}\right], \text{ for } 5 \le t \le 10 + \text{ year}$$

where $\delta = 4.3 \times 10^4$ hrs
λ = random time dependent failure rate
t = mission time
α = Weibull model scale factor
β = Weibull model shape factor
δ = delay factor.

Failure Rate Uncertainty Distribution

Log Normal

Coefficient of Variation	$\eta = 4.18$
Mean	$\mu = -17.38$
Standard Deviation	$\sigma = 1.7083$

Failure Rate Mean and Bounds, Metallic

5% Lower Bound	Median	Mean	95% Upper Bound
$\lambda_{.05}$	$\lambda_{.5}$	$E\{\lambda\}$	$\lambda_{.95}$
.0017	0.028	.122	.471

$$X\ 10^{-6}\ \text{per hour}$$

Weibull Scale Factor Mean and Bounds

5% Lower Bound	Median	Mean	95% Upper Bound
$\alpha_{.05}$	$\alpha_{.5}$	α_E	$\alpha_{.95}$
2.42×10^6	4.079×10^7	9.36×10^6	6.72×10^8

Weibull Shape Factor, $\beta = 1.2$

PROPELLANT FEED LINES

While the feed line environments and propellants are quite different for the two propulsion system classes, certain similarities override from the reliability point of view. Failure modes of leakage and rupture are common to both. Manufacturing process such as welding and swaging are also common potential sources of damage. Further, the available reliability data for each group overlap in comparison. Therefore, a single reliability and uncertainty model set will be formulated.

Component Reliability Model

$$R = \exp(-\lambda t)$$

where t = operating time
λ = failure rate

Failure Rate Uncertainty Distribution

Log normal

Coefficient of variation $\eta = .42$

Mean $\mu = \cdot 16.4$

Standard Deviation $\sigma = .592$

Failure Rate Mean and Bounds

5% Lower Bound	Median	Mean	95% Upper Bound
$\lambda_{.05}$	$\lambda_{.5}$	$E\{\lambda\}$	$\lambda_{.95}$
0.0235	.076	0.09	0.2

$$X10^{-6} \text{ per hour}$$

FILL VALVE

This component is used to introduce the pressurant or propellant into its storage tank. Upon completion of fluid loading the valve is closed and if launch occurs on schedule it remains in this position throughout the remainder of the mission. Failure modes of this component are rupture and internal leakage of the valve seat. Rupture can be caused by flaws appearing randomly in the material and by stresses during launch. Redundancy for this component is achieved by capping with valve closure caps:

Component Reliability Model

$$R = \exp(-\lambda t)$$

where t = pressurized time
λ = failure rate

Failure Rate Uncertainty Distribution

Lognormal

Coefficient of Variation	$\eta = 10.5$
Mean	$\mu = -16.21$
Standard Deviation	$\sigma = 2.1703$

Valves in general are exposed to repeated cyclic operation and their reliability models reflect the situation with cyclic dependent functions that can often drive the overall expression. Fill valves however, can be expected to be cycled only a few times in system pressure tests and finally once more upon charging the propellant storage tank prior to launch. It will then become a passive component of the system; expected to last the mission in the finally closed condition. Therefore its reliability model includes a time dependent function only. The deleterious effects of test cycling prior to final charging are included in the

developed failure rate to be applied throughout the mission.

Failure Rate Mean and Bounds

5% Lower Bound	Median	Mean	95% Upper Bound
$\lambda_{.05}$	$\lambda_{.5}$	$E\{\lambda\}$	$\lambda_{.95}$
.003	0.091	.09	.323

$$X10^{-6} \text{ per hour}$$

REGULATOR

The function of the regulator is to maintain a set pressure of pressurant gas delivered to the propellant tanks. This component would not be required in a blow-down system. Its failure modes include (1) leakage to space due to case failure, (2) fail open and fail closed due to erosion of the seat, (3) contamination, and (4) corrosion. Contamination can cause deformation of valve seals and added friction between moving parts, resulting in reduced ability to open and close.

Component Reliability Model

$$R = \exp\left[-\lambda_d(t - t_{op}) - \lambda_{op}t_{op} - \lambda_c N\right]$$

Where λ_d = failure rate for non-firing mission phases

t = total mission time

t_{op} = operating time

λ_{op} = failure rate for firing mission phases

λ_c = failure rate per cycle

λ_N = total cycles

Failure Rate Uncertainty Distributions

Lognormal		λ_d	λ_{op}	λ_c
Coefficient of variation, η		1.48	2.09	1.35
Mean	μ	-12.77	-7.41	-12.09
Standard Deviation	σ	1.0765	1.2965	1.0188

Failure Rate Mean and Bounds

	5% Lower Bound $\lambda_{.05}$	Median $\lambda_{.5}$	Mean $\{E\}\lambda$	95% Upper Bound $\lambda_{.95}$
λ_d	.48	2.86	5.1	16.5
λ_{op}	71.7	605	1402	5106
λ_c	.048	5.6	9.42	30.0

$$X10^{-6} \text{ per hour (cycle)}$$

Partition by Failure Modes

1. Fail Low

1.1 Model $R = \exp\left[- \lambda_{dl}t_{dl} - \lambda_{opl}t_{op} - \lambda_{cl}N\right]$

1.2 Failure Rates

$$E\{\lambda_{dl}\} = 40\%\{E\ \lambda_d\}$$
$$E\{\lambda_{opl}\} = 40\%\{E\ \lambda_{op}\}$$
$$E\{\lambda_{cl}\} = 40\%\{E\ \lambda_c\}$$

1.3 Failure Rate Mean and Bounds

	5% Lower Bound $\lambda_{.05}$	Median $\lambda_{.5}$	Mean $\{E\}\lambda$	95% Upper Bound $\lambda_{.95}$
λ_{dl}	0.197	1.14	2.04	6.6
λ_{opl}	28.5	242	5.61	2054
λ_{cl}	0.418	2.24	3.77	12

$$X10^{-6} \text{ per hour (cycle)}$$

2. Fail High or Oscillatory

   2.1 Model $R = \exp\left\{-\lambda_{dh}t_d\ -\lambda_{oph}t_{op}\ -\lambda_{ch}N\right\}$

   2.2 Failure Rates

   $$E\left\{\lambda_{dh}\right\} = 60\%\ E\left\{\lambda_{ds}\right\}$$

   $$E\left\{\lambda_{oph}\right\} = 60\%\ E\left\{\ _{r}\right\}$$

   $$E\left\{\lambda_{ch}\right\} = 60\%\ E\left\{\lambda_{c}\right\}$$

   2.3 Failure Rate Mean and Bounds

	5% Lower Bound $\lambda_{.05}$	Median $\lambda_{.5}$	Mean $E(\lambda)$	95% Upper Bound $\lambda_{.95}$
λ_{dh}	0.295	1.71	3.06	9.9
λ_{oph}	43	363	841	3064
λ_{ch}	0.63	3.36	5.65	18

$$X10^{-6}\ \text{per hour (cycle)}$$

CHECK VALVE

The function of the check valve is to control the direction of flow through the system and to isolate the thruster from interconnecting systems. The failure modes are leakage, fail open, and fail closed. The failure mechanisms are metal-to-metal valve seat fretting for hard seat valves, polymer seat material flow under load or high temperature, binding and seizing of closure guide elements due to contamination, and fatigue.

Component Reliability Model

$$R = \exp[-\lambda_c N - \lambda_m t]$$

where λ_c = cycle failure rate

       N = number of cycles

       λ_m = failure rate per hour

       t = mission time

Failure Rate Uncertainty Distribution Model

Log normal		λ_t	λ_c
Coefficient of Variation	$\eta =$	1.91	11.9
Mean	$\mu =$	-13.4	-10.05
Standard Deviation	$\sigma =$	1.2402	2.2273

Failure Rate Mean and Bounds

	5% Lower Bound $\lambda_{.05}$	Median $\lambda_{.5}$	Mean $E\{\lambda\}$	95% Upper Bound $\lambda_{.95}$
λ_c	.68	26.4	315	1029
λ_t	.197	1.52	3.28	11.7

Partition by Failure Mode

1. Fail Open

   1.1 Model: $R = \exp(-\lambda_c N - \lambda_f t)$

   1.2 Failure Rates

   $$E\{\lambda_{co}\} = 25\% \{E\ \lambda_c\}$$

   $$E\{\lambda_{fo}\} = 25\% \{E\ \lambda_f\}$$

   1.3 Failure Rate Mean and Bounds

	5% Lower Bound $\lambda_{.05}$	Median $\lambda_{.5}$	Mean $E\{\lambda\}$	95% Upper Bound $\lambda_{.95}$
λ_c	0.169	6.59	78.8	257
λ_f	0.0493	0.38	0.82	2.93

   $X10^{-6}$ per hour (cycle)

2. Fail Closed

   2.1 See 1.1

   2.2 See 1.2

   2.3 See 1.3

3. Fail Partial

    3.1 Model: $R = \exp(-\lambda_{cp}N - \lambda_{fp}t)$

    3.1 Failure Rates

$$E\{\lambda_{cp}\} = 50\% \; E\{\lambda_c\}$$

$$E\{\lambda_{fp}\} = 45\% \; E\{\lambda_f\}$$

    3.2 Failure Rate Mean and Bounds

	5% Lower Bound $\lambda_{.05}$	Median $\lambda_{.5}$	Mean $E\{\lambda\}$	95% Upper Bound $\lambda_{.95}$
λ_c	0.338	13.2	158	515
λ_f	0.042	0.486	1.476	5.64

$$X10^{-6} \text{ per hour (cycle)}$$

4. Leak to space

    4.1 Model: $R = \exp(\lambda_{fL})t$

    4.2 Failure Rate

$$E\{\lambda_{fL}\} = 5\% \; E\{\lambda_f\}$$

    4.3 Failure Rate Mean and Bounds

	5% Lower Bound $\lambda_{.05}$	Median $\lambda_{.5}$	Mean $E\{\lambda\}$	95% Upper Bound $\lambda_{.95}$
λ_{fL}	0.00064	0.019	.164	0.58

$$X10^{-6} \text{ per hour}$$

ISOLATION VALVE

This component used to isolate portions of a fluid
system (such as pressurant gas from propellant tanks or
stored propellant from downstream components). Solenoid
valves are most commonly used in this capacity although
explosive actuated valves find use in systems where no
pressurant leakage is desired for long durations. Failure
mode for the explosively activated valve include failure of
the electrical leads, failure of the initiator, failure of
the explosive and rupture of the housing under explosive
pressure. Failure modes for the reusable solenoid configu-
rations include fail open, fail closed, internal leakage
and leak to space. Fail open/Fail closed mechanism include
electrical failure, seizure of the armature in the coil
housing, contamination or fretting between moving parts.
Internal leakage mechanisms include metal-to-metal seat
fretting from vibrational exposure, particulate contamina-
tion, imperfection in fabrication and loss of spring
strength.

Component Reliability Model - Solenoid Valve

$$R = \exp(-\lambda_c N - \lambda_f t)$$

where t = mission time
N = number of cycles
λ_c = cyclic failure rate
λ_f = time dependent failure rate

Failure Rate Uncertainty Distribution - Solenoid Valve

Log Normal	λ_c	λ_f
Coefficient of Variation	$\eta = 10.5$	8
Mean	$\mu = -17.31$	-17.14
Standard Deviation	$\sigma = 2.1707$	2.0431

Failure Rate Mean and Bounds - Solenoid Valve

	5% Lower Bound $\lambda_{.05}$	Median $\lambda_{.5}$	Mean $E\{\lambda\}$	95% Upper Bound $\lambda_{.95}$
λ_c	.001	0.03	.32	1.08
λ_f	.001	0.036	.29	1.04

$$X10^{-6} \text{ per hour (cycle)}$$

Partition by Failure Modes

1. Fail Open

    1.1 Model: $\quad R = \exp\left[-\lambda_{co} N - \lambda_{fo} t\right]$

    1.2 Failure Rates: $E\{\lambda_{fo}\} = 10\%\{E\lambda_f\}; \quad E\{\lambda_{c\mu}\} = 10\%\{E\lambda_c\}$

    1.3 Failure Rate Mean and Bounds

	5% Lower Bounds $\lambda_{.05}$	Median $\lambda_{.5}$	Mean $E\{\lambda\}$	95% Upper Bounds $\lambda_{.95}$
λ_{fo}	0.00013	0.0036	0.029	0.104
λ_{co}	0.00008	0.003	0.032	0.108

$$X10^{-6} \text{ per hour (cycle)}$$

I-142

2. Fail Closed

    2.1 Model:
$$R = \exp\left[\lambda_{co}N - \lambda_{fo}t\right]$$

    2.2 Failure Rates: $E\{\lambda_{f_C}\} = 30\% \; E\{\lambda_f\}; E\{\lambda_{cp}\} = 60\% \; E\{\lambda_c\}$

2.3 Failure Rate Mean and Bounds

	5% Lower Bounds	Median	Mean	95% Upper Bounds
	$\lambda_{.05}$	$\lambda_{.5}$	$E\{\lambda\}$	$\lambda_{.95}$
λ_{fo}	0.0004	0.0108	0.087	0.312
λ_{co}	0.00025	0.009	0.096	0.324

$$X10^{-6} \text{ per hour (cycle)}$$

3. Fail Partial

    3.1 Model:
$$R = \exp\left[-\lambda_{cp} \, N - \lambda_{fp} \, t\right]$$

    3.2 Failure Rates: $E\{\lambda_{fp}\} = 55\% \; E\{\lambda_f\}; \; \lambda_{cp} = 60\% \; E\{\lambda_c\}$

3.3 Failure Rate Mean and Bounds

	5% Lower Bounds	Median	Mean	95% Upper Bounds
	$\lambda_{.05}$	$\lambda_{.5}$	$E\{\lambda\}$	$\lambda_{.95}$
λ_{fp}	0.0006	0.020	0.16	0.624
λ_{cp}	0.0005	0.018	0.192	0.648

$$x10^{-6} \text{ per hour (cycle)}$$

4. Leak to Space

    4.1 Model: $R = \exp\left[-\lambda_{fL}t\right]$

    4.2 Failure Rate: $E\{\lambda_{fl}\} = 5\% \ E\{\lambda_f\}$

    4.3 Failure Rate Mean and Bounds

	5% Lower Bounds	Median	Mean	95% Upper Bounds
	$\lambda_{.05}$	$\lambda_{.5}$	$E\{\lambda\}$	$\lambda_{.95}$
λ_{fL}	0.00006	0.0018	0.0145	0.052

$$x10^{-6} \text{ per hour}$$

Component Reliability Model - Explosive Valve

The reliability of this device is driven by the actuator (explosive) and as such is best modelled by a lognormal success probability distribution. Prior to activation the device can be expected to have a reliability of 1.0. The lognormal model is applied to determine the probability of success at the expected time of activation.

Uncertainty Distribution Parameters and Reliability Values Means and Bounds - Explosive Valve

	5% Lower Bound $R_{.05}$	Mean $E\{R\}$	95% Upper Bound $R_{.95}$
σ	.3991	.3991	.3991
R(1yr)	>.99997	≫.99997	≫.99997
R(3yrs)	.899⌐	.9948	.9983
R(5yrs)	.5	.9	.95
R(7yrs)	.1996	.6689	.7887
R(10yrs)	.0412	.324	.4634

LATCH VALVE

The function of this valve is to provide selected interconnection and isolations between the propellant tanks, and multiple thrusters. These are solenoid actuated valves and they experience failure modes and mechanism similar to the solenoid isolation valves. The reliability model developed for the solenoid isolation valves should apply here as well.

Component Reliability Model

$$R = \exp\left[-\lambda_c N - \lambda_f t\right]$$

where t = mission time
N = number of cycles
λ_c = cyclic failure rate
λ_f = time dependent failure rate

Failure Rate Uncertainty Distribution

see Solenoid Isolation Valves

Failure Rate Mean and Bounds

see Solenoid Isolation Valves

RELIEF VALVE

The function of this component is to protect the propellant tanks from overpressurization. Its failure modes and mechanisms are: failure to open due to armature sticking, failure to close due to spring failure or armature sticking, and seal leakage. Spring failures can result from material imperfections and fatigue; armature sticking can result from contamination; and seal leakage can result from contamination on the seat.

Component Reliability Model

$$R = \exp\left[-\lambda_m t_m - \lambda_c N\right]$$

where λ_f = failure rate per mission hour

λ_c = failure rate per cycle

t_m = mission time

N = number of cycles

Failure Rate Uncertainty Distribution Model

Log normal		λ_f	λ_c
Coefficient of Variation	$\eta =$	12.94	1.12
Mean	$\mu =$	-15.03	-13.178
Standard Deviation	$\sigma =$	2.2642	.9018

Failure Rate Mean and Bounds

	5% Lower Bound $\lambda_{.05}$	Median $\lambda_{.5}$	Mean $E\{\lambda\}$	95% Upper Bound $\lambda_{.95}$
λ_f	.0072	0.297	3.857	12.32
λ_c	.43	1.892	2.841	8.34

$$X10^{-6} \text{ per hour (cycle)}$$

BURST DIAPHRAGM

A burst diaphragm, like an electrical fuse, has a different purpose in a nonrepairable system than in a conventional application. In conventional applications, such devices may be intended either to limit damage to the equipment in which they are installed or to protect a system in which the equipment is nonessential. In nonrepairable systems, only the latter function is meaningful because it may involve personnel safety.

Premature bursting of a diaphragm results in equipment failure; failure to burst when intended constitutes system failure. For purposes of the second failure mode, the burst diaphragm is redundant with (strictly speaking, is a backup to) the relief valve and should be regarded as having failed only if pressure containment is lost and injury or system damage results.

Tradeoff between the two failure modes is inherent: reducing the probability of premature bursting virtually guarantees an increased probability of failure to burst, and conversely, the existence of redundancy in the failure-to-burst mode influences the tradeoff.

The reliability estimation problem is compounded further by the fact that burst diaphragm failure must be defined in somewhat complicated forms. Premature bursting occurs if pressure exceeds burst strngth and is less than the lower of actual or intended relief valve setting. Failure to burst occurs when burst strength of the diaphragm exceeds that elsewhere in the fluid containment and pressure becomes excessive, the latter being possible if the relief valve malfunctions. Such compound phenomena must be dealt with above the component level. At the system level, components such as the burst diaphragm can be treated by assuming that their reliability can be made high enough (when used with another component such as a relief valve) to yield negligible system level effect.

FILTER

Propellant leakage due to loss of integrity of the filter housing or welds can be characterized by a constant failure rate, mission-time dependent, exponential model. Clogging and the associated failure rate tend to increase this time; this suggests a Weibul model using operating time as the variable. The shape parameter should not be much greater than one since longevity depends on variable contamination levels and is not defined sharply; $\beta = 1.5$ was selected.

Component Reliability Model

$$R = \exp\left[-\lambda_L t - \frac{t_{op}^{\beta}}{\alpha_c}\right]$$

λ_L = leakage failure rate
t = mission time
t_{op} = operating time
β = shape factor = 1.5
α_c = scale factor

The values for the failure rate (λ_L) and the scale factor (α_c) were determined in the following manner. Available data (eight sources) for filter failure rates indicated an expected total failure rate value of $E\{\lambda\} = 0.0863 \times 10^{-6}$/hr

The data base further indicated an approximately equal apportionment to leakage and clogging yielding

$$\lambda_L t = .043 \times 10^{-6}/hr$$

$$\lambda_c = .043 \times 10^{-6}/hr$$

In order to transform the clogging failure rate to the more appropriate Weibull model, the exponential model and the Weibull model were set equal (equal expected reliability) at 10,000 mission hours.

$$R = \exp(-\lambda_c t) = \exp - \left[\frac{t_{op}}{\alpha_c} \right]^{\beta}$$

and a ratio of 10:1 used for mission time to operating time. Using previously estimated values

$$\beta = 1.5$$

$$E\{\lambda\}_c\} = .043 \text{ X.} 10^{-6}/\text{hr}$$

a value for the scale factor at $E\{\lambda_c\}$ was obtained

$$\alpha_c = 7.35 \text{X} 10^7$$

Failure Rate Uncertainty Distribution Model (Leaking)

Lognormal

Coefficient of Variation	$\eta = 4$
Mean	$\mu = -18.345$
Standard Deviation	$\sigma = 1.66$

Failure Rate Mean and Bounds (Leaking)

5% Lower Bound	Median	Mean	95% Upper Bound
$\lambda_{.05}$	$\lambda_{.5}$	$E\{\lambda_L\}$	.95
.0007	0.0107	.043	.166

$$\text{X} 10^{-6} \text{ per hour}$$

Clogging Failure Weibull Model Mean and Bounds

5% Lower Bound	Median	Mean	95% Upper Bound
$\alpha_{c.05}$	$\lambda_{.5}$	α_{CE}	$\alpha_{c.95}$
1.9×10^7	2.94×10^8	7.35×10^7	4.5×10^9

Partition by Failure Modes

1. Leakage

    1.1 Model $R = \exp(-\lambda t)$

    1.2 Failure Rate Mean and Bounds

5% Lower Bound	Median	Mean	95% Upper Bound
$\lambda_{.05}$	$\lambda_{.5}$	$E\{\lambda\}$	$\lambda_{.95}$
.0.0007	0.0107	0.043	0.166

$$X10^{-6} \text{ per hour}$$

2. Clogging

    1.1 Model $R = \exp \left[\dfrac{-(t_{op})^\beta}{\alpha} \right]$

    1.2 Weibull Parameter Values and Bounds

5% Lower Bound	Equivalent Mean	Median	95% Upper Bound
$\alpha_{.05}$	α_E	$\alpha_{.5}$	$\alpha_{.95}$
1.9×10^7	7.35×10^7	2.94×10^8	4.5×10^9

HEATER (tank, line and valve)

To prevent the freezing of propellant which produces either degraded performance or catastrophic failure previously described, electrical heaters are used to maintain a satisfactory thermal environment. Heater locations need to be determined as the thruster system is adapted to the spacecraft. There may be as many as three heaters applied to the tank, line, and propellant control valve, although a smaller number is more likely.

A heater failure rate contained in the NRN[*] for the satellite environment is:

$$\lambda = 0.450 + 350\%, -95\% \text{ per } 10^6 \text{ part hours.}$$

Lacking any information to the contrary, it is believed that the heaters on which the data were accumulated had an environmental conditioning function similar to the present application. Therefore, this rate is estimated as appropriate. The question that cannot be definitely answered is the extent of the duty cycle since it will be dependent on the satellite orbit and the need for environmental protection at the spacecraft location.

The kinds of failures expected exclude those arising from wide temperature excursions and other stress-inducing phenomena. More likely sources of failure are imperfections which occur randomly. A constant failure is appropriate.

Component Reliability Model

$R = \exp(-\lambda t)$ where t = mission hours

Failure Rate Uncertainty Distribution Model

Log Normal

Coefficient of Variation	$\eta = 2.016$
Mean	$\mu = -17.68$
Standard Deviation	$\sigma = 1.27$

---

[*] NEDCO Reliability Notebook

Failure Rate Mean and Bounds

5% Lower Bound	Median	Mean	95% Upper Bound
$\lambda_{.05}$	$\lambda_{.5}$	$E\{\lambda\}$	$\lambda_{.95}$
0.0025	0.021	0.047	0.169

$$x \ 10^{-6} \text{ per hour}$$

HEATER, EXTERNAL THRUSTER APPLICATION

The operational environment of the heater in this application is characterized by thermal cycling and thermal gradient. At low duty cycles, cooling between firings can lead to thermal excursions of nearly 1000 F. Prolonged exposure to high temperatures results from its position on the thrust chamber wall. Under these conditions fractures can result from the induced thermal stresses. Insulation failure can lead to shorting between the conducting heater element and the sheath. Hot spots can develop in the heater element at capacity locations or at necked areas produced in the drawing process. Another potential failure occurs at the joints of the heater filament and adjacent conductors. Over stress can occur in brazing or welding during the fabrication process. Most insulator materials used are hygroscopic. Without proper control in the fabrication process, absorbed moisture can lead to insulator breakdown in operation.

This component is further characterized by a "burn in" or "in/out" mortality period. This effect was incorporated in the model by using an initial reliability value less than 1.0.

Component Reliability Model

$$R = P \cdot \exp\left[-\lambda_c N - \frac{t_{op}^{\beta}}{\alpha}\right]$$

where P = infant mortality factor

λ_c = heater cycle failure rate

t_{op} = heater operating time

β = Weibull shape factor = 3

α = Weibull scale factor

N = number of heater cycles

Cyclic Failure Rate Uncertainty Distribution

  Log normal

  Coefficient of variation $\eta =$ 3.09

  Mean $\mu =$ -17.1482

  Standard Deviation $\sigma =$ 1.5354

Cyclic Failure Rate Mean and Bounds

5% Lower Bound	Median	Mean	95% Upper Bound
$\lambda_{c.05}$	$\lambda_{.5}$	$E \lambda_c$	$\lambda_{c.95}$
0.00286	0.0357	0.116	0.446

$$X10^{-6} \text{ per cycle}$$

Operating Time (Weibull Scale Factor) Mean and Bounds

5% Lower Bound	Mean	Median	95% Upper Bound
$\alpha_{.05}$	α_E	$\alpha_{.5}$	$\alpha_{.95}$
1.64×10^{12}	6.3×10^{12}	2.046×10^{13}	2.56×10^{14}

Infant Mortality, P, Mean and Bounds

5% Lower Bound	Median/Mean	95% Upper Bound
$P_{.05}$	$E\{P\}$	$P_{.95}$
.977	.99	~.999

HEATER, INTERNAL THRUSTER APPLICATION

Notwithstanding the presence of the protective tube, the cycle of the heater is severe. In the pulse mode of operation, the heater is in a transient state as it delivers heating effects over a short period of time and is further heated by the reaction. At duty cycles below 4 percent, cooling between pulses can bring the temperature down so that the excursion can be nearly 1,000°F. Under thermal cycling conditions, stress cycling is inevitable. In addition to cycling, there are thermal gradients under near steady-state operating conditions. For the case of the axial heaters, after current is turned off, the filaments will be conducting heat away as the protective tube rises in temperature under the influence of the decomposition reaction. Additionally, the dissimilar materials on the metal parts and insulator of the heating element, having different expansion rates, will compound the stresses due to nonuniform temperature distribution.

The failure modes and mechanisms are in general the same for the internal application and to the external application thruster heater. The resulting model is therefore the same. The heightened severity of the internal heater environment is reflected in the model parametic valves.

The limited experience base (one firm) with heaters in this application is reflected in the magnitude of the uncertainty distribution parameters.

The complex model developed initially was replaced with one following the general form of the external heater reliability model. The parameter values differ since the only internal heater configuration assessed in the study differs from other sheath heaters. This dual inconel filament sheath heater was designed and produced by one firm.

Component Reliability Model

$$R = P \exp\left[-\lambda_c N - \frac{t_{op}}{\alpha}^{\beta}\right]$$

where P = Infant Mortality factor
λ_c = cyclic failure rate
N = number of heater cycles

t_{op} = heater operating time
β = Weibull shape factor = 3.5
α = Weibull scale factor

Cyclic Failure Rate Uncertainty Distribution Model

Log Normal

Coefficient of Variation η = 7.32

Mean μ = -17.182

Standard Deviation σ = 2.0

Cyclic Failure Rate Mean and Bounds

5% Lower Bound	Median	Mean	95% Upper Bound
λ_{05}	$\lambda_{.5}$	$E\{\lambda\}$	$\lambda_{.95}$
.0012	0.0345	.255	.926

$$X10^{-6} \text{ per cycle}$$

Infant Mortality, P, Mean and Bounds

5% Lower Bound	Mean	95% Upper Bound
$P_{.05}$	$E\{P\}$	$P_{.95}$
.91	.96	.99

Operating Time (Weibull Scale Factor) Mean and Bounds

5% Lower Bound	Mean	Median	95% Upper Bound
$\alpha_{.05}$	α_E	$\alpha_{.5}$	$\alpha_{.95}$
7.07×10^{13}	2.568×10^{14}	1.9×10^{15}	5.08×10^{16}

ENGINE VALVES

Torque motor valves have few or no sliding parts that would be subject to wear binding or seizing. However, this is achieved by introducing flexure tubes that may be subject to fatigue and fracture. The four data points available on torque motor valves indicated no apparent difference in the expected failure rate of torque motor and solenoid engine valves (fourteen data points were available for the engine valves).

Some bipropellant system employ an engine valve with a single actuation (solenoid or torque motor) used to drive two valve poppets. Examination of the data base resulted in no identifiable difference in failure rate for this type of valve when compared to single seat valves. Series redundant dual seat valves are employed in some monopropellant systems. While this arrangement reduces the possibility of seat leakage due to contamination it introduces additional parts subject to wear, erosion and corrosion effects.

The overall failure rate for this type of valve falls in the central range of the total valve data base. This indicated no significant advantage (or penalty) at the total failure rate level.

Finally the engine valve data, including electrothermal monopropellant, catalytic monopropellant and hypergolic bipropellant system component, could identify no credible base for alternate reliability models.

Component Reliability Model

The single engine valve model consists of three components, cyclic, operating time and mission time. Each of these components is characterized with growing failure rates. Valve cycling involves wear, fatigue, and a growing possibility of leakage due to upstream and internally generated contaminants. Operating time and flight time allow for erosion and corrosion of valve parts, respectively.

The failure rate growth phenomena was characterized by Weibull models. This yielded

$$R = \exp\left[\frac{-N^{\beta}}{\alpha_c} - \frac{t_{op}^{\beta}}{\alpha_{op}} - \frac{t_f^{\beta}}{\alpha_f} \right]$$

where β = Weibull shape factor = 1.5

N = number of cycles

t_{op} = operating time

t_f = flight time

α_c = Cycle scale factor

α_{op} = Operating time scale factor

α_f = Flight time scale factor

A shape factor of β = 1.5 was used. The scale factors (α) were determined from the exponential model failure rates in the same manner as used in previous components. However, a specific point for equivalency of the two models was not used. Because of the wide range of mission lengths, thrust levels, operating lives, etc. encountered by this type of valve, a more flexible approach reflecting design life was was selected. The exponential and Weibull models were then set equal at half the design life of the valve yielding the following scale factors (α)

$$\text{Cyclic scale factor, } \alpha_c = \frac{(.5N_D)^{.5}}{\lambda_c}$$

$$\text{Operating scale factor, } \alpha_{op} = \frac{(.5\,t_{opD})^{.5}}{\lambda_{op}}$$

$$\text{Fight time scale factor, } \alpha_f = \frac{(.5\,t_{fD})^{.5}}{\lambda_f}$$

where
- N_D = Total design life cycles
- t_{opD} = Total operating time design life
- t_{fD} = Total flight time design life
- λ_c = Cycle failure rate
- λ_{op} = Operating time failure rate
- λ_f = Flight time failure rate

Failure Rate Uncertainty Model

Log normal		λ_c	λ_{op}	λ_f
Coefficient of Variation	$\eta =$	.8	1.52	2
Mean	$\mu =$	-15.2	-9.81	-14.6
Standard Deviation	$\sigma =$	.704	1.0936	1.268

Exponential Failure Rate Mean and Bounds

(Used to determine scale factors α_c, α_{op}, α_f)

	5% Lower Bound $\lambda_{.05}$	Median $\lambda_{.5}$	Mean $E\{\lambda\}$	95% Upper Bound $\lambda_{.95}$
Cyclic failure rate λ_c	.079	.25	.322	.8
Operating time failure rate λ_{op}	9.1	55	100	332
Flight time failure rate λ_f	.056	0.45	1.0	3.63

$$X10^{-6} \text{ per cycle or hour.}$$

Weibull Model Scale Factor Mean and Bounds

	5% Lower Bound $\alpha_{.05}$	Mean α_E	95% Upper Bound $\alpha_{.95}$
Cycle Scale Factor α_c	$\dfrac{(.5N_D)^{.5}}{\lambda_{c.95}}$	$\dfrac{(.5N_D)^{.5}}{E\{\lambda_c\}}$	$\dfrac{(.5N_D)^{.5}}{\lambda_{c.05}}$
Operating time scale factor α_{op}	$\dfrac{(.5t_{cpD})^{.5}}{\lambda_{op.95}}$	$\dfrac{(.5t_{opD})^{.5}}{E\{\lambda_{op}\}}$	$\dfrac{(.5t_{opD})^{.5}}{\lambda_{op.05}}$
Flight time scale factor α_f	$\dfrac{(.5t_{fD})^{.5}}{\lambda_{f.95}}$	$\dfrac{(.5t_{fD})^{.5}}{E\{\lambda_f\}}$	$\dfrac{(.5t_{fD})^{.5}}{\lambda_{f.05}}$

Partition by Failure Modes

1. Fail Open

    1.1 Model: $R = \exp\left[\dfrac{-N^{\beta}}{\alpha_{co}} \quad \dfrac{-t_{op}^{\beta}}{\alpha_{opo}} \quad \dfrac{-t_f^{\beta}}{\alpha_{fo}}\right], \beta = 1.5$

    1.2 Failure Rates and Weibull Scale Factors

$$E\{\lambda_{co}\} = 10\% \; E\{\lambda_c\}$$

$$E\{\lambda_{opo}\} = 10\% \; E\{\lambda_{op}\}$$

$$E\{\lambda_{fo}\} = 10\% \; E\{\lambda_f\}$$

    1.3 Weibull Parameter Values and Bounds

	5% Lower Bound $\alpha_{.05}$	Equiv. Mean α_E	Median $\alpha_{.5}$	95% Upper Bound $\alpha_{.95}$
α_{co}:	$\dfrac{(.5N_D)^{.5}}{8\times10^{-8}}$	$\dfrac{(.5N_D)^{.5}}{3.22\times10^{-8}}$	$\dfrac{(.5N_D)^{.5}}{2.5\times10^{-8}}$	$\dfrac{(.5N_D)^{.5}}{7.9\times10^{-9}}$
α_{opo}:	$\dfrac{(.5t_{opo})^{.5}}{332\times10^{-5}}$	$\dfrac{(.5t_{opo})^{.5}}{1\times10^{-5}}$	$\dfrac{(.5t_{opo})^{.5}}{5.5\times10^{-6}}$	$\dfrac{(.5t_{opo})^{.5}}{9.1\times10^{-7}}$
α_{fo}:	$\dfrac{(.5t_{fo})^{.5}}{3.63\times10^{-7}}$	$\dfrac{(.5t_{fo})^{.5}}{1\times10^{-7}}$	$\dfrac{(.5t_{fo})^{.5}}{4.5\times10^{-8}}$	$\dfrac{(.5t_{fo})^{.5}}{5.6\times10^{-9}}$

2. Fail Closed

    2.1 Model $R = \exp\left[\dfrac{-N^{\beta}}{\alpha_{cc}} \quad \dfrac{-t_{op}^{\beta}}{\alpha_{opc}} \quad \dfrac{-t_f^{\beta}}{\alpha_{fc}}\right], \; \beta = 1.5$

2.2 Failure Rates and Weibull Scale Factors

$$E\{\lambda_{cc}\} = 30\% \ E\{\lambda_c\}$$

$$E\{\lambda_{opc}\} = 30\% \ E\{\lambda_{op}\}$$

$$E\{\lambda_{fc}\} = 30\% \ E\{\lambda_f\}$$

2.3 Weibull Parameter Values and Bounds

	5% Lower Bound	Equiv. Mean	Median	95% Upper Bound
	$\alpha_{.05}$	α_E	$\alpha_{.5}$	$\alpha_{.95}$
α_{cc}	$\dfrac{(.5N_D)^{.5}}{2.4 \times 10^{-7}}$	$\dfrac{(.5N_D)^{.5}}{9.66 \times 10^{-8}}$	$\dfrac{(.5N_D)^{.5}}{7.5 \times 10^{-8}}$	$\dfrac{(.5N_D)^{.5}}{2.37 \times 10^{-8}}$
α_{opc}	$\dfrac{(.5t_{opD})^{.5}}{9.96 \times 10^{-3}}$	$\dfrac{(.5t_{opD})^{.5}}{3 \times 10^{-5}}$	$\dfrac{(.5t_{opD})^{.5}}{1.65 \times 10^{-6}}$	$\dfrac{(.5t_{opD})^{.5}}{2.73 \times 10^{-6}}$
α_{fc}	$\dfrac{(.5t_{fD})^{.5}}{1.1 \times 10^{-6}}$	$\dfrac{(.5t_{fD})^{.5}}{3 \times 10^{-7}}$	$\dfrac{(.5t_{fD})^{.5}}{1.35 \times 10^{-7}}$	$\dfrac{(.5t_{fD})^{.5}}{1.68 \times 10^{-8}}$

3. Fail Partial

3.1 Model

$$R = \exp\left[\frac{-N^{\beta}}{\alpha_{cp}} \quad \frac{-t_{op}^{\beta}}{\alpha_{opp}} \quad \frac{-t_f^{\beta}}{\alpha_{fp}} \right], \ \beta = 1.5$$

3.2 Failure Rates

$$E\{\lambda_{cp}\} = 60\% \ E\{\lambda_c\}$$

$$E\{\lambda_{opp}\} = 55\% \ E\{\lambda_{op}\}$$

$$E\{\lambda_{fp}\} = 55\% \ E\{\lambda_f\}$$

3.3 Weibull Parameter Values and Bounds

	5% Lower Bound	Equiv. Mean	Median	95% Upper Bound
α_{cp}	$\dfrac{(.5N_D)^{.5}}{4.8 \times 10^{-7}}$	$\dfrac{(.5N_D)^{.5}}{1.93 \times 10^{-7}}$	$\dfrac{(.5N_D)^{.5}}{1.5 \times 10^{-7}}$	$\dfrac{(.5N_D)^{.5}}{4.74 \times 10^{-8}}$
α_{opp}	$\dfrac{(.5t_{opD})^{.5}}{1.83 \times 10^{-4}}$	$\dfrac{(.5t_{opD})^{.5}}{5.5 \times 10^{-5}}$	$\dfrac{(.5t_{opD})^{.5}}{3.03 \times 10^{-5}}$	$\dfrac{(.5t_{opD})^{.5}}{5.01 \times 10^{-6}}$
α_{fp}	$\dfrac{(.5t_{fD})^{.5}}{2 \times 10^{-6}}$	$\dfrac{(.5t_{fD})^{.5}}{5.5 \times 10^{-7}}$	$\dfrac{(.5t_{fD})^{.5}}{2.48 \times 10^{-7}}$	$\dfrac{(.5t_{fD})^{.5}}{3.08 \times 10^{-8}}$

4. Leak to Space

4.1 Model $R = \exp\left\{ \lambda_{op} t_{op} - \lambda_f t_f \right\}$

4.2 Failure Rates

$$E\left\{ \lambda_{opl} \right\} = 5\% \; E\left\{ \lambda_{op} \right\}$$

$$E\left\{ \lambda_{fl} \right\} = 5\% \; E\left\{ \lambda_{f} \right\}$$

4.3 Failure Rate Mean and Bounds

	5% Lower Bound	Median	Mean	95% Upper Bound
	$\lambda_{.05}$	$\lambda_{.5}$	$E\{\lambda\}$	$\lambda_{.95}$
λ_{op}	0.455	2.75	5	16.6
λ_f	0.0028	0.0225	0.05	0.182

THRUSTER CHAMBER (MONOPROPELLANT)

The principal failure mechanisms for this component include nitriding, cyclic thermal and pressure stressing and fatigue. These mechanisms are time dependent and indicative of increasing failure rates. Weibull models were again used in a manner similar to the injector and catalyst bed. Transition from exponential failure rate data to the Weibull models was accomplished using a 50% design life point of equivalency.

Component Reliability Model

$$R = \exp \left[\frac{-N^{\beta}}{\alpha_c} - \frac{t_{op}^{\beta}}{\alpha_{op}} \right]$$

Where α_c = pulse failure rate scale factor

N = number of pulses

t_{op} = operating time

α_{op} = operating time scale factor

Failure Uncertainty Distribution

Log normal		λ_c	λ_{op}
Coefficient of Variation	$\eta =$	1.8	1.5
Mean	$\mu =$	-18.45	-16.10
Standard Deviation	$\sigma =$	1.2019	1.0875

Exponential Model Failure Rate Mean and Bounds

	5% Lower Bound $\lambda_{.05}$	Median $\lambda_{,5}$	Mean $E\{\lambda\}$	95% Upper Bound $\lambda_{.95}$
Pulse failure rate, λ_c	.0013	0.0097	.02	.07
Operating time failure rate, λ_{op}	.017	0.102	.184	.609

$$\times 10^{-6} \text{ per hour (cycle)}$$

Weibull Model Parameters Mean and Bounds

	5% Lower Bound $\alpha_{.05}$	Median $\alpha_{.5}$	Mean α_E	95% Upper Bound $\alpha_{.95}$
Pulse scale factor	$\dfrac{(.5N_D)^{.5}}{\lambda_{c.95}}$	$\dfrac{(.5N_D)^{.5}}{\lambda_{c.5}}$	$\dfrac{(.5N_D)^{.5}}{E\{\lambda_c\}}$	$\dfrac{(.5N_D)^{.5}}{\lambda_{c.05}}$
Operating time scale factor	$\dfrac{(.5t_{opD})^{.5}}{\lambda_{op.95}}$	$\dfrac{(.5t_{opD})^{.5}}{\lambda_{op.95}}$	$\dfrac{(.5t_{opD})^{.5}}{E\{\lambda_{op}\}}$	$\dfrac{(.5t_{opD})^{.5}}{\lambda_{op.05}}$

where N_D = design life pulses

t_{opD} = design life operating time

Shape factor β = 1.5 for both pulse and operating time components of model

THRUST CHAMBER (BIPROPELLANT)

This component has potential failure modes that in general will tend to increase with accumulated operating time. They are (1) rupture of the chamber due to flaws in material or stresses for thermal and pressure cycling; (2) failure of weld joints due to imperfections in the weldments; (3) change in nozzle contour due to thermal stresses and erosion; (4) spalling of the chamber protective coating.

Component Reliability Model

$$R = \exp\left[\frac{-N^{\beta}}{\alpha_p} - \frac{t_{op}^{\beta}}{\alpha_{op}}\right]$$

where N = number of engine pulses

t_{op} = operating time

α_p = pulse scale factor

α_{op} = operating time scale factor

β = shape factor = 1.5

Exponential Model Failure Rate Uncertainty Distribution

Lognormal		λ_c	λ_{op}
Coefficient of Variation	η =	1.86	1.86
Mean	μ =	-19.73	-11.676
Standard Deviation	σ =	1.223	1.223

Exponential Model Failure Rate Mean and Bounds

	5% Lower Bound $\lambda_{.05}$	Median $\lambda_{.5}$	Mean $E\{\lambda\}$	95% Upper Bound $\lambda_{.95}$
Pulse failure rate, λ_c	.00013	0.0027	.0057	0071
Operating time failure rate, λ_{op}	1.14	8 497	17.95	63.5

$$\times 10^{-6} \text{ per hour (pulse)}$$

Weibull Model Scale Factor Mean and Bounds

	5% Lower Bound $\alpha_{.05}$	Mean α_E	Median $.5$	95% Upper Bound $\alpha_{.95}$
Pulse scale factor	$\dfrac{(.5N_d)^{.5}}{\lambda_{p.95}}$	$\dfrac{(.5N_d)^{.5}}{E\{\lambda_p\}}$	$\dfrac{(.5N_d)^{.5}}{\lambda_{p.5}}$	$\dfrac{.5(N_d)^{.5}}{\lambda_{p.05}}$
Operating time Scale Factor	$\dfrac{(.5t_{opd})^{.5}}{\lambda_{op.95}}$	$\dfrac{(.5t_{opd})^{.5}}{E\{\lambda_{op}\}}$	$\dfrac{(.5t_{opd})^{.5}}{\lambda_{op.5}}$	$\dfrac{(.5t_{opd})^{.5}}{\lambda_{op.95}}$

where N_d = design life pulses
t_{opd} = design life operating time

INJECTOR MONOPROPELLANT

Failure modes for this component include metal fatigue, cracking, and nitriding as well as plugging of the injector orifices. These failure modes indicate increasing failure rates with time. As in previous components Weibull models were used to approximate the situation. Leaking at the injector to chamber seals is also a significant failure mode. While the probability of its occurrence increases with time, the failure rate can be expected to remain constant.

Component Reliability Model

$$R = \exp\left[\frac{-N^{\beta}}{\alpha_c} - \frac{t_{op}^{\beta}}{\alpha_{op}} - \lambda_L t_{op}\right]$$

where: α_c = cyclic failure rate scale factor

N = Number of cycles

t_{op} = operating time

α_{op} = operating time scale factor

λ_L = leakage failure rate

β = shape factor

Failure Rate Uncertainty Distribution

Log normal		λ_c	λ_{op}	λ_L
Coefficient of Variation	$\eta =$	1.5	1.2	1.5
Mean	$\mu =$	-17.91	-14.57	-19.01
Standard Deviation	$\sigma =$	1.0857	.9445	1.0857

Exponential Model Failure Rate Mean and Bounds

	5% Lower Bound	Median	Mean	95% Upper Bound
	$\lambda_{.05}$	λ_5	$E\{\lambda\}$	$\lambda_{.95}$
λ_c	.0028	0 0166	.03	.099
λ_{op}	.10	0 471	.736	2 228
λ_L	.001	0.0056	01	033

$$X10^{-6} \text{ per hour (cycle)}$$

where λ_c = cyclic failure rate

λ_{op} = operating time failure rate

λ_L = leakage failure rate

Weibull Reliability Model Shape Factor Mean & Bounds

5% Lower Bound	Median	Mean	95% Upper Bound
$\alpha_{.05}$	α_E	$\alpha_{.5}$	$\alpha_{.95}$

α_c

$$\frac{(.2N_D)^{.5}}{\lambda_{c.95}} - \qquad \frac{(.2N_D)^{.5}}{E\,\lambda_c} \qquad \frac{(.2N_D)^{.5}}{\lambda_{.5}} \qquad \frac{(.2N_D)^{.5}}{\lambda_{c.05}}$$

α_{op}

$$\frac{(.2t_{opD})^{.5}}{\lambda_{op.95}} - \quad \frac{(.2t_{opD})^{.5}}{E\{\lambda_{op}\}} - \quad \frac{(.2t_{opD})^{.5}}{\lambda_{op.5}} - \quad \frac{(.2t_{opD})^{.5}}{\lambda_{op.05}}$$

where

α_c = shape factor for cycles

α_{op} = shape factor for operating time

$\lambda_{c.95}$ = 95% Upper Bound for exponential model cyclic failure rate

$\lambda_{c.05}$ = 5% Lower Bound for exponential model cyclic failure rate

N_d = design life cycles

t_{opD} = design operating time (hours)

$\lambda_{op.05}$ = analagous to $\lambda_{c.95}$

$\lambda_{op.05}$ = analagous to $\lambda_{c.05}$

Partition by Failure Modes

1. Clogging

   1.1 Model : $R = \exp\left[\dfrac{-t_{op}^{\beta}}{\alpha_{cl}}\right]$, $\beta = 1.5$

   1.2 Failure Rate

   $E\left\{\lambda_{cl}\right\} = 50\% \; E\left\{\lambda_{op}\right\}$

   1.3 Weibull Parameter Values and Bounds

5% Lower Bound	Equiv. Mean	Median	95% Upper Bound
$\alpha_{.05}$	α_{E}	$\alpha_{.5}$	$\alpha_{.95}$
$\alpha_{cl} \quad \dfrac{(.2t_{opo})^{.5}}{2.79 \times 10^{-6}}$	$\dfrac{(.2t_{opo})^{.5}}{3.68 \times 10^{-7}}$	$\dfrac{(.2t_{opo})^{.5}}{1.87 \times 10^{-7}}$	$\dfrac{(.2t_{opo})^{.5}}{1.25 \times 10^{-8}}$

2. Leaking, Excessive flow

   2.1 Model : $R = \exp\left[\dfrac{-N^{\beta}}{\alpha_{Lc}} - \dfrac{t_{op}^{\beta}}{\alpha_{Lop}} - \lambda_L t_{op}\right]$

   2.2 Failure Rates

   $E\left\{\lambda_{Lc}\right\} = 100\% \; E\left\{\lambda_c\right\}$

   $E\left\{\lambda_L\right\} = 100\% \; E\left\{\lambda\;\right\}$

   $E\left\{\lambda_{Lop}\right\} = 50\% \; E\left\{\lambda_{op}\right\}$

   2.3 Failure Rate Mean and Bounds

	5% Lower Bound	Median	Mean	95% Upper Bound
	$\lambda_{.05}$	$\lambda_{.5}$	$E\{\lambda\}$	$\lambda_{.95}$
λ_L	.001	.0056	.01	.033

   $\times 10^{-6}$ per hour

2.4 Weibull Parameter Mean and Bounds

	5% Lower Bound $\alpha_{.05}$	Equiv. Mean α_E	Median $\alpha_{.5}$	95% Upper Bound $\alpha_{.95}$
d_{Lc}	$\dfrac{(.2N_D)^{.5}}{.099 \times 10^{-6}}$	$\dfrac{(.2N_D)^{.5}}{.03 \times 10^{-6}}$	$\dfrac{(.2N_D)^{.5}}{.0166 \times 10^{-6}}$	$\dfrac{(.2N_D)^{.5}}{2.8 \times 10^{-9}}$
Lop	$\dfrac{(.2t_{opn})^{.5}}{2.79 \times 10^{-6}}$	$\dfrac{(.2t_{opn})^{.5}}{3.68 \times 10^{-7}}$	$\dfrac{(.2t_{opn})^{.5}}{1.8 \times 10^{-7}}$	$\dfrac{(.2t_{opn})^{.5}}{1.25 \times 10^{-8}}$

INJECTOR BIPROPELLANT

Failure modes of this component include plugging and fatigue induced by pressure and temperature cycling. These modes indicate an increasing failure rate model should be used. The scale parameter for the Weibull (increasing failure rate) model was made dependent on design life to increase model responsiveness to the broad range of bipropellant thruster systems performance levels. The point of equivalency used for transition from exponential model data to Weibull scale factor was 50% of design life. Internal and external thruster leakage are also principal failure modes. These, however, were expected to be random failure situations and therefore were represented using a constant failure rate.

Component Reliability Model

$$R = \exp\left[- \lambda_L t_{op} - \frac{N^\beta}{\alpha}\right]$$

where λ_L = internal leakage failure rate

t_{op} = operating time

N = number of engine pulses

β = Weibull shape factor = 1.5

α = Weibull scale factor

Failure Rate Uncertainty Distribution-Internal Leakage

Log normal

Coefficient of variation	η = 1.86
Mean	μ = -12.77
Standard Deviation	σ = 1.2254

Failure Rate Mean and Bounds-Internal Leakage

	5% Lower Bound	Median	Mean	95% Upper Bound
	$\lambda_{L.05}$	$\lambda_{L.5}$	$E\{\lambda_L\}$	$\lambda_{L.95}$
Internal Leakage Failure Rate	.378	2.84	6.02	21.3

$$x10^{-6} \text{ per hour}$$

Failure Rate Uncertainty Distribution - Pulse

Lognormal

Coefficient of variation	$\eta = 1.94$
Mean	$\mu = -21.15$
Standard Deviation	$\sigma = 1.25$

Failure Rate Mean and Bounds - Pulse

	5% Lower Bound	Median	Mean	95% Upper Bound
	$\lambda_{C.05}$	$\lambda_{C.5}$	$E\{\lambda_C\}$	$\lambda_{C.95}$
Pulse Failure Rate	.00008	.0006	.00143	.0051

$$x10^{-6} \text{ per hour}$$

Weibull Scale Factor Mean and Bounds

	5% Lower Bound	Median	Mean	95% Upper Bound
	$\alpha_{.05}$	$\alpha_{.05}$	α_E	$\alpha_{.95}$
Scale factor	$\dfrac{(.5N_D)^{.5}}{\lambda_{C.95}}$	$\dfrac{(.5N_D)^{.5}}{\lambda_{C.5}}$	$\dfrac{(.5N_D)^{.5}}{E\{\lambda_C\}}$	$\dfrac{(.5N_D).5}{\lambda_{C.05}}$

CATALYST BED (INCLUDING RETENTION SCREENS)

The principal identified failure mechanisms for catalyst bed assembly (catalyst poisoning, particle structural breakdown, fines migration and bed packing, catalyst erosion, catalyst bed voids and nitriding of screen retainers) indicate growing failure rates with thruster use. Weibull models were used to reflect these situations. The catalyst bed assembly is also sensitive to the mode of operation of the thruster (cold start, hot pulsing and steady state). Some catalytic hydrazine thruster are designed to operate in the cold start mode. Others employ heaters to avoid cold starting. While one general model was used for all cases, three sets of failure rates and Weibull scale and shape factors were employed to yield models for the cold start, hot pulsing and steady state situations. In calculating the Weibull scale factors from constant failure rate data, the same approach was used as was employed in the injector reliability models. The equivalent point between exponential and Weibull models was selected at 50% of design life. This approach will allow 1) a more definitive assessment of cold start and hot start thruster in the context of the design and mission requirements 2) an alternate mode of assessment for hot start thruster if the thruster heaters have failed.

Component Reliability Models

$$R_{pulse} = \exp\left[\frac{-N^{\beta}}{\alpha_c} - \frac{n^{\beta}}{\alpha_{cs}} - \frac{t_{op}^{\beta}}{\alpha_{op}} - \lambda_d t_d\right]$$

$$R_{steady\ state} = \exp\left[-\frac{N_{ss}^{\beta}}{\alpha_{ns}} - \frac{n^{\beta}}{\alpha_{cs}} \frac{t_{ss}^{\beta}}{\alpha_{ss}} - \lambda_d t_d\right]$$

where N = number of pulses excluding cold starts
N_{ss} = number steady state cycles
n = number of cold starts

t_{op} = operating time, pulse mode

t_{ss} = operating time, steady state

t_d = dormant time

α_c = pulse scale factors

α_{NS} = steady state pulse scale factor

α_{cs} = cold start scale factor

α_{ss} = steady state operating time scale factor

α_{op} = operating time scale factor

λ_d = dormant failure rate

β = shape factor

Exponential Model Failure Rates Mean and Bounds

	5% Lower Bound $\lambda_{.05}$	Median $\lambda_{.5}$	Mean $E\{\lambda\}$	95% Upper Bound $\lambda_{.95}$
cyclic failure rate, pulsing, λ_c	.0067	0.049	.10	.35
operating time failure rate, λ_{op}	.256	1.53	2.76	9.16
cold start failure rate, λ_{cs}	1.04*	6.2*	11.2*	37.2*
steady state operating time failure rate, λ_{ss}	12.8	76.4	138	458
dormant failure rate, λ_d	.00067	.0049	.01	.035
Steady state cycles failure rate, λ_{NS}	.485	2.77	5	16.6

$$X10^{-6} \text{ per hour (cycle)}$$

$$*X10^{-6} \text{ per cold start}$$

I-178

Weibull Reliability Model (Pulse Mode) Scale Factor Mean and Bounds

	5% Lower Bound	Mean	95% Upper Bound
Pulse scale factor α_c	$\sqrt{\dfrac{.5N_D}{\lambda_{c.95}}}$	$\sqrt{\dfrac{.5N_D}{E\{\lambda_c\}}}$	$\sqrt{\dfrac{.5N_D}{\lambda_{c.05}}}$
Operating time scale factor α_{op}	$\sqrt{\dfrac{.5t_{opD}}{\lambda_{op.95}}}$	$\sqrt{\dfrac{.5t_{opD}}{E\{\lambda_{op}\}}}$	$\sqrt{\dfrac{.5t_{opD}}{\lambda_{op.05}}}$
Cold start scale factor α_{cs}	$\dfrac{(.5n_D)^2}{\lambda_{cs.95}}$	$\dfrac{(.5n_D)^2}{E\{\lambda_{cs}\}}$	$\dfrac{(.5n_D)^2}{\lambda_{cs.05}}$

$$\text{where } N_D = \text{design life pulses}$$
$$t_{opD} = \text{design operating time}$$
$$n_D = \text{design cold starts}$$

Weibull Shape Factor (β) Values

Model Component	Value
Pulse $\dfrac{N^\beta}{\alpha_c}$	$\beta = 1.5$
Cold Start $\dfrac{n^\beta}{\alpha_{cs}}$	$\beta = 3.0$
Cyclic Operating time $\dfrac{t_{op}^{\beta}}{\alpha_{op}}$	$\beta = 1.5$
Steady State operating time $\dfrac{t_{ss}^{\beta}}{\alpha_{ss}}$	$\beta = 2.0$
Steady state pulse $\dfrac{ns^{\beta}}{\alpha_{ns}}$	$\beta = 2.0$

Weibull Reliability Model (Steady State Mode) Mean and Bounds

	5% Lower Bound	Mean	Median	95% Upper Bound
	$\alpha_{.05}$	α_E	$\alpha_{.5}$	$\alpha_{.95}$
Steady state pulse scale factor α_{ns}	$\dfrac{.5N_{SSD}}{\lambda_{NS.95}}$	$\dfrac{.5N_{SSD}}{E\{\lambda_{NS}\}}$	$\dfrac{.5N_{SSD}}{\lambda_{NS.5}}$	$\dfrac{.5N_{SSD}}{\lambda_{NS.05}}$
Steady state operating time scale factor α_{ss}	$\dfrac{.5t_{SSD}}{\lambda_{ss.95}}$	$\dfrac{.5t_{SSD}}{E\{\lambda_{ss}\}}$	$\dfrac{.5t_{ss}}{\lambda_{ss.5}}$	$\dfrac{.5t_{SSD}}{\lambda_{ss.05}}$

where N_{ssd} = design steady state state pulses

t_{ssd} = design steady state operating time

Failure Rate Uncertainty Distributions

Lognormal		λ_c	λ_{op}	λ_{cs}
Coefficient of Variation	$\eta =$	1.8	1.5	1.5
Mean	$\mu =$	-16.84	-13.392	-11.991
Standard Deviation	$\sigma =$	1.2019	1.0875	1.0875

Lognormal		λ_{ss}	λ_d	λ_{ns}
Coefficient of Variation	$\eta =$	1.5	1.8	1.5
Mean	$\mu =$	-9.48	-19.143	-12.797
Standard Deviation	$\sigma =$	1.0875	1.2019	1.0875

THRUSTER SCREEN AND RETAINER PACKS (ELECTROTHERMAL)

The principal mode of failure of this component was assessed to be loss of structural integrity of the platinum screen pack retainer. The identified failure mechanism was nitriding of the retainer (currently Haynes 25). Due to the lack of directly applicable data for the retainer the reliability model was limited to a Weibull component used to characterize the increasing failure rate due to nitriding. The scale factor depending on design life was employed to reflect the broad scope of potential thruster operating times and cycles.

Component Reliablity Model

$$R = \exp\left[-\frac{t_{op}^{\beta}}{\alpha}\right]$$

where t_{op} = operating time

β = shape factor = 2.5

α = scale factor

Exponential Model Failure Rate Mean and Bounds*

*(Estimated using limited catalyst bed retainer data as a guide)

5% Lower Bound	Median	Mean	95% Upper Bound
$\lambda_{.05}$	$\lambda_{.5}$	$E\{\lambda\}$	$\lambda_{.95}$
.019	0.1107	.2	.662

$$\times 10^{-6} \text{ per hour}$$

Exponential Model Failure Rate Uncertainty Distribution

Lognormal

Coefficient of Variation	$\eta = 1.504$
Mean	$\mu = -16.016$
Standard Deviation	$\sigma = 1.0875$

Scale Factor Mean and Bounds

Based on limited data available for catalyst bed re-
tainers, the following scale factors were determined. The
transition from exponential model data to Weibull model
scale factor was made using a point of equivalency of 10%
the design life.

	5% Lower Bounds	Median	Mean	95% Upper Bound
	$\alpha_{.05}$	α_E	$\alpha_{.5}$	$\alpha_{.95}$
Operating time	$(.1t_{opd})^{1.5}$	$(.1t_{opd})^{1.5}$	$(.1t_{opd})^{1.5}$	$(.1t_{opd})^{1.5}$
Scale factor	$\lambda_{op.95}$	$\lambda_{op.5}$	$E\{\lambda_{op}\}$	$\lambda_{op.05}$

SYSTEM LEVEL FAULT TREES

The seven systems generically represented in figures 2 through 8 of this report were analyzed using the fault tree approach discussed earlier. Regardless of approach a greater degree of specifity concerning system configuration was required to conduct a system analysis. AFRPL provided the required information including number and deployment of thrusters, valves and redundant components. The resulting fault trees are presented in this section in the following format. For each system:

- A brief description of the system is provided

- A schematic of the system showing redundancies and numbers of components is included

- The fault tree analysis is presented.

The symbology used in the fault tree logic diagrams is defined in Table 8.
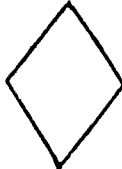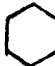
Cesium Ion Electron-Bombardment Thruster. The following requirements of the mercury electron-bombardment engine apply to the cesium engine:

- The thrust level for stationkeeping is approximately 1 millipound

- The orbit adjustment operations extend over 10,000 hours, including 2555 firing cycles.

The 1-millipound cesium ion thruster system has been developed for this kind of mission. Its specific application is on board the ATS-F (later designated ATS-6) satellite for north-south stationkeeping on the synchronous orbit, but it is also compatible with the USAF stationkeeping mission. Functionally comparable to the mercury thruster, the 1-millipound cesium ion thruster system will be the focus of this analysis.

A schematic of the system analyzed is shown in Figure 11. The fault tree analysis is presented in Figure 12. (For component level detail of the "THRUSTER" element of Figure 11 refer to Figure 2 Cesium Ion Electron Bombardment Generic Systems Layout, page I-4).

Table 8

Fault Tree Analysis Symbology

An event, usually a fault, resulting from the combination of more basic faults.

Basic component fault which can be assigned A probability of occurrence based on test results or physics of failure analysis.

A fault not developed further as to its causes because of lack of information, time, or value in doing so. Also used here for external faults.

A conditional event—one which must occur in order for an input fault (cause) to result in an output fault (effect).

An event expected to occur in normal operation.

And gate—the output event occurs only when all of the input events are present.

Or gate—the output event occurs when one or more of the input events are present.

Reference key to another part of the fault tree where the identical sequence of events is shown.

Inhibit gate—used to indicate application of a conditional event C, which may be a fault in itself or an event normal to system operation.

Reference key to another fault tree—perhaps for another major subsystem.

I-184

UNPRESSURIZED SURFACE TENSION
PROPELLANT STORAGE RESERVOIRS
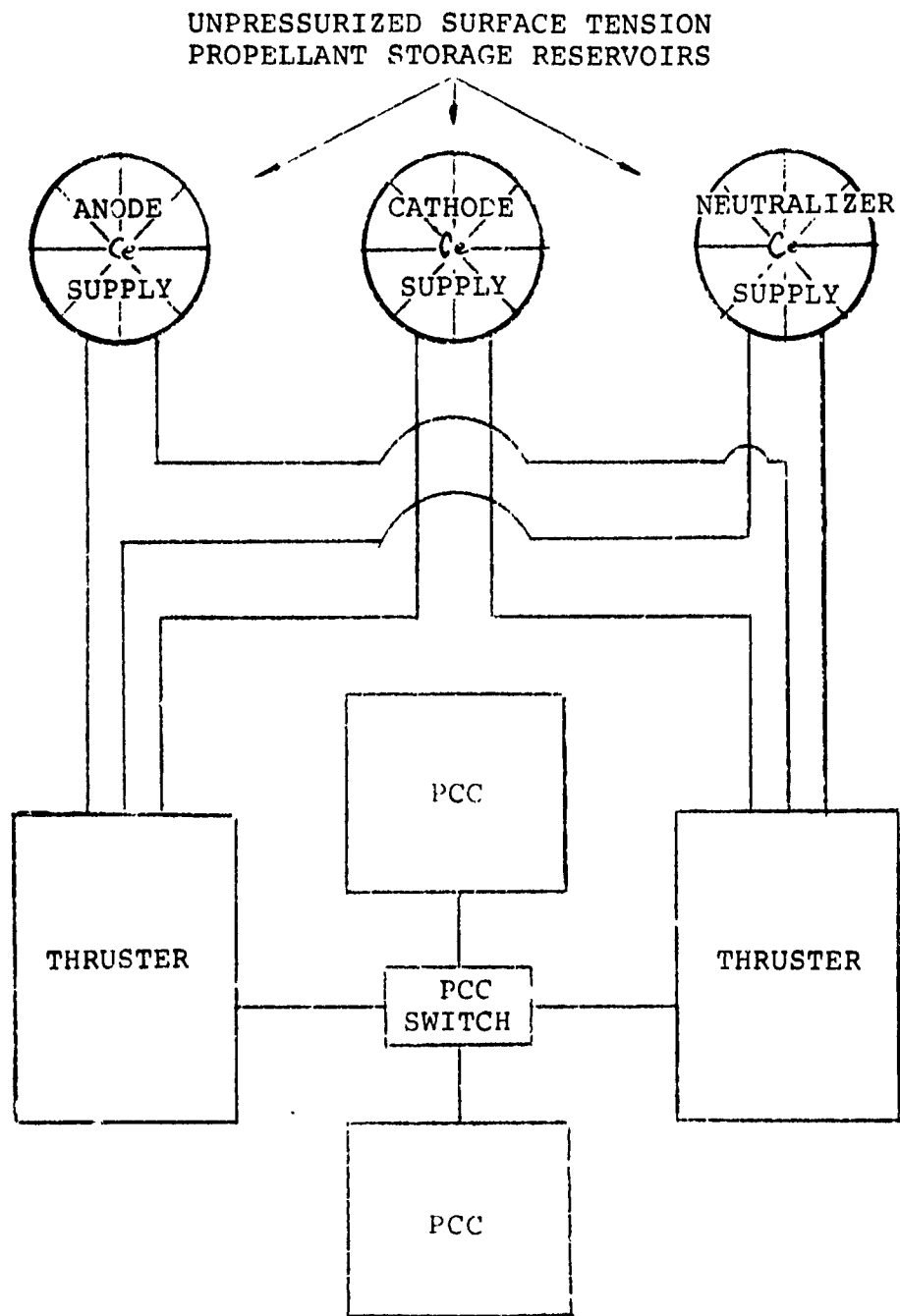
Figure 11   Cesium Ion System Schematic

CESIUM ION ELECTRON BOMBARDMENT SYSTEM
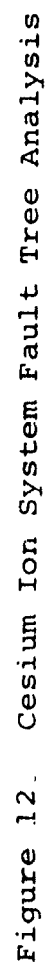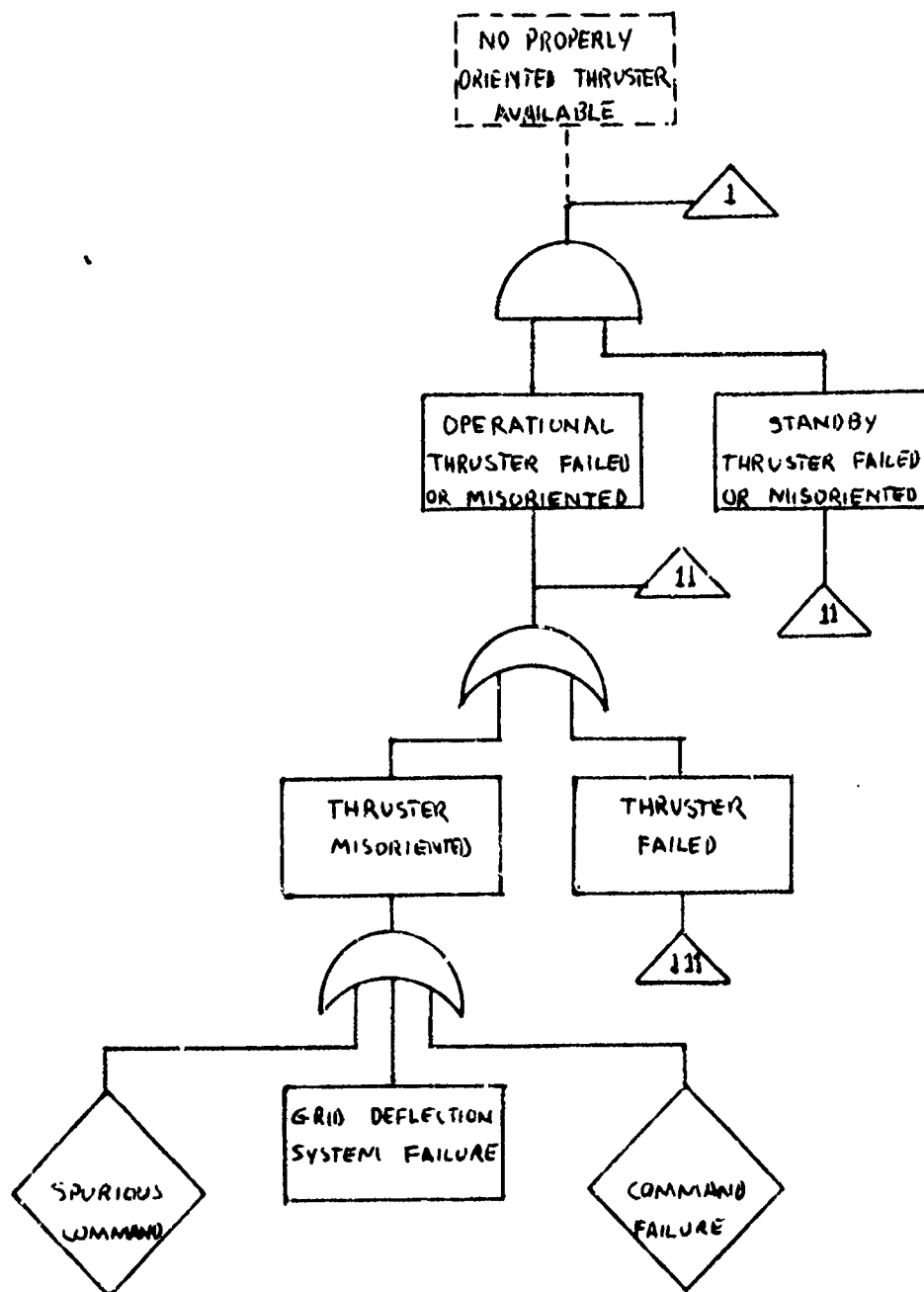
FAULT TREE ANALYSIS

Figure 12. Cesium Ion System Fault Tree Analysis

Figure 12 (Continued)
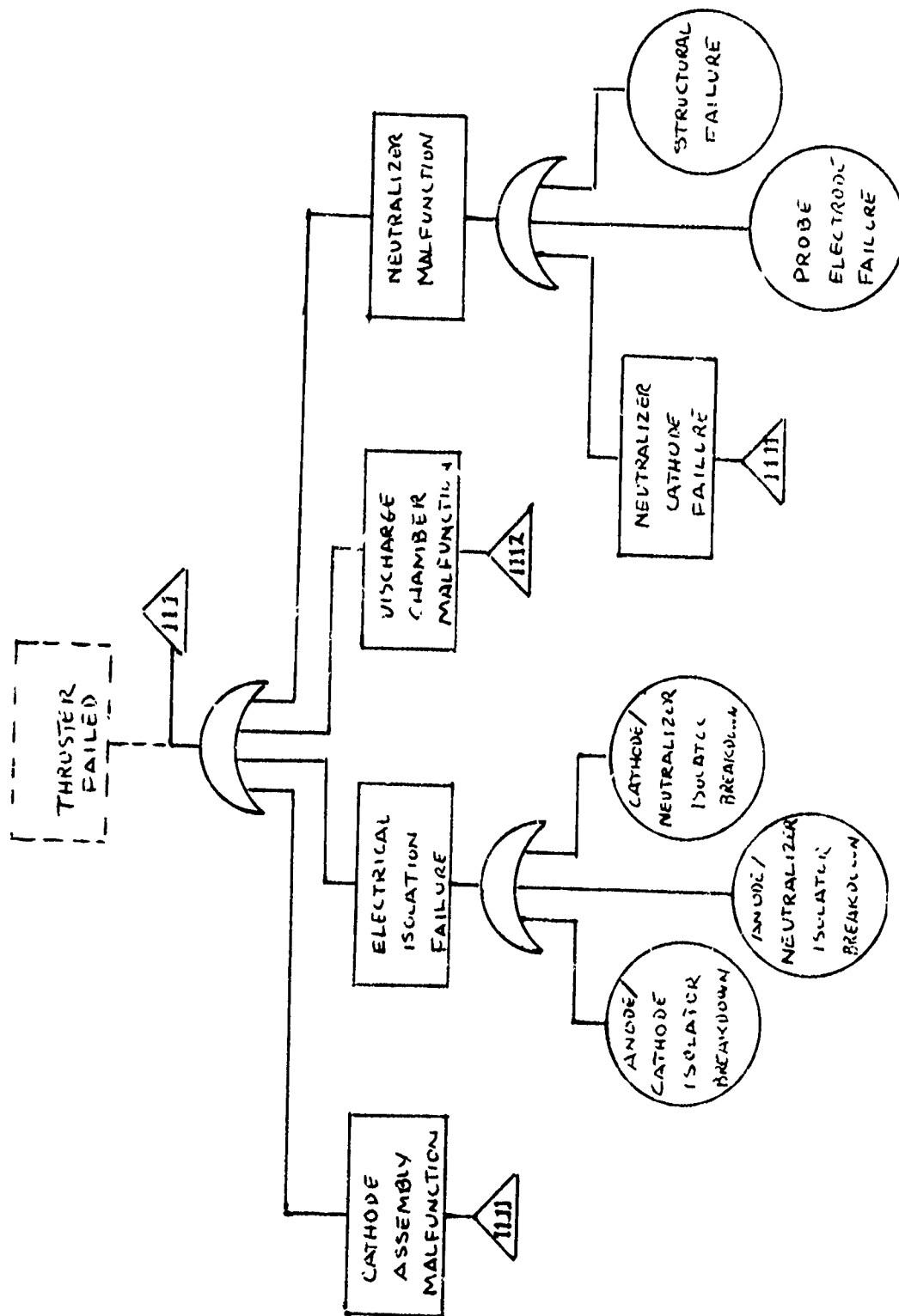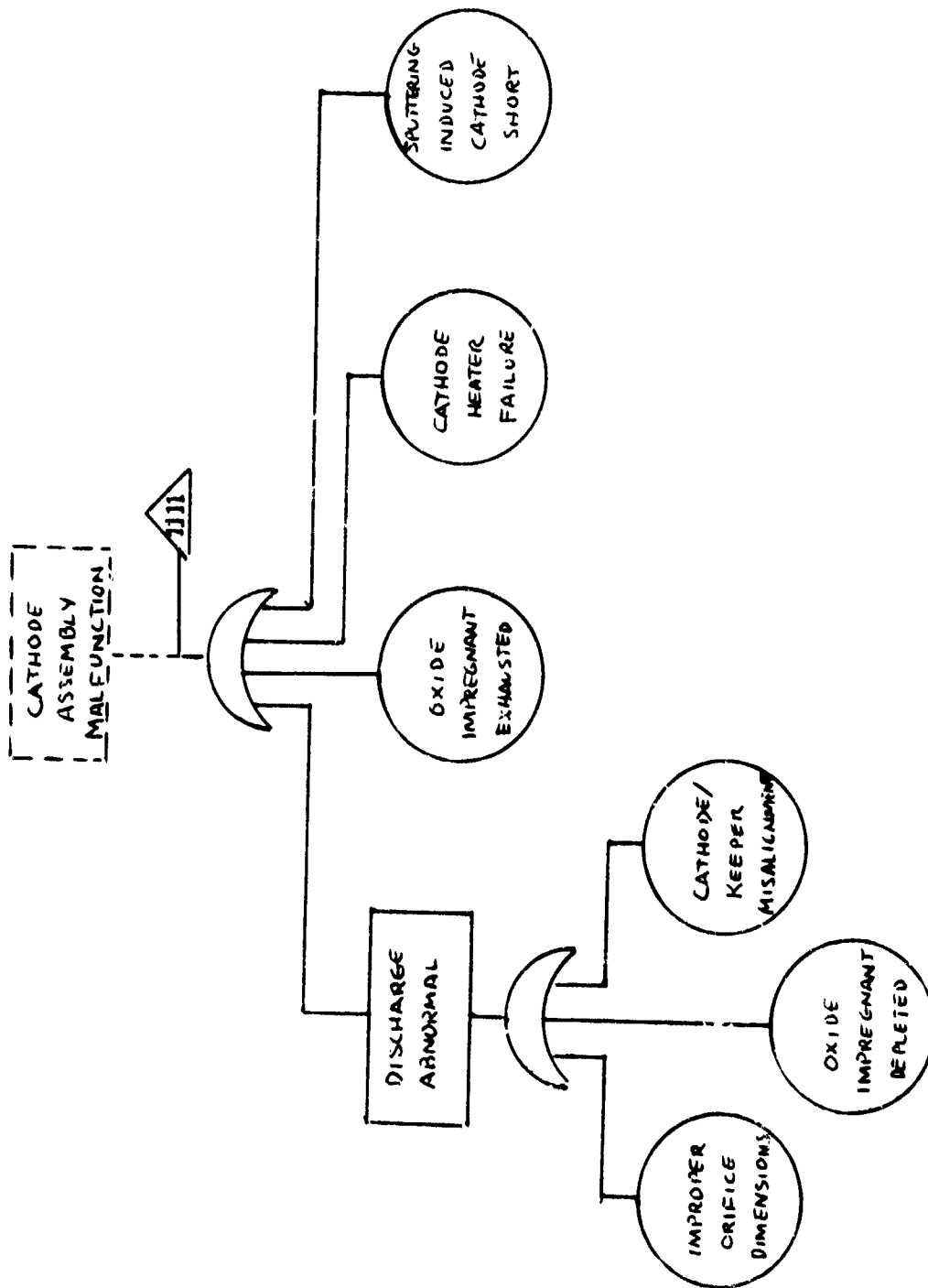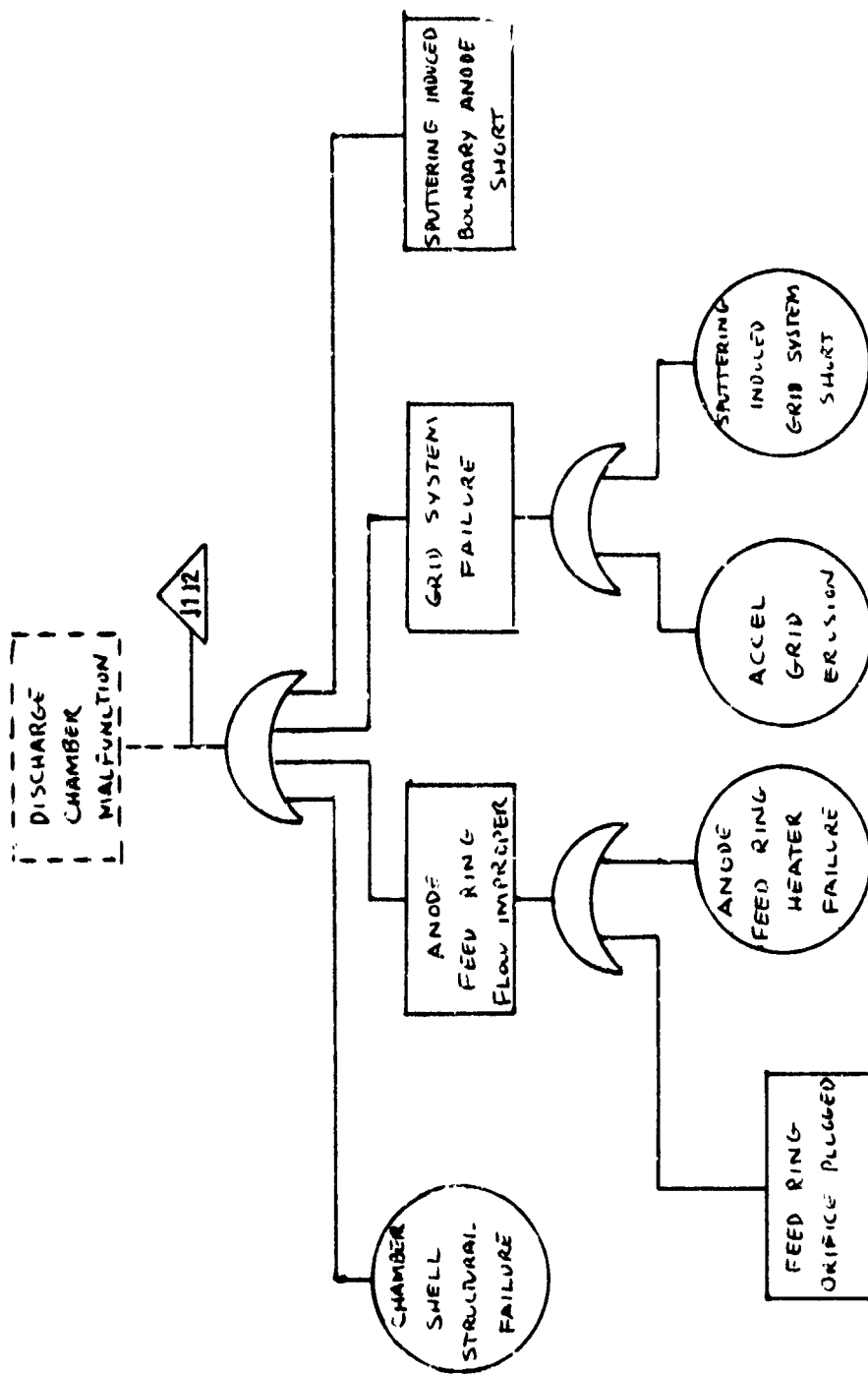
Figure 12 (Continued)

Figure 12 (Continued)

Figure 12 (Continued)
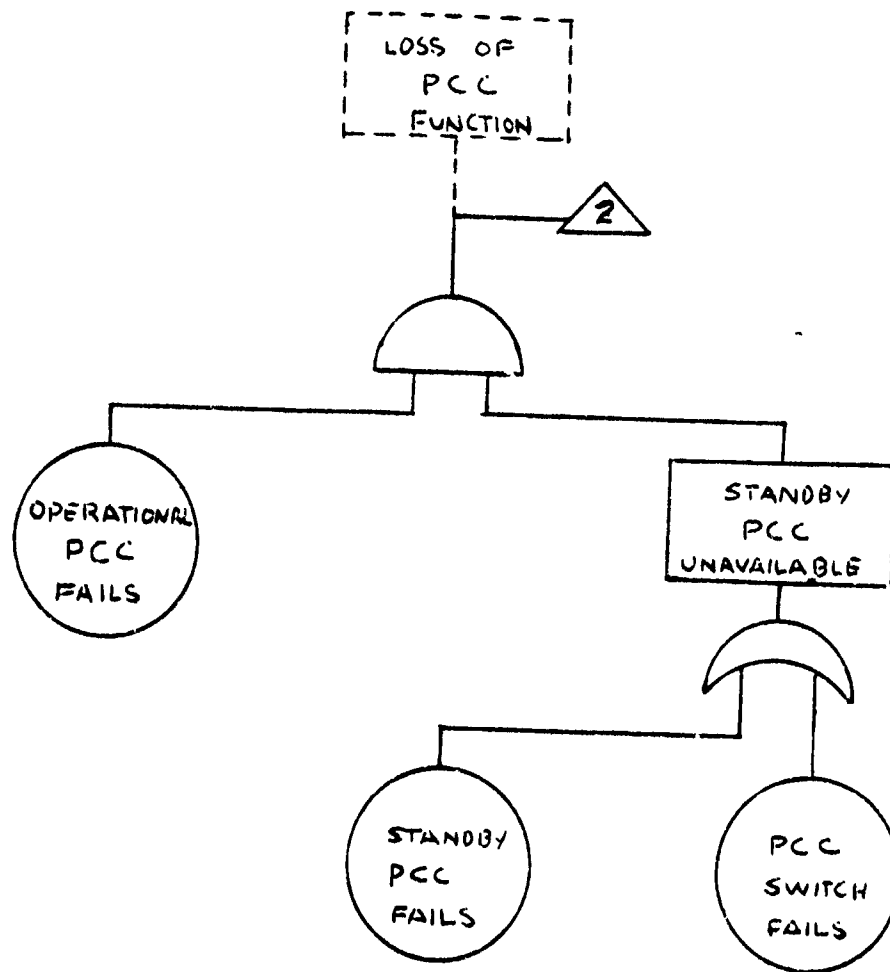
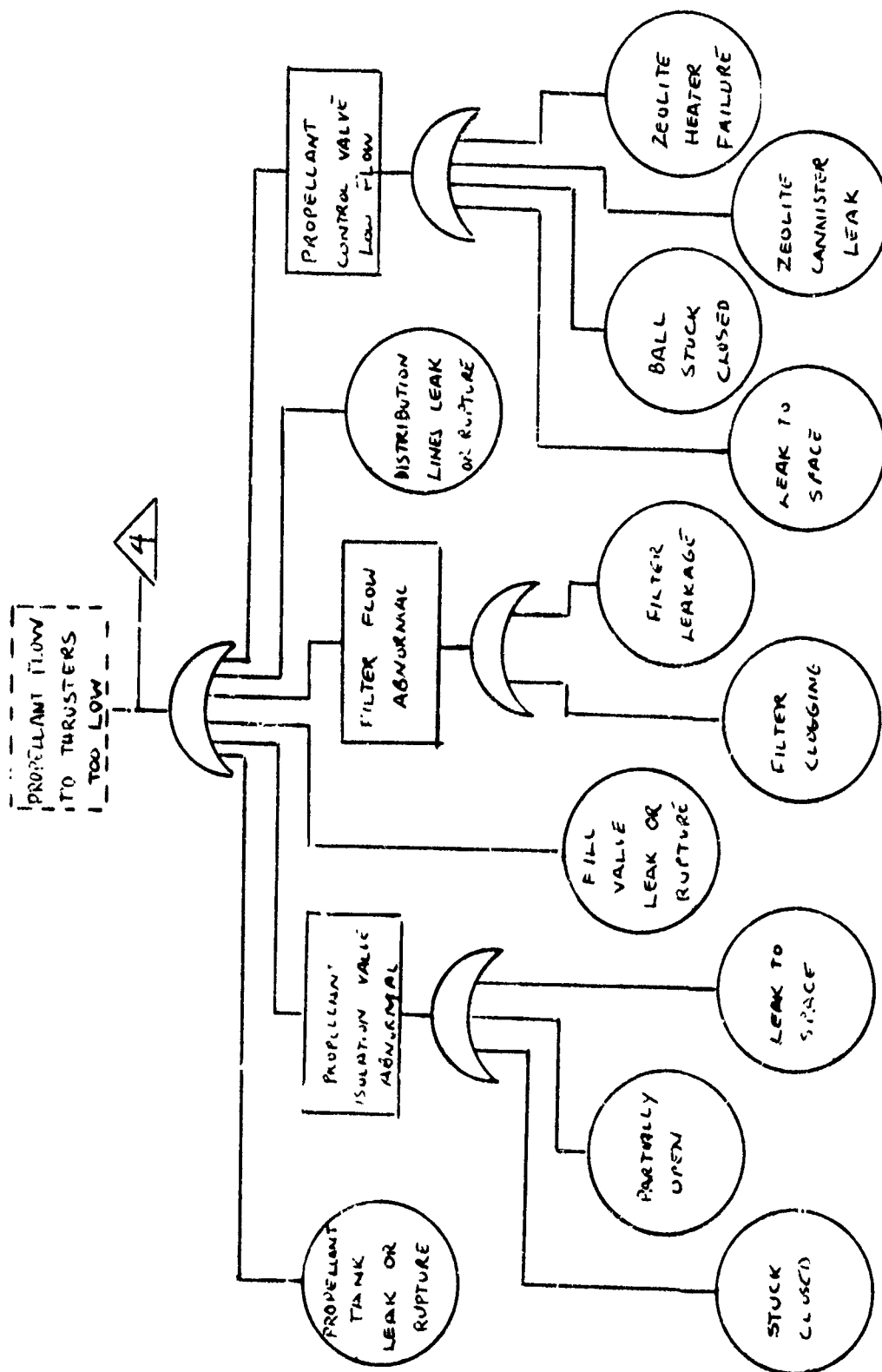Figure 12 (Continued)
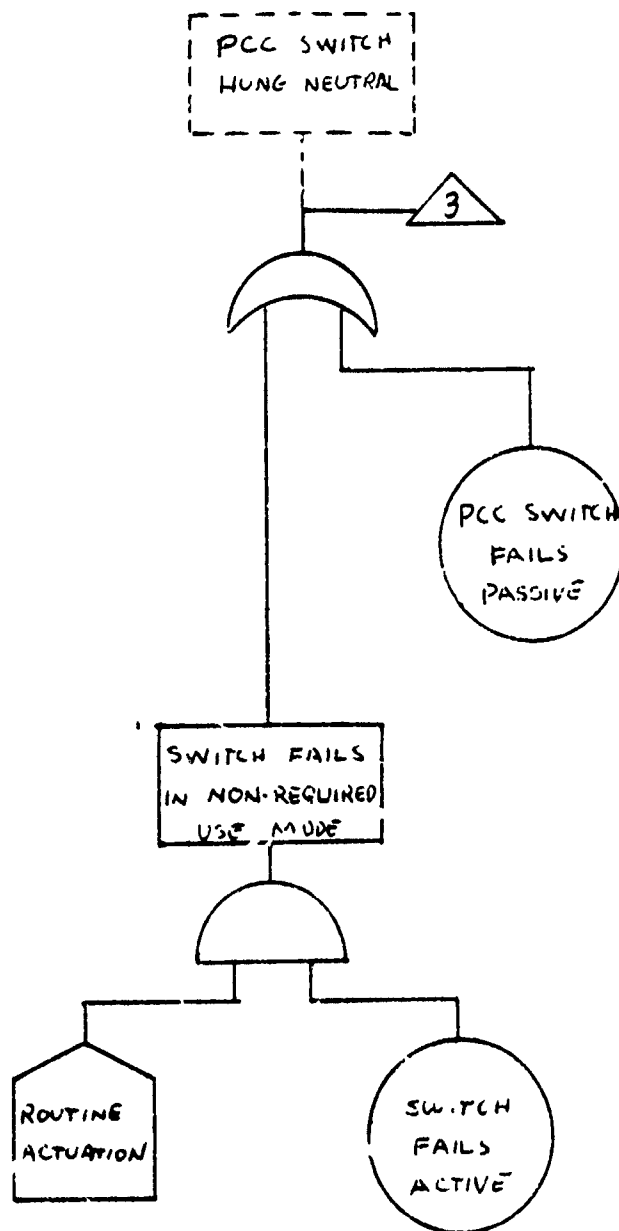
Figure 12 (Continued)
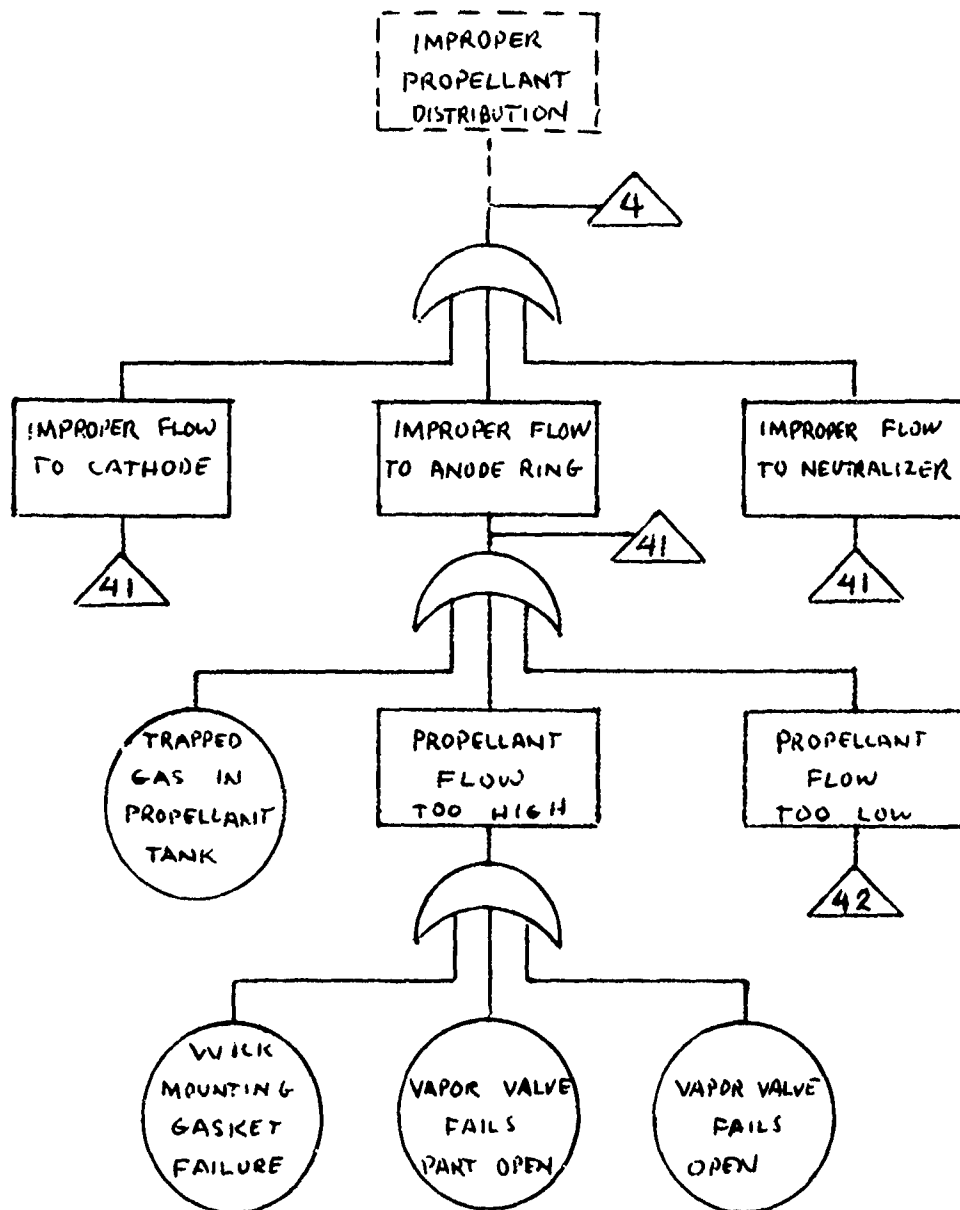
Figure 12 (Continued)
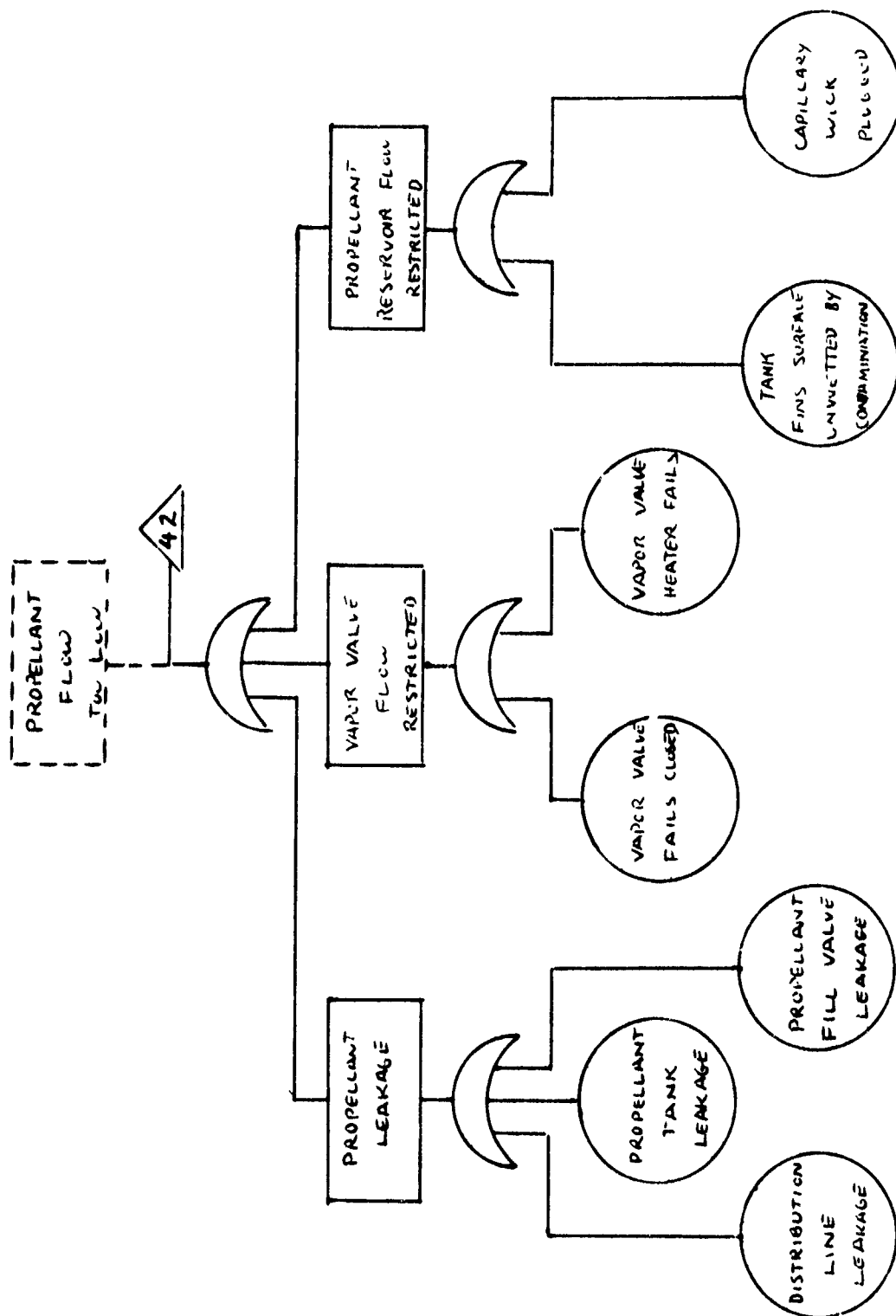
Figure 12 (Continued)

Mercury Ion Electron-Bombardment Thruster. Because of the
very limited developmental activity in ion thrusters, the
analysis presented here was based heavily on one specific
design, the 8-centimeter (cm) Structurally Integrated Thrus-
ter (SIT-8), which produces the thrust level required for the
missions of interest. Generally, this unit is regarded
as a second generation of evolution in mercury (Hg)-ion
electron-bombardment technology. The experience accrued
through the SIT-5 development, which included extensive
laboratory testing to establish durability and predict
useful life, provides the foundation for the new design.
Additionally, experience gained in development of 15-
and 30-cm primary propulsion units is available, in-
cluding the successful flight results of thousands of
hours of operation aboard SERT II.

Despite this existing development background, the
technology of Hg-vapor electron-bombardment thrusters is
very low in maturity from the reliability viewpoint. The
vital components are unique designs without series produc-
tion and without statistically valid failure rates.

In an ion engine, the propellant is transformed to an
emitted stream of ions which have been electrostatically
accelerated to produce thrust forces. The SIT-8 propellant
storage and distribution subsystem contains liquid Hg under
pressure. Since the porous plugs in the feed lines cannot
be wetted by liquid Hg, the propellant is positively con-
tained until the vaporizer is activated. With the vaporizer
heater on, flow is initiated and maintained. The single
Hg reservoir serves both the main cathode and the neutralizer
through branched feed lines, each with its own plug-vaporizer.
Physically, the cathode-isolator-vaporizer (CIV) components
are closely integrated and often referred to as the CIV
assembly.

A schematic of the system analyzed is shown in
Figure 13. The fault tree analysis is presented in
Figure 14. (For component level detail of the "THRUSTER"
element of Figure 13, refer to Figure 3, Mercury Ion
Electron Bombardment Generic System Layout, page I-5).
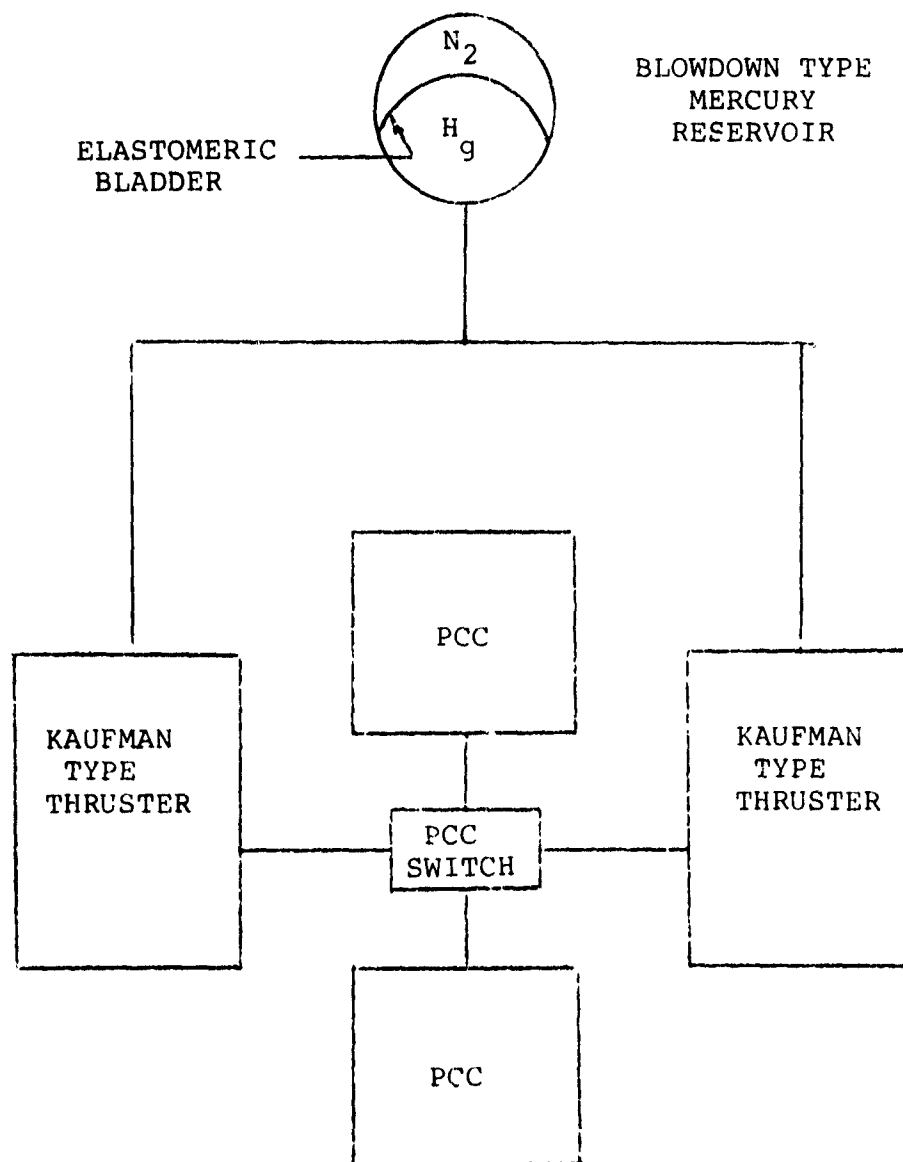
Figure 13. Mercury Ion System Schematic

MERCURY ION ELECTRON BOMBARDMENT SYSTEM
FAULT TREE ANALYSIS
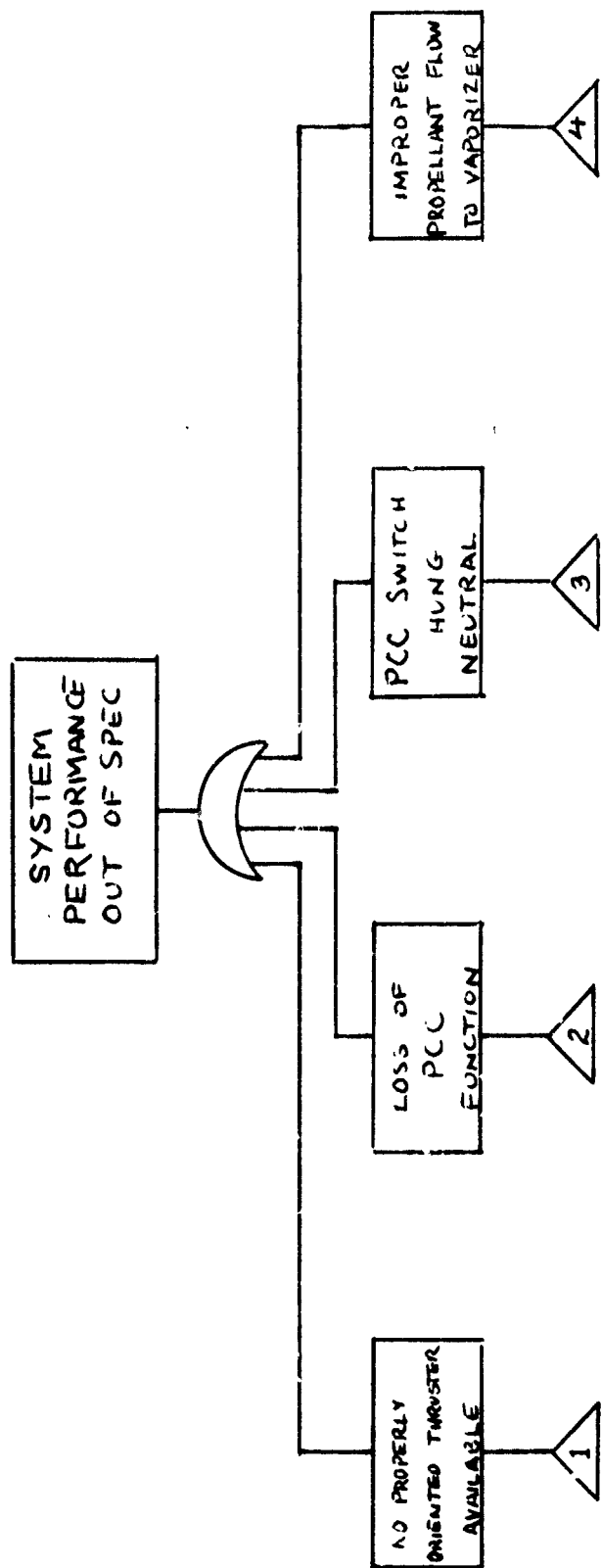
Figure 14   Mercury Ion System Fault Tree Analysis
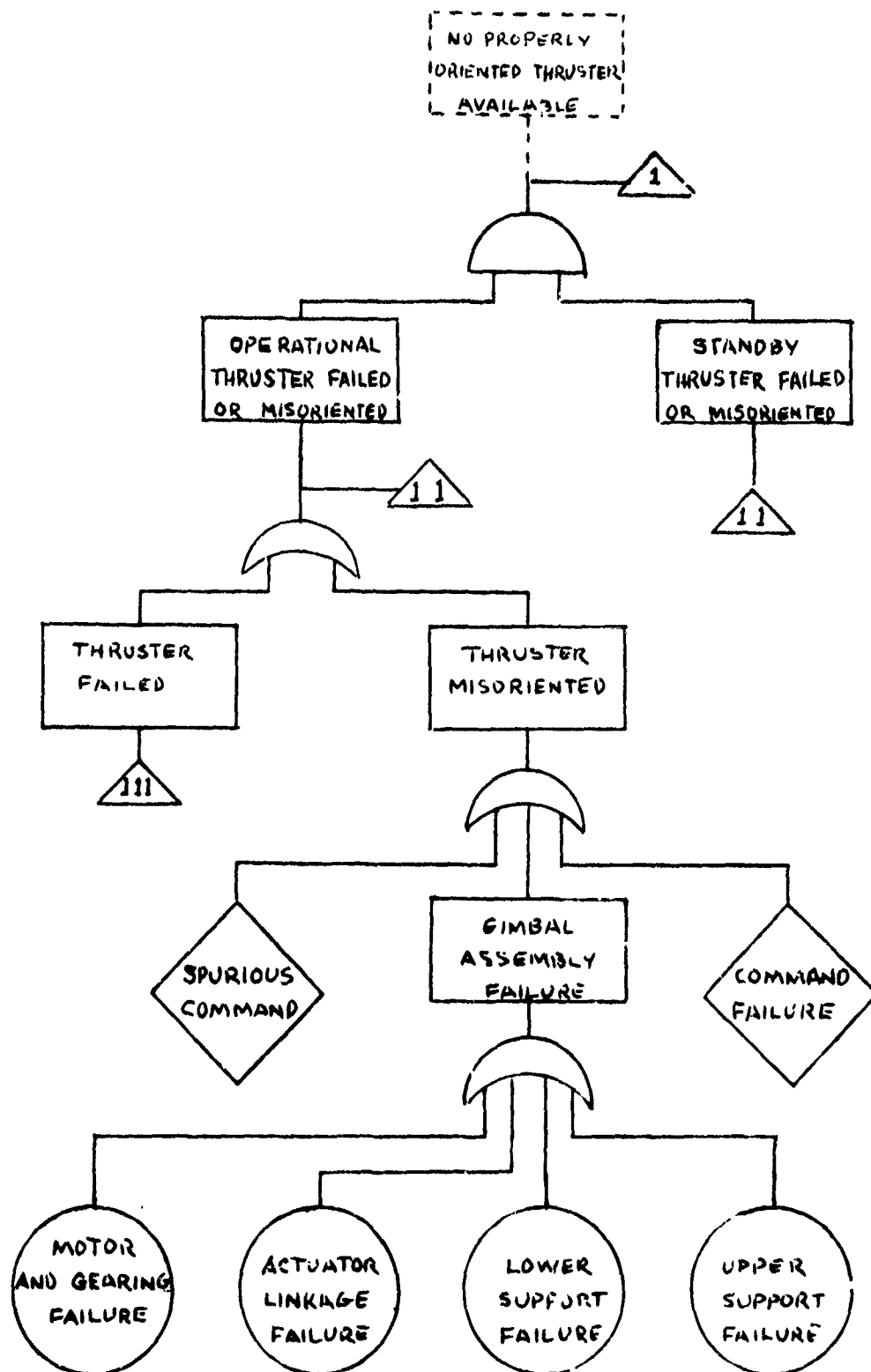
Figure 14 (Continued)
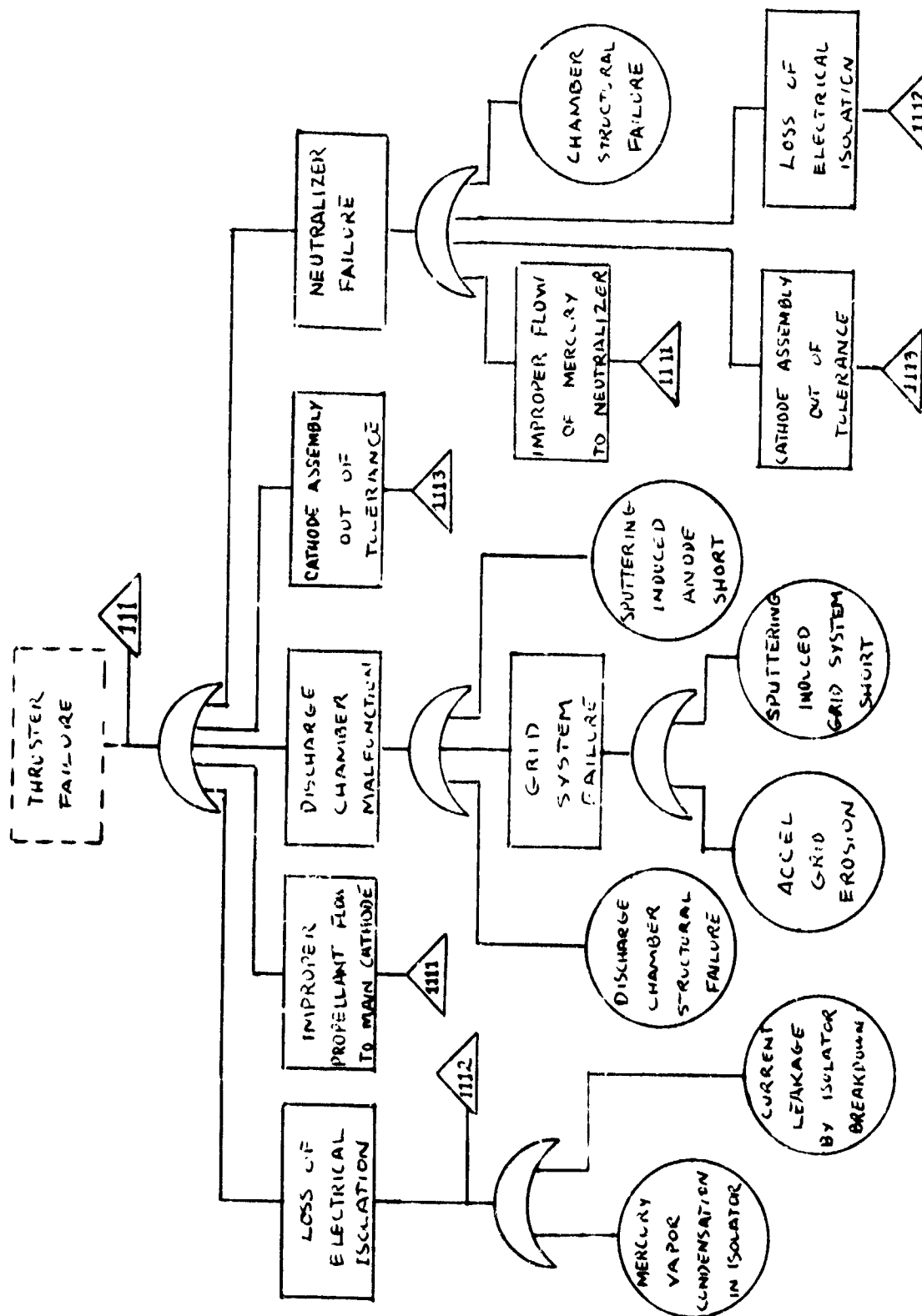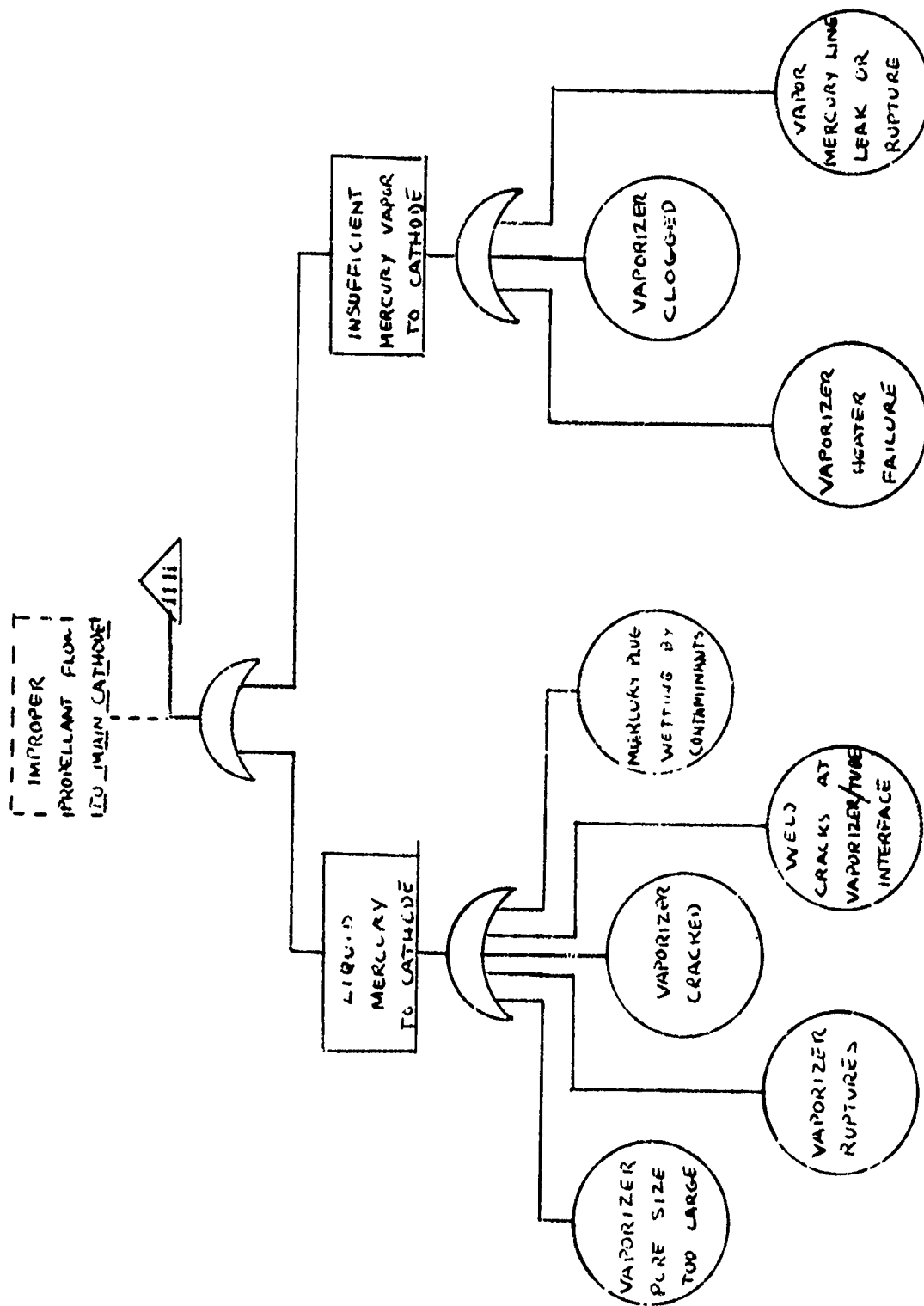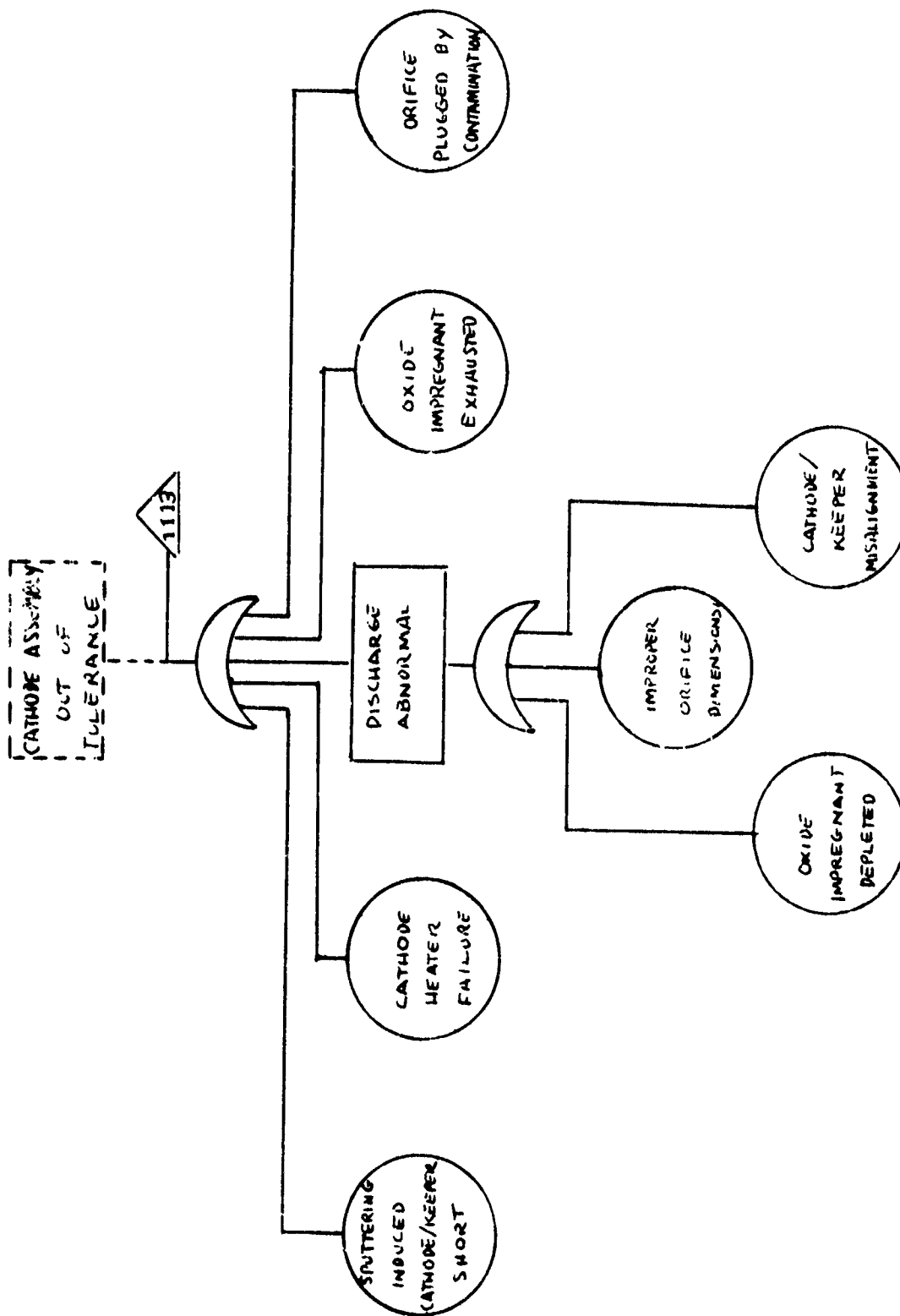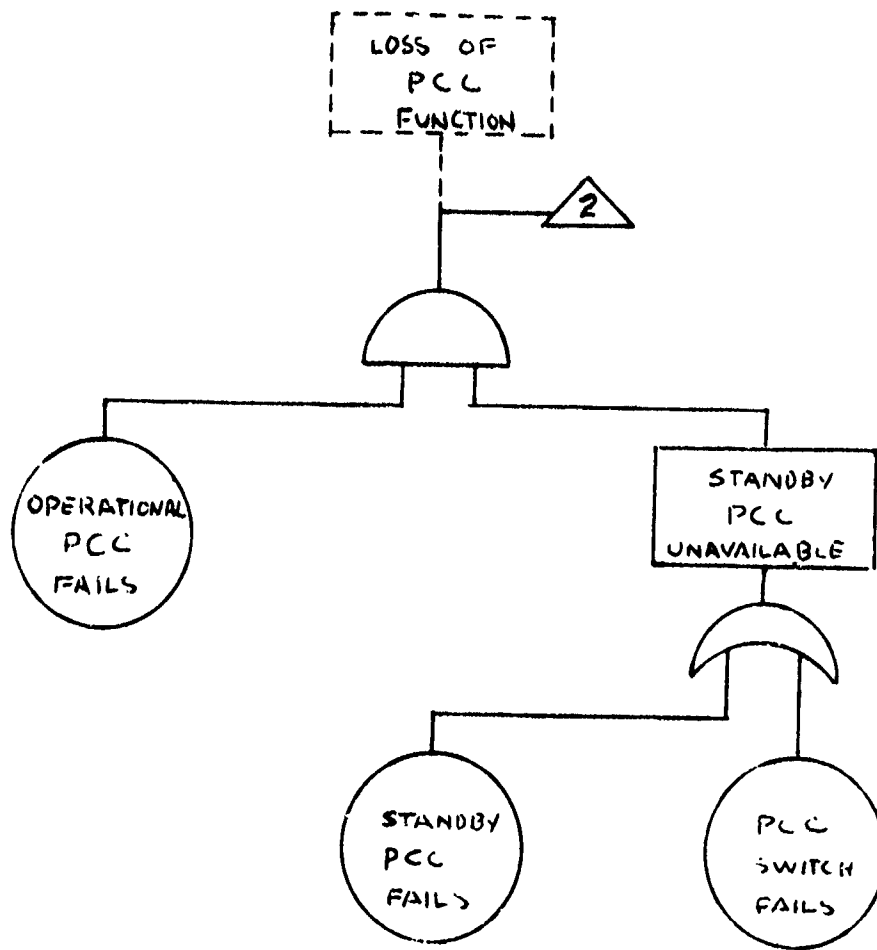
I-200

Figure 14 (Continued)

Figure 14 (Continued)

Figure 14 (Continued)

CATHODE ASSEMBLY OUT OF TOLERANCE

1113

DISCHARGE ABNORMAL

ORIFICE PLUGGED BY CONTAMINATION

OXIDE IMPREGNANT EXHAUSTED

CATHODE HEATER FAILURE

SPUTTERING INDUCED CATHODE/KEEPER SHORT

CATHODE/KEEPER MISALIGNMENT

IMPROPER ORIFICE DIMENSIONS

OXIDE IMPREGNANT DEPLETED

Figure 14 (Continued)

I-204

Figure 14 (Continued)

Figure 14 (Continued)

I-206
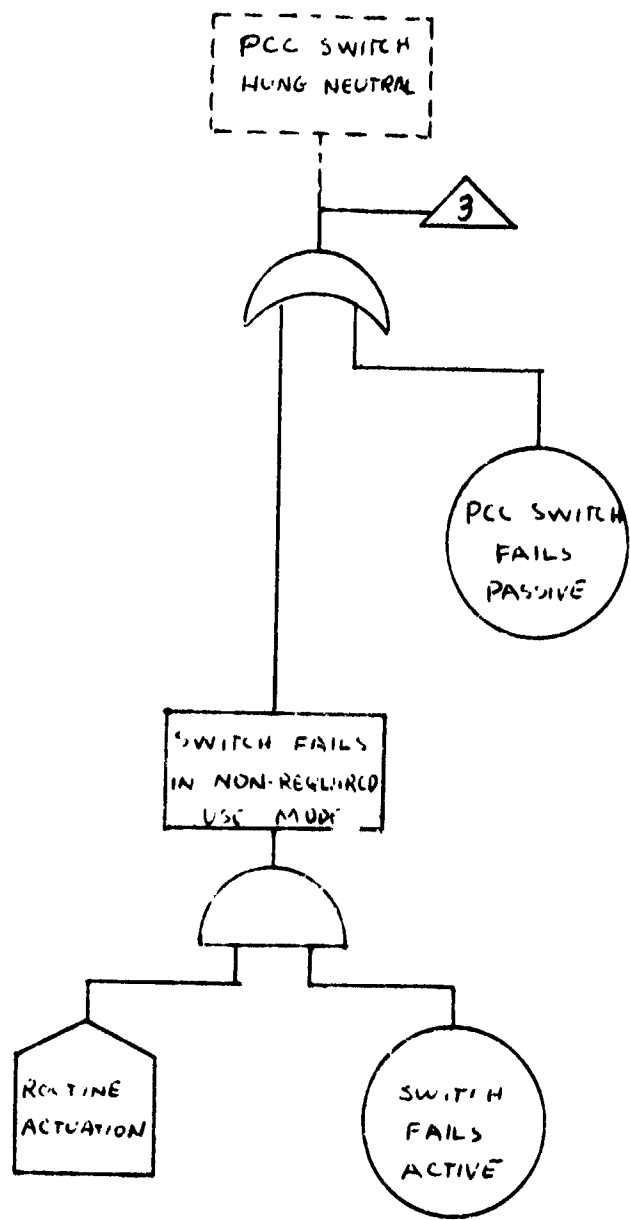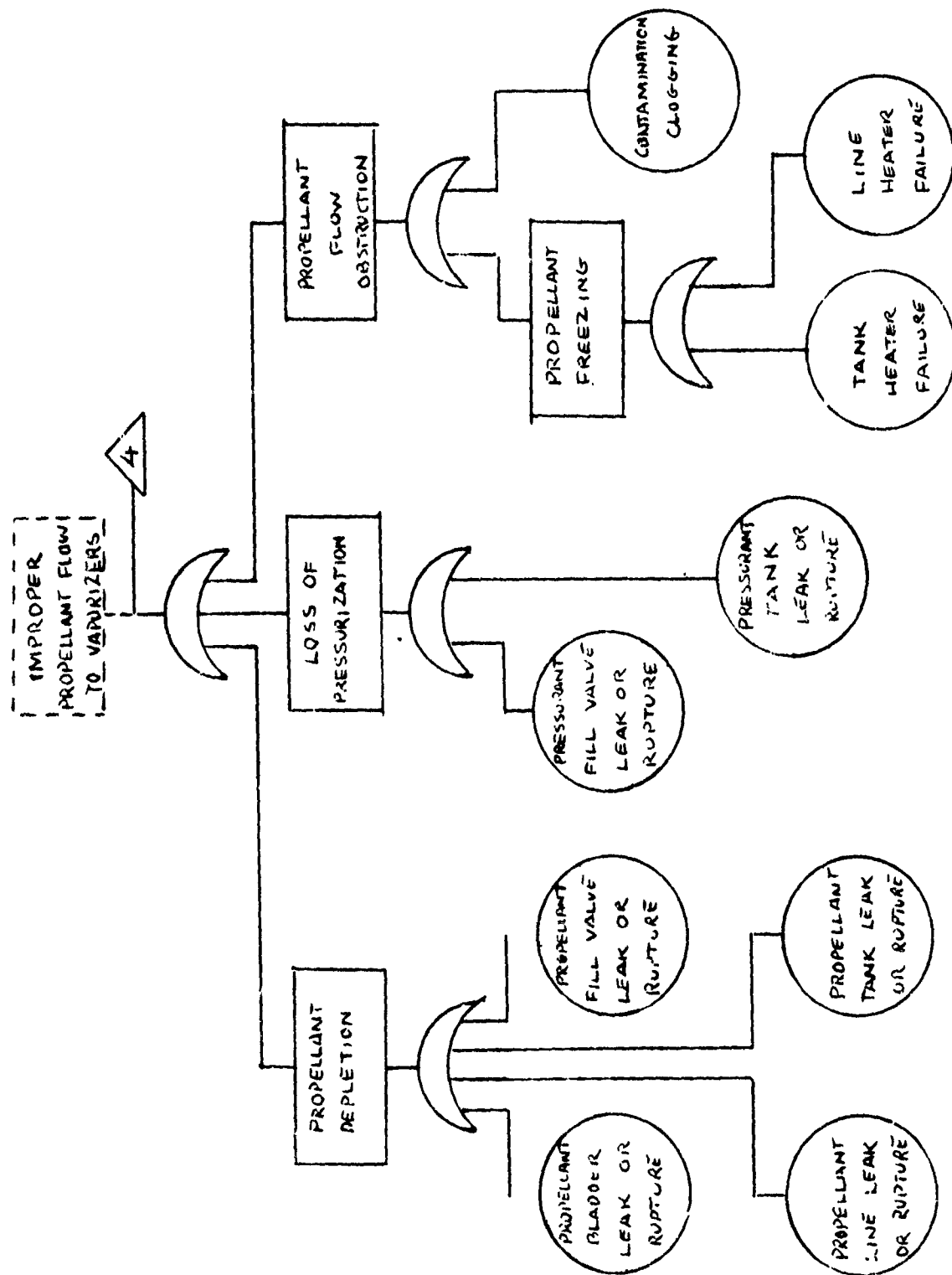
Solid Propellant Pulsed Plasma System. Current solid pro-
pellant pulsed plasma systems employ polytetraflouroethylene
(Teflon) as the propellant. The exposed face(s) of the
Teflon are subjected to electrical discharges that ablate
and depolymerize surface layers and convert the products
into a plasma that is ejected through a nozzle. Each pulse
involves initiating a discharge by an igniter that generates
a "microplasma" which, in turn, initiates the discharge across
the Teflon. Energy for the discharge is obtained from one
or more high-voltage, high-capacitance energy storage capa-
citors. The capacitors, in turn, are fed from conventional
spacecraft d.c. busses through stepup and charge control
circuitry. Capacitor charging occurs between pulses but
does not necessarily occupy the entire interval between
discharges.

No fuel feed control is required. The thruster struc-
ture accommodates the Teflon in the form of solid rods which
may be straight or curved and have rectangular cross sections.
As ablation takes place, constant-force (Negator) springs
advance the remaining Teflon to a shoulder of the discharge
electrodes. The Teflon is, of course, self-lubricating in
its feed guides. Since there are no significant cyclic
loads on the feed system, the failure rate is expected to
be negligible.

The mechanical simplicity of the solid propellant pulsed
plasma thruster causes reliability to be dominated by the
electronic aspects. Reliability analysis for charging,
discharge-initiating, and associated circuitry is to be
performed by the methods outlined in the Electronic Compo-
nents and Assemblies section, where detailed discussion of
two special electronic components, the energy storage capa-
citor and the ignitor, also appears.

A schematic of the system analyzed is shown in Figure
15.   The fault tree analysis is presented in figure 16.
(For component level detail of the "THRUSTER" element of
Figure 15, refer to Figure 4, Pulsed Plasma Generic Sys-
tem Layout, page I-6).
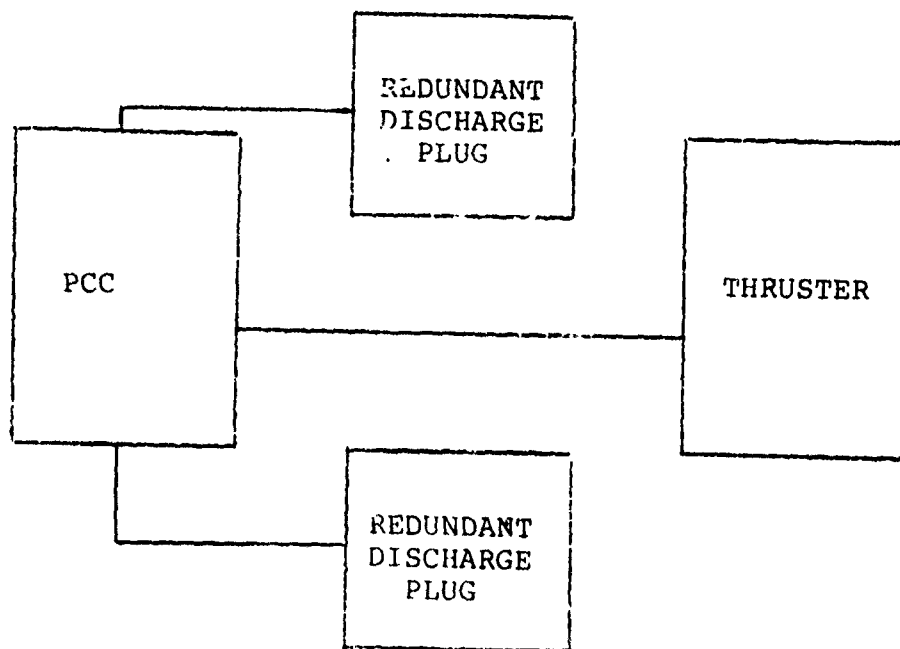
Figure 15 Pulsed Plasma System Schematic

PULSED PLASMA SYSTEM
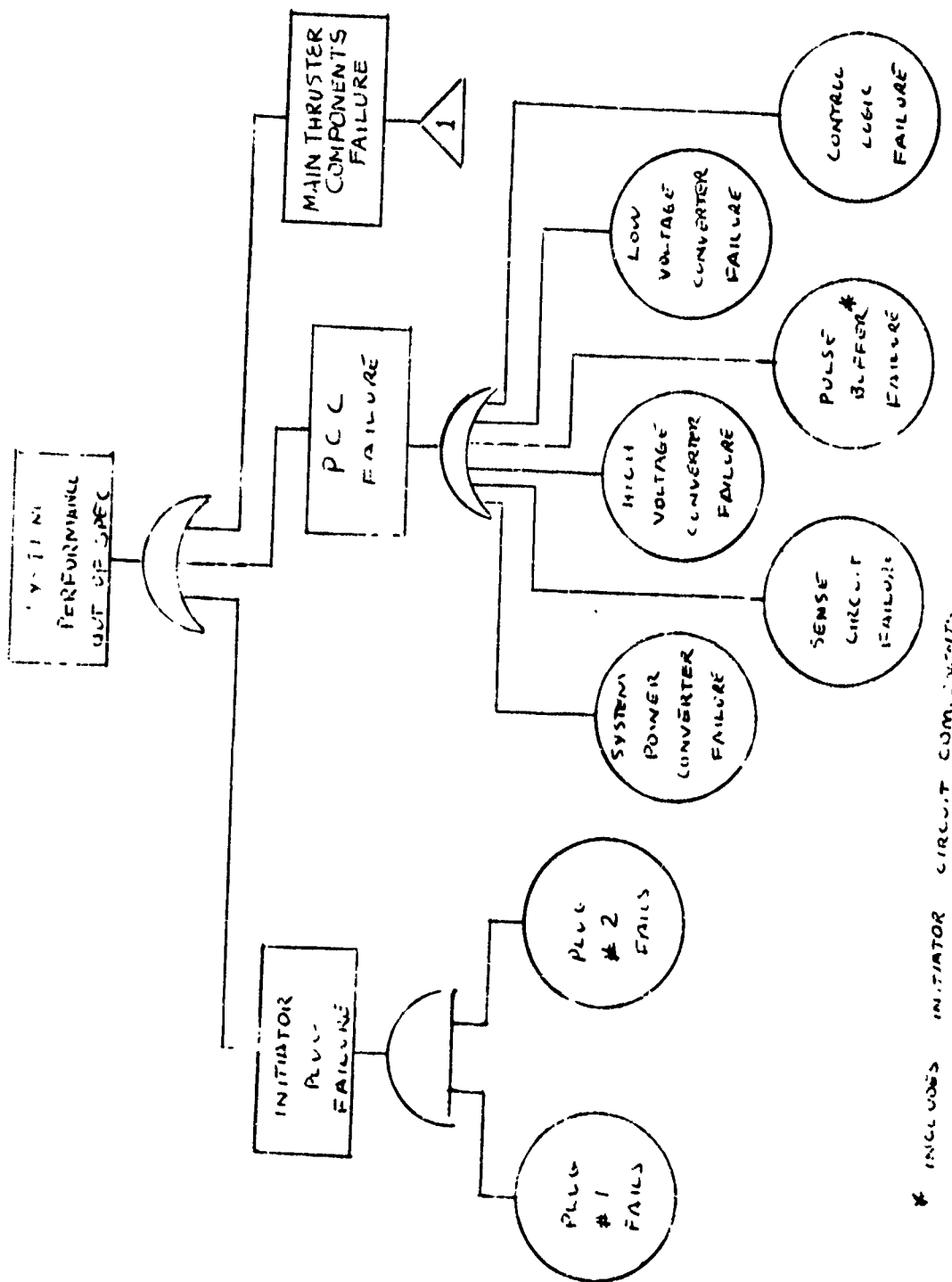
FAULT TREE ANALYSIS

Figure 16. Pulsed Plasma System Fault Tree Analysis
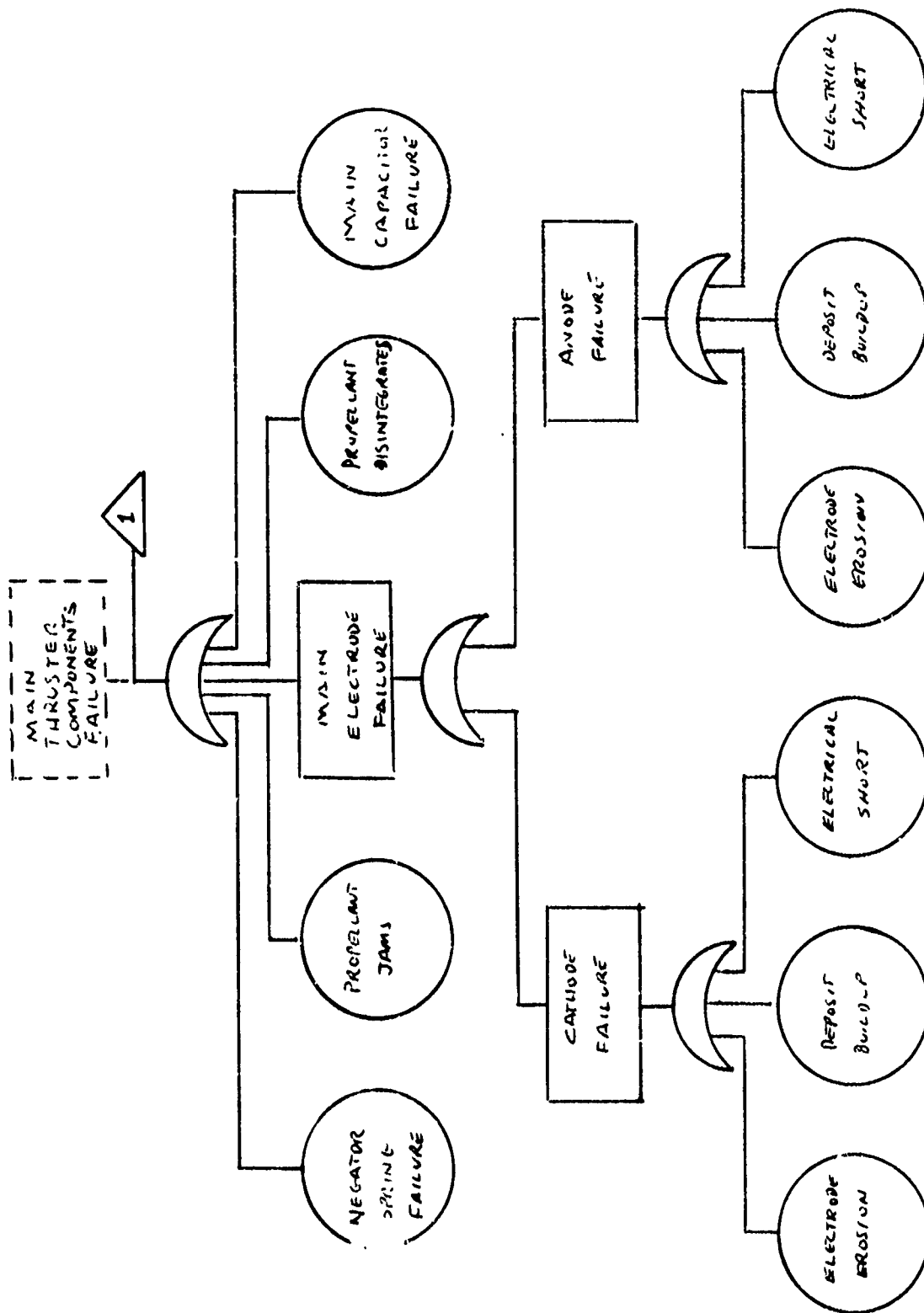
Figure 16 (Continued

Colloid Electric Propulsion System. The thruster is comprised of 12 modules, each of which consists of 36 hollow tubes (needles). The propellant (sodium iodide-doped glycerol) is fed through the needles to their tips, where it is exposed to a vacuum and a high voltage gradient ($\approx 14kv$) between the needles and the extractor plate. The voltage gradient breaks the propellant into droplets that have a positive electron charge, and accelerates them to provide the thrust. Test verify that specification level performance can be achieved and that nonwetting films of oil-like contamination must be prevented from accumulating on the needle tips.

The feed system consists of a storage bellows and a flow controller. In addition to containing the propellant until demanded by the thruster, the bellows has a spring force that pressurizes the propellant so that it can flow against the various impedances of the system. The controller acts as a propellant shutoff device and regulates flow through a ball seat to meet thrusted demands. Flow regulation and termination were found to be sensitive to voids within the propellant to the controller.

The neutralizer is a thin (0.002 in. diameter) tungsten wire, which is heated until a sufficient quantity of electrons is emitted to equal the positive current from the thruster. Accelerated life tests demonstrated that analytical derived lifetime projections were conservative and that lifetime is not substantially influenced by exposure to vapor (propellant).

The power conditioner converts input power from the spacecraft into the forms (voltage and frequency) required by the various elements of the thruster system. In addition, it controls system operating functions, accepts and implements ground commands, and provides a telemetry output of critical operating parameters. Its basic function is to provide high-voltage power to the thruster by means of an inductive storage circuit.

(For component level detail of the "THRUSTER" element of Figure 17 refer to Figure 5, Colloid Generic System Layout, page I-7).
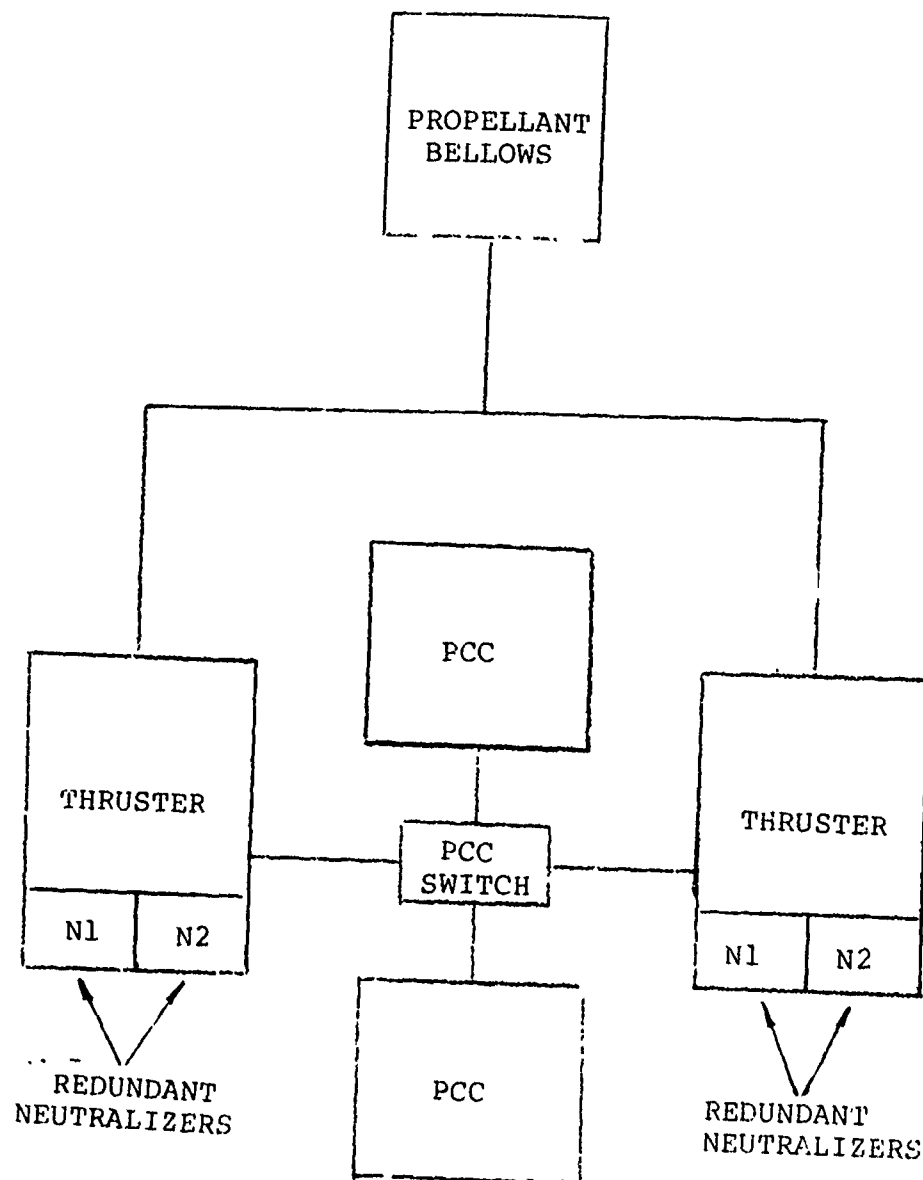
Figure 17. Colloid System Schematic

COLLOID SYSTEM

FAULT TREE ANALYCIS
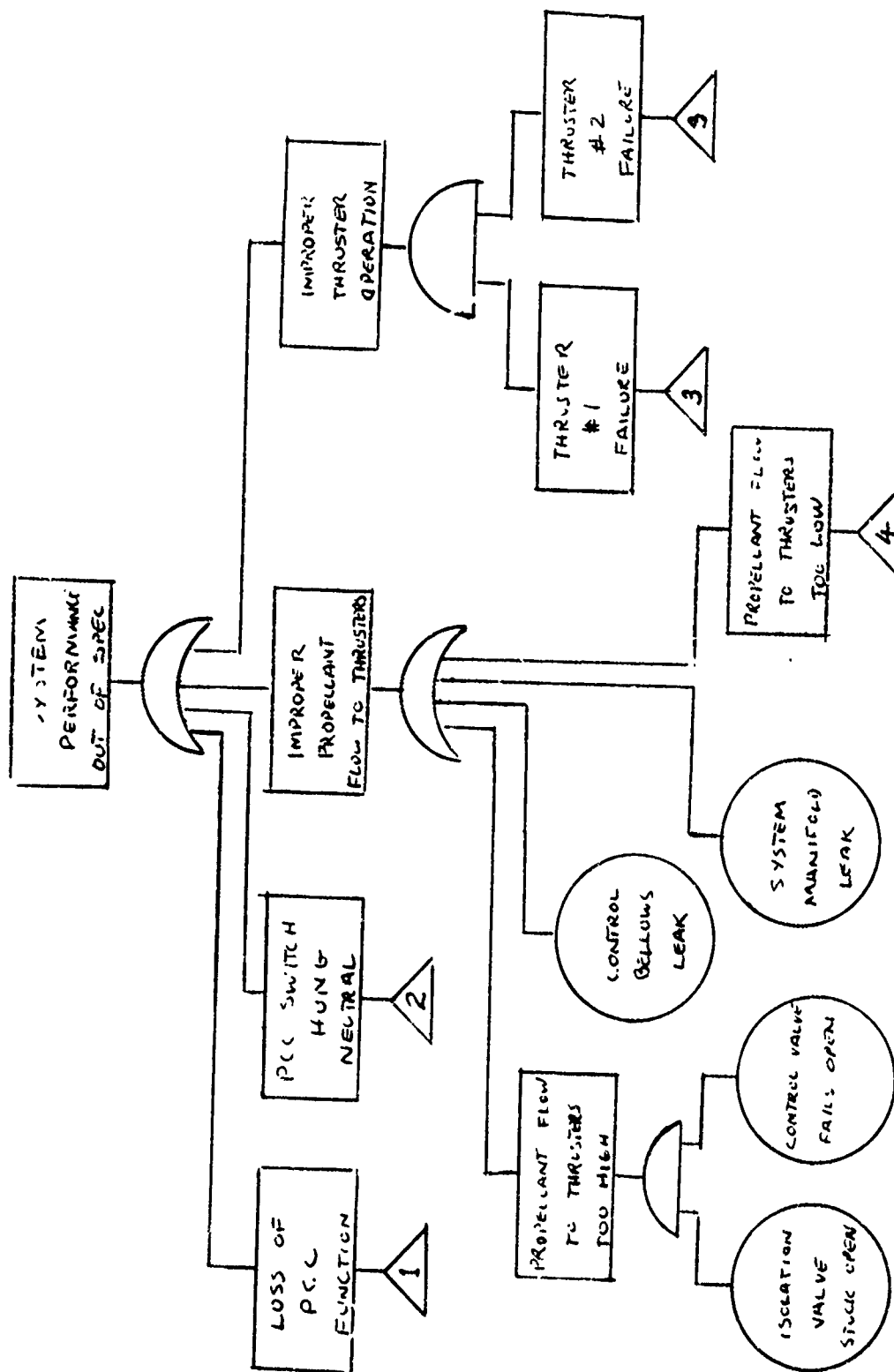
Figure 18. Colloid System Fault Tree Analysis
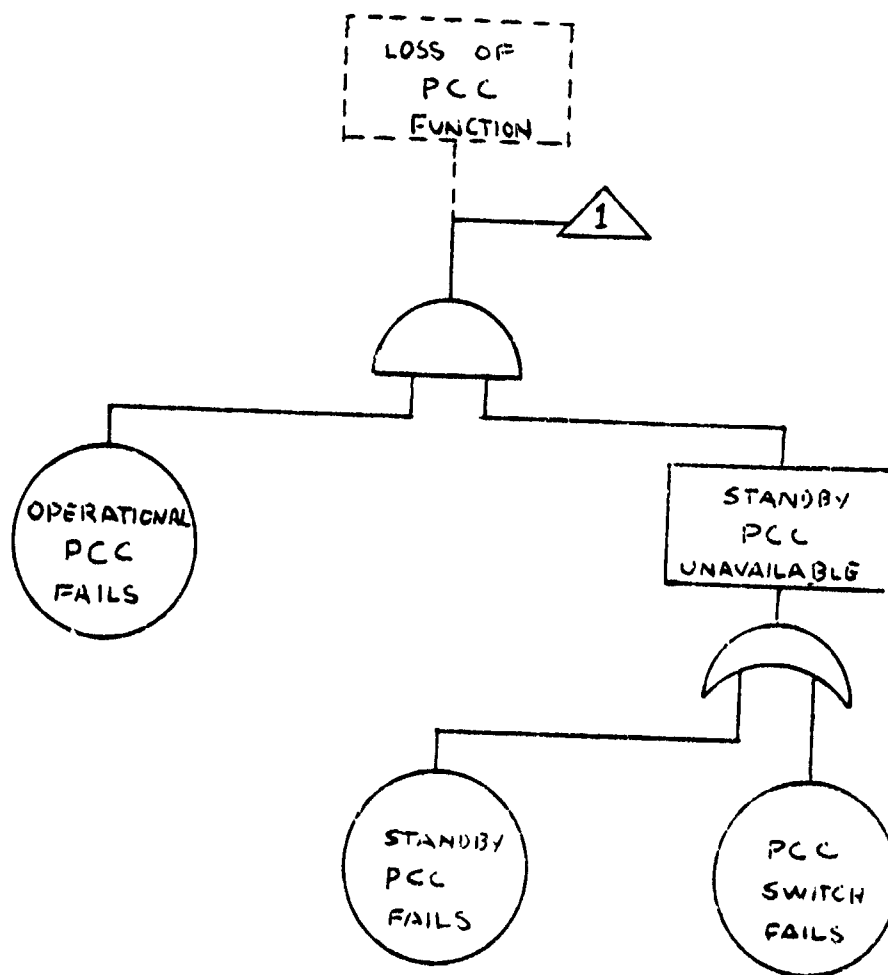
Figure 18 (Continued
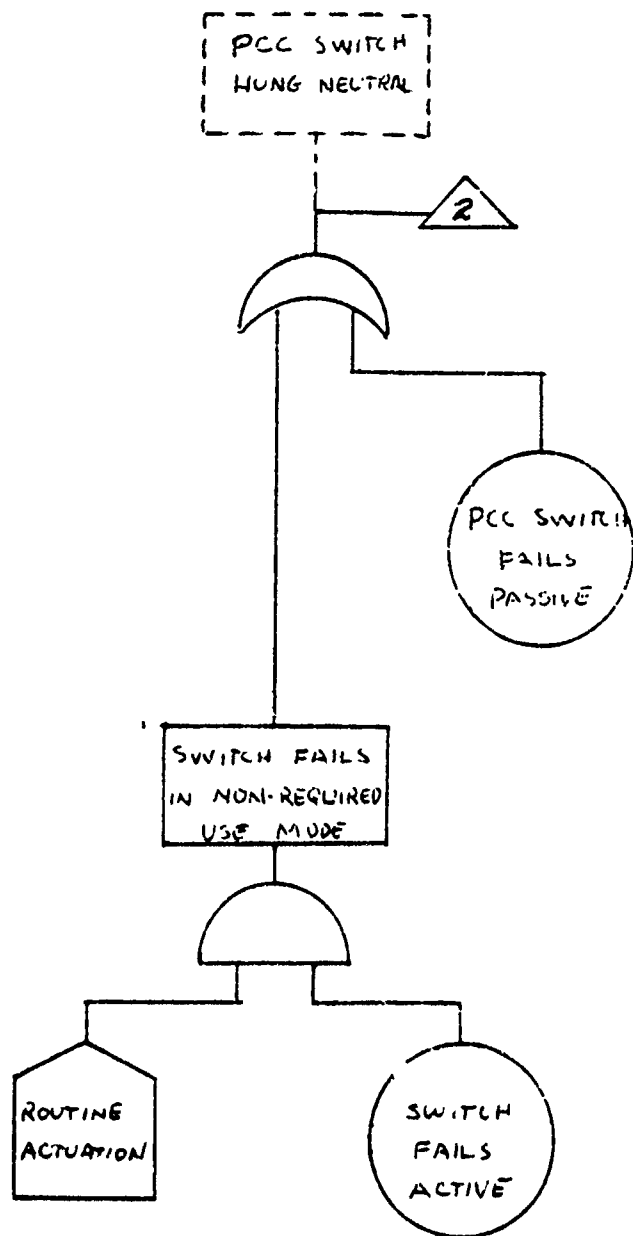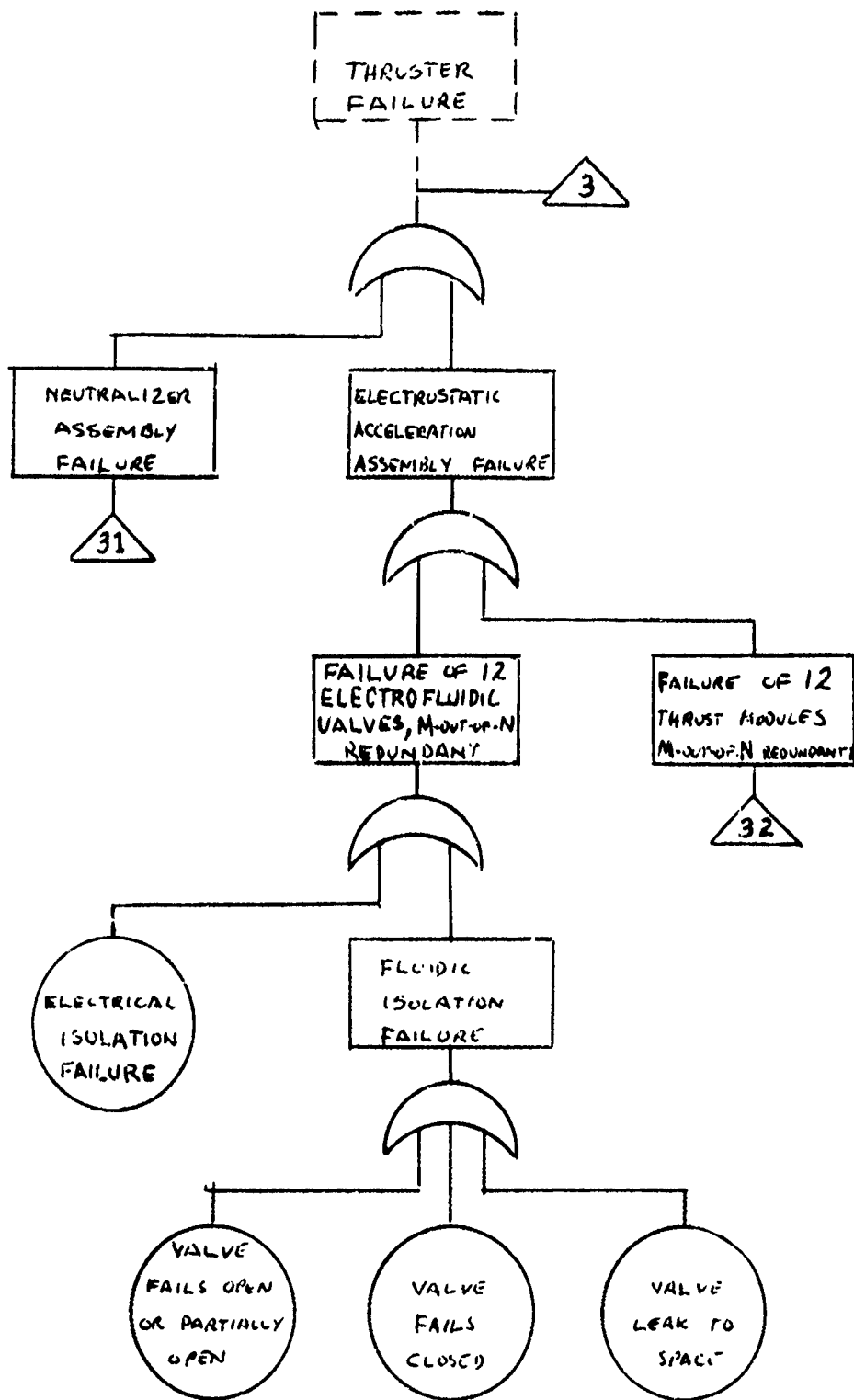
Figure 18 (Continued)

I-217
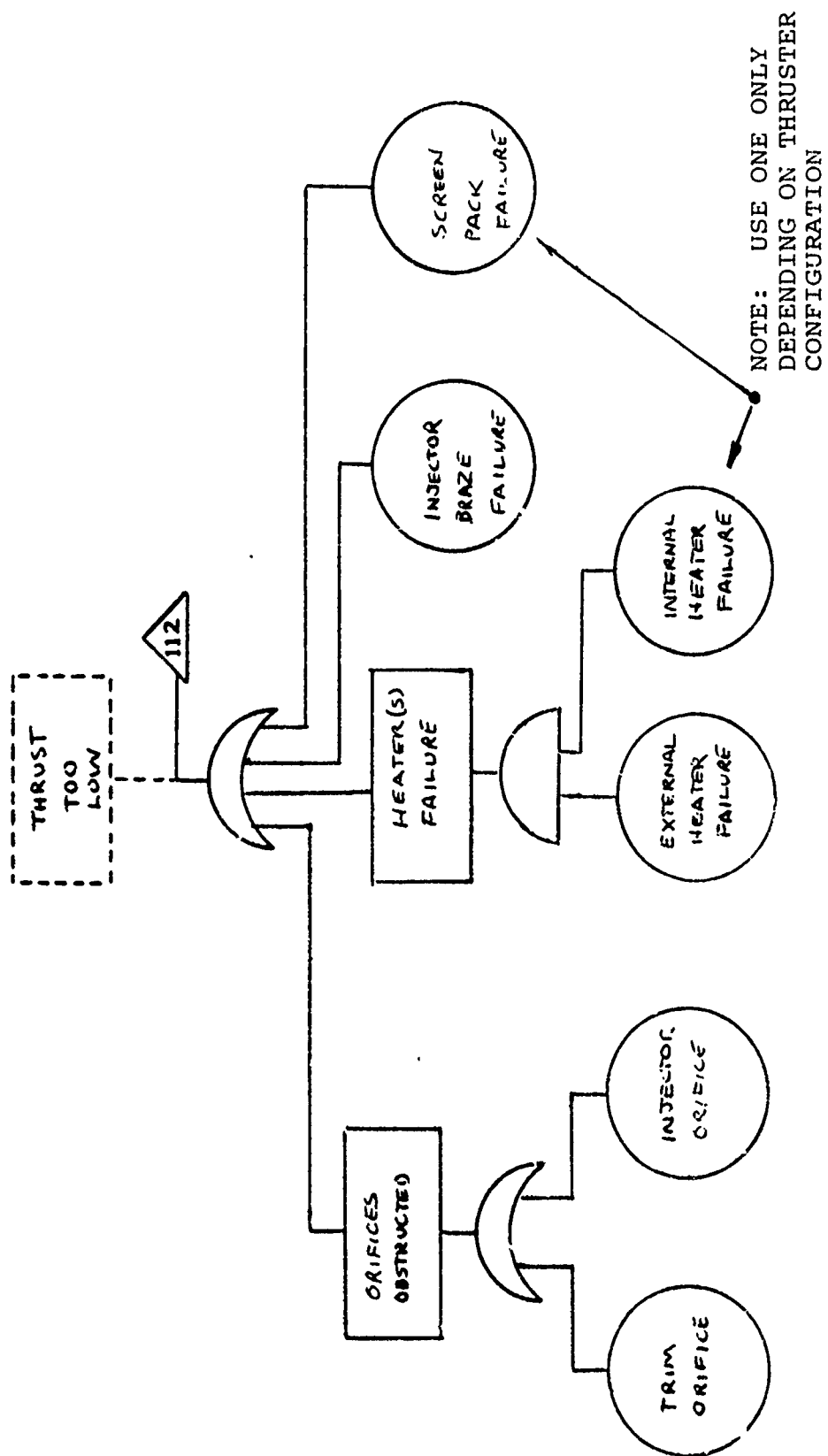
Figure 18 (Continued)

I-218

Figure 18 (Continued)

Figure 18 (Continued)

I-220
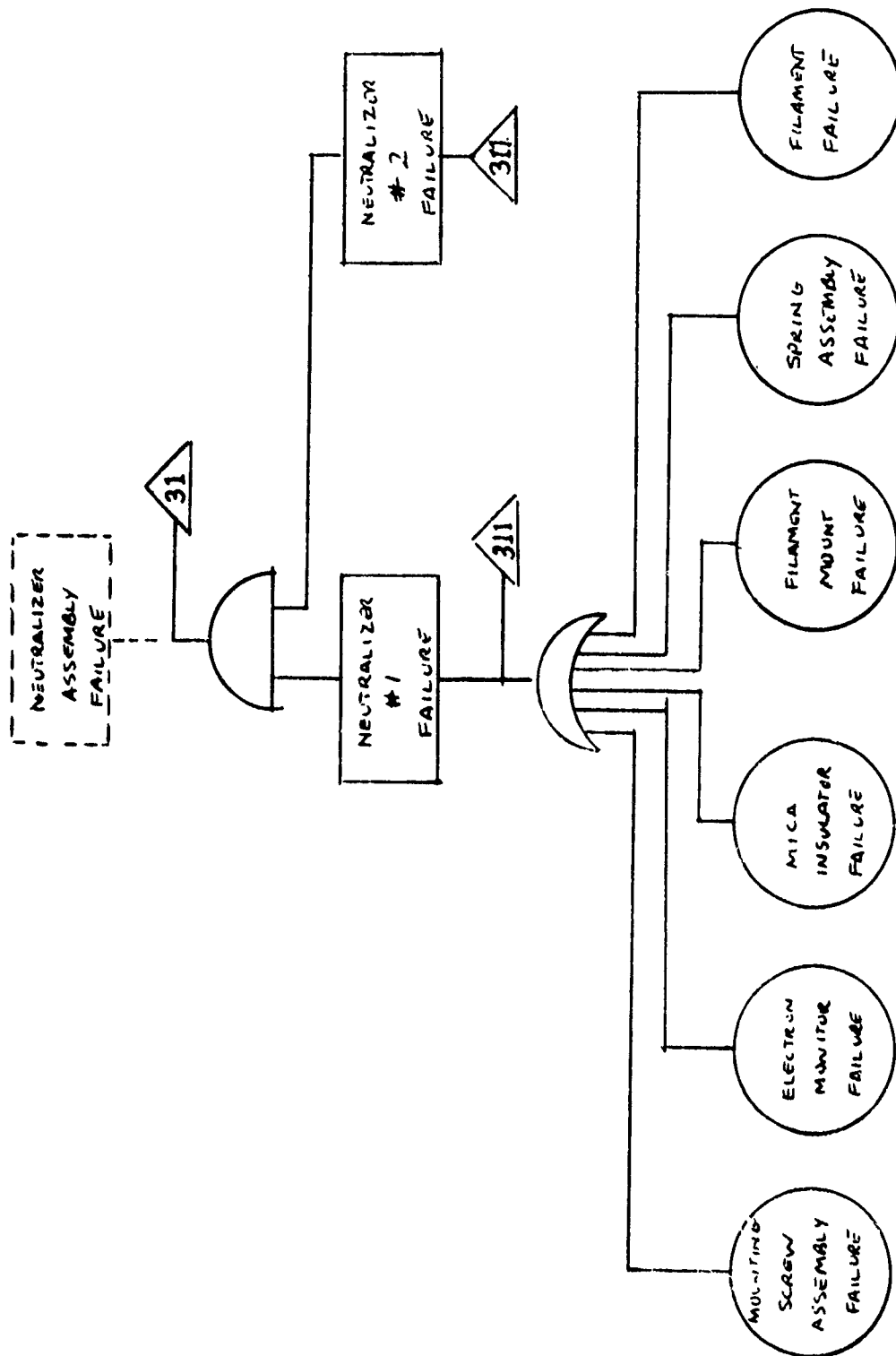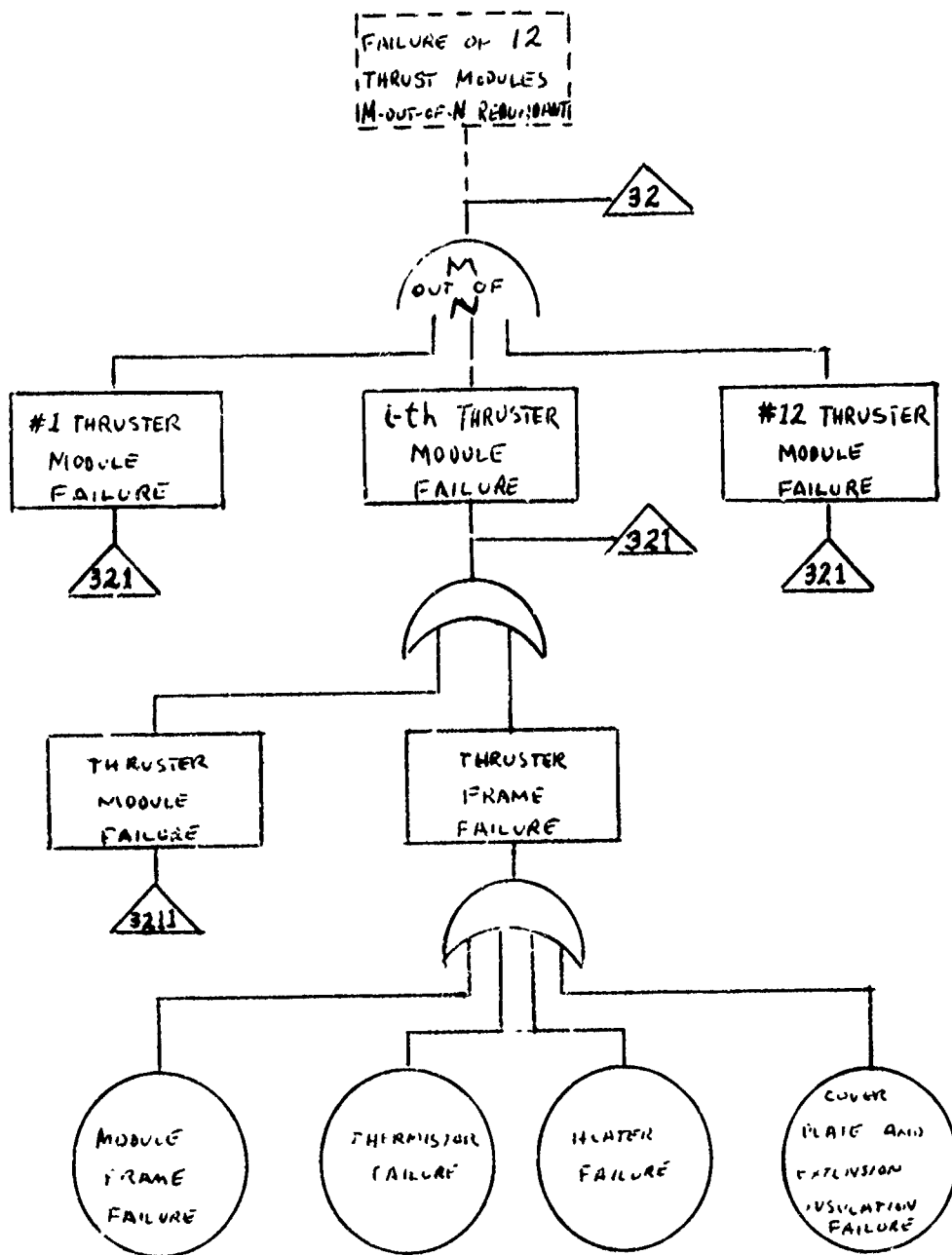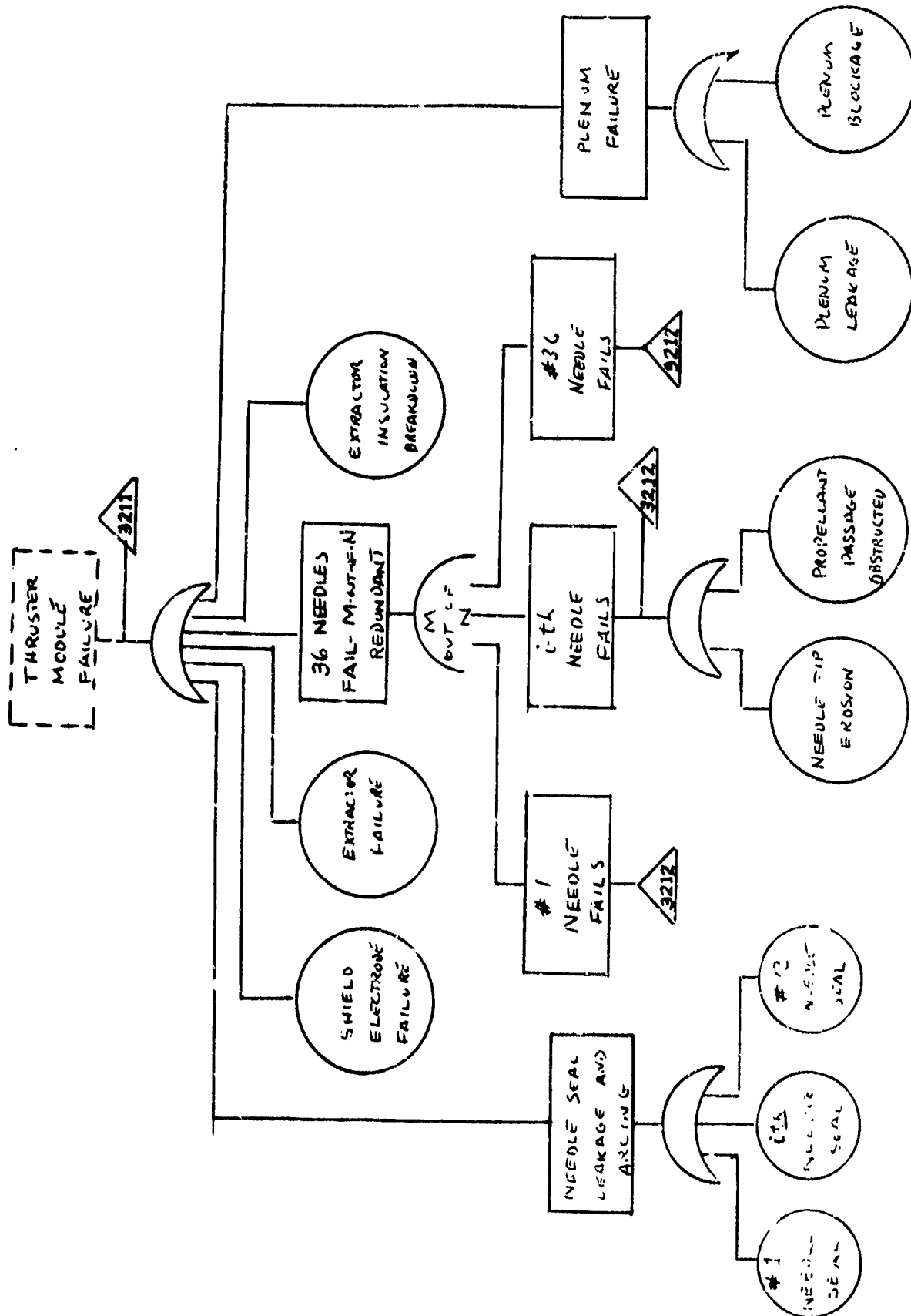
Figure 18 (Continued)

Figure 18 (Continued)

Catalytic Monopropellant. This is one of the most widely
used auxiliary propulsion systems. It has been applied over
a broad spectrum of thrust levels and mission times. The
basic scheme derives thrust from the spontaneous exothermic
decomposition of hydrazine when it is brought into contact
with a catalyst: Initially a catalyst was used (H-7) that
required heating. The catalyst currently employed is
Shell 405 granule forms of various sizes. Developmental
work is underway on monolithic catalyst system, but the
Shell 405 catalysts are in use exclusively at this time
and comprise the catalyst bed analyzed in this study. Mild
heating of the catalyst bed is employed in some designs
to prolong catalyst life and minimize rough start conditions.
"Cold start" designs have also been produced and employed
with success. A blowdown pressurization system was used
in conjunction with the catalytic thruster in this analysis.
However, pressurized surface tension schemes and constant
regulated pressure schemes may also be employed. Each of
these alternatives ahs been assessed: pressurized surface
tension in conjunction with the electrothermal thruster
and constant pressure with the bipropellant thruster. The
three thruster types and the three pressurization systems
are completely interchangeable.

The interchanging of appropriate fault tree branches
will yield "synthesized" fault trees for all desired
combinations.

A schematic of the system analyzed is shown in Figure
19. The fault tree analysis is presented in Figure 20.

(For additional system details refer to Figure 6, Catalytic
Monopropellant Generic System Layout page I-8).
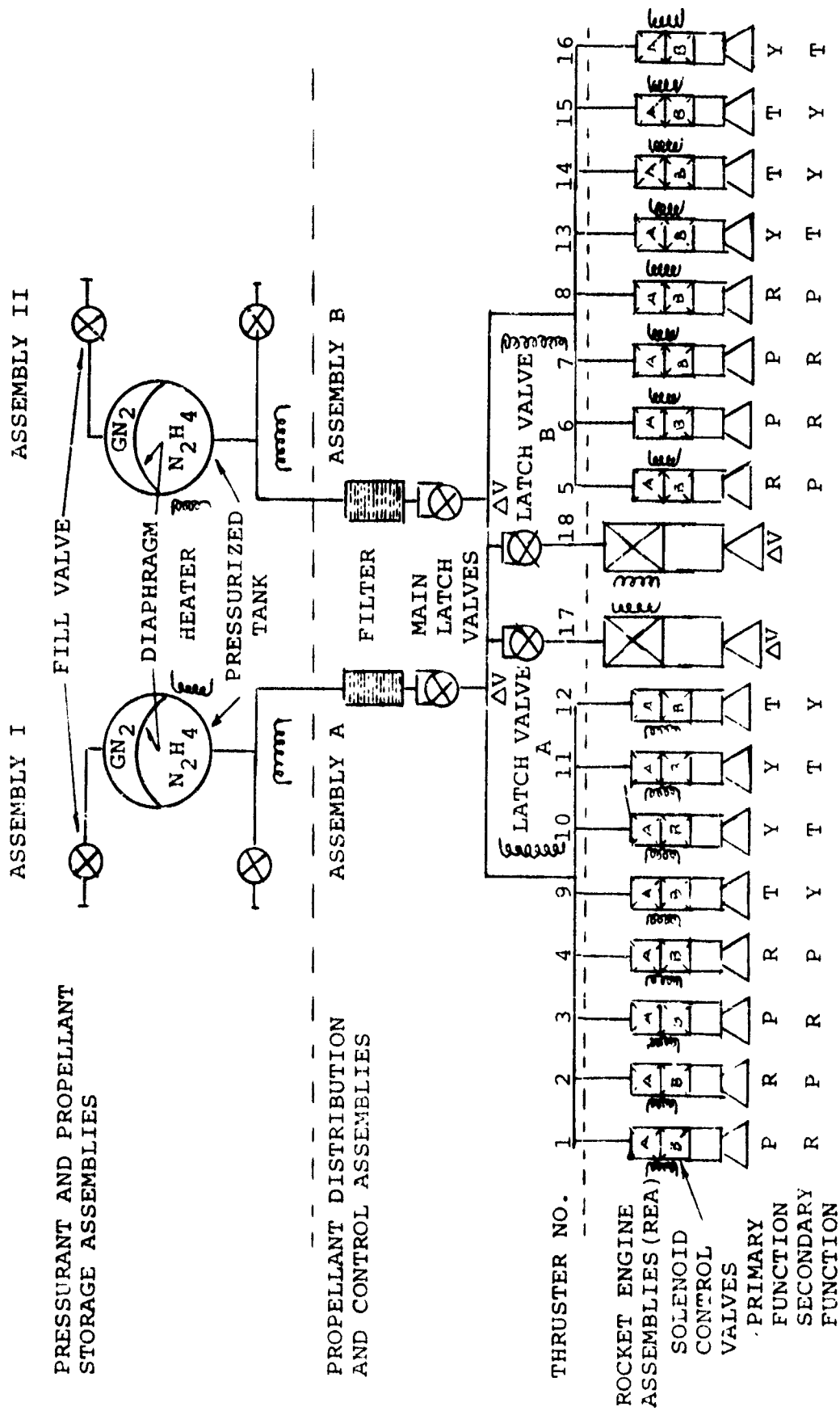
Figure 19. Catalytic Monopropellant System Schematic

CATALYTIC MONOPROPELLANT SYSTEM

FAULT TREE ANALYSIS
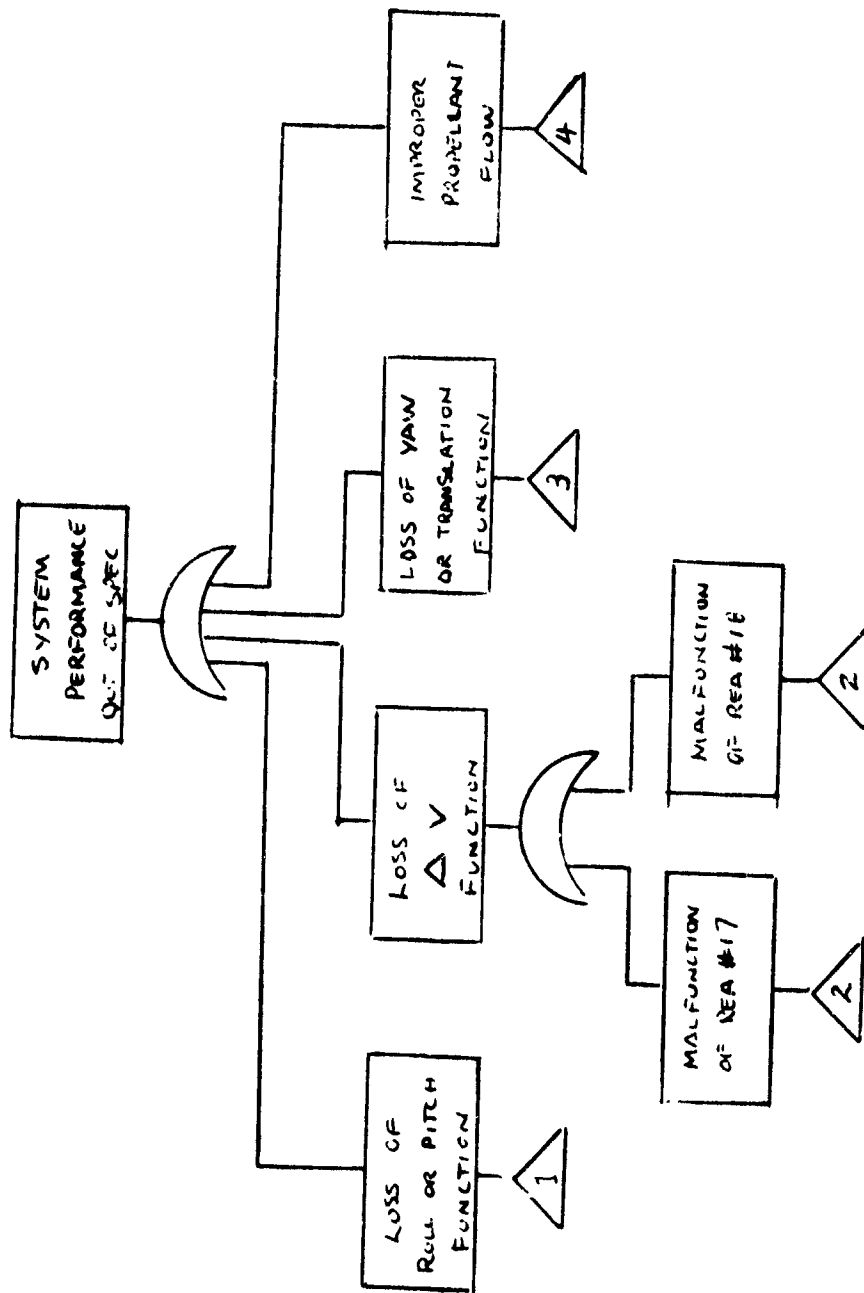
Figure 20   Catalytic Monopropellant System Fault Tree Analysis
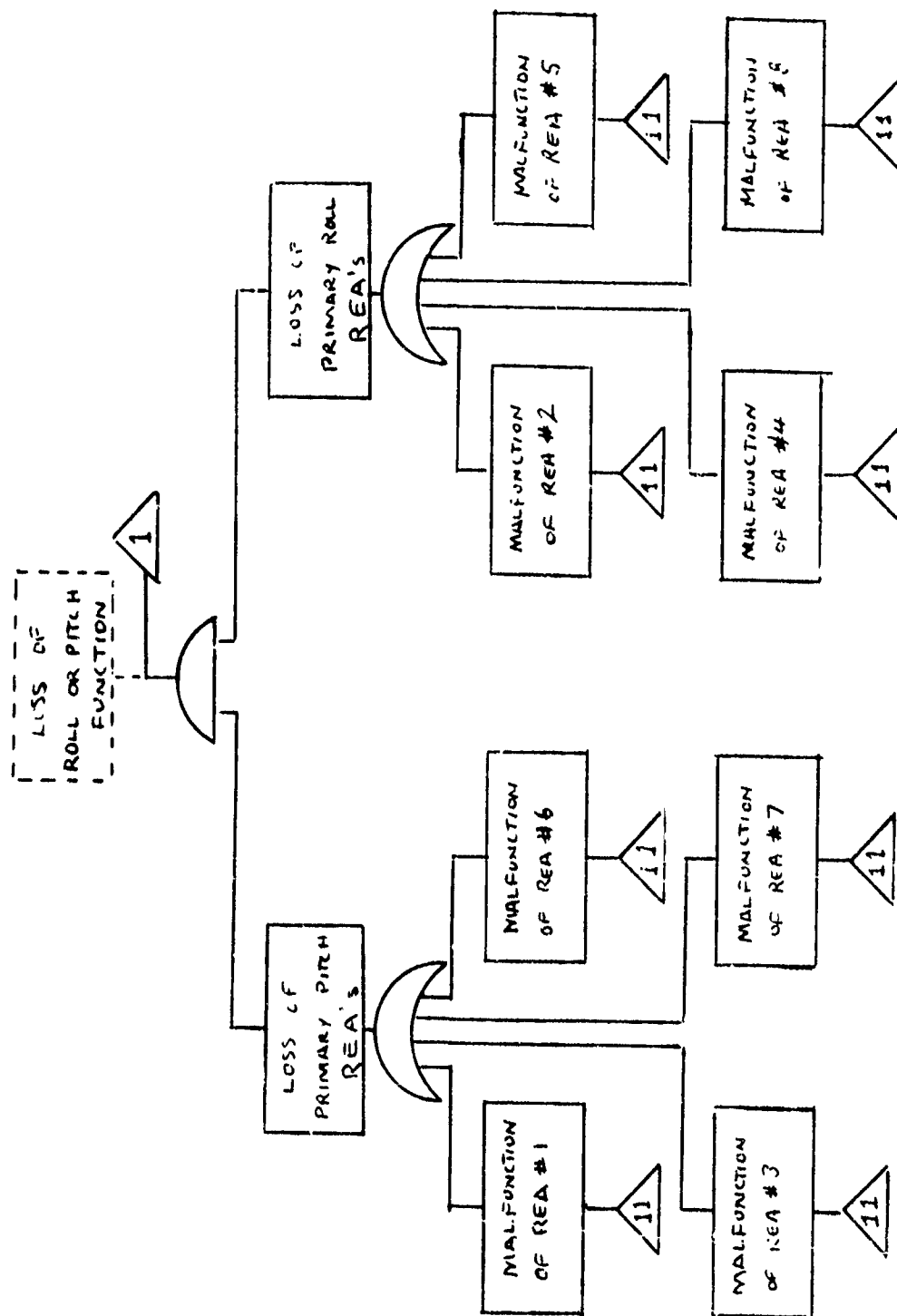
Figure 20 (Continued)
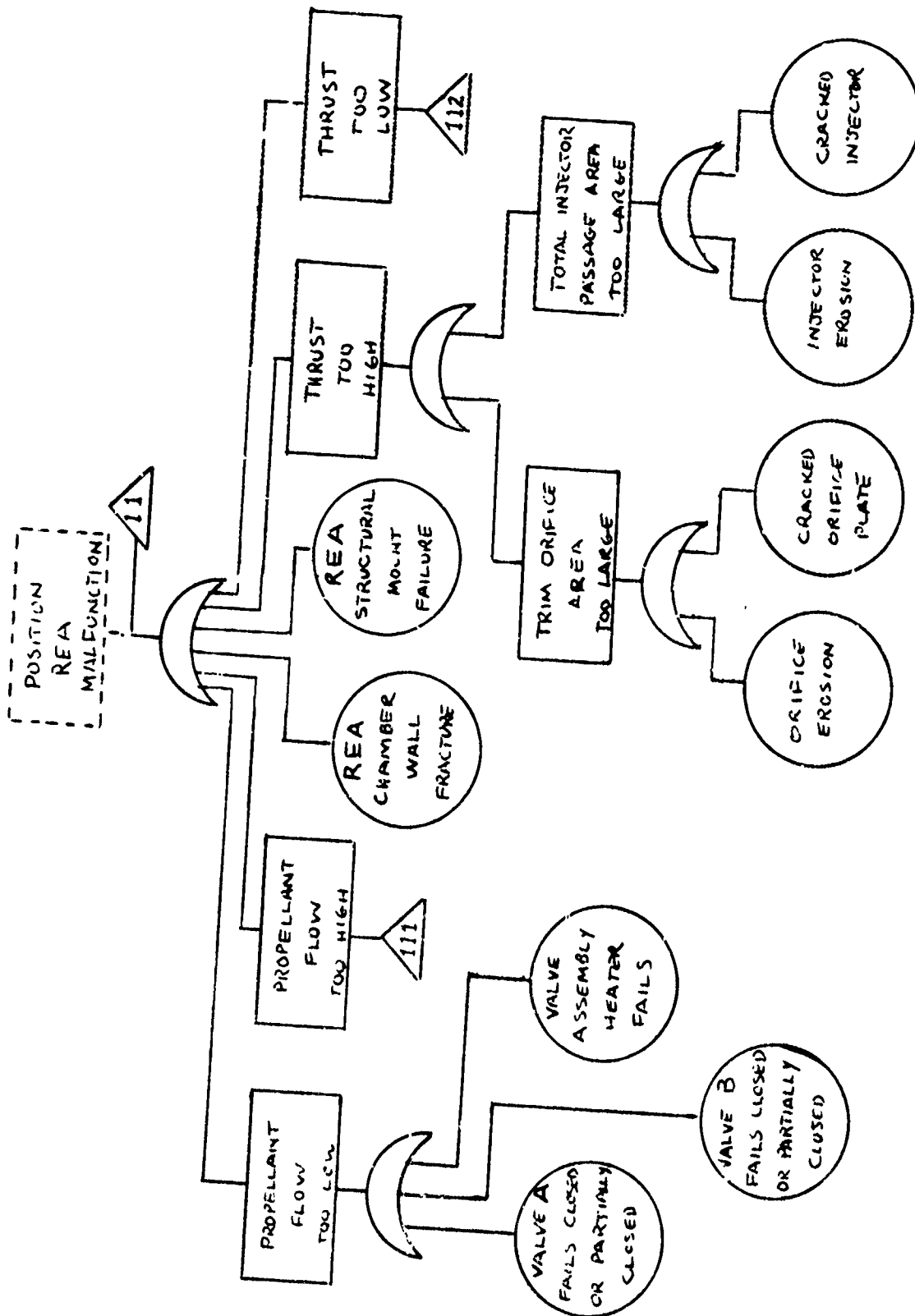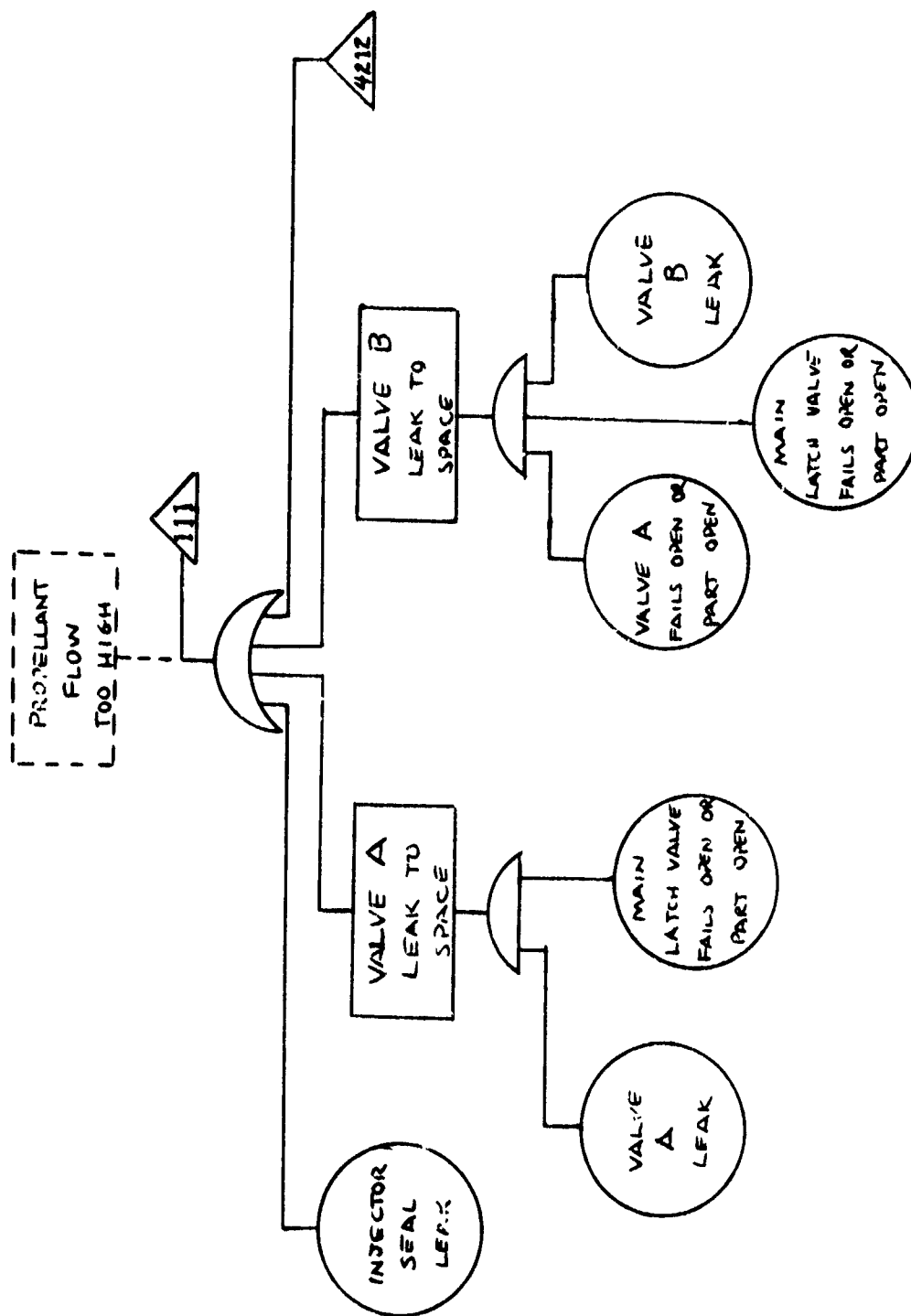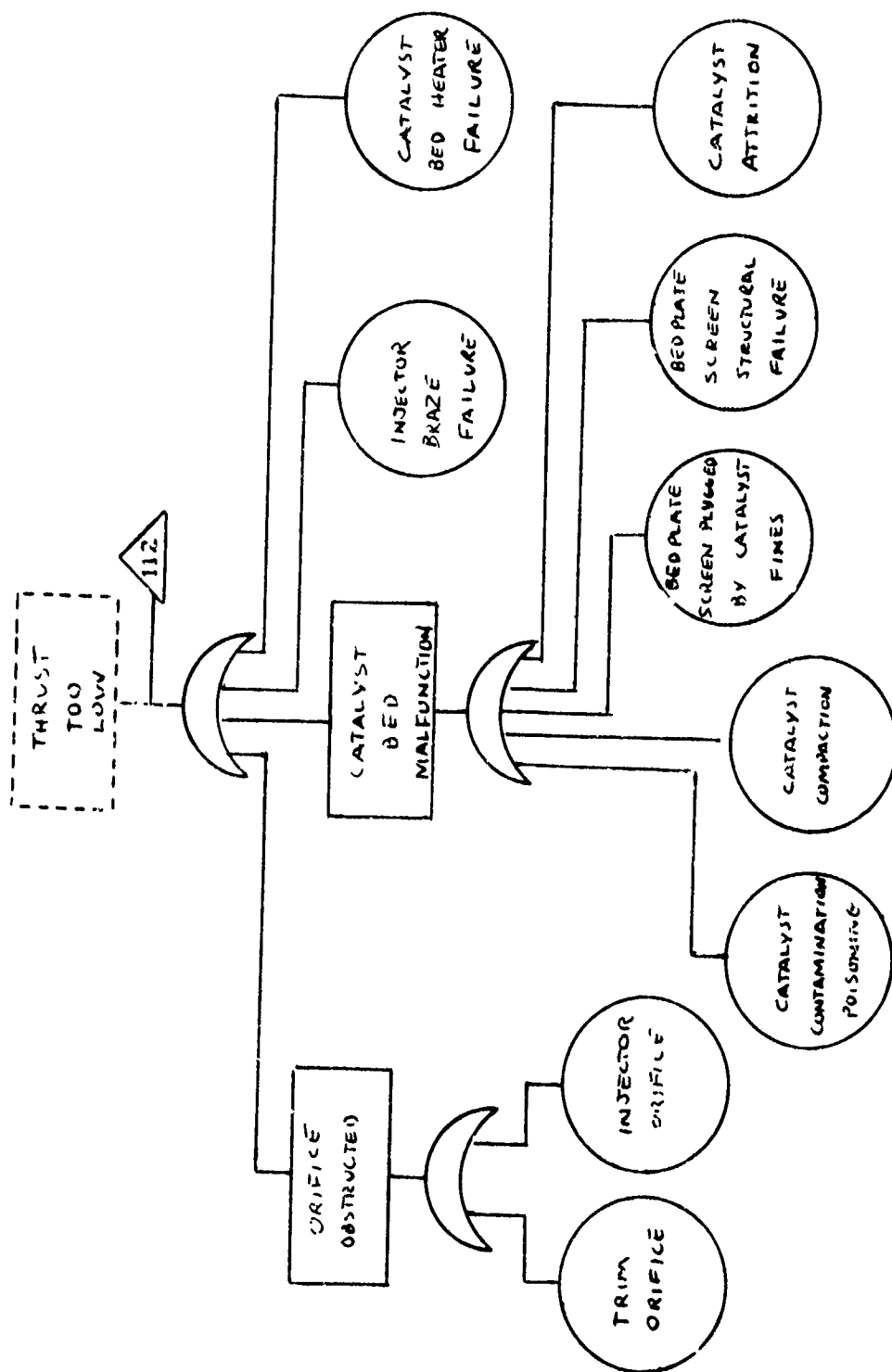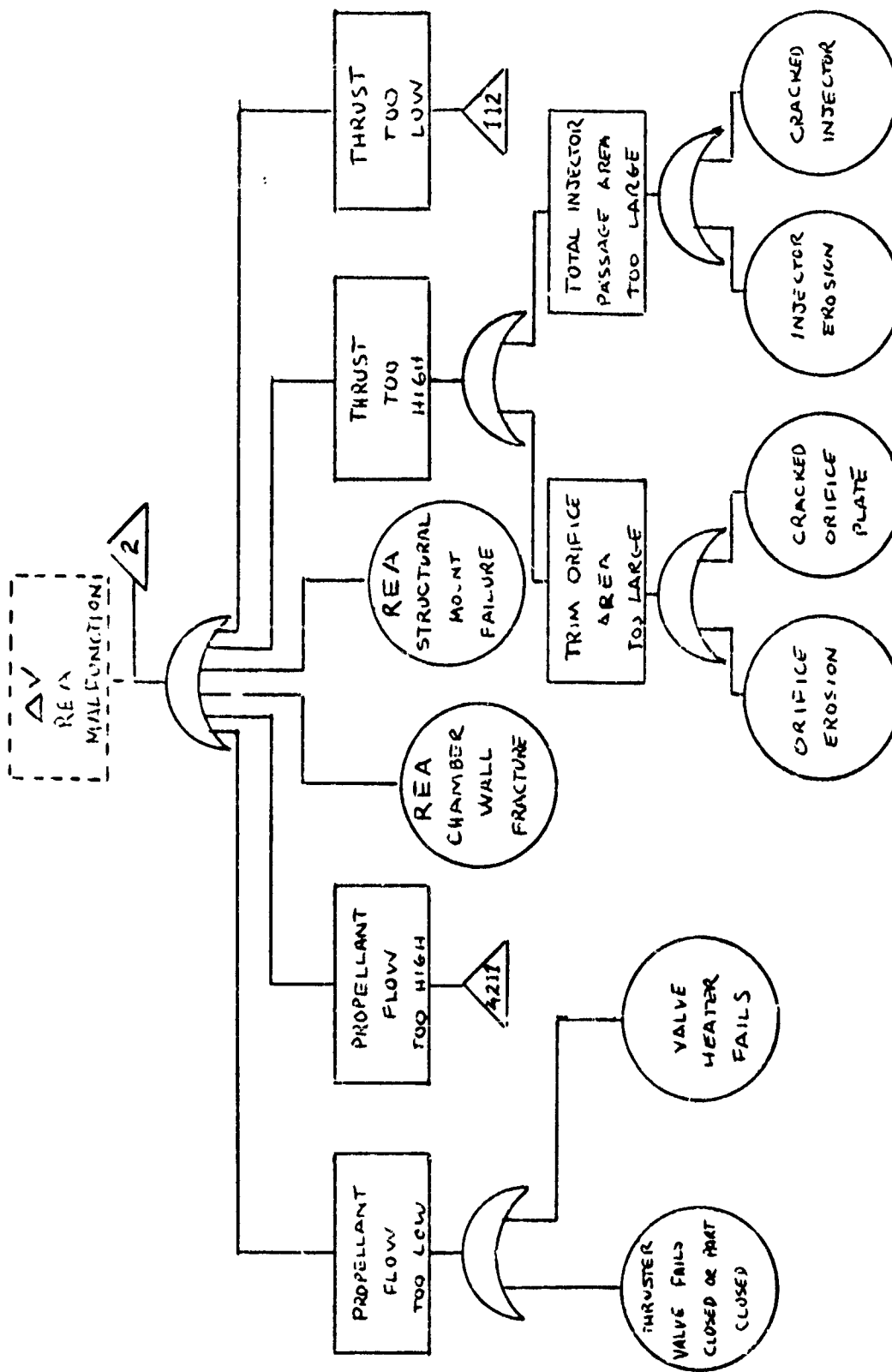
I-227

Figure 20 (Continued)

Figure 20 (Continued)

Figure 20 (Continued)

I-230

Figure 20 (Continued)

Figure 20 (Continued)

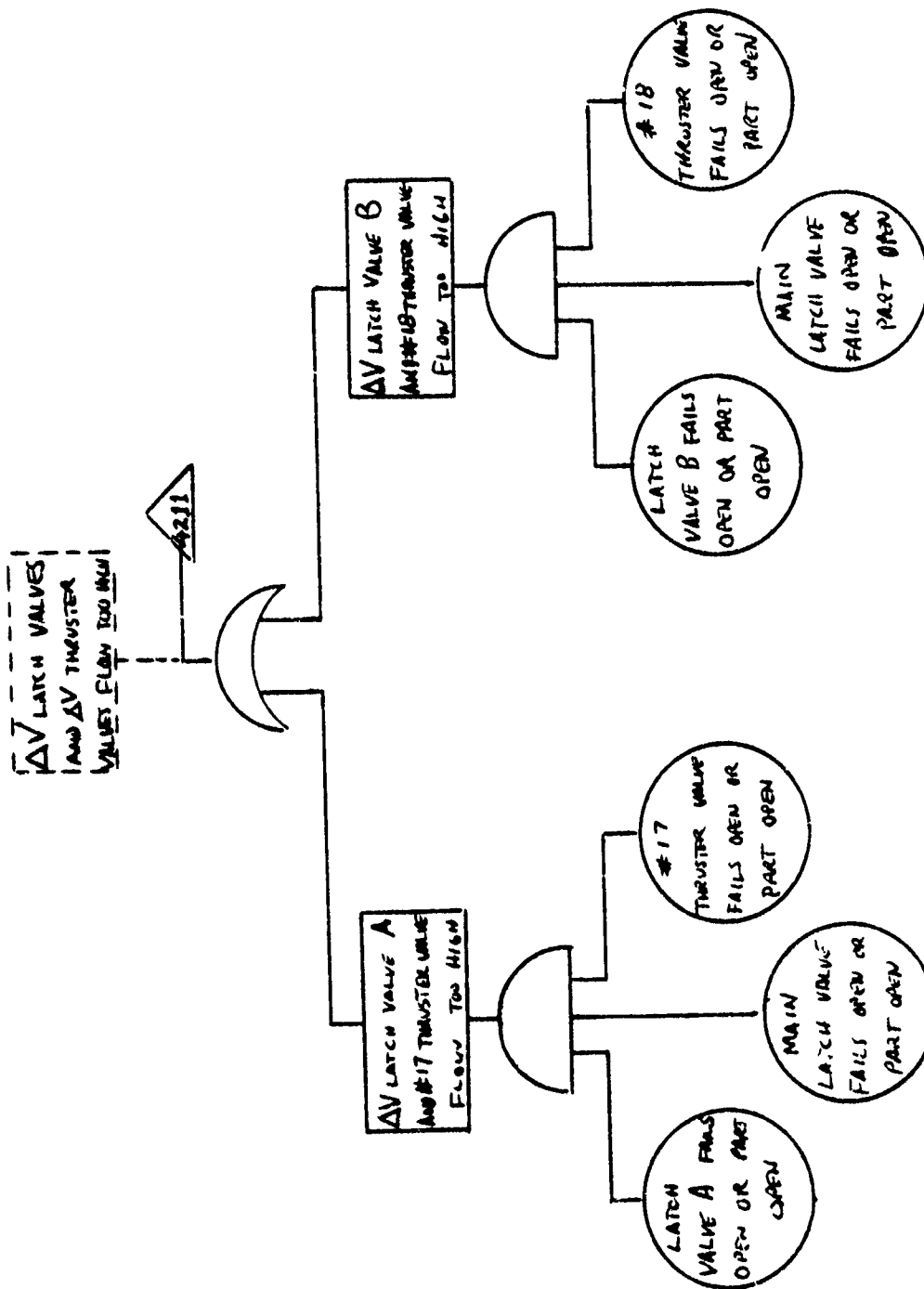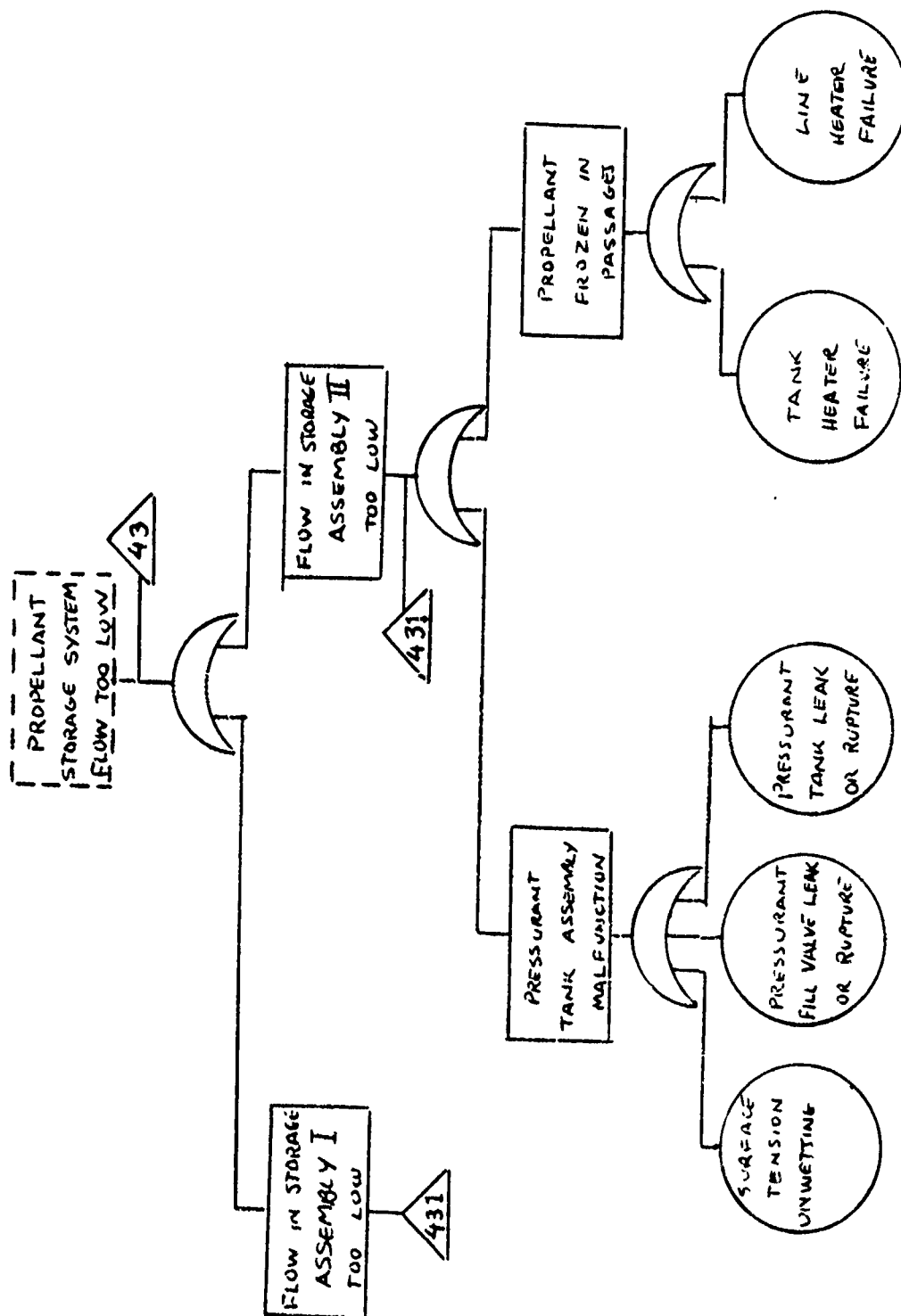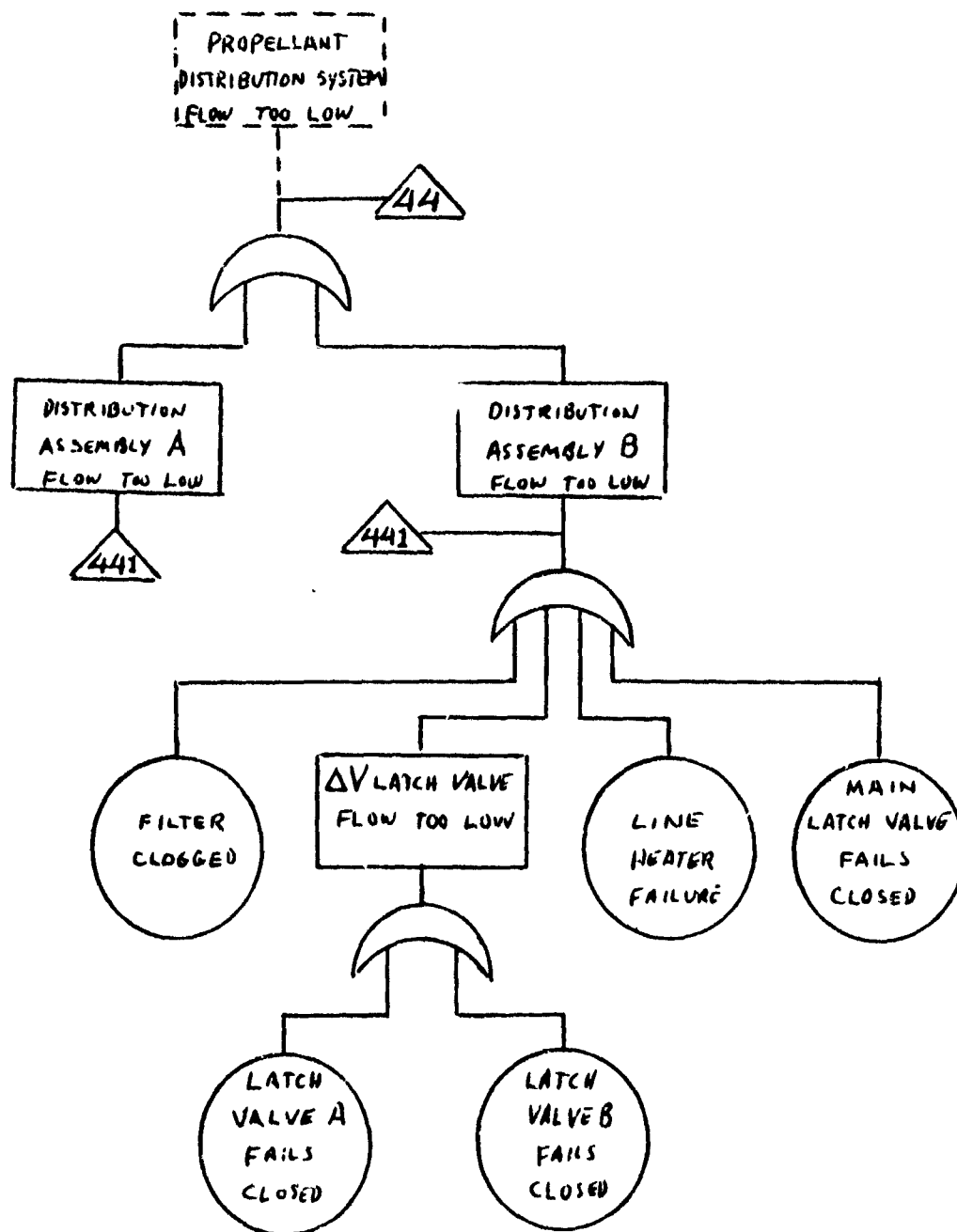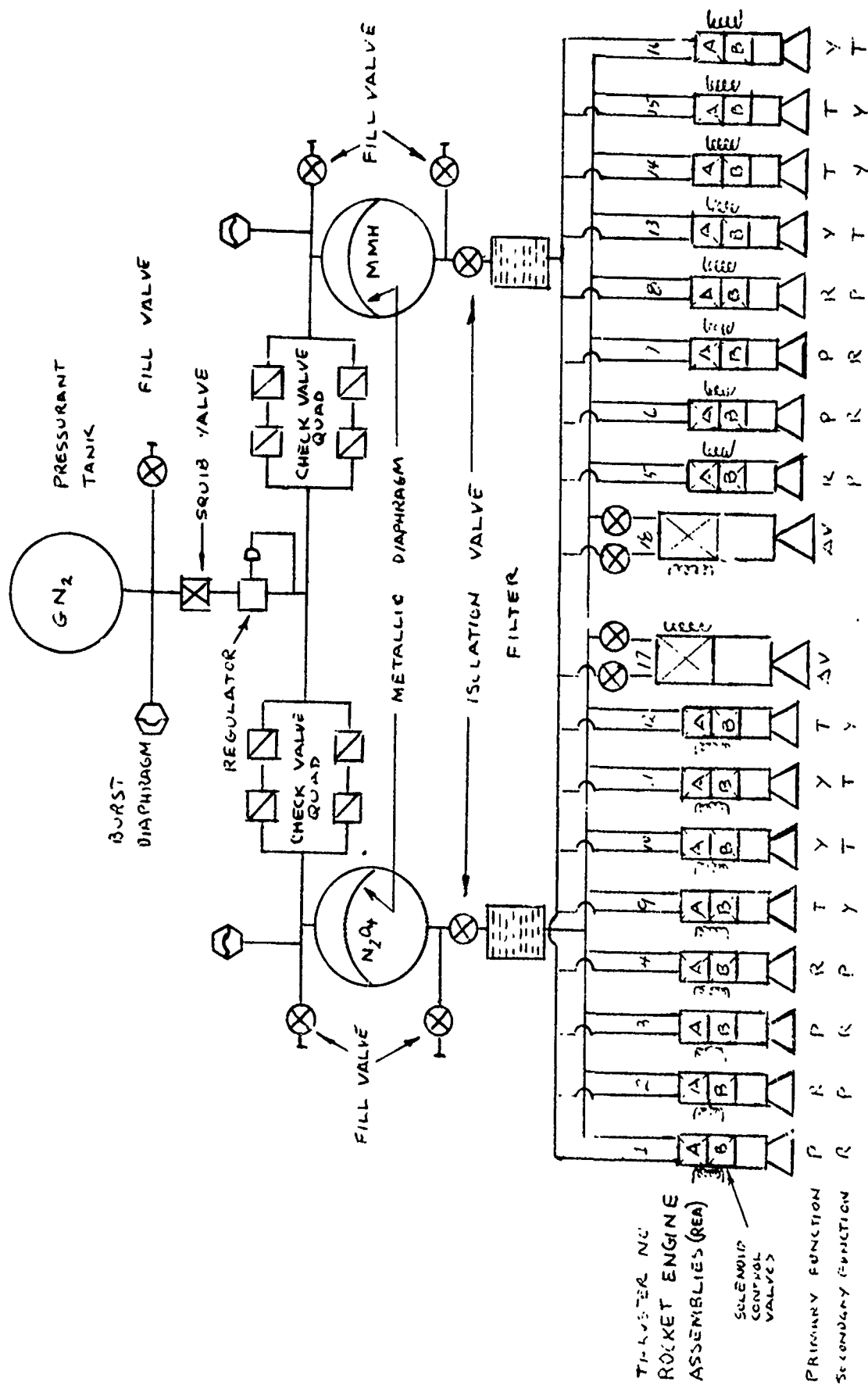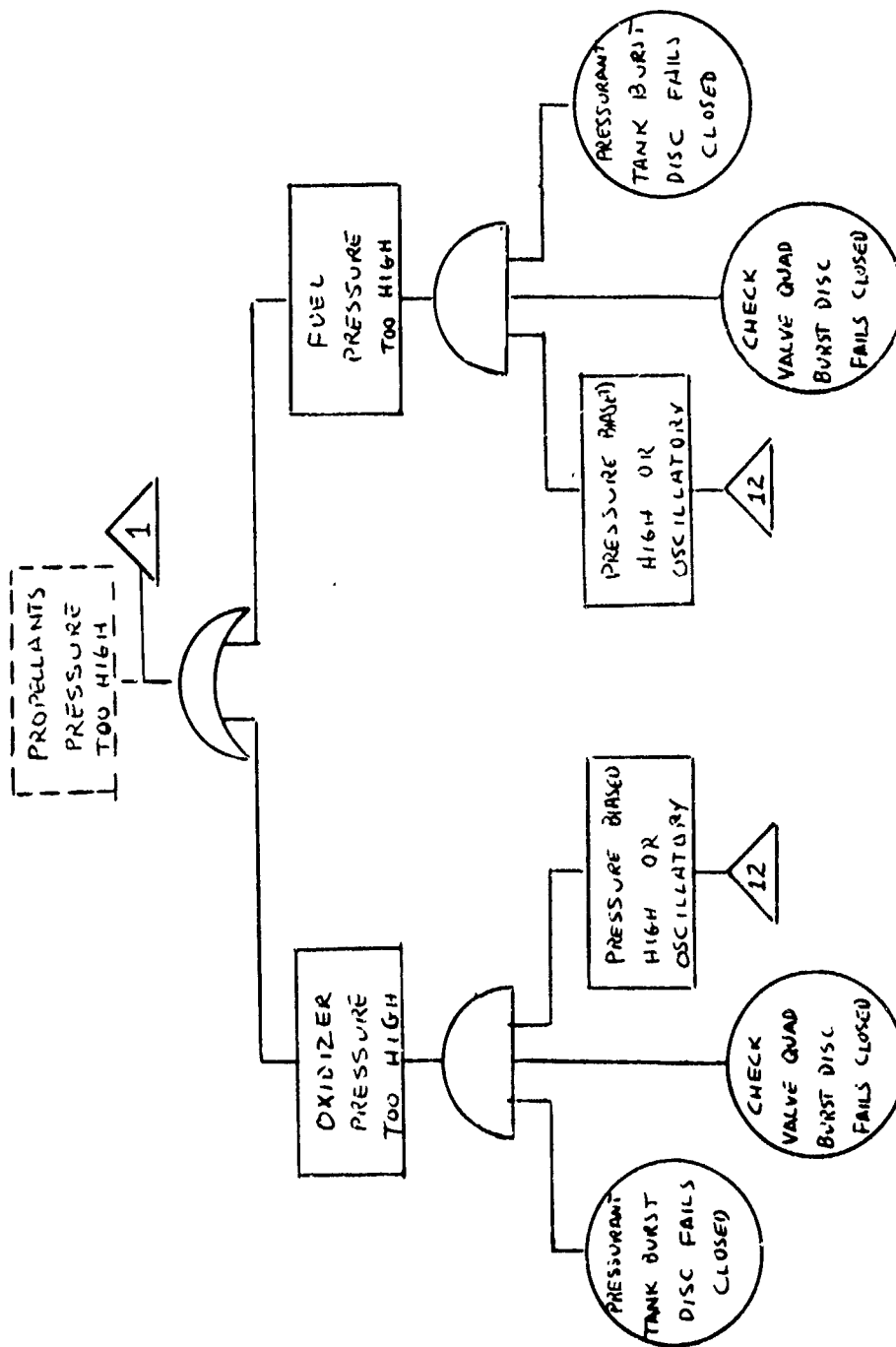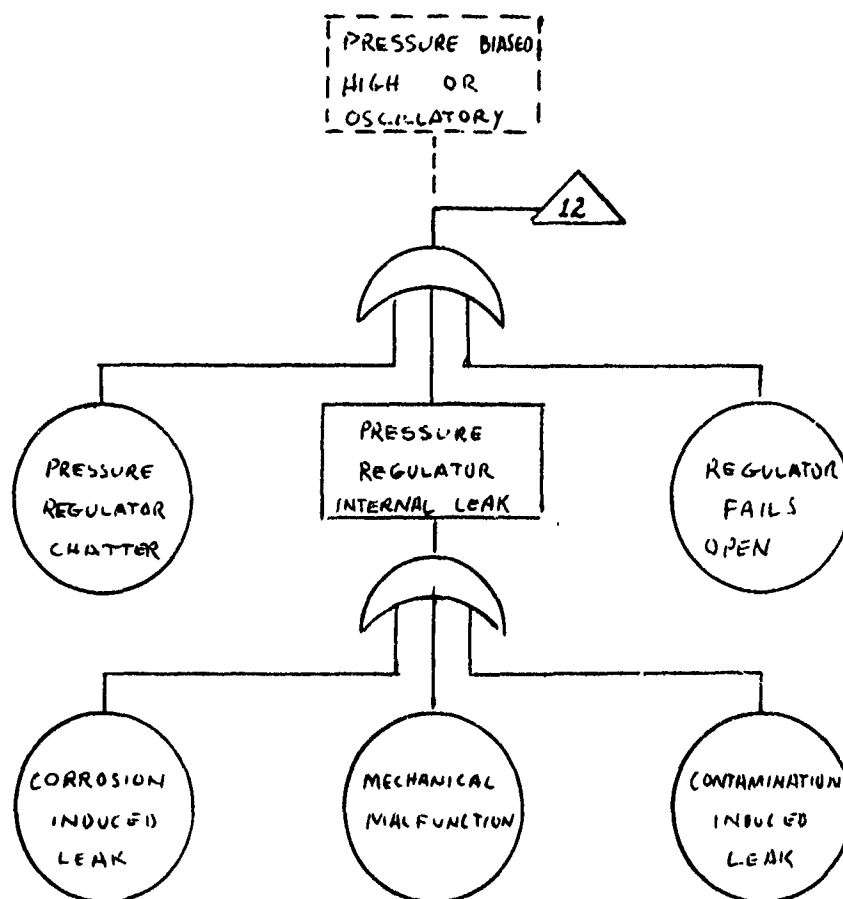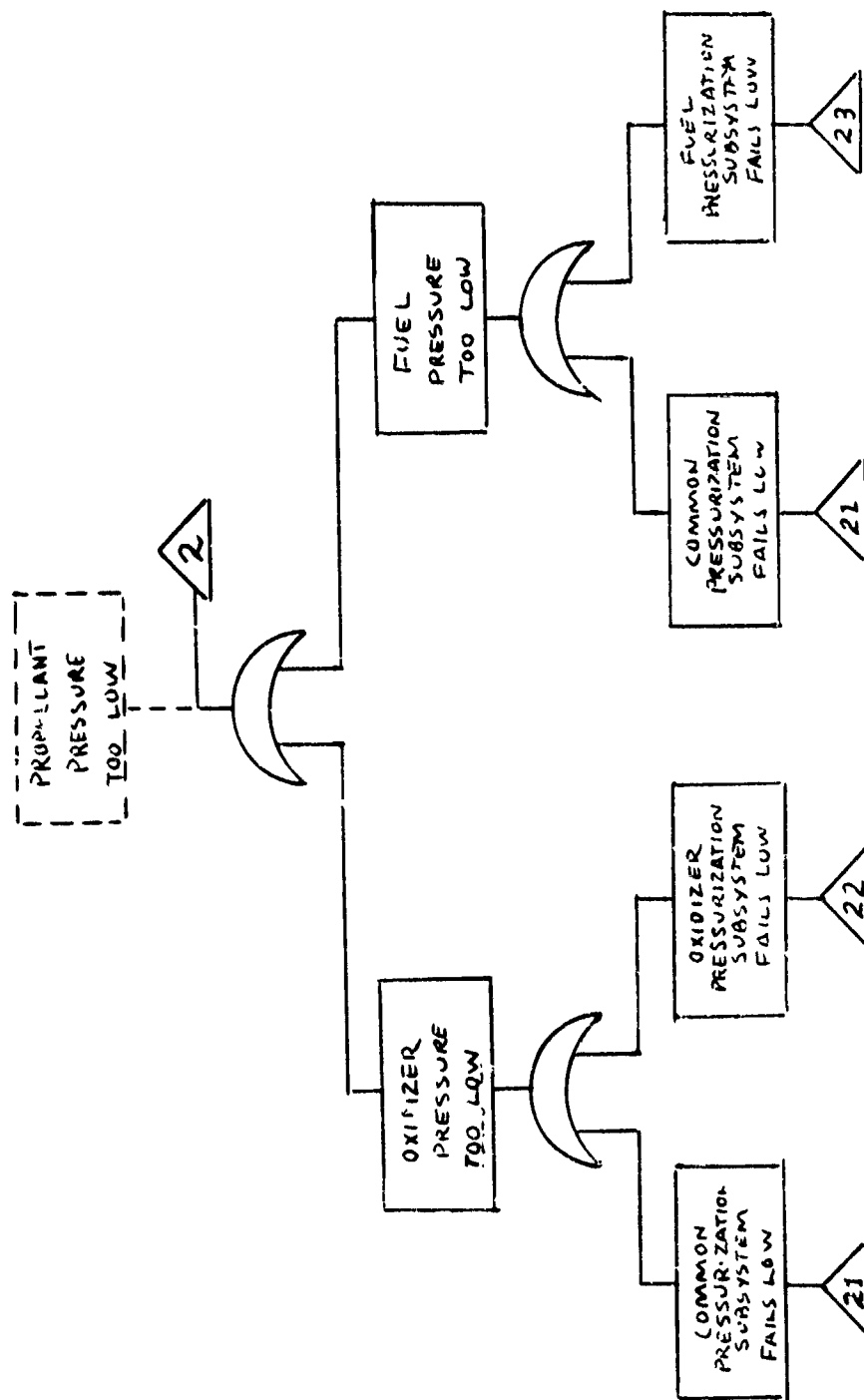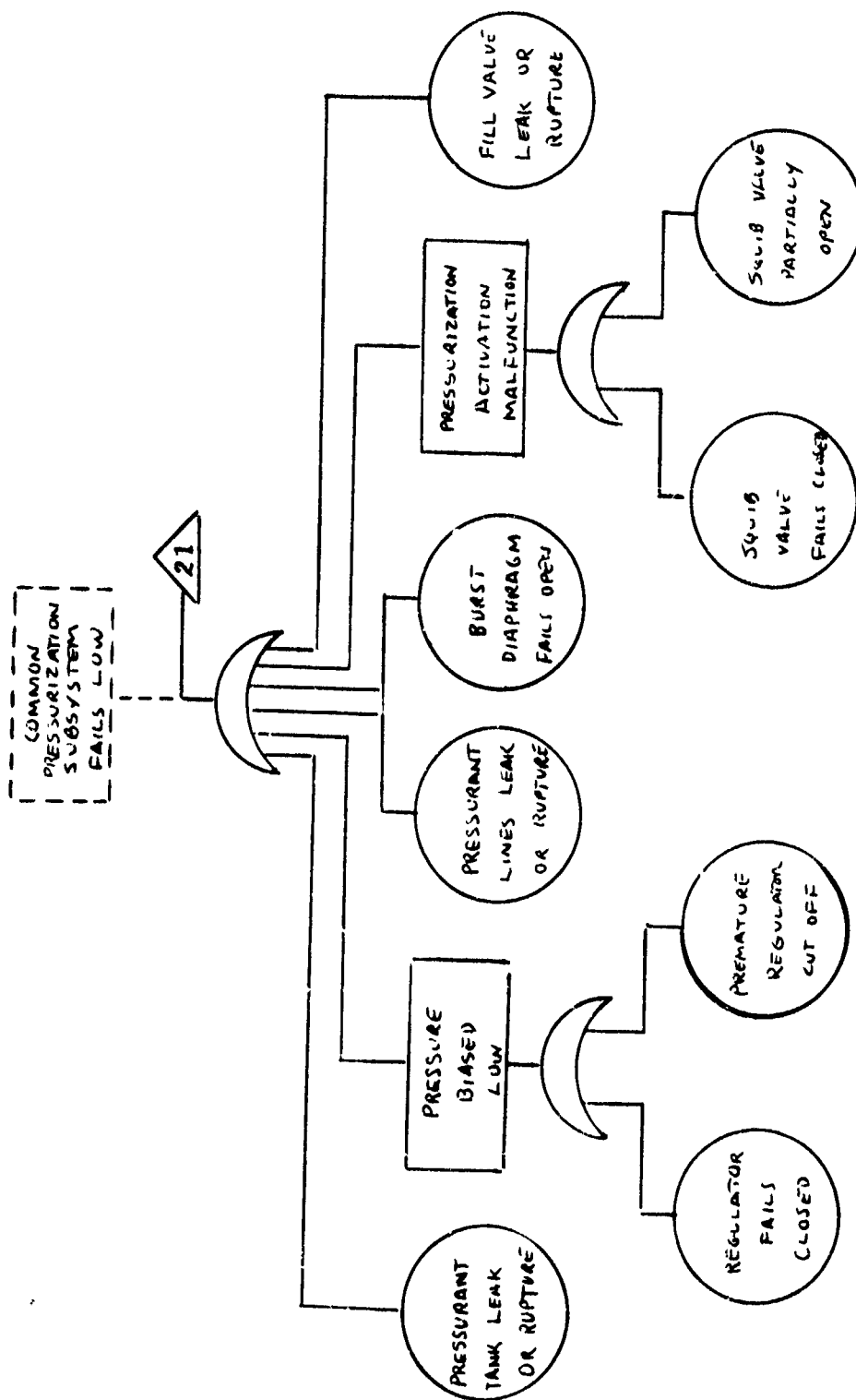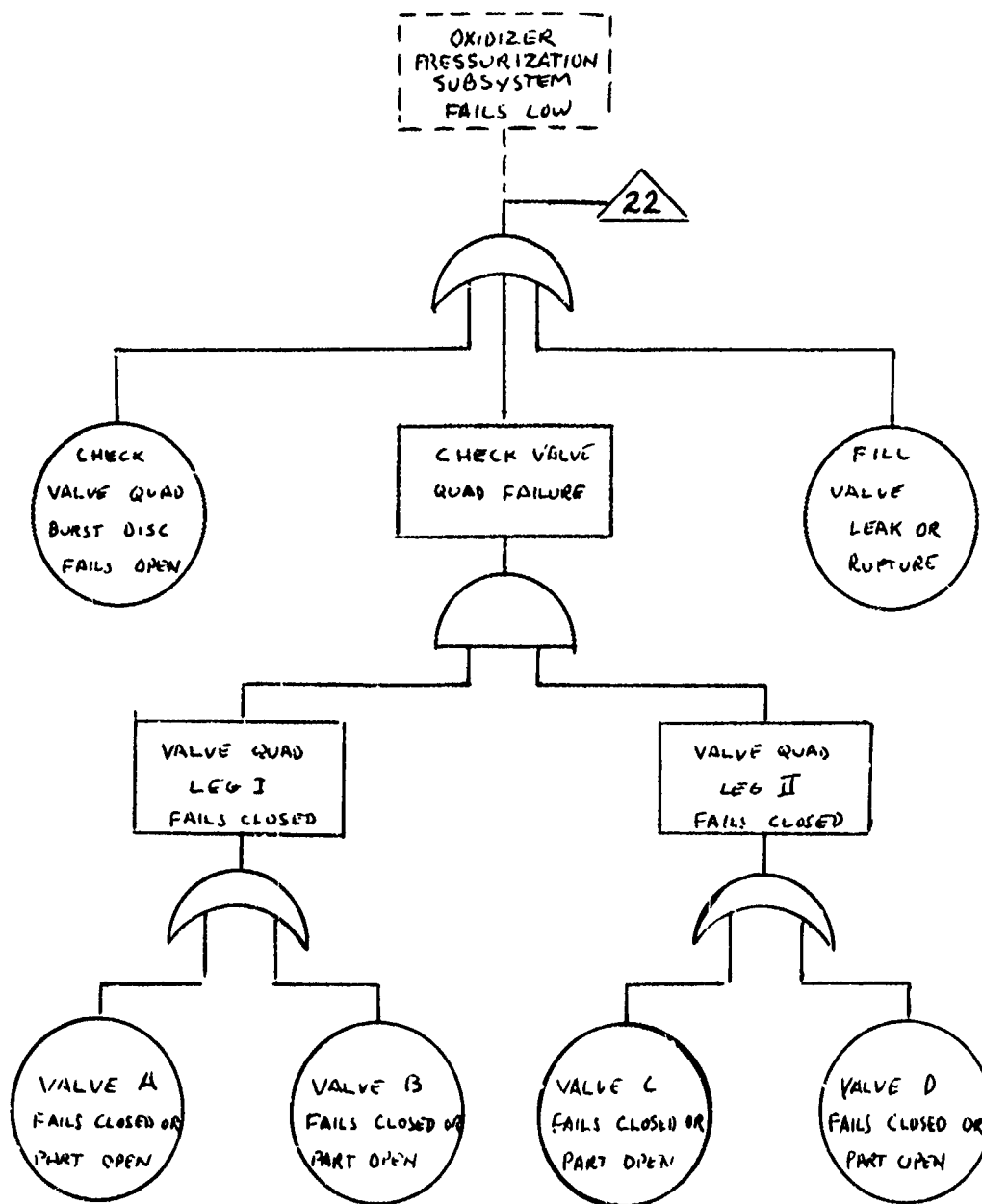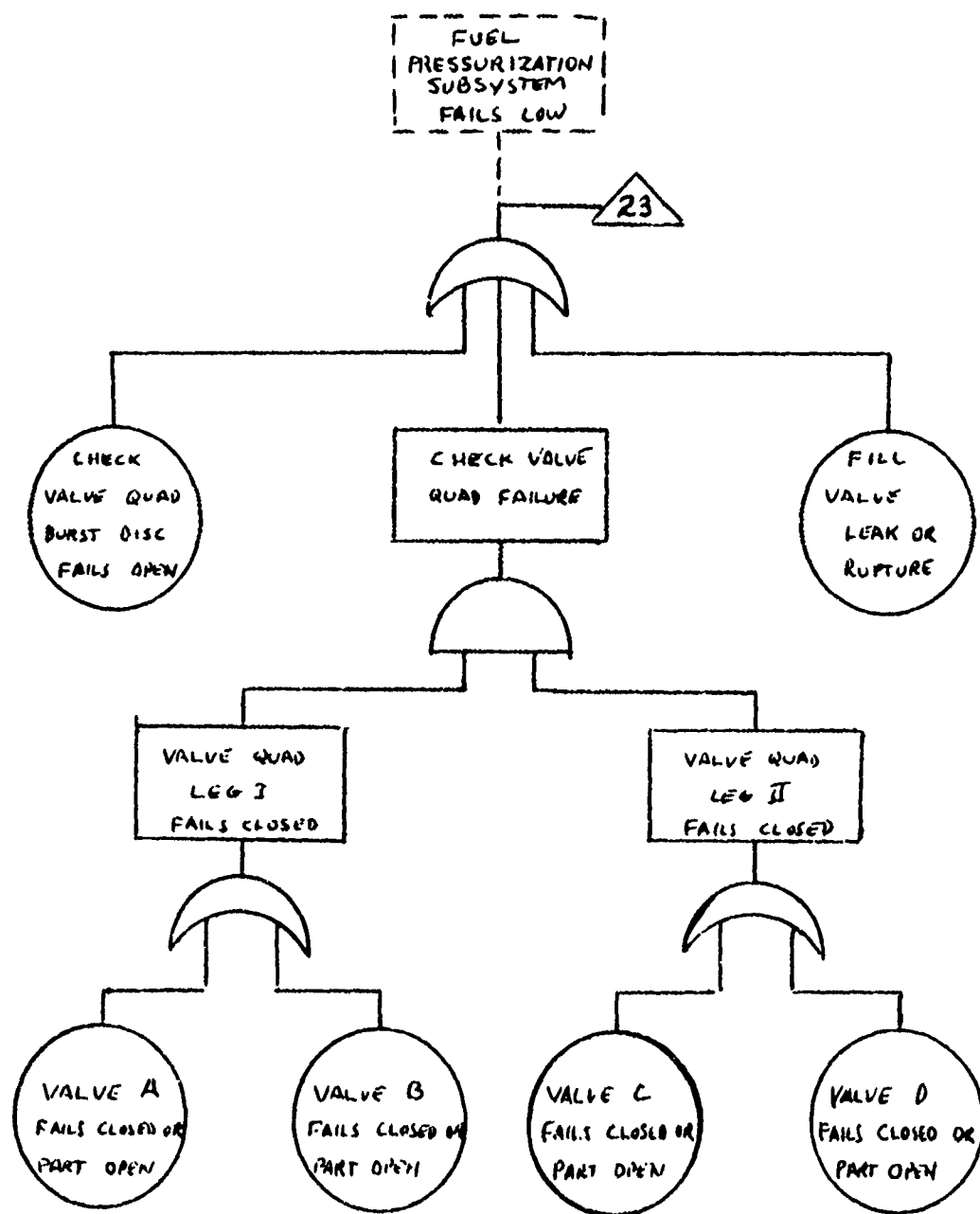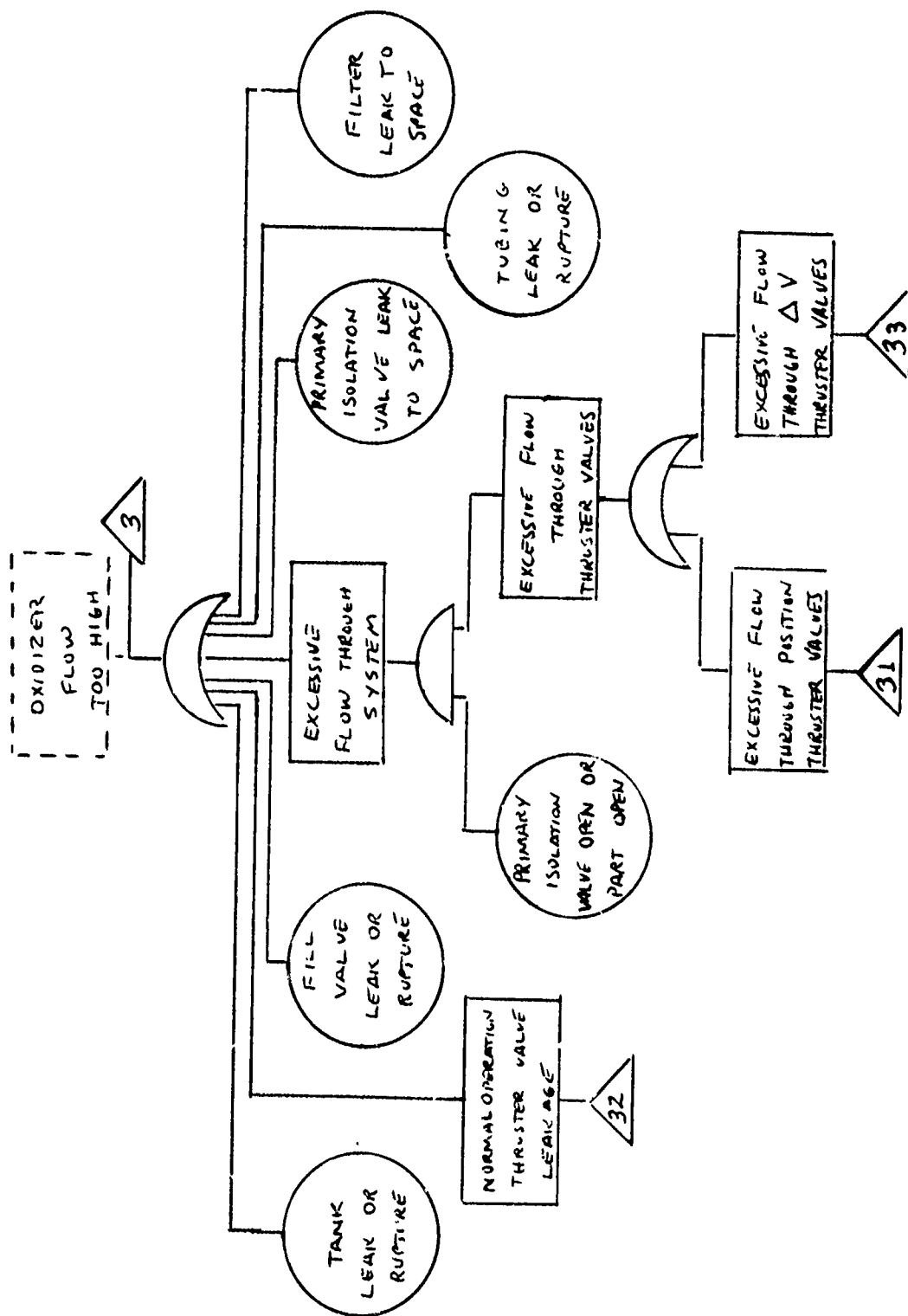Figure 20 (Continued)

Figure 20 (Continued)

Figure 20 (Continued)

Figure 20 (Continued)

I-236

Figure 20 (Continued)

I-237
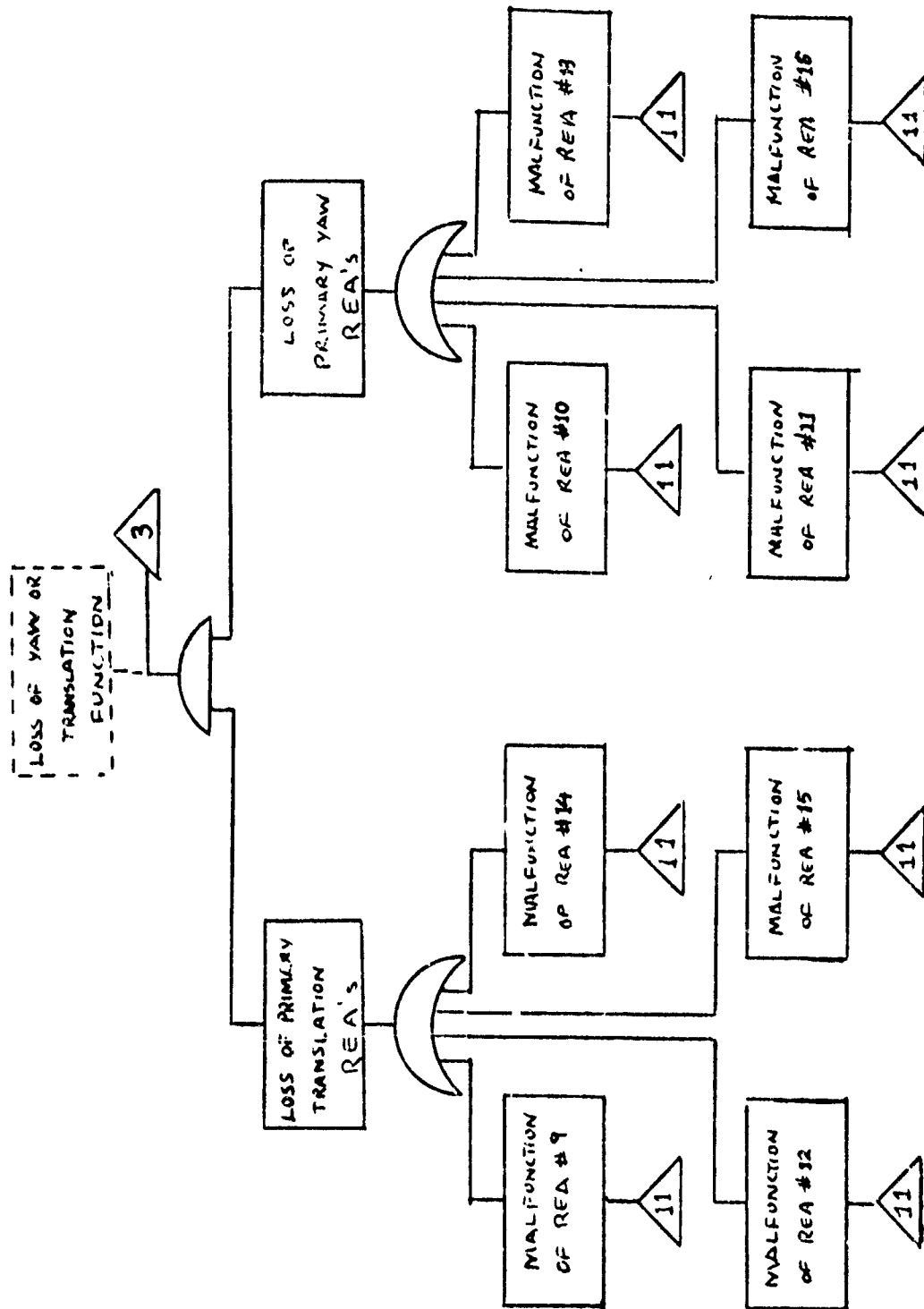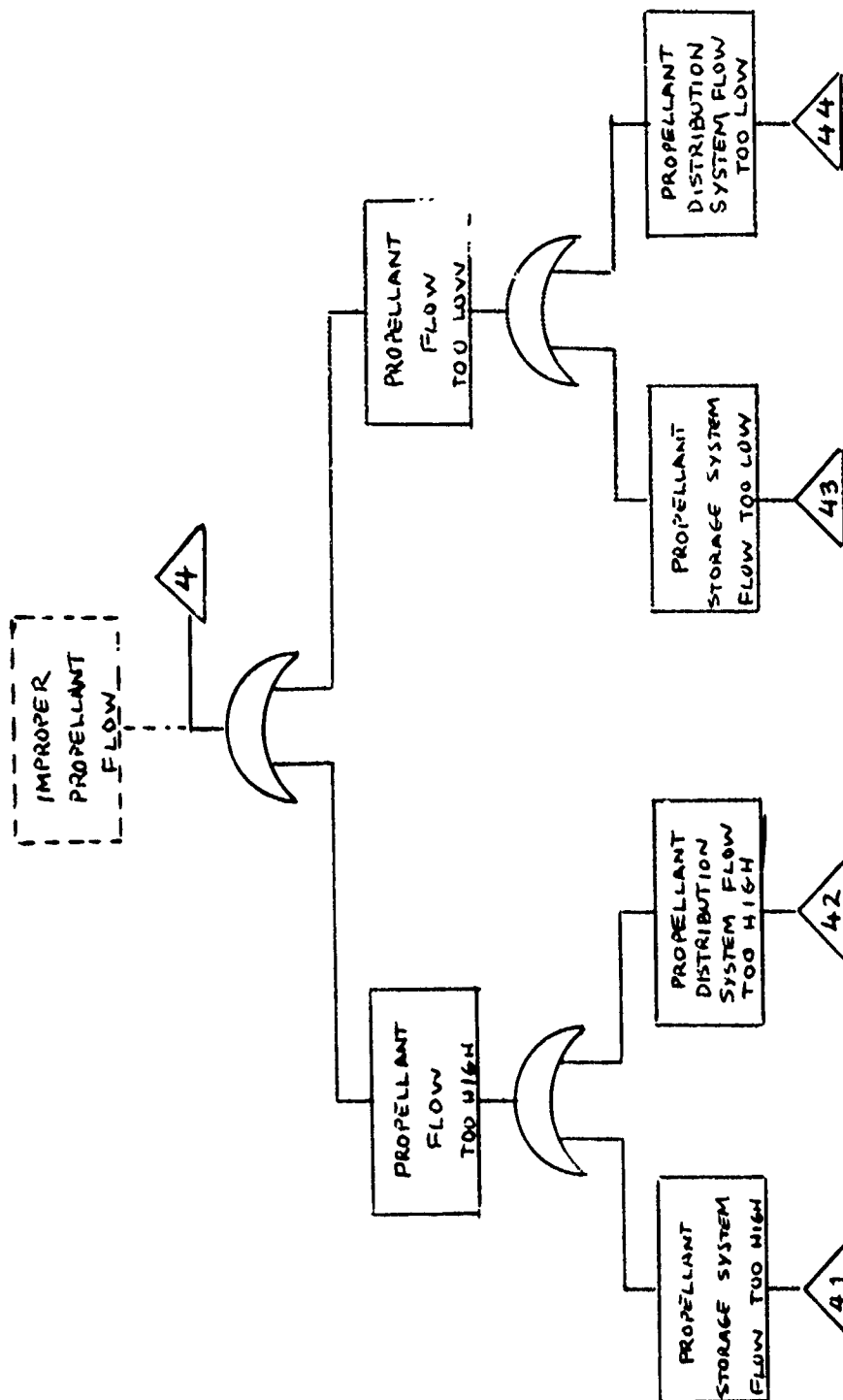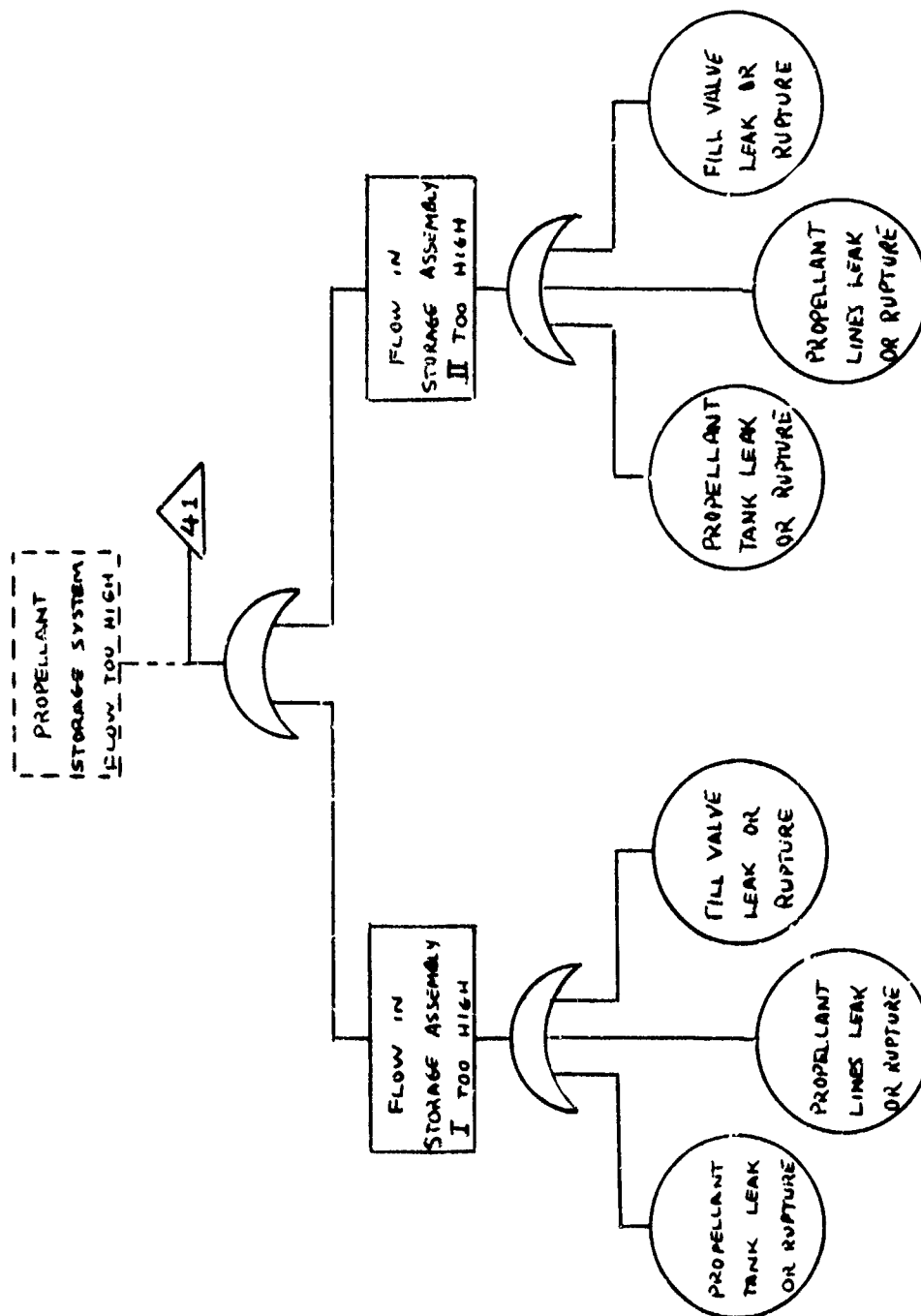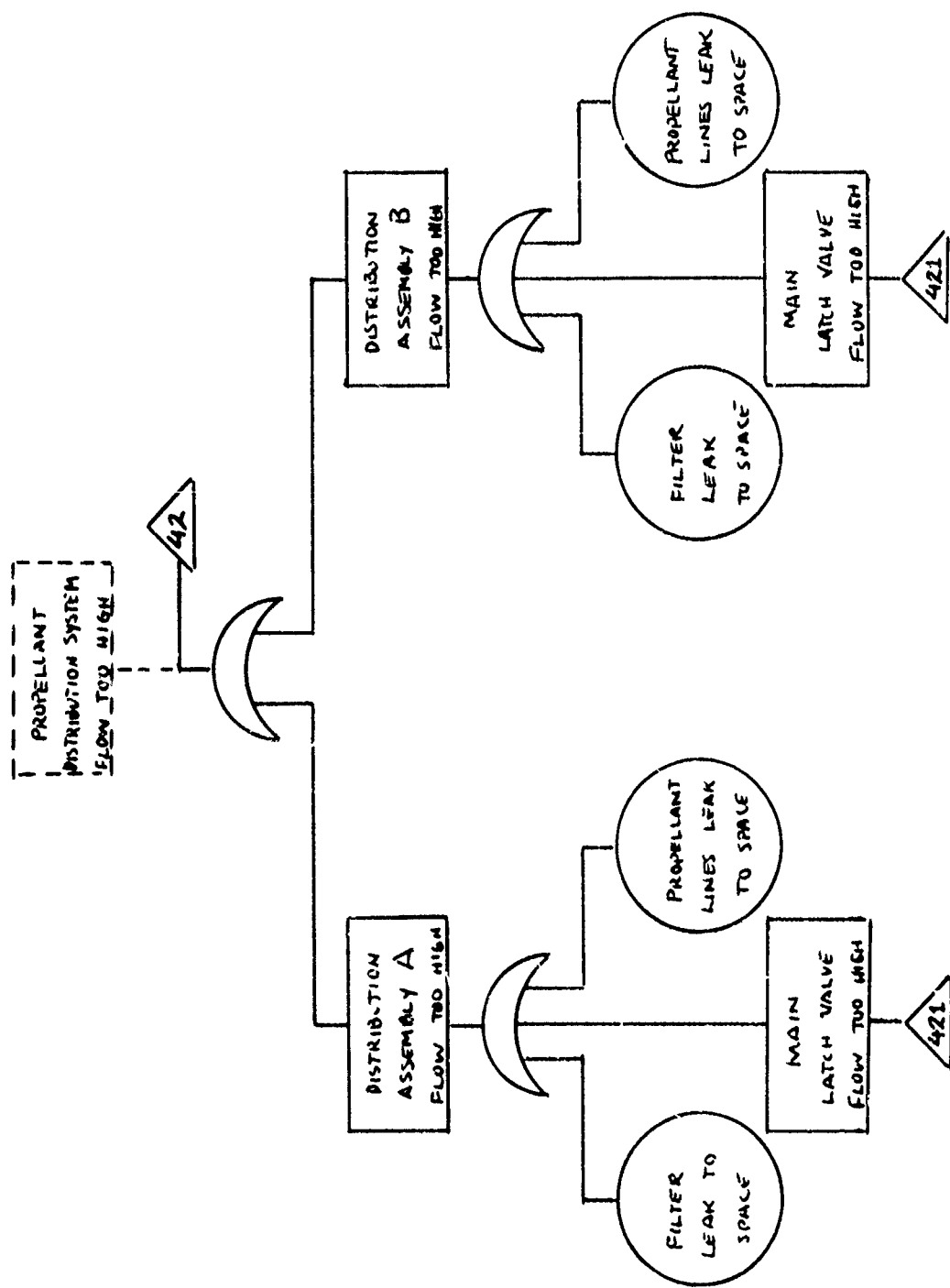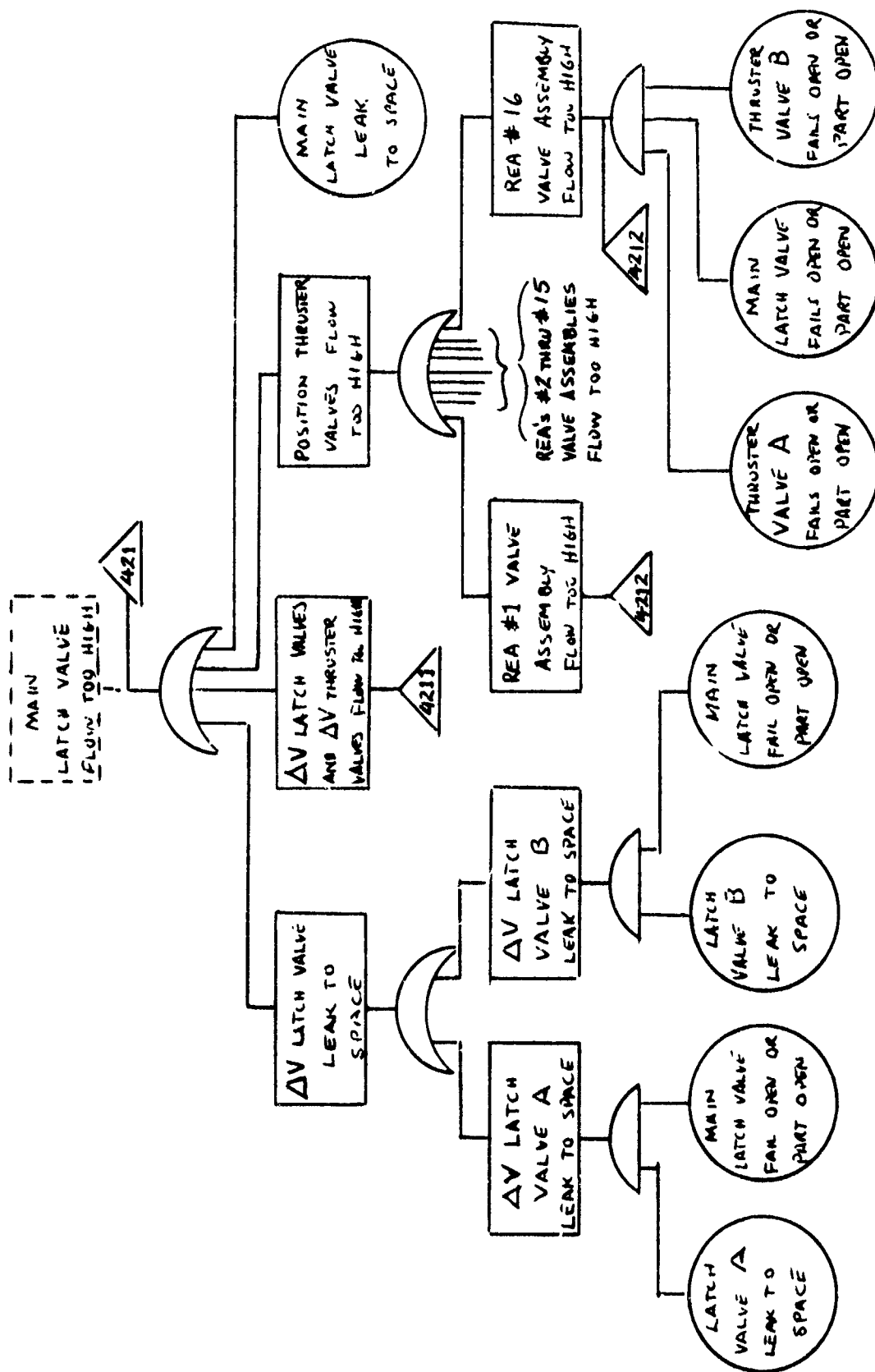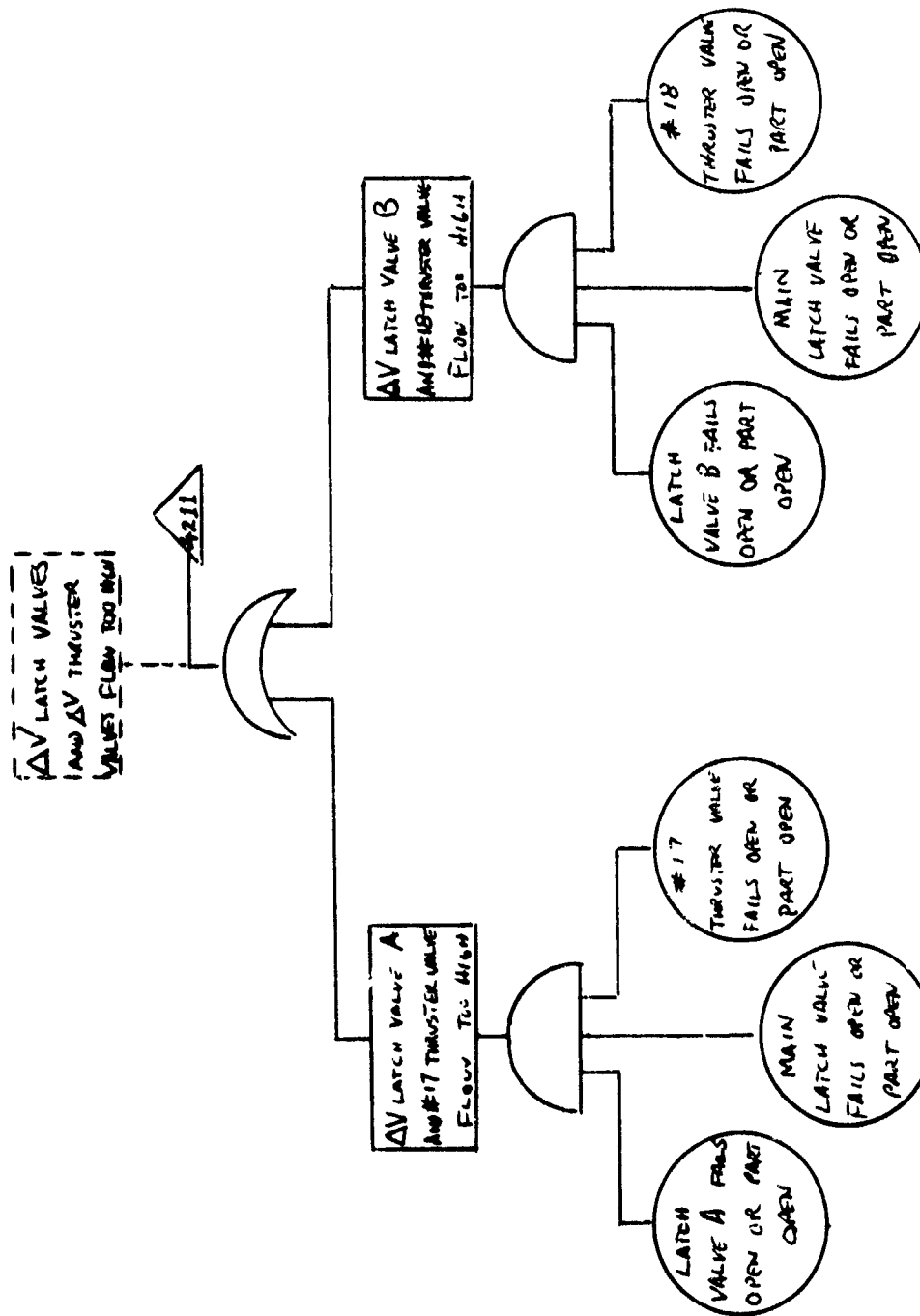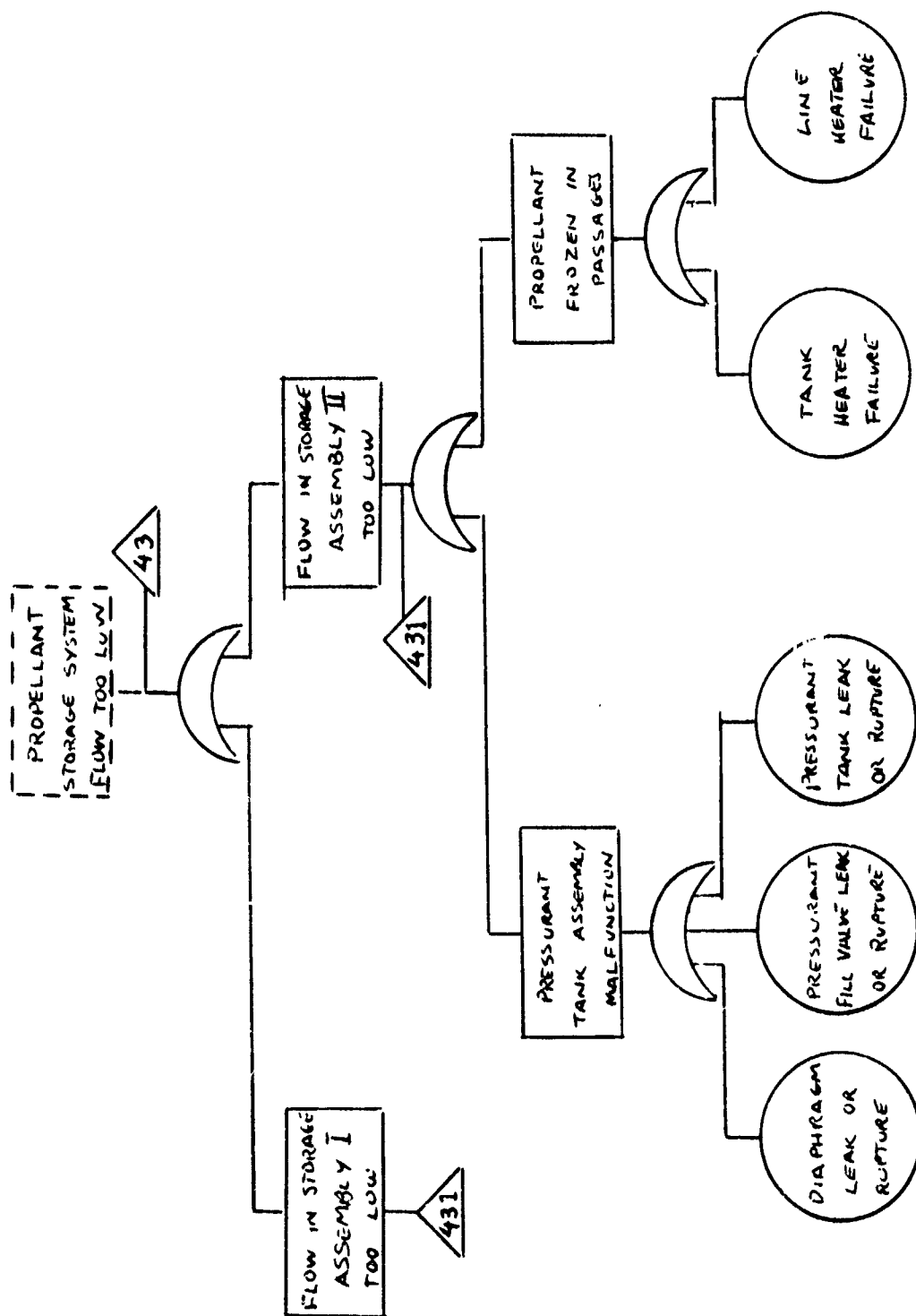
Figure 20 (Continued)
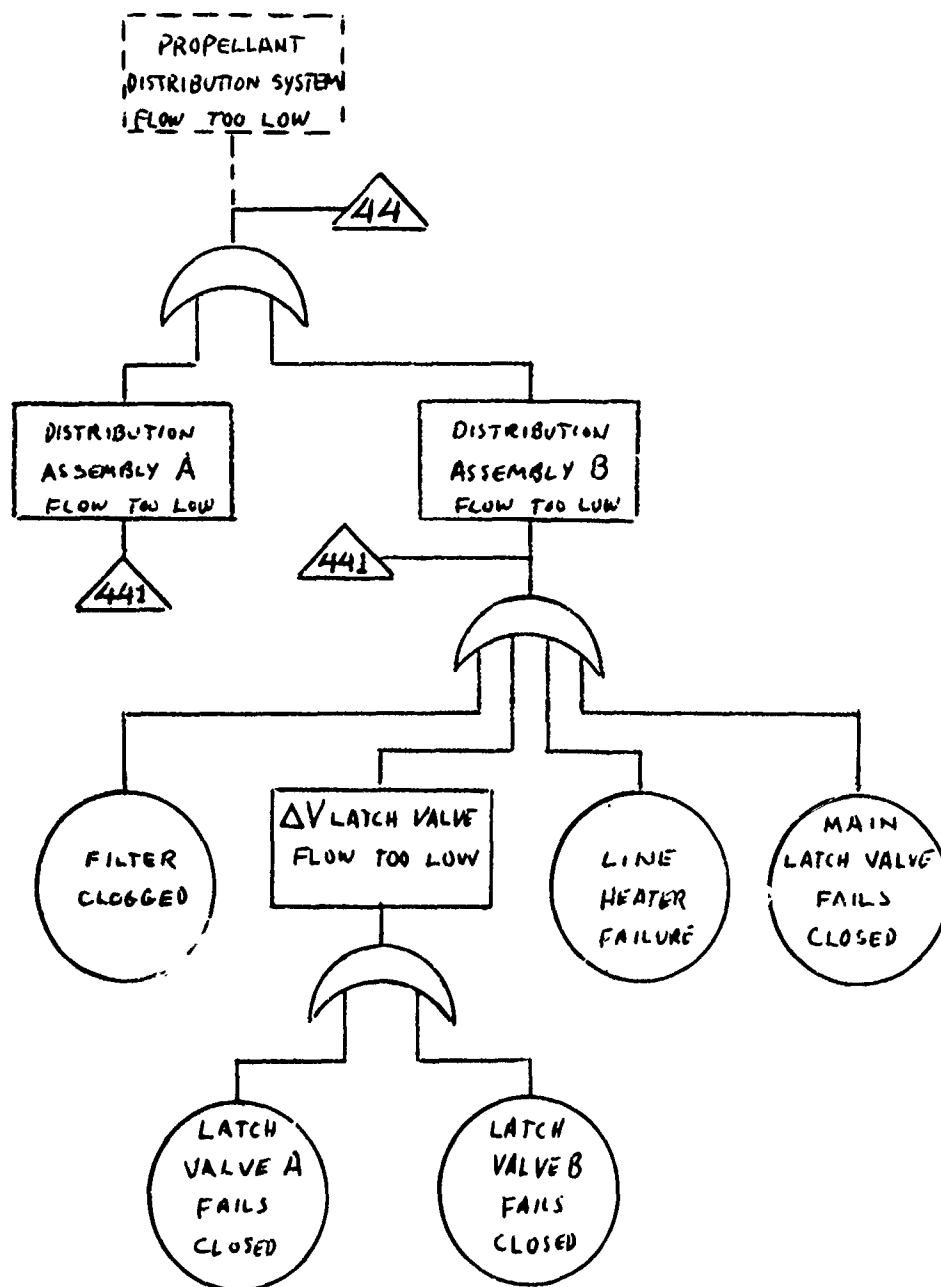
Figure 20 (Continued)

Electrothermal Thruster. Like the catalytic monopropellant
thruster described above, the electrothermal thruster de-
rives thrust from the exothermic decomposition of hydrazine.
It differs, however, in the method of initiation of the de-
composition reaction. Instead of using a catalyst bed, the
reaction is thermally induced with sheath heaters serving
as the heat sources. Two design approaches to heating the
thrust chamber were analyzed. The first employs heaters
externally mounted on the thrust chamber. These heating
elements provide thermal energy to platinum screen packs
housed within the thrust chamber. Decomposition of the
hydrazine is initiated as the monopropellant comes in con-
tact with the heated screen pack. The second approach em-
ploys a heating rod mounted on the main axis within the
thrust chamber as the principal heat source. The swirled
injection of hydrazine results in a cylindrically shaped,
thermally induced decomposition zone about the internal rod
heater. This approach also employs external heating elements
to supplement the internal heater.

Either electrothermal approach requires power levels of
only 3 to 5 watts to initiate operation for medium milli-
pound units. If the duty cycle is greater than approximately
5 percent, and cooldown between pulses does not occur, the
electric heaters can be turned off. The decomposition
reaction is sustained by the self generated heat.

A pressurized surface tension propellant containment/
delivery system was used in conjunction with the electro-
thermal thruster in this analysis. However, the blowdown
pressurization and the regulated constant pressure schemes
(analyzed in conjunction with the catalytic monopropellant
thruster and hypergolic bipropellant thruster, respectively)
may also be employed. The interchangeability of the appro-
priate fault tree branches will yield "synthesized" fault
trees for all desired combinations.

A schematic of the system is shown in Figure 21. The
fault tree analysis is presented in figure 22. For addi-
tional details of the alternate thruster configurations and
other system components refer to Figure 7, Electrothermal
Monopropellant Generic System Layout, page I-9.
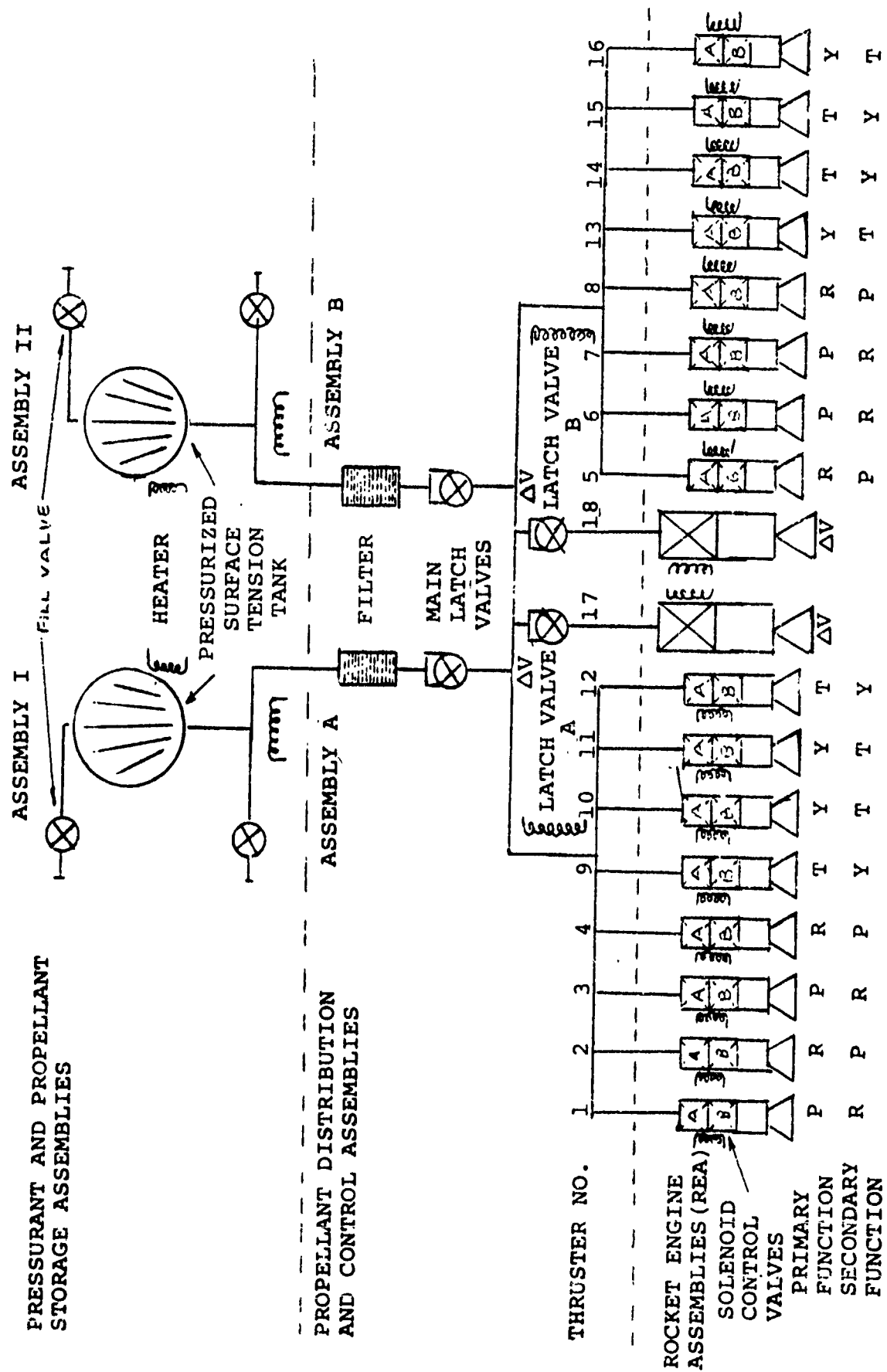
Figure 21. Catalytic Electrothermal Monopropellant System Schematic

ELECTROTHERMAL MONOPROPELLANT SYSTEM

FAULT TREE ANALYSIS
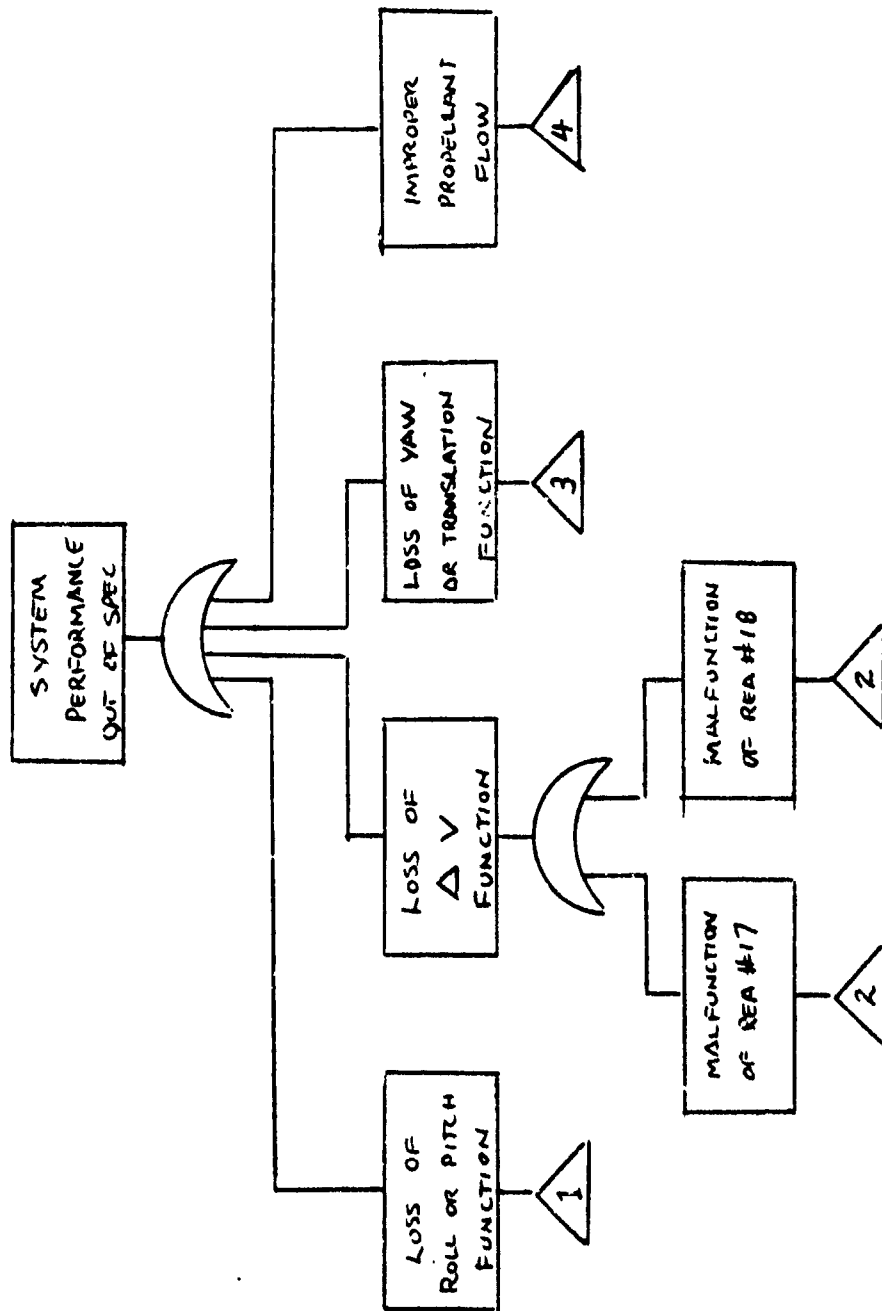
Figure 22. Electrothermal Monopropellants System Fault Tree Analysis
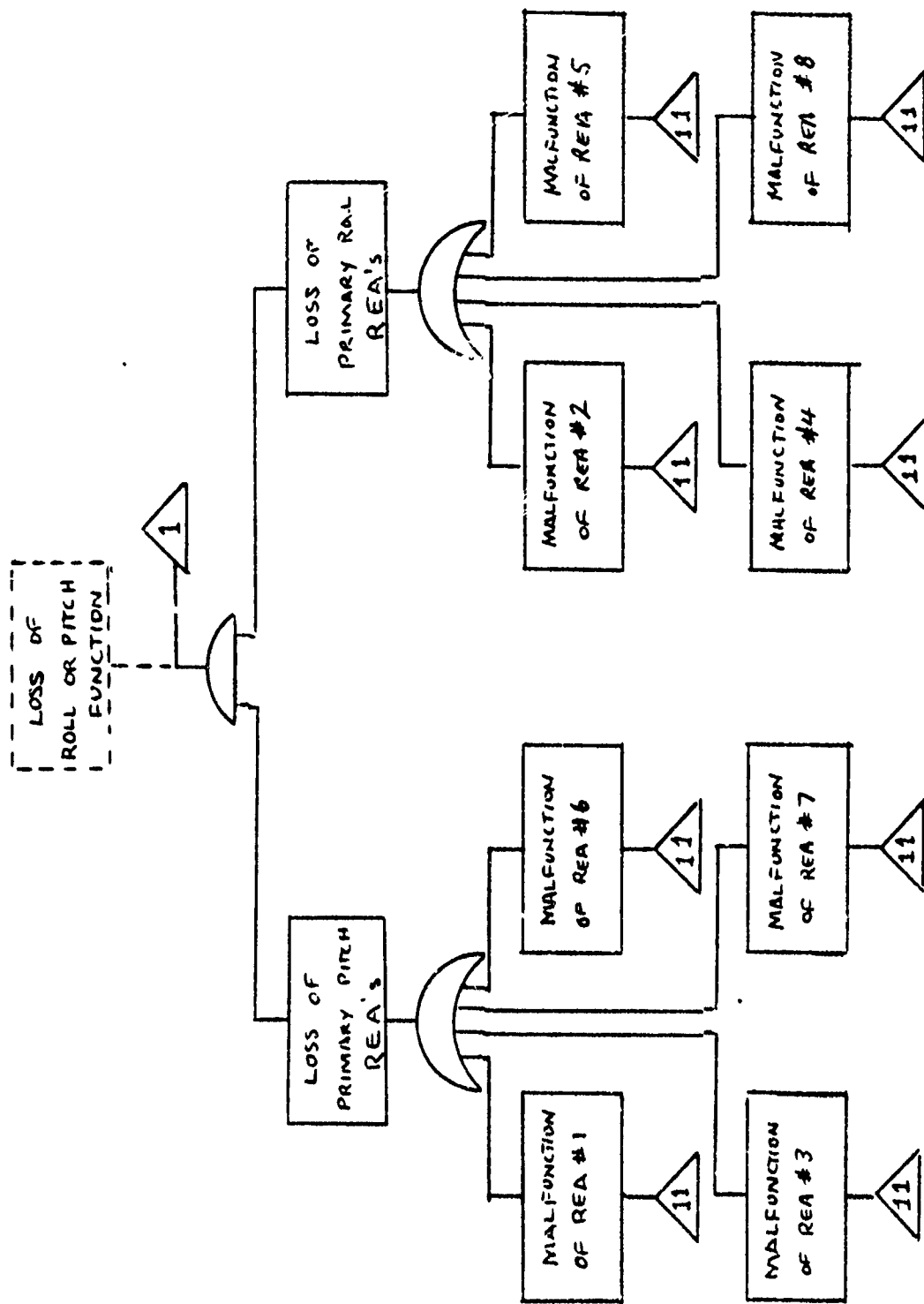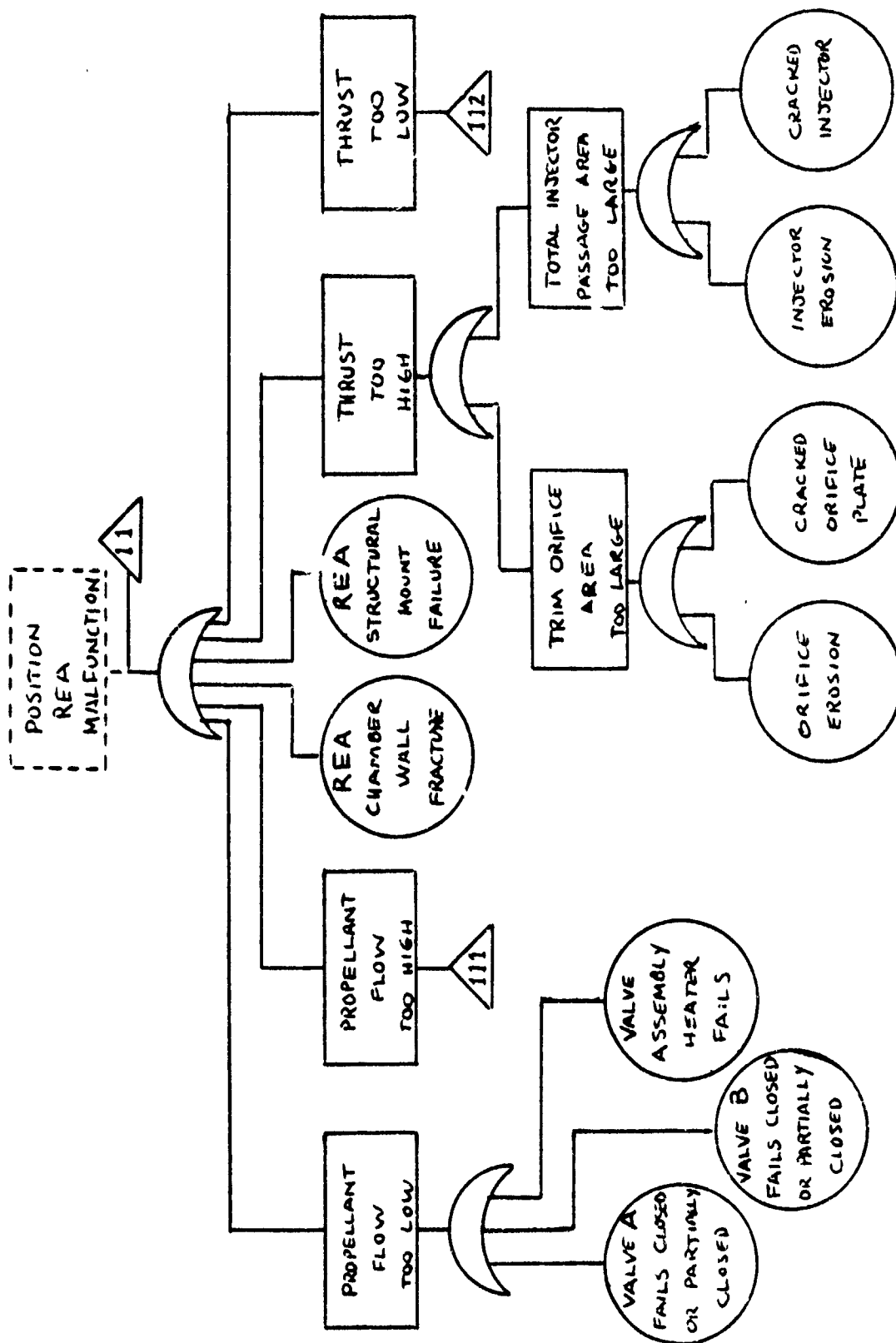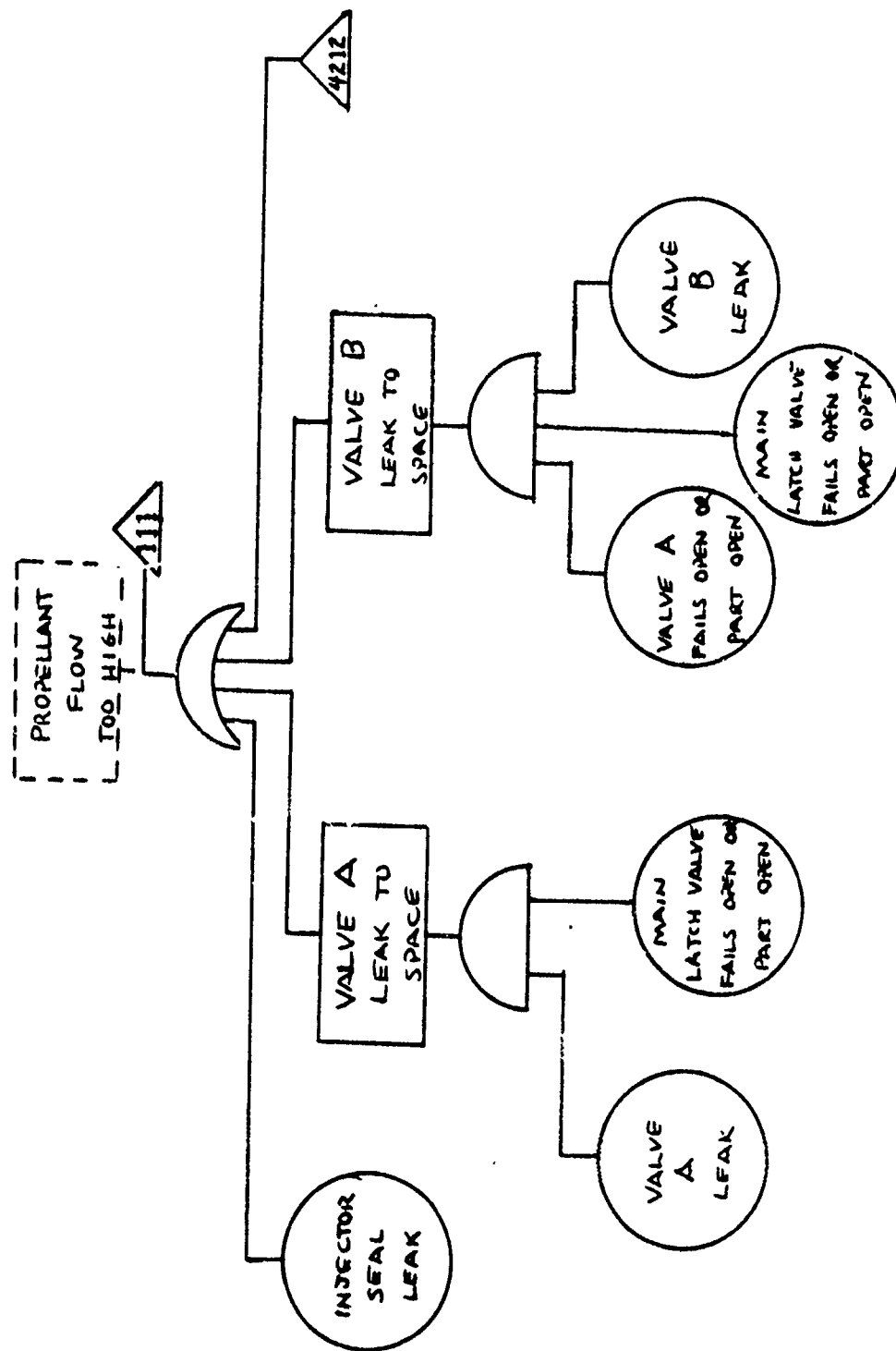
I-243

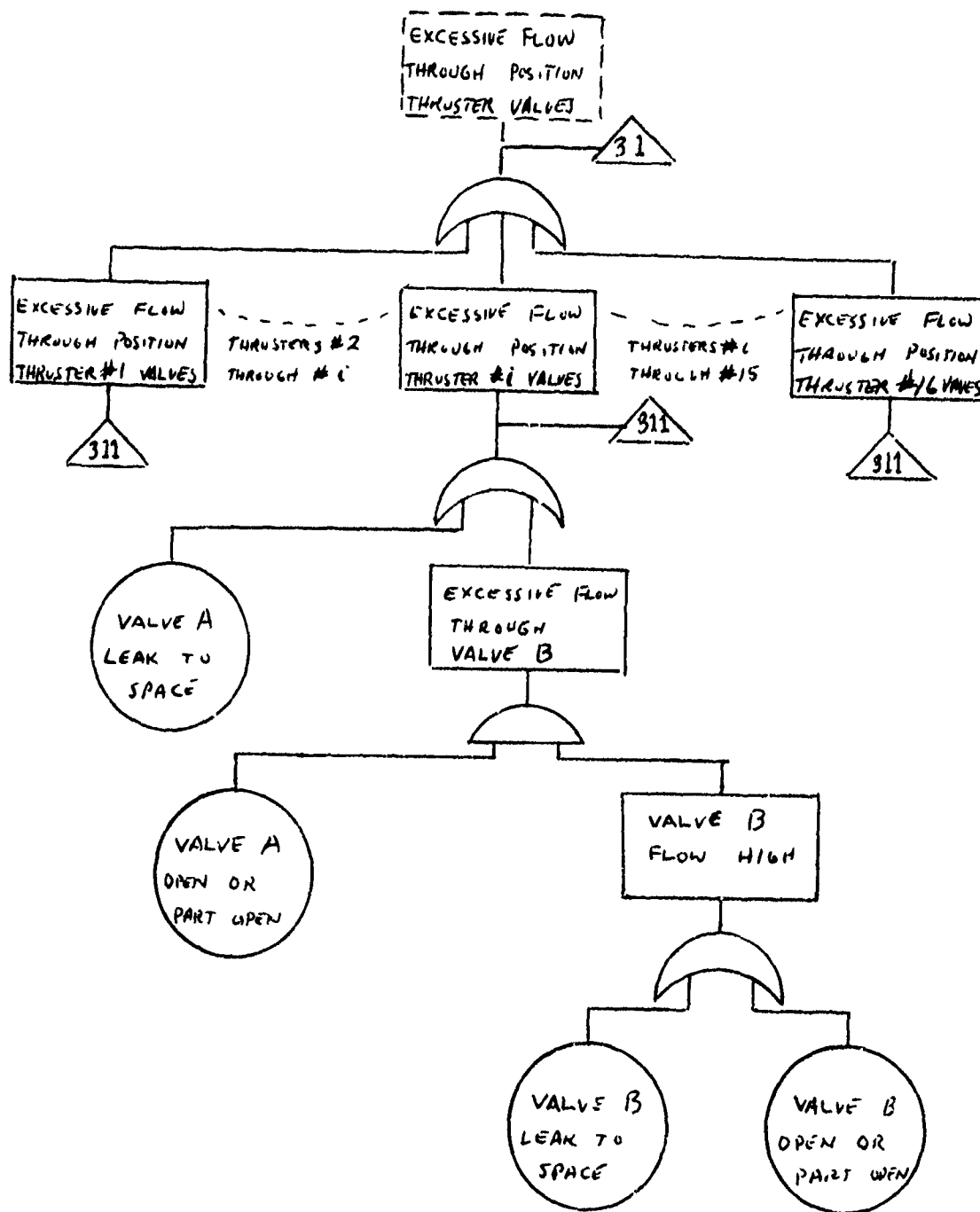Figure 22 (Continued)

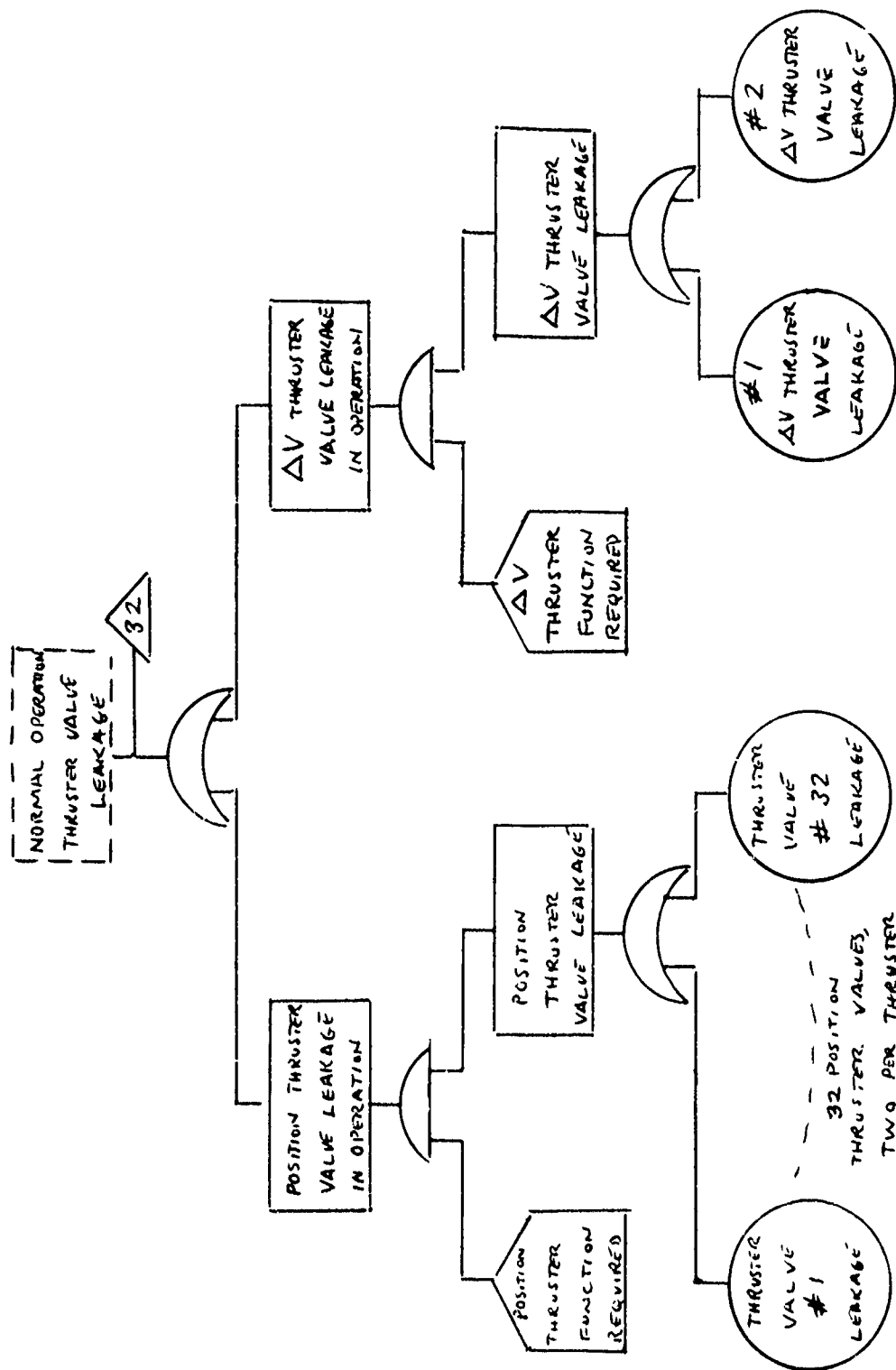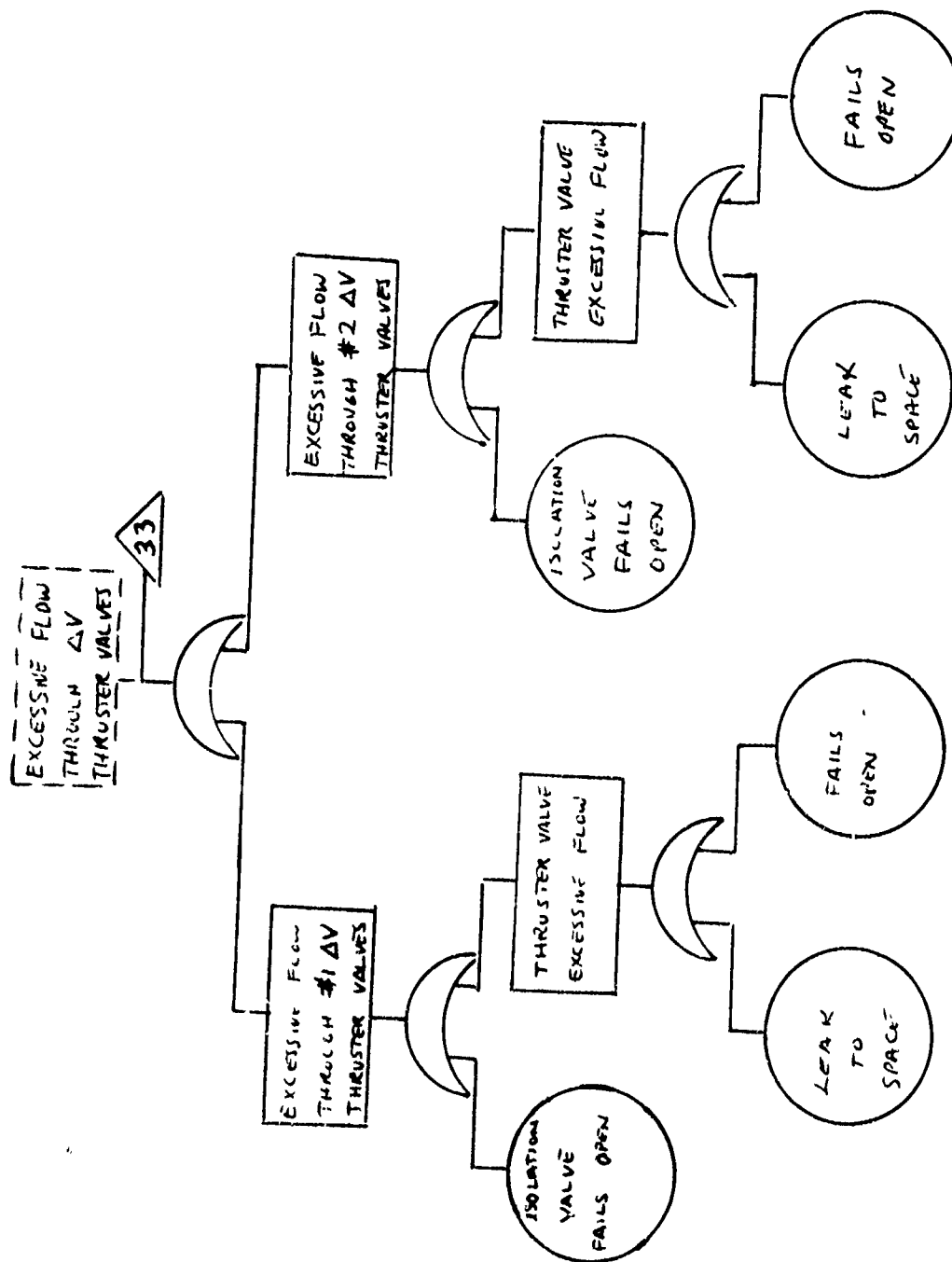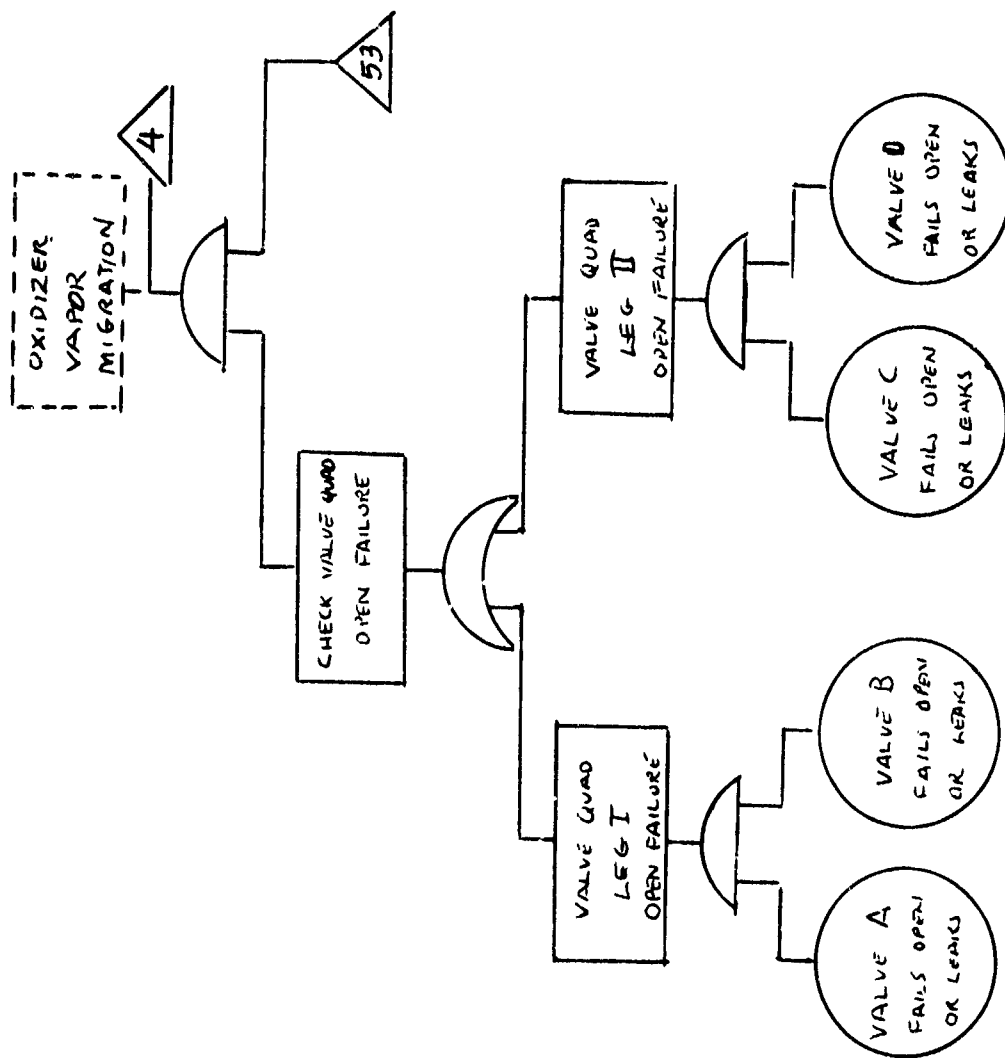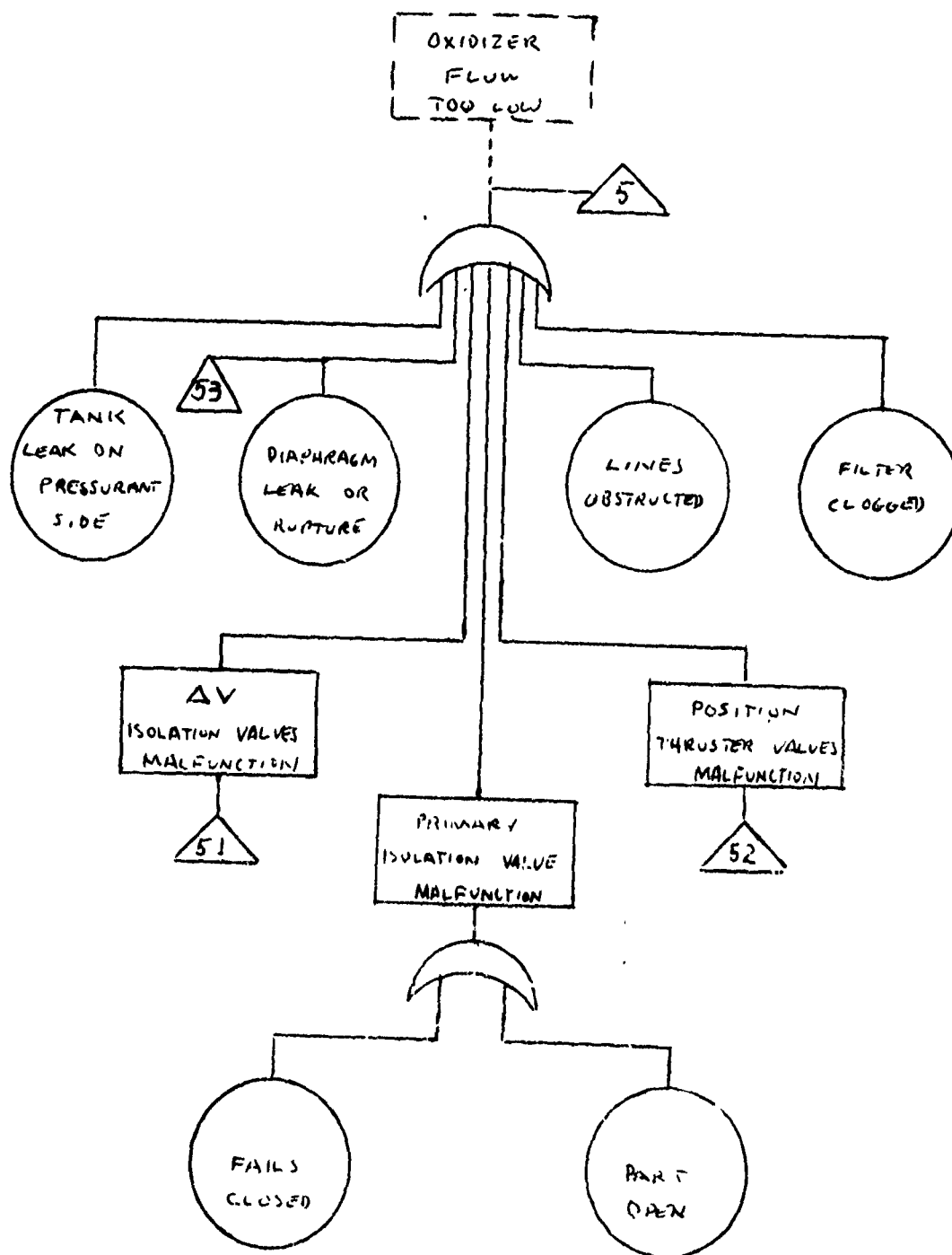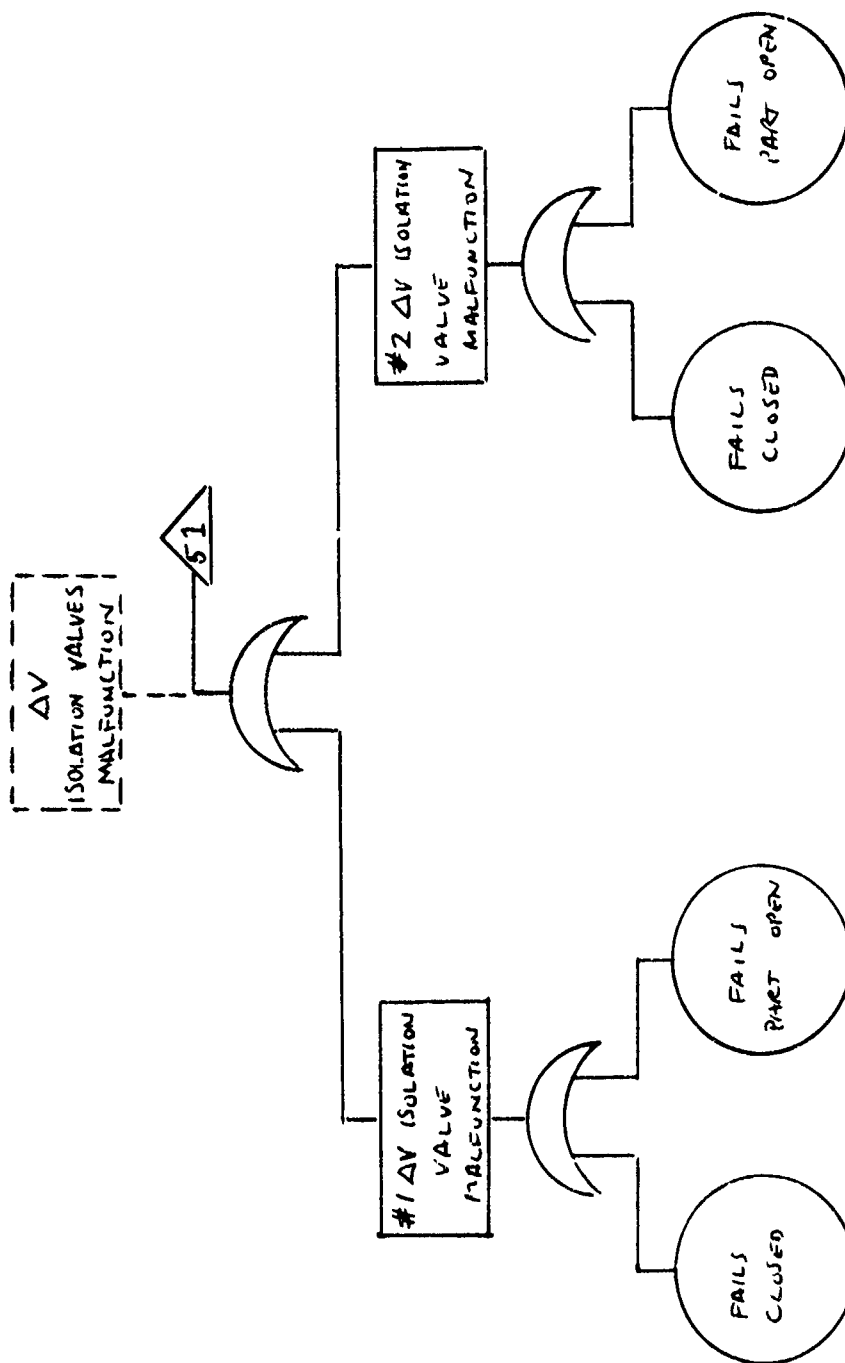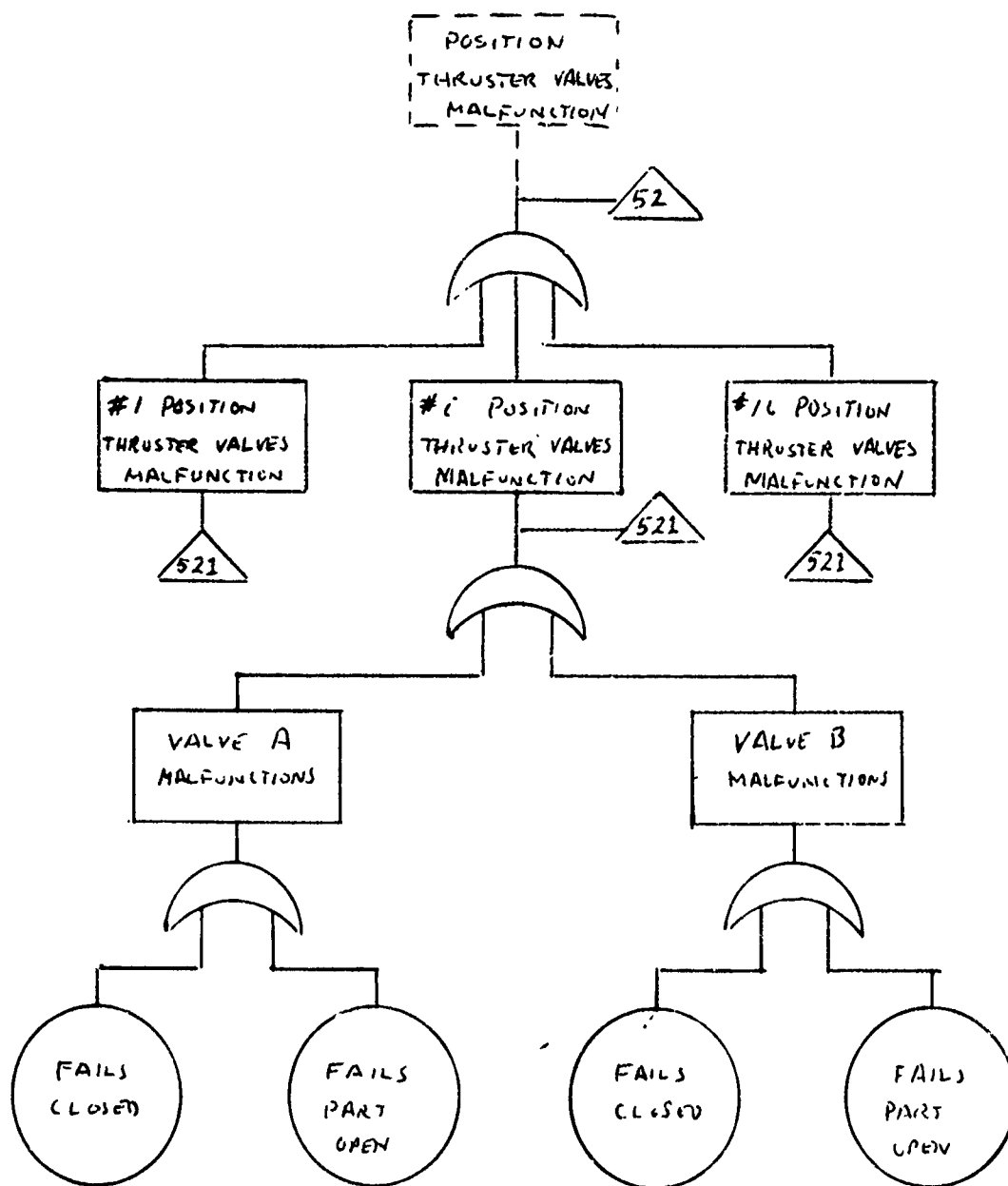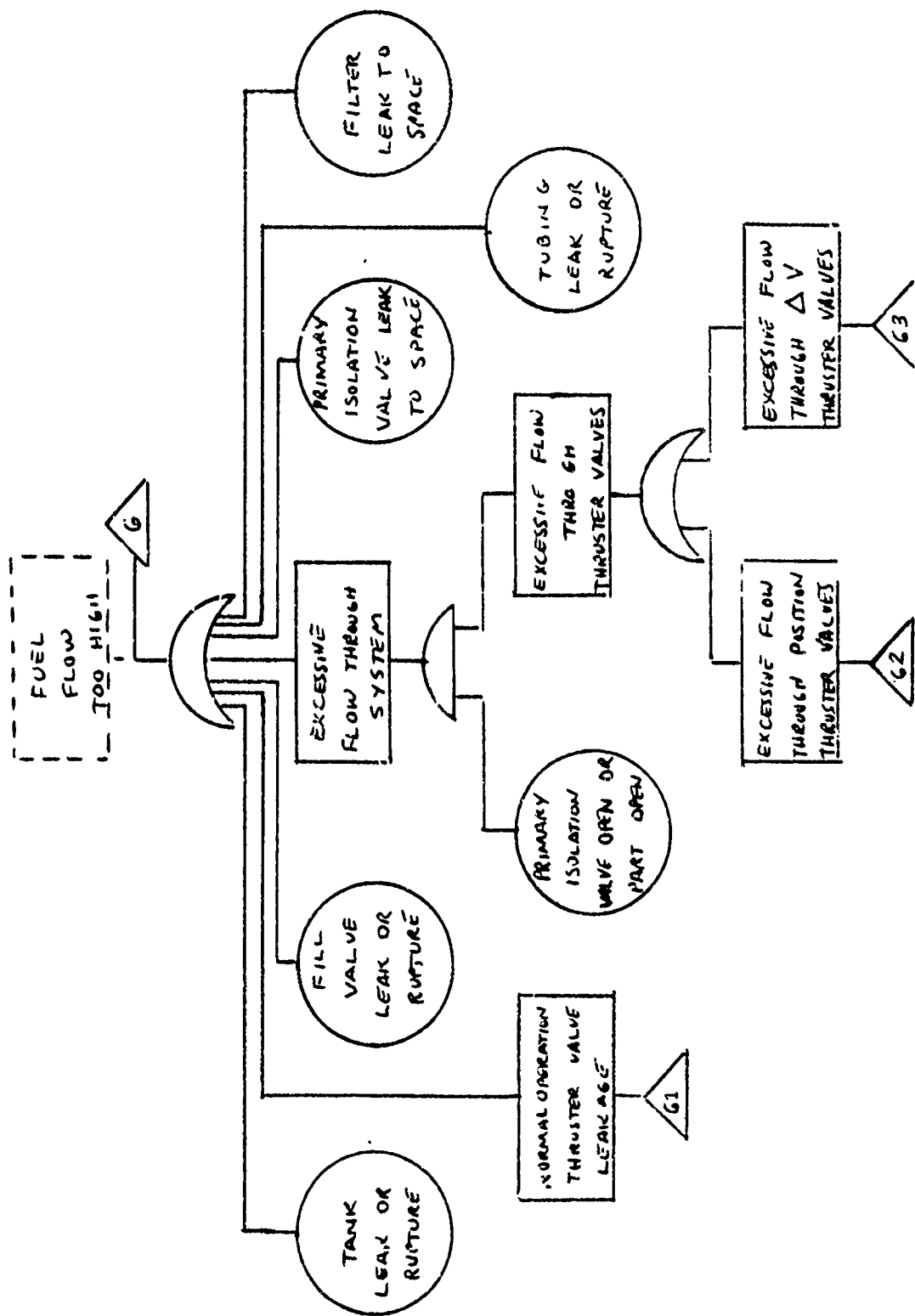Figure 22 (Continued)

Figure 22 (Continued)

Figure 22 (Continued)

NOTE: USE ONE ONLY
DEPENDING ON THRUSTER
CONFIGURATION

Figure 22 (Continued)

I-248

Figure 22 (Continued)

I-249
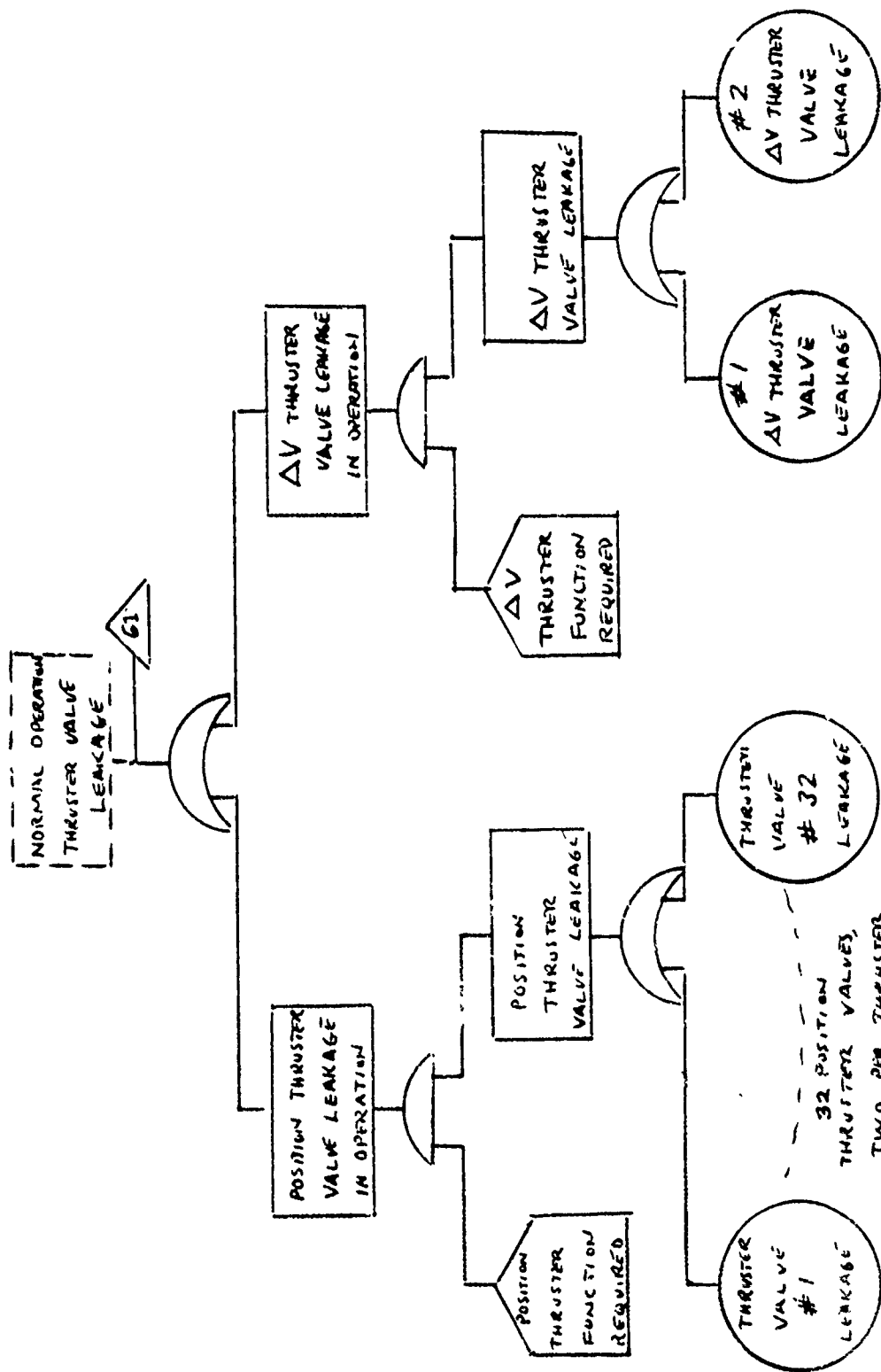
Figure 22 (Continued)

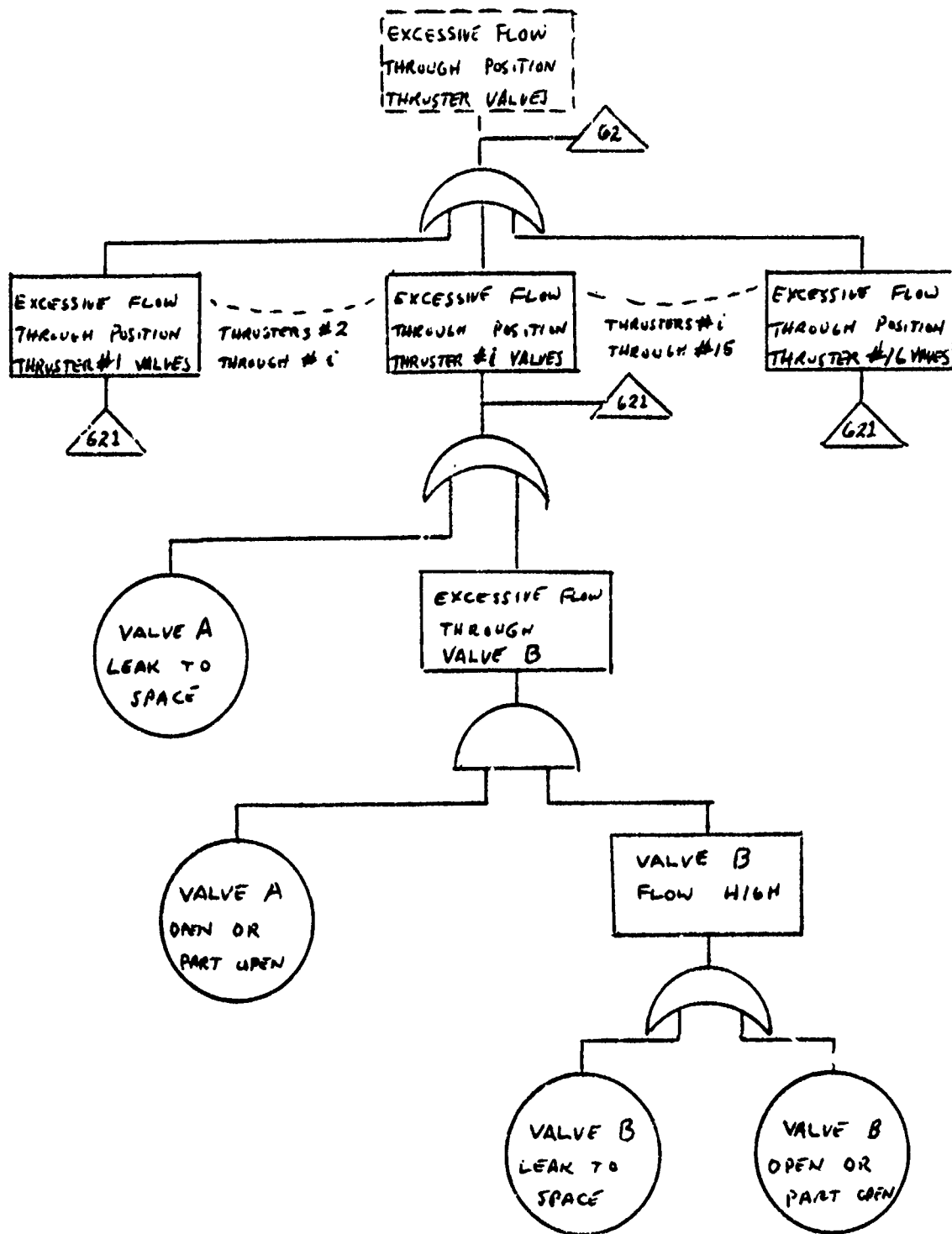Figure 22 (Continued)

Figure 22 (Continued)

Figure 22 (Continued)

I-253

Figure 22 (Continued)

I-254

Figure 22 (Continued)

Figure 22 (Continued)

I-256
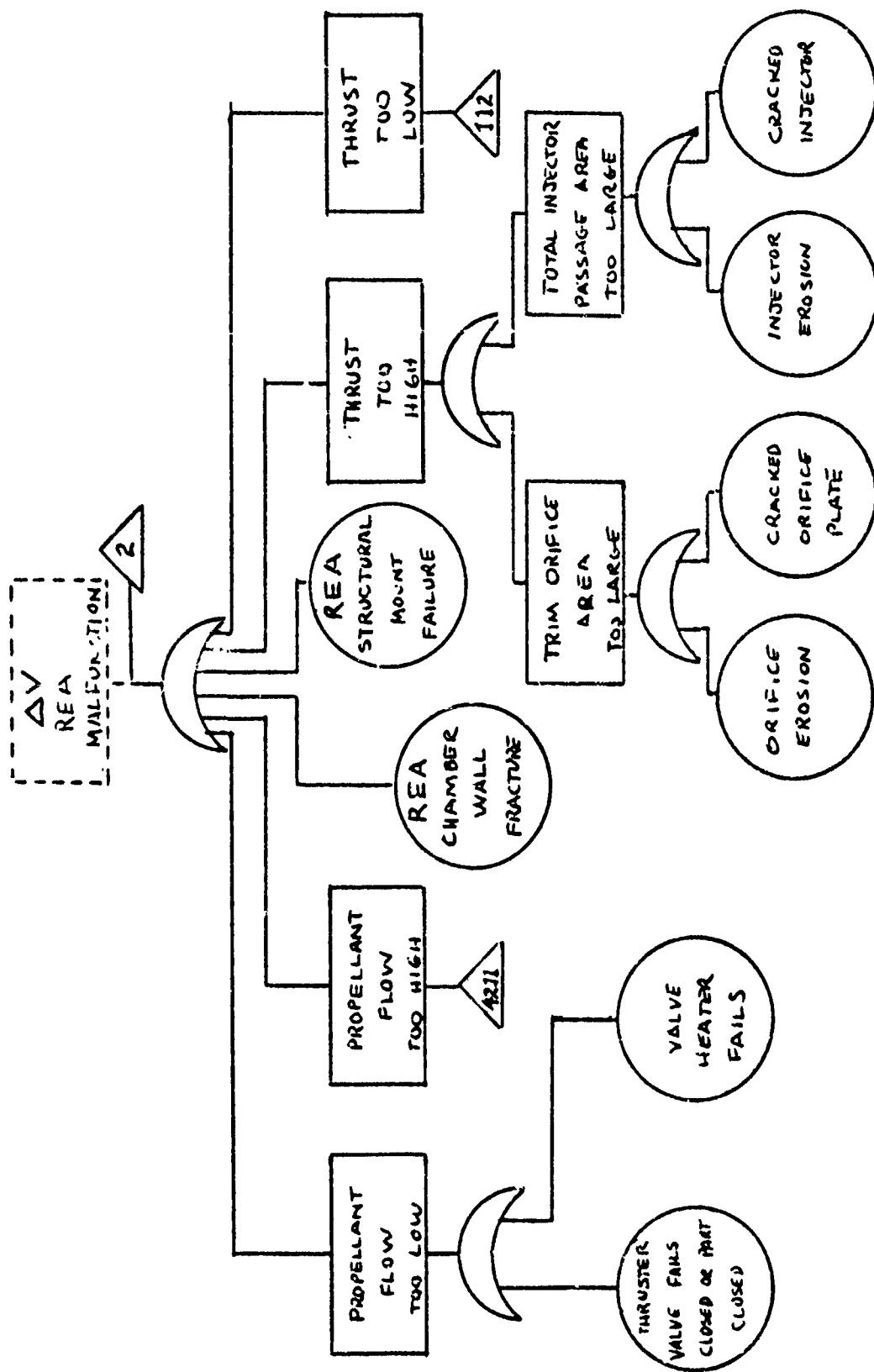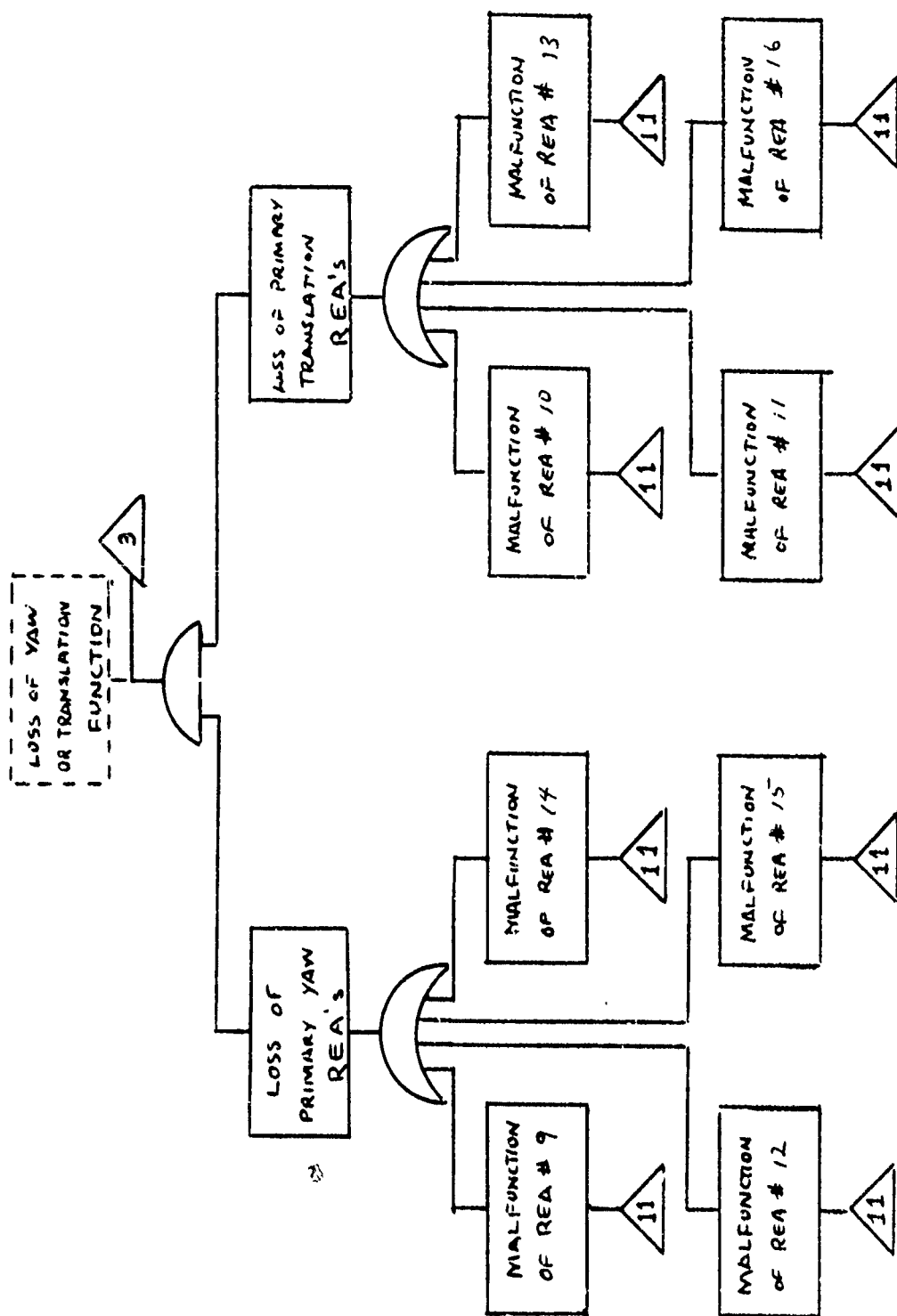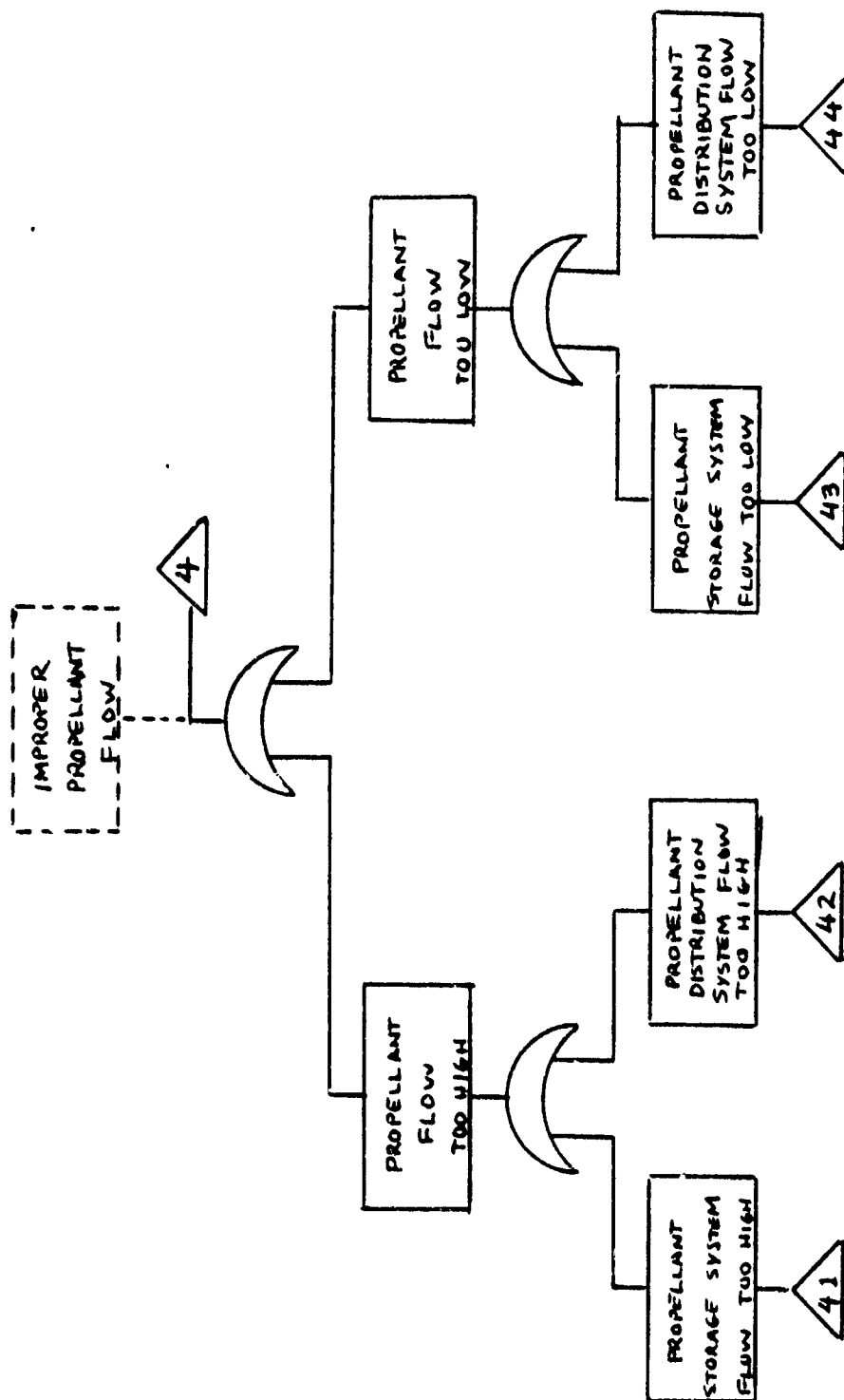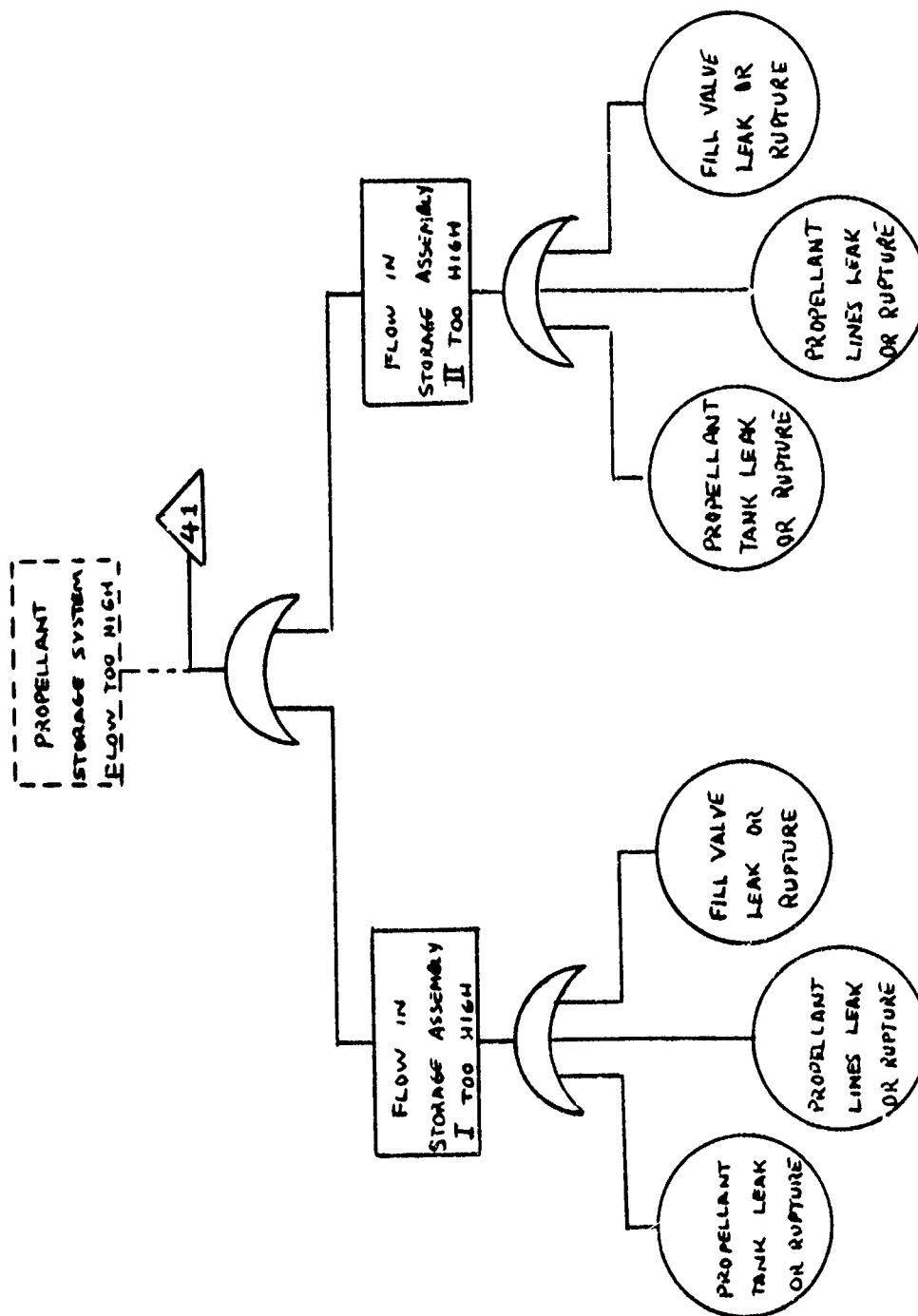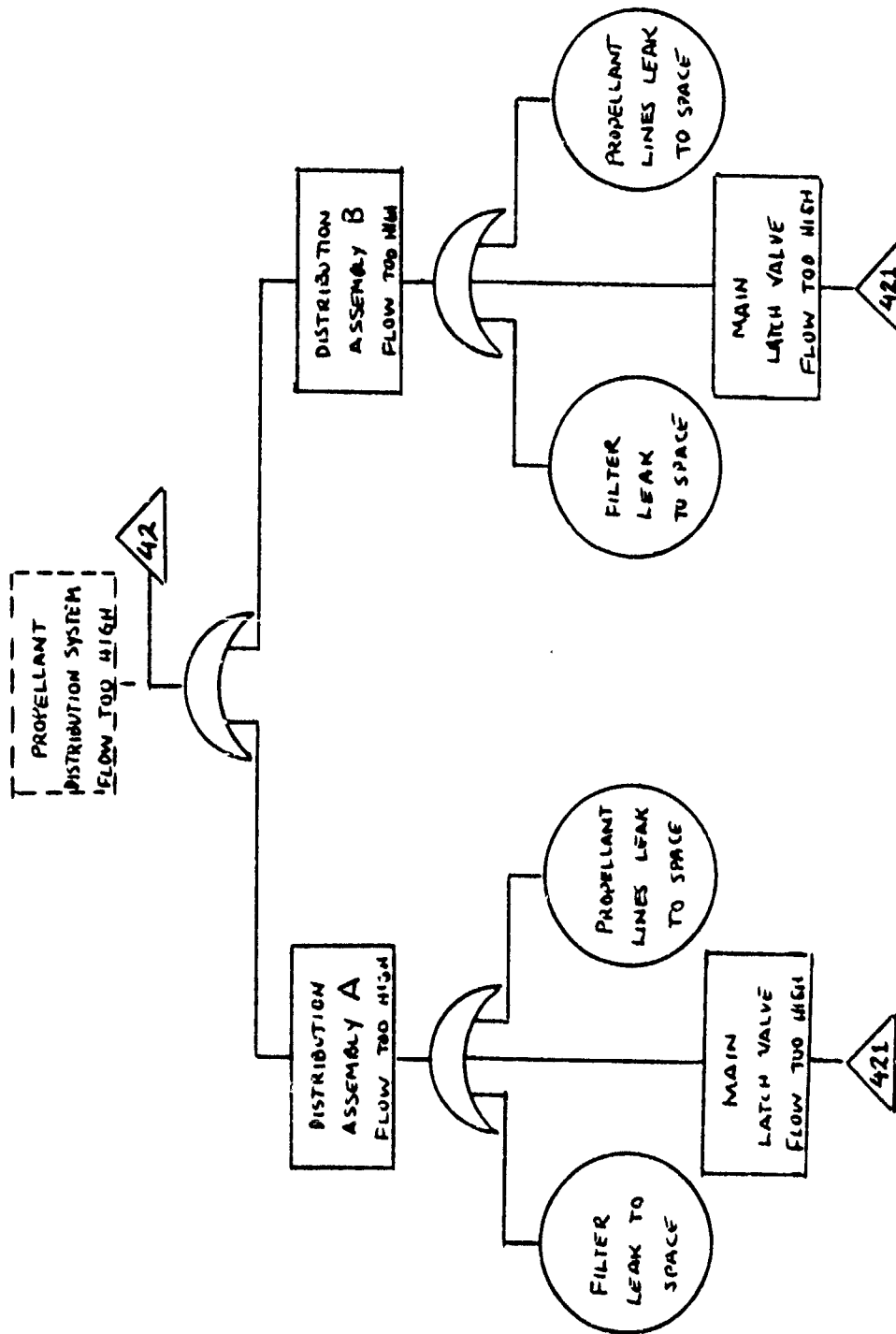
Bipropellant Thruster. The bipropellant thruster analyzed
in this study is of the hypergolic type. It derives thrust
from the spontaneous exothermic reaction which results when
monomethyl hydrazine and nitrogen tetroxide are brought
into contact with each other.

As discussed in the previous thermochemical propulsion
systems, three pressurization schemes may be used inter-
changeably with the three propulsion systems. For the
purposes of this study, each propulsion system used a dif-
ferent pressurization approach. The constant regulated
pressure approach was used in conjunction with the bipro-
pellant thruster. The interchanging of appropriate fault
tree branches will yield fault trees for all desired com-
binations.

A schematic of the system is shown in Figure 23. The
fault tree analysis is presented in Figure 24. For addi-
tional detail on system components refer to Figure 8, Bi-
propellant Generic System Layout, page I-8.

Figure 23. Hypergolic Bipropellant System Schematic

HYPERGOLIC BIPROPELLANT SYSTEM
FAULT TREE ANALYSIS
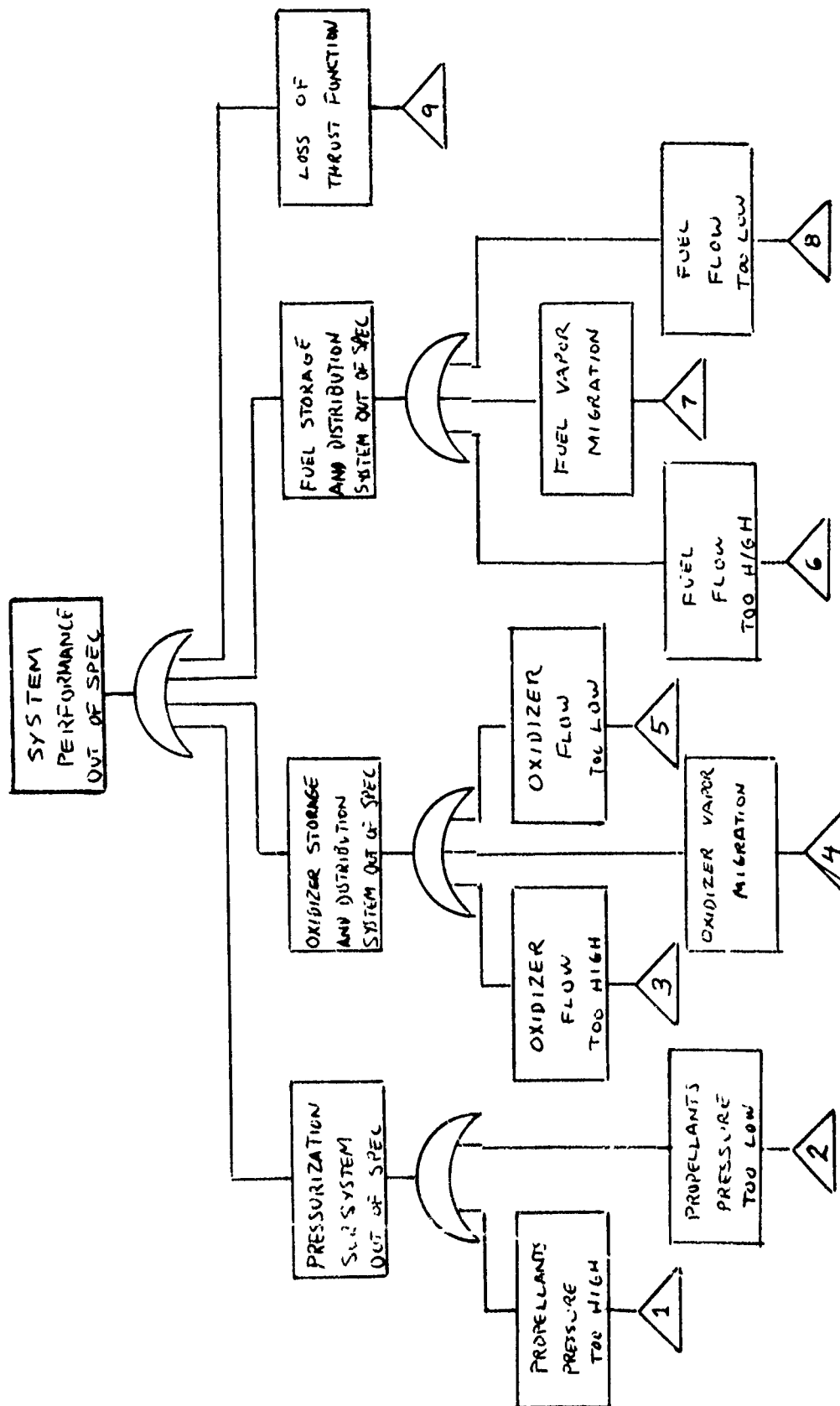
Figure 24. Hypergolic Bipropellant System Fault Tree Analysis

I-260

Figure 24 (Continued)

Figure 24 (Continued)

Figure 24 (Continued)

Figure 24 (Continued)

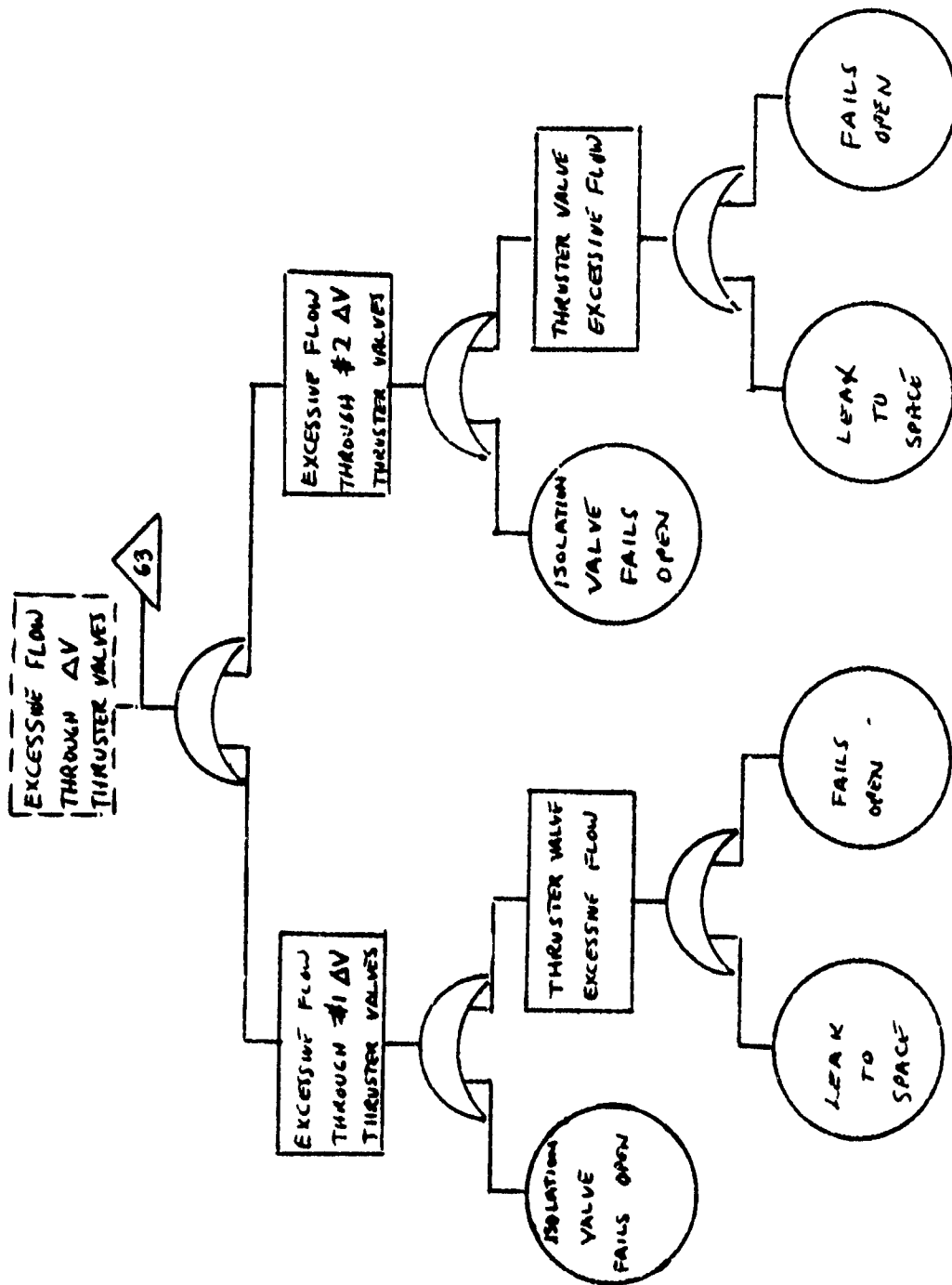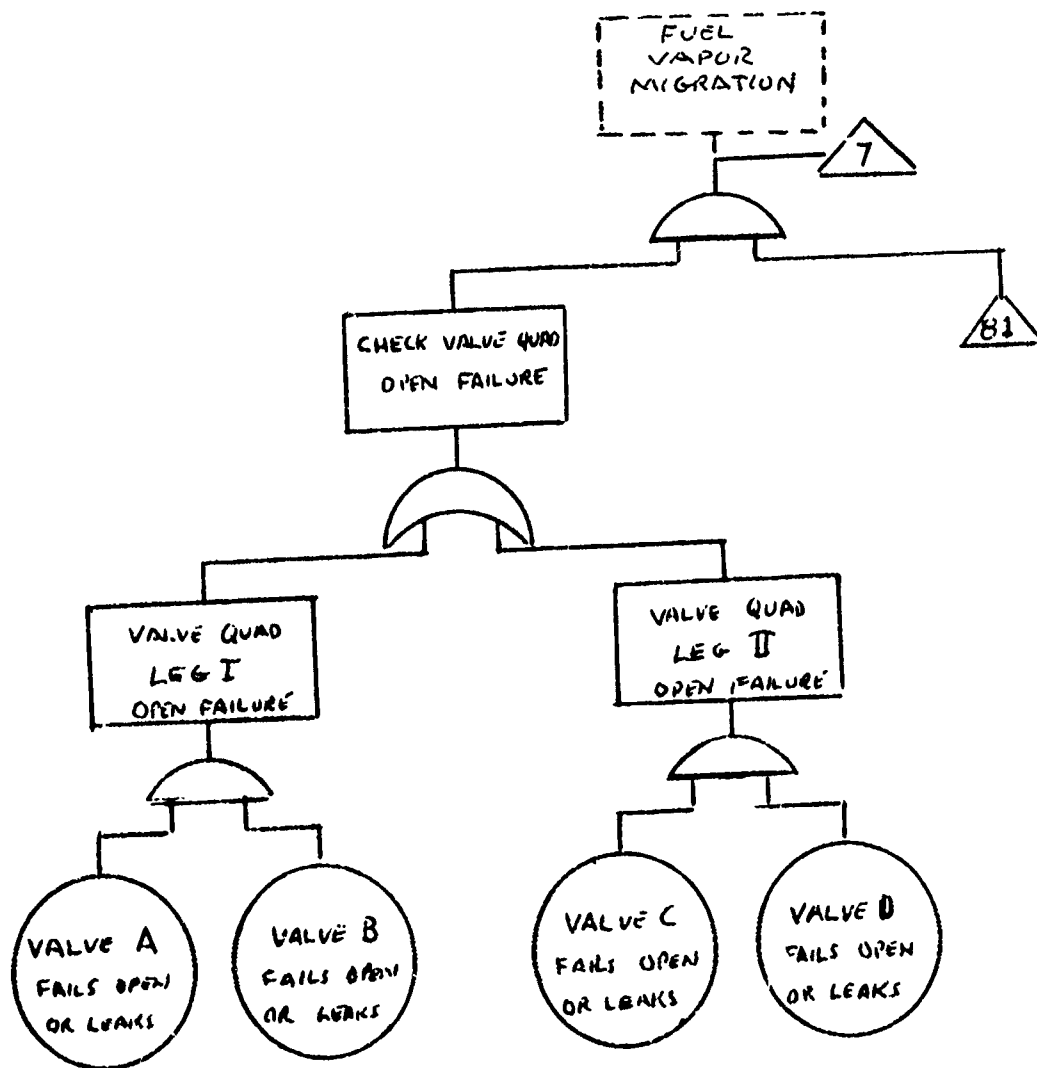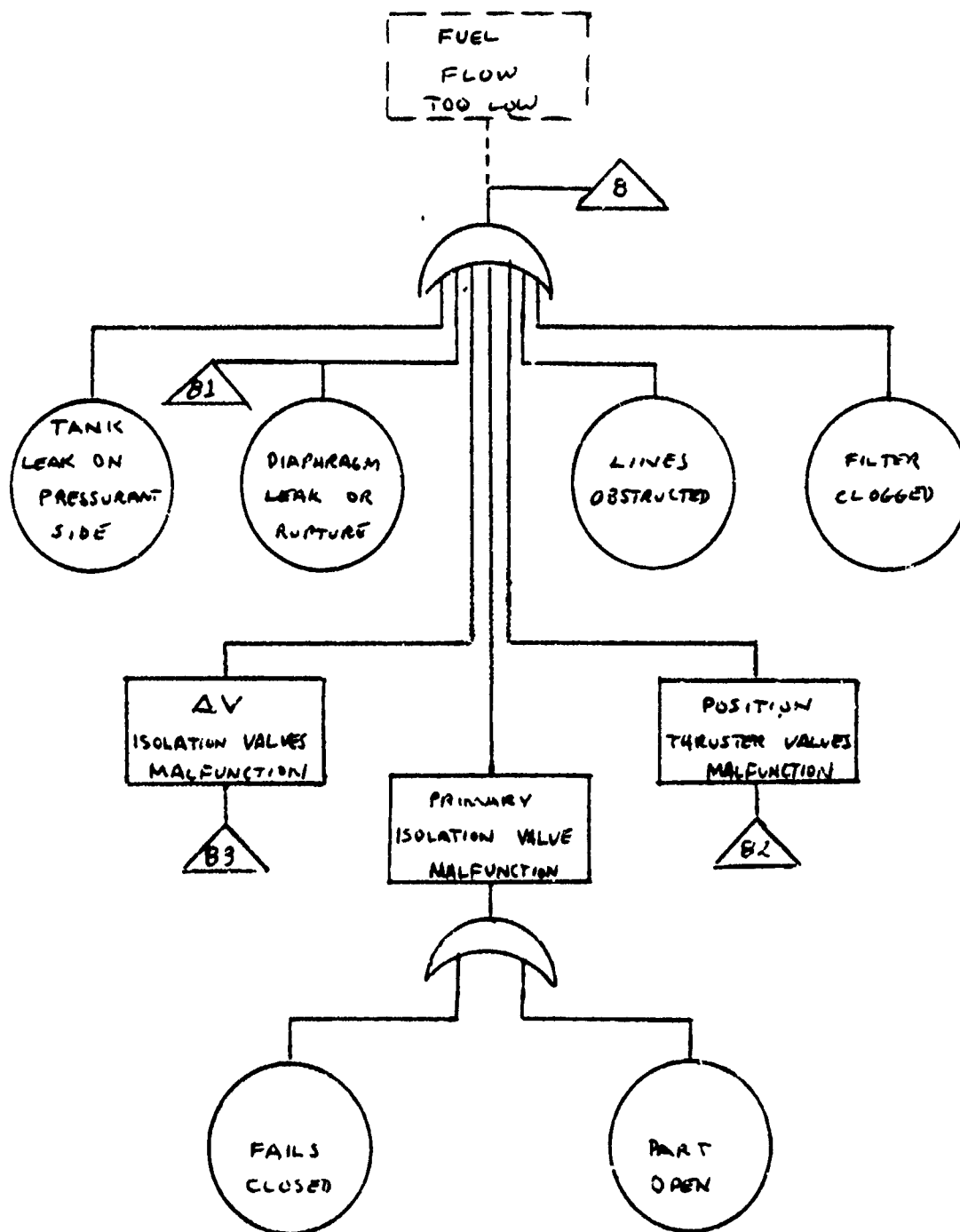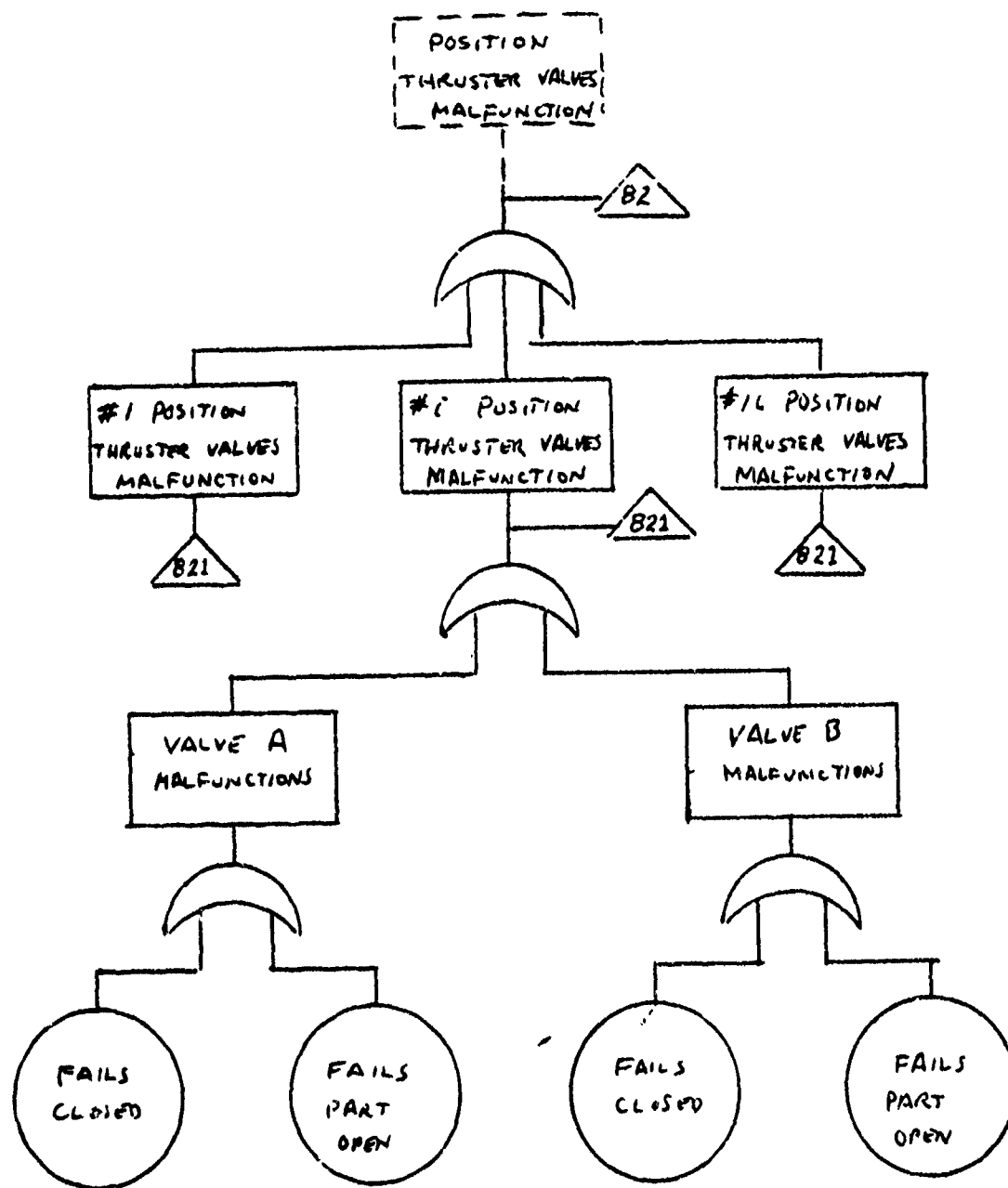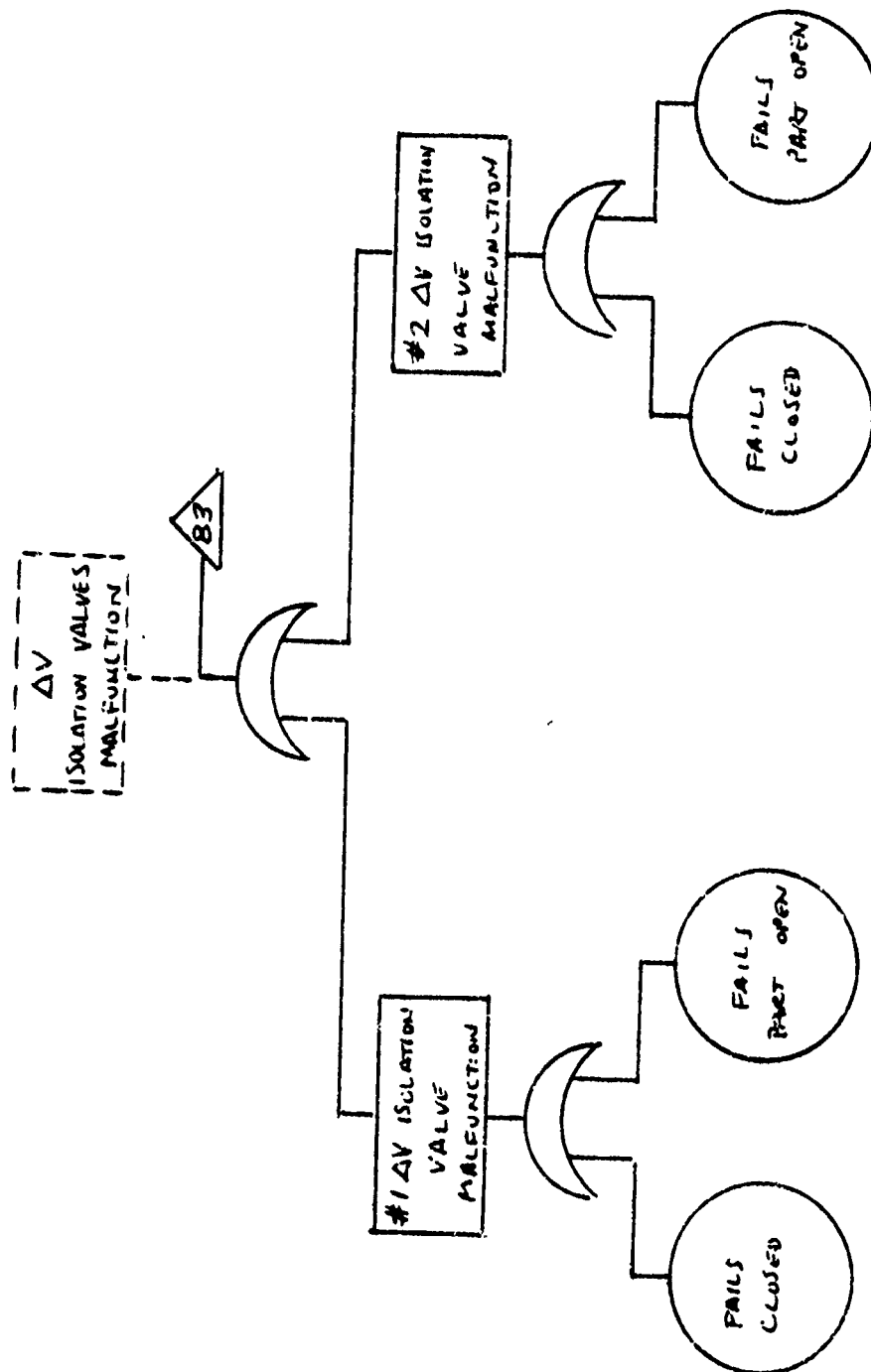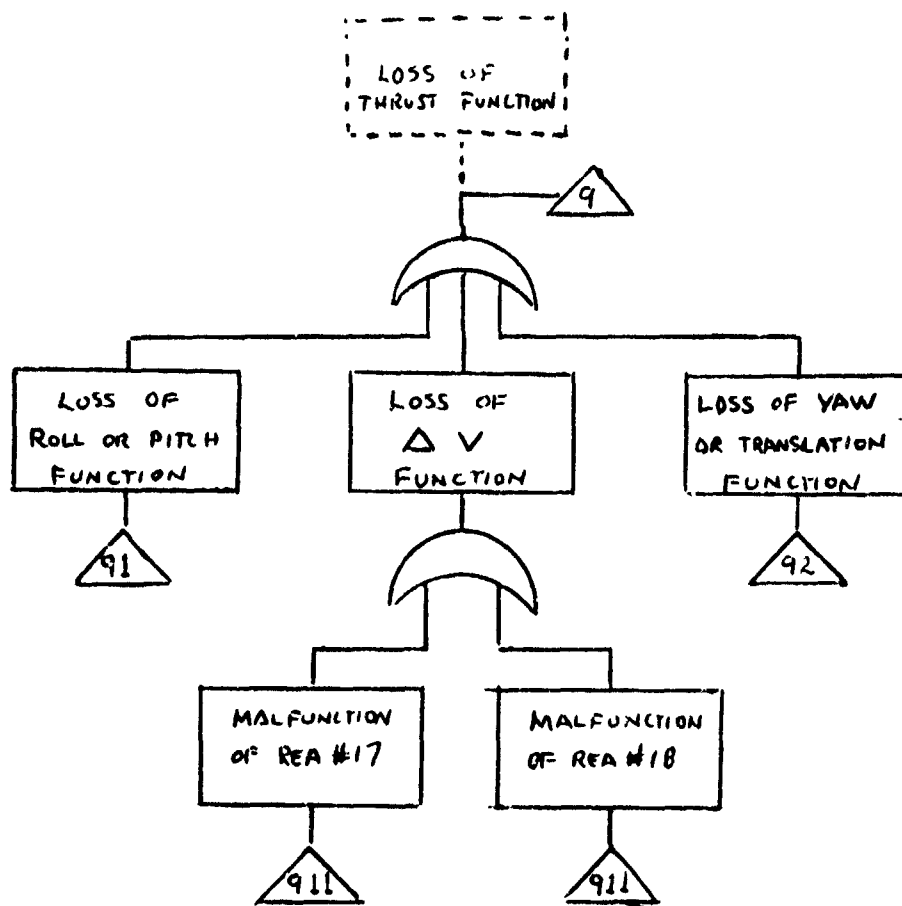Figure 24 (Continued)

Figure 24 (Continued)

Figure 24 (Continued)
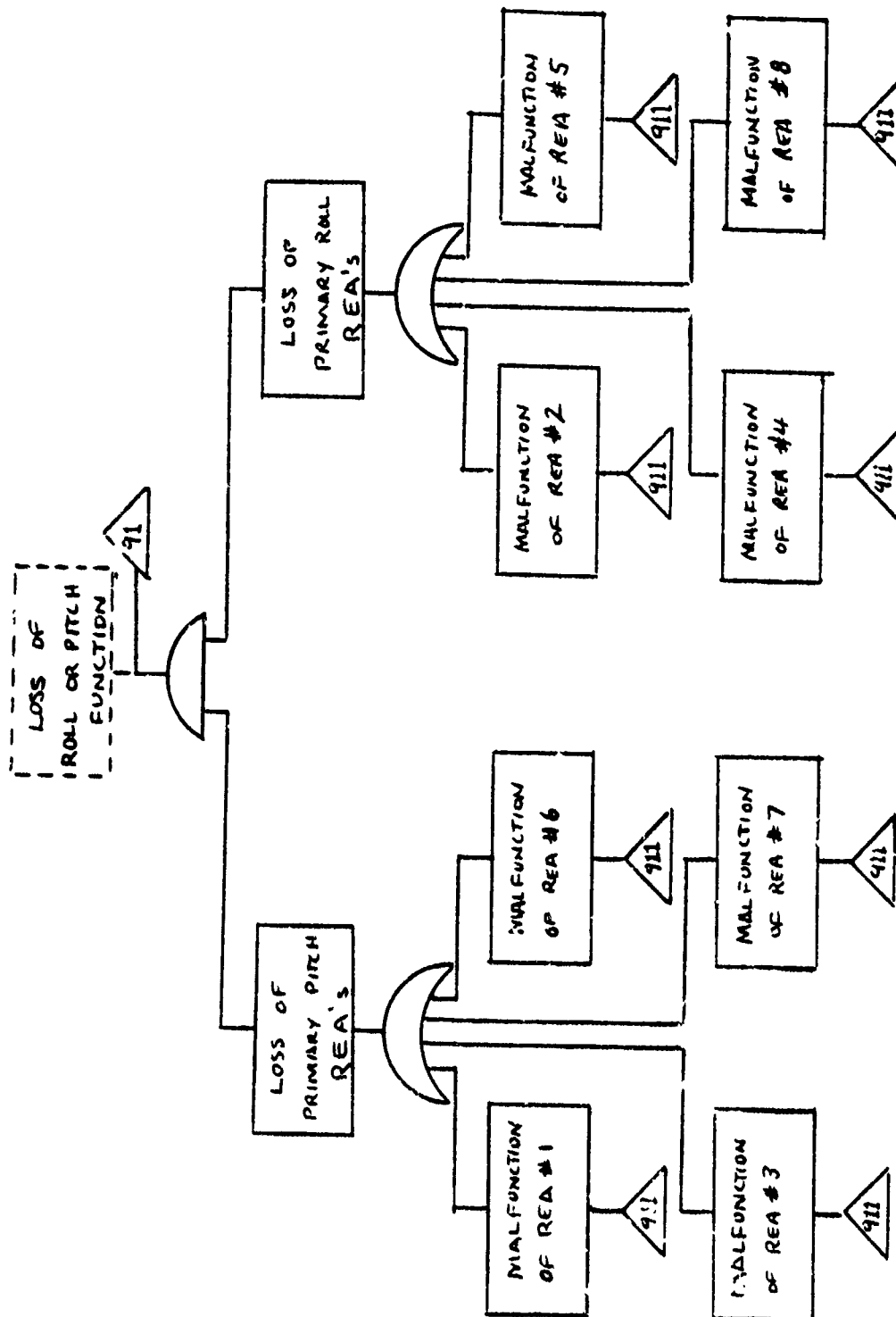
Figure 24 (Continued)

Figure 24 (Continued)

Figure 24 (Continued)

Figure 24 (Continued)

Figure 24 (Continued)

Figure 24 (Continued)

Figure 24 (Continued)

Figure 24 (Continued)
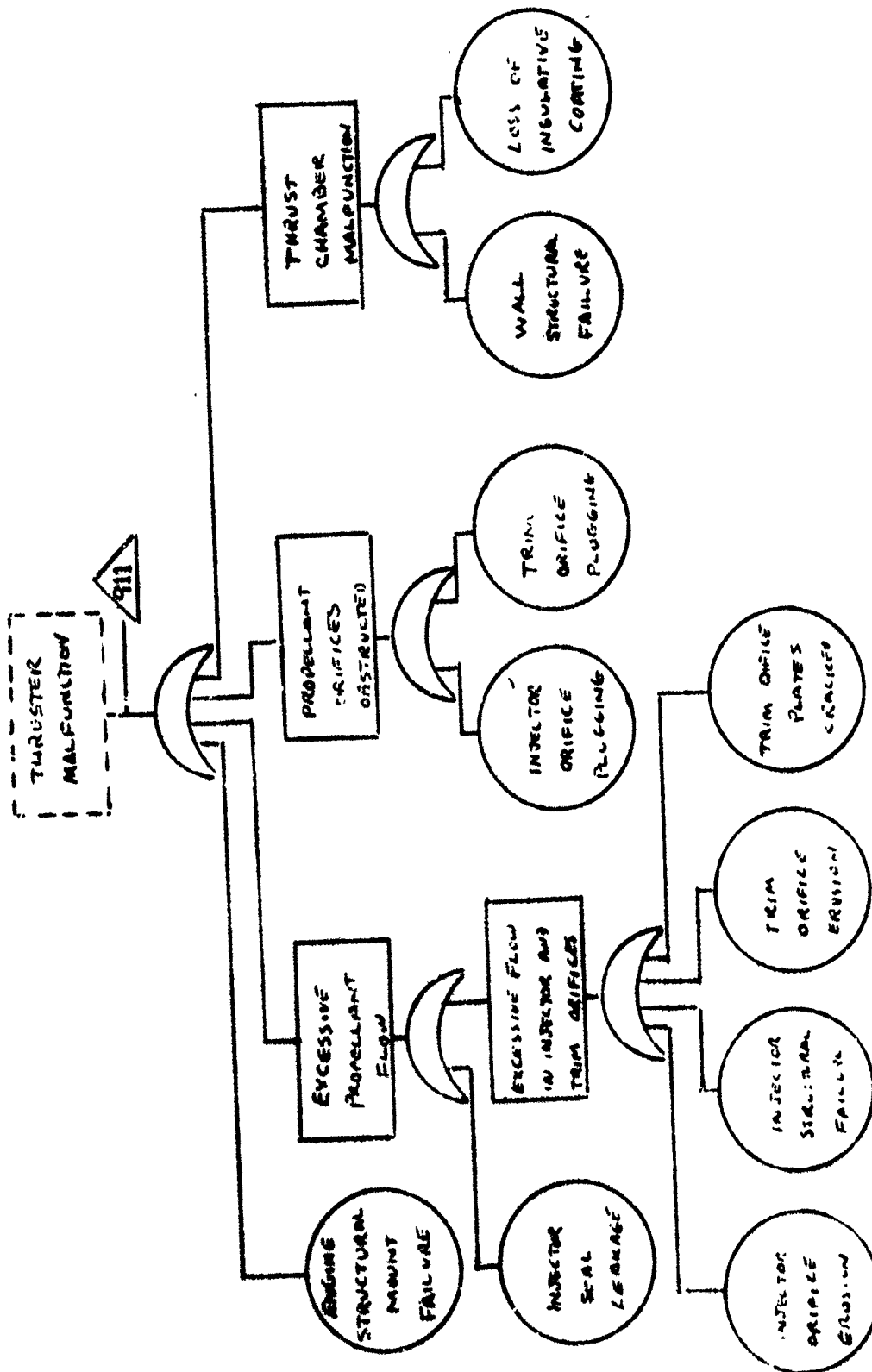
Figure 24 (Continued)

Figure 24 (Continued)

Figure 24 (Continued)

Figure 24 (Continued)

Figure 24 (Continued)

Figure 24 (Continued)

I-281

Figure 24 (Continued)

Figure 24 (Continued)

Figure 24 (Continued)

Figure 24 (Continued)

Figure 24 (Continued)